LED lighting in greenhouse horticulture: Photosynthesis

Craig R. Taylor

Propositions

1. The importance of far-red light to enhancement of photosynthesis reveals the inadequacy of the PAR definition.
(this thesis)

2. The inattention towards light-limited CO_2 fixation has led to significant gaps in the understanding of fundamental aspects of photosynthesis.
(this thesis)

3. Vertical farming is not a sustainable means of food production on local and global scales.

4. The frequent outsourcing of experimental set-up to technicians or university workshops by PhD candidates means that many candidates do not develop the skills needed to be truly independent scientists.

5. Foundational electronics and computer programming courses should be a prerequisite for undergraduate students of the natural sciences.

6. Merit is the only criterion which should matter for any position.

7. Meetings seldom achieve much more than keeping people from work which they are supposed to be doing.

Propositions belonging to the PhD thesis entitled

LED lighting in greenhouse horticulture: Photosynthesis

Craig Robert Taylor
Wageningen, 31 May 2022

LED lighting in greenhouse horticulture:

Photosynthesis

Craig R. Taylor

Thesis committee

Promotor
Prof. dr. ir. L.F.M. Marcelis
Professor of Horticulture and Product Physiology
Wageningen University

Thesis co-supervisors
Dr. J. Harbinson
Associate professor of Biophysics
Wageningen University

Dr. ir. W. van Ieperen
Assistant Professor of Horticulture and Product Physiology
Wageningen University

Other members:
Prof. dr. ir. N. Anten, Wageningen University
Prof. dr. X. Yin, Wageningen University
Prof. dr. R. Croce, Vrije Universiteit Amsterdam
Prof. dr. E. Murchie, Nottingham University, United Kingdom

LED lighting in greenhouse horticulture: Photosynthesis

Craig R. Taylor

Thesis
submitted in fulfilment of the requirements for the degree of doctor
at Wageningen University
by the authority of the Rector Magnificus Prof. dr. ir. A.P.J. Mol,
in the presence of the
Thesis Committee appointed by the Academic Board
to be defended in public
on Tuesday 31 May 2022
at 11:00 a.m. in the Groot Auditorium.

Abstract

Light spectrum has a significant impact on a wide variety of plant processes including photosynthesis and photomorphogenesis which in turn impact plant productivity. The choice of supplementary light spectrum in greenhouses is therefore not trivial, and this is especially so given the diverse spectral possibilities afforded by increasingly popular LED supplementary lighting. The main focus of this thesis is on spectral impacts of light-limited quantum yield of CO_2 fixation in leaves of tomato, a common greenhouse-grown crop. Some attention is also given to the photomorphogenetic impacts of spectrum as well as the impact of temperature on Φ_{CO2}.

Enhancement of photosynthesis is examined using diverse actinic spectra. Leaves were grown in either an artificial daylight or an artificial shade spectrum. Gas exchange was measured using each of 17 narrowband irradiances, a nearly identical irradiance to growth irradiance, and a combination of the narrowband irradiances and growth irradiance in a 1:1 ratio on an absorbed PAR basis. Enhancement was calculated to be 23% in the shade spectrum whereas enhancement did not occur in the sun spectrum. In the spectral combination experiments, maximum enhancement of 76% occurred when 720 nm was combined with the shade spectrum; enhancement across all other wavelengths added to the shade spectrum ranged between 17 and 27%. No, or negligible, enhancement occurred in the daylight spectrum or when wavelengths of 660 nm or shorter were combined with the daylight spectrum. However, enhancement of 4.7, 7.6 and 43% was observed when 680, 700 and 720 nm were combined with the daylight spectrum, respectively. Taken together, a commonality of instances where enhancement was found to occur was a spectrum rich in far-red light (>700 nm) which highlights the inadequacy of the PAR definition.

Another experiment examined how leaves acclimate to spectral fluctuations in the short-term and what impact this may have on Φ_{CO2}. State transitions were induced by subjecting leaves grown in an artificial daylight irradiance or artificial shade irradiance to alternating irradiances which are extreme in terms of their PSII and PSI over-excitation. A relationship between Φ_{CO2} and the occurrence of state transitions is revealed in a higher plant for the first time. The accompanying increase in Φ_{CO2} from commencement to completion of a state transition was found to be between 10-13%.

A third experiment examines the combined spectral impacts of blue light on photosynthesis, plant morphology, and whole-plant light interception. The wide variety of leaf-level and whole-plant impacts regulated by blue light makes it an interesting candidate to explore these relationships, further stimulated by the absence of study of blue light doses in a more natural daylight background. Blue light inhibition of etiolation was preserved under a simulated daylight background and this inhibition increased with blue light fraction while whole-plant light absorption decreased. Photosynthetic effects of blue light fraction were unremarkable, with Φ_{CO2} and maximum photosynthetic capacity (A_{max}) negligibly affected, the latter of which may already have been saturated by the blue fraction of the daylight spectrum itself. With limited impact on Φ_{CO2}, the primary impact of blue light fraction on plant biomass appears to be through whole-plant light absorption.

A final experiment examines the impact of temperature on Φ_{CO2}, Φ_{PSII}, Φ_{PSI}, and the electrochromic shift at 2% and 21% O_2 and between 15 and 35 °C. Φ_{CO2} was predictably greater at 2% O_2 at all temperatures due to the suppression of photorespiration. Φ_{CO2} showed a temperature optimum at 18 °C in 2% and 21% O_2 but the extent of the temperature dependency at 2% O_2, being 29% lower at 35 °C, was unexpected given the practical absence of photorespiration. Whereas Φ_{PSII} was mostly independent of temperature at 2% O_2, it showed a parabolic response in 21% O_2 with a temperature optimum at 25 °C. Surprisingly, Φ_{PSII} and qP were lower in 2% O_2 than 21% O_2, which may be the result of cyclic electron transport to accommodate for shortfalls in ATP production.

Keywords: enhancement, gas exchange, light emitting diodes, light spectrum, photosystem balance, photomorphogenesis, photoreceptors, photosynthesis, state transitions, temperature, tomato, quantum yield.

CONTENTS

LIST OF ABBREVIATIONS

Φ_{CO2}, $\Phi_{CO2(LL)}$ maximum (light-limited) quantum yield of CO_2 fixation

Φ_{PSII}, quantum yield of PSII electron transport

A_{max}, light saturated rate of CO_2 assimilation

ATP, adenosine triphosphate

BBC, Benson-Bassham-Calvin cycle

ECS, Electrochromic shift

Fd, ferrodoxin

Fm, dark adapted maximum fluorescence

Fm' light adapted maximum fluorescence

Fo, dark adapted minimum fluorescence

Fo', light adapted minimum fluorescence

Fv'/Fm', maximum light adapted efficiency of PSII

LET, linear electron transport

LHCII, light-harvesting complex II

NADPH, nicotinamide adenine dinucleotide phosphate

P700, photosystem I primary donor

Pi, inorganic phosphate

PCB, printed circuit board

PCO, photosynthetic carbon oxidation

PGO, phosphoglycolate

PPFD, photosynthetic photon flux density

PSI, photosystem I

PSII, photosystem II

PQ, plastoquinone

PQH2, plastoquinol

SEM, standard error of the mean

Q_A, primary quinone acceptor of PSII

CHAPTER 1

General Introduction

1.1. Background

Oxygenic photosynthesis is a process of energy transduction in which light energy is absorbed by photosynthetic tissues and converted to metabolically useful forms of chemical energy. The primary function of photosynthesis is to fix carbon dioxide, ultimately derived from the air or water surrounding the plant, alga, or bacteria, into carbohydrates for maintenance and growth. Carbon fixation requires chemical energy in two forms. First substantial reducing power in the form of NADPH and, second, a source of energy in the form of ATP, specifically the phosphoanhydride bounds linking the phosphate groups. ATP is made from ADP and Pi, and NADPH from NADP, by the action of light-driven reactions and they drive the metabolic process of carbon dioxide fixation in the Benson-Bassham-Calvin cycle (BBC). In the viridiplantae (the land plants and green algae) this results in the formation of starch and triose phosphates, with the latter being exported from the chloroplast to make sucrose in the cytosol. These metabolic reactions release the ADP, Pi and NADP needed for the continued activity of the light-driven reactions of photosynthesis.

Given the primary importance of light to photosynthesis, this study was stimulated by the increasing popularity of LED lighting as supplementary assimilation lighting in greenhouses in the Netherlands and how the relatively narrow emission spectrum of LEDs commonly used in greenhouses might influence the efficiency of photosynthesis. At the high latitudes in which the Netherlands is located, the average light intensity during the darker months of late autumn, winter and early spring is too low for high crop yields and supplementary lighting is therefore employed to overcome this problem (Heuvelink *et al.*, 2005). LEDs have been in existence for several decades, with use in consumer electronics dating as far back as the 1960s (Gayral, 2017). Initial attempts to use LED lighting for plant growth around the early 1990's were limited by light output, the limited range of useful output spectra available (especially in those LEDs with reasonably high output efficiency), and high cost. Their use was therefore confined to small-scale proof-of-principle tests of LEDs in plant lighting applications (Morrow, 2008). Subsequent improvements in LED light output (both in terms of the total output power per LED and the quantum efficiency of this output) and lower production costs (Haitz and

Tsao, 2011) enabled their transition from low output applications to dedicated illuminance applications including horticultural lighting.

A discussion of the advantages of LEDs as horticultural lighting can only be done in relation to other horticultural lighting technologies of which high pressure sodium (HPS) lighting is most commonly used. Given the continued widespread use of HPS lighting and the rising popularity of LEDs, together with the vast amount of electrical energy consumed by horticultural lighting in general, various comparisons of the two lighting technologies have been made from financial, energetic and productivity standpoints (Nelson and Bugbee, 2014; Kowalczyk *et al.*, 2020; Ouzounis *et al.*, 2018; Kusuma *et al.*, 2020; Katzin *et al.*, 2020; Katzin *et al.*, 2021). Such has been the pace of improvement in LED technology that some of these comparisons are already outdated. The theoretical limit of LED efficiency is close to being reached, with blue, white and red LEDs having energy conversion efficiencies of around 93%, 81% and 76%, respectively (Kusuma *et al.*, 2020). Expressed as moles of quanta output per Joule of electrical energy input, the most energy-efficient LED fixtures currently range between about 2.5 and 3 μmol J^{-1} depending on which LEDs colours are used; by comparison the most efficient HPS lamps have an efficiency of about 1.7 μmol J^{-1} (Radetsky, 2018; Kusuma *et al.*, 2020). An electrical energy saving of 60% was found when LEDs were used instead of HPS lamps (Ouzounis *et al.*, 2018). This reduction in energy when using LEDs is mainly due to the lower radiative heat production by LEDs together with their lower operating temperature compared to HPS lamps (which are gas discharge lamps). LEDs can therefore be positioned closer to plants without the risk of burning them (Morrow, 2008), something which is not possible with HPS lighting. This has led to research into the novel positioning of LEDs within the canopy, such as intra-canopy lighting (Trouwborst *et al.*, 2010), which also reduces radiative losses due to backscattering of light which occur when the lamps are positioned above the canopy. To compensate for the lower heat production of LEDs, however, more energy is required for heating (Katzin *et al.*, 2021). Those authors have estimated that a transition from HPS lighting to LEDs reduces total greenhouse energy consumption by between 10 – 25% depending mostly on climate.

Alongside their lower operating temperature, another less frequently mentioned benefit of LEDs is that they are remarkably small and compact devices which allows designers to better position LEDs above and within the canopy in ways that allow for improved coverage and

more even light distribution, a feature not possible with other considerably more bulky lighting technologies. The light output of LEDs is easily adjustable from zero to maximum illuminance by simply controlling the current through the LED or the duty cycle of pulse width modulation. The straightforward and precise control of LED output intensity might be significant in cases where certain narrowband spectra exert strong physiological responses at low fluence (e.g. Nagy *et al.*, 1993). In contrast, it is not recommended for HPS lamps to be dimmed below about 50% as this leads to changes in electrical properties, spectral shifts and accelerated lamp ageing (Correa *et al.*, 2002). Though LEDs show spectral shifts and efficiency droop depending on junction temperature (Senawiratne *et al.*, 2010), these are relatively small and manageable with adequate cooling and lower drive currents. When used correctly LEDs have a notably long lifespan. An extensive collation of manufacturer's data for various horticultural LED luminaires reveals a reported range between about 24000 and 53000 hours (within which 90% of the initial output is maintained) (Paucek *et al.*, 2020). For comparison, HPS lamps have a useable lifespan of about 16000 hours (Tähkämö *et al.*, 2016).

Perhaps the most conspicuous aspect of LEDs compared with traditional light sources is the variety of spectra which LEDs can provide: nowadays LEDs producing virtually any desired narrowband spectra are readily available as well as many 'white' light sources. The narrow emission spectra allow for a more specific choice of wavelengths than is possible with HPS lamps, and this flexibility in output wavelength allows for adjustment of the light source to maximise light absorption or penetration of the canopy and to manipulate photomorphogenetic effects. This makes LEDs unique amongst traditional lighting technologies and presents a potentially beneficial avenue for increased crop production if the spectral effects can be better understood and harnessed appropriately. However, horticultural LED lighting is still a relatively nascent technology and the combination of wavelengths to use to achieve optimal physiological responses and plant productivity for a given crop is still incompletely understood. At the leaf-level, it seems most reasonable to employ lighting which results in efficient photosynthesis since this should, all other things being equal, translate to high yields while potentially increasing energy efficiency of supplementary LED-lit greenhouses. An important caveat regarding this general assumption are the parallel spectral impacts on plant morphology which receive attention in section 1.8. of this introduction.

A metric of photosynthesis efficiency is its quantum yield which expresses the number of moles of CO_2 fixed in photosynthesis per moles of absorbed photons. This can be mathematically expressed as:

$$\Phi CO_2 = \frac{A}{\gamma}$$

where A is the rate of CO_2 assimilation per unit leaf area (usually expressed as $\mu mol\ m^2\ s^{-1}$), γ is the photon flux absorbed by a leaf (usually expressed as $\mu mol\ m^2\ s^{-1}$) and Φ_{CO2} is quantum yield. If γ is taken as the rate of photons incident on the leaf (rather than what is absorbed) then Φ_{CO2} is distinguished as quantum yield on an incident light basis. In this work the amount of light absorbed by a leaf is of interest as it provides an intrinsic measure of Φ_{CO2}. To understand what is meant by the term 'light-limited', it is necessary to examine the general response of CO_2 assimilation by leaves to incident light intensity or irradiance, referred to as a photosynthetic light-response curve. A non-rectangular hyperbola is commonly used to describe this response mathematically (Thornley, 1976):

$$A = \frac{\Phi CO_2.PPFD + A_{max} - \sqrt{(\Phi CO_2.PPFD + A_{max})^2 - 4\theta.\Phi CO_2.PPFD.A_{max}}}{2\theta}$$

where A is net photosynthesis, Φ_{CO2} is maximum quantum yield, PPFD is photosynthetic photon flux density, A_{max} is maximum (light saturated) photosynthesis and θ is a curvature factor.

A basic, generalised, light response is presented in Fig. 1 and shows three distinct regions. Apart from an area of potential non-linearity at very low light intensities (Kok, 1948; Sharp, 1984), the slope of the relationship between incident or absorbed irradiance and CO_2 fixation assimilation at low light intensities is so nearly linear that is treated as such and the slope of this line is the maximum (apparent) quantum efficiency for carbon dioxide fixation for a given set of measurement conditions (Fig. 1(A)). The measurement conditions are important since, apart from light intensity, a variety of environmental factors (e.g. carbon dioxide mole fraction, oxygen mole fraction, irradiance spectrum, temperature, etc.) exert a significant influence on maximum Φ_{CO2}. As the maximum Φ_{CO2} for a given set of measurement conditions occurs when CO_2 fixation is, practically, directly proportional to light intensity (i.e. light is the primary limitation to the rate of CO_2 fixation), photosynthesis under these conditions is said

to be 'light-limited'. At higher light intensities the response of A to PAR becomes curvilinear (Fig. 1(B)) which is due to the effect of underlying biochemical limitations to efficient light utilisation, including the dissipation of excess light energy (which cannot be used by photosynthesis) by protective non-photochemical mechanisms. At even higher light intensities photosynthesis becomes light-saturated and the addition of more light is not accompanied by any increase in assimilation (Fig. 1(C)). At this point the maximum assimilation rate, A_{max}, is reached. Though much attention has been given to light-saturated photosynthesis, light-limited Φ_{CO2} is a potentially very influential parameter since most leaves in the field (and greenhouse) are to some extent light-limited (Long and Drake, 1991; Long *et al.*, 1996) and the maximum quantum yield of Φ_{CO2} is a major factor affecting the assimilation rate under non-light-limited conditions. Φ_{CO2} is an even more relevant parameter in greenhouses in the Netherlands during wintertime when daylight levels are low. Supplementary LED lighting will typically contribute about 200 μmol m^{-2} s^{-1} at canopy level (Katzin *et al.*, 2021) and the contribution to total irradiance from daylight in winter can be about the same (depending greatly on weather conditions and light transmission of a given greenhouse). In these environments even leaves in the upper canopy may still be light-limited, or nearly so, during photoperiod extension by supplementary lighting. The majority of leaves within the canopy are likely to be light-limited to some extent, even in some instances where intra-canopy lighting is used.

This introduction proceeds further by exploring the light environment in natural and (supplementary-LED-lit) greenhouse environments. The relevance of the latter environment to (a) short-term light-limited photosynthesis at the leaf level and (b) whole-plant morphology will be discussed in relation to fundamental plant-light interactions. Finally, an approach towards resolving certain key questions is presented.
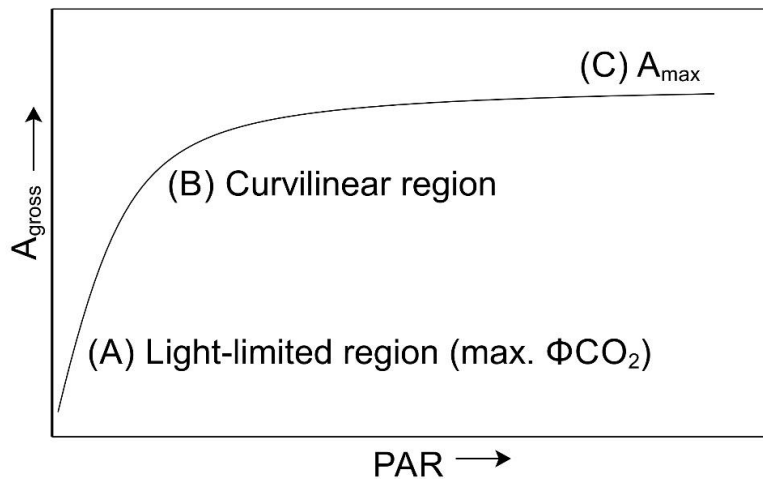
Figure 1: Generalised photosynthetic light response curve showing response of gross assimilation (A_{gross}) to light intensity (PAR) with three distinct regions: (A) Highly linear light-limited region occurring at low light intensities and coinciding with maximum Φ_{CO2} for a given set of measurement conditions, (B) curvilinear region indicating exit from light-limitation and onset of biochemical limitations to efficient light utilisation, and (C) Maximum assimilation rate (A_{max}) under high, saturating, light intensity.

1.2. Light in the natural environment

Practically all light on earth originates from the Sun. Other stars, even those which are visible to the naked eye, are far too distant to provide sufficient light energy to drive CO_2 fixation at the earth's surface (Raven and Cockell, 2006). Two properties of sunlight are especially relevant to plants given their dependence on light for survival:

(i) As an approximately blackbody emitter, the Sun does not emit all wavelengths with equal photon flux densities. As sunlight passes through the atmosphere, its spectrum is modified by atmospheric and meteorological conditions which attenuate different bands of the visible and non-visible spectrum through a variety of physical processes. For example, absorption by H_2O, O_2, O_3, and other gases to a lesser extent, create distinct bands of reduced intensity (Bird *et al.*, 1982). Light scattering, which depends on solar angle and atmospheric particulates, diffuses sunlight in a spectrally dependent way. Meteorological features such as clouds impose spectral changes to incident light through a combination of selective absorption and scattering (Bird *et al.*, 1982).

(ii) Over short distances where atmospheric scattering can be ignored, light travels in straight lines through space. This makes light a directional resource but one that changes with time and meteorological conditions. Plants, by virtue of their positioning, architecture and spectral

properties of light absorption and scattering will interact with the incident daylight, absorbing, transmitting and backscattering light within and from the canopy. The spectrum and intensity of light reaching lower leaves therefore varies considerably depending on the development of the canopy and the angular spectral distribution of the daylight irradiance. The impact of leaves on the spectrum of the light environment in the photosynthetically active and near-infra-red spectral regions occurs because green leaves absorb almost all light in the red and blue part of the spectrum but less green and even less far-red light. The result of this selective filtering is that leaves shaded by other leaves receive a considerably different spectrum than do unshaded leaves. The impact of leaf light absorption on light intensity incident on the lower leaves is self-evident given that a significant amount of light energy in the PAR region is absorbed as it passes through leaves. Physical factors such as wind routinely alter the position of photosynthetic surfaces, often only temporarily, causing a sunfleck: the intermittent exposure of a shaded leaf to daylight via a sunfleck can occur in a matter of seconds or less. Equally, in the much longer term, seasonal changes and the formation of canopy gaps affect light spectrum and intensity. The result of some or all of the factors listed here is that spectrum and intensity of daylight incident on a given leaf is highly variable across timescales ranging from seconds to days, weeks, and even months.

1.3. Light environment in greenhouses with supplementary LED lighting

The greenhouse with supplementary lighting can represent an even more complex and spectrally variable light environment than that of the natural environment. This is because daylight which penetrates through transparent greenhouse materials combines with the supplementary LED light. If supplementary LED lighting spectra were closely matched to daylight, the impact of supplementary LED lighting would likely be of little consequence beyond light intensity effects on photosynthesis (and plant morphology) which are relatively better understood than responses to complex spectral mixtures. An example of red and blue narrowband LED spectra, which are more or less ubiquitous spectral choices for LED supplementary lighting, are presented in Fig. 2 to show the contrast between these spectra and that of a daylight reference spectrum (the G173 spectrum, https://www.astm.org/Standards/G173.htm). As is evident from that figure, the single colour LEDs emit all their irradiance within a narrow band of wavelengths with an emission spectrum characterised by a defined peak and small full width at half maximum (FWHM). Depending on

the variety of narrowband LEDs used, this can result in many missing spectral regions which are otherwise present in daylight. Therefore, narrowband spectra comprise only a fraction of the wavelengths of daylight which span not only the PAR region (400-700 nm) but also spectral regions outside the range of PAR (daylight is commonly defined to range between 280 to 3000 nm). These spectral 'gaps' where spectral region(s) are deficient, can, nonetheless, have impacts on photosynthesis and photomorphogenesis. While the presence of some large spectral 'gaps' may have no detrimental impact on plant function others may, in specific cases, be detrimental. For example, when plants are grown under narrowband red light alone, several photosynthetic and morphological aberrations develop, including suppressed Fv/Fm, low A_{max}, and unresponsive stomata (Hogewoning *et al.*, 2010a; Trouwborst *et al.*, 2016). The addition of narrowband blue light to this red light has been shown to eliminate these aberrations leading to normal functioning of photosynthesis (Hogewoning *et al.*, 2010a; Miao *et al.*, 2019). Spectral 'gaps' in supplementary lighting may however be of less relevance given the presence of daylight in the greenhouse for at least some of the photoperiod. Although other supplementary lighting technologies such as HPS lamps also produce a greatly different spectrum to that of natural daylight, the properties of narrowband LED emission make LEDs unique lighting sources in a horticultural context.
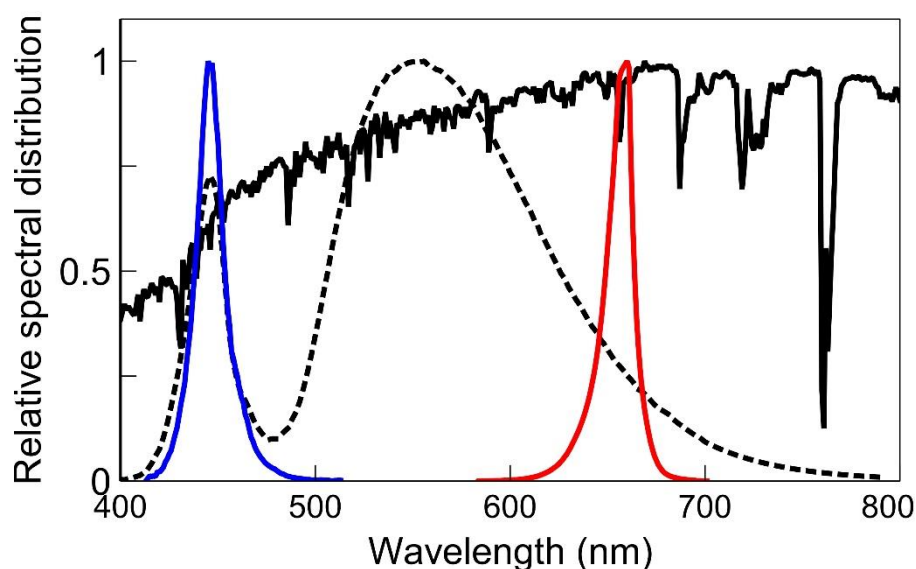

Figure 2: Relative spectral distributions of example LED spectra compared with that of a standard daylight spectrum (solid line; G173, https://www.astm.org/Standards/G173.htm) shown for comparison. Narrowband red (peak wavelength = 660 nm) and blue (peak wavelength = 445 nm) LED spectra are shown by their respective colours and a 'warm white' white LED spectrum is shown by the dashed line.

Even broadband white LEDs, including those which produce an irradiance which visually resembles daylight, produce, in most cases, a markedly different spectrum to that of actual daylight. Figure 2 also shows how the relative spectral distribution of a typical white LED (dashed line) differs considerably from that of the daylight reference spectrum. Note the peak at 450 nm in the white LED and deficiency in the longer-wave blue and far-red spectral regions. While several tuneable solar simulators comprising different narrowband LEDs have been reported (e.g. Fujiwara and Sawada, 2006; Kolberg *et al.*, 2011; Tavakoli *et al.*, 2021), these are generally intended for small-scale research or industrial testing applications. Therefore, the current state of horticultural LED lighting, and LED technology in general, limits supplementary LED spectra to 'unnatural' spectra which differ, typically greatly, from that of sunlight. This need not be a disadvantage of LED supplementary lighting; the benefits of a carefully selected narrowband irradiance (or combination of irradiances) may lead to better light-use efficiency by leaves compared with broadband sources and allow the ability to manipulate plant morphology in a potentially beneficial way.

An inevitable consequence of LED supplementary lighting and variable daylight levels is that the spectrum incident to a leaf can change dramatically, broadly along a continuum between these two spectra in various proportions. For example, a decrease in daylight intensity as twilight approaches inevitably leads to a spectrum which is increasingly skewed towards that of the LED spectrum until LED light is the only irradiance in the greenhouse. At sunrise the opposite occurs i.e. the spectrum gradually skews towards that of daylight. Increased cloud cover within a day, though also associated with its own spectral shift, can also skew spectrum in the greenhouse towards that of LED supplementary lighting and *vice versa*. How photosynthesis responds to short term spectral variability is one area of interest of this work.

1.4. Spectral dependency of quantum yield of CO_2 fixation

The spectral composition and variability of the light environment would be of less ecophysiological significance if leaves were able to utilise different wavelengths for photosynthesis with equal efficiency. However, intensive study on the wavelength dependence of Φ_{CO2} (on an absorbed light basis) over the past half-century has revealed the same general trend: a peak in the red region, a trough in the green region, and a shoulder in the blue region (McCree, 1972a; Inada, 1976; Evans, 1987). The underlying cause of this spectral dependency is broadly threefold. Leaf photosynthetic pigments are comprised of

chlorophylls a and b and carotenoids and there may also be non-photosynthetic pigments such as flavonoids. In photosynthesis it is necessary for the excited state formed when light is absorbed by photosynthetic pigments in either photosystems I and II to be transferred to chlorophyll a and then to a reaction centre. In the reaction centres of PSI and PSII the excited state of a chlorophyll a molecule is used to drive a chemical change, so stabilising some of the energy in the form of chemical energy. This process depends on the transfer of an excited state from one molecule to another. While chlorophyll to chlorophyll energy transfer takes place with near-perfect efficiency, transfer from a carotenoid molecule to a chlorophyll takes place with an efficiency of only about 70% (Croce *et al.*, 2001). As the carotenoids absorb light most strongly in the blue part (400-500 nm) of the spectrum (Lichtenthaler, 1987), light use efficiency in this spectral region is lower than in the red part of the spectrum where the only photosynthetic pigments that absorb light are the chlorophylls. In addition, non-photosynthetic pigments present in the leaf (e.g. flavonoids and anthocyanins) act as a sunscreen by absorbing light energy but not transmitting this energy to the photosynthetic apparatus. The flavonoids, in particular, absorb in the blue to green spectral regions and have no conspicuous effect on the colour of normal, healthy green leaves, but their absorption of blue and green light will also result in a loss of light-use efficiency in the blue-green spectral regions.

Another reason for the wavelength dependence of photosynthesis is due to the configuration of the electron transport chain which operates with two photosystems in series with one another. These photosystems – photosystem I (PSI) and photosystem II (PSII) – are distinct in terms of pigment composition and hence absorption spectrum. Whereas most wavelengths in the PAR region are preferentially absorbed by PSII, PSI absorbs far-red light more strongly. It is understood that CO_2 fixation is most efficient when electron transport between the photosystems is linear and that non-linear, cyclic electron flows, lower CO_2 fixation (Pfannschmidt, 2005). Linear electron transport depends on the photosystems operating at similar rates yet the intrinsic maximum efficiency of the photosystems is quite different. Out of 44 species from diverse taxa, the maximum (dark adapted) PSII efficiency (i.e. Fv/Fm) did not exceed 0.86 (Björkman and Demmig, 1987) whereas the maximum efficiency of PSI is close to 1 (Hogewoning *et al.*, 2012). These differences in photosystem efficiency mean that PSII must be comparatively more excited by absorbed irradiance. Therefore, what is meant

by 'balanced' excitation of the photosystems is excitation which leads to similar electron fluxes and linear electron transport (LET).

1.5. Photosynthetic acclimation to light spectrum

It follows that the variable and unpredictable nature of spectrum in the natural environment has the potential to disrupt optimal LET (i.e. equal potential electron transport rates through both photosystems). The importance of maintaining high photosynthetic efficiency is evidenced by the existence of mechanisms which attempt to restore balance following imbalanced excitation. These mechanisms are referred to as long- or short-term mechanisms based on the timescales over which they occur.

State transitions are a short-term acclimation mechanism which operates over a matter of minutes. The function of a state transition is to adjust the energy balance between PSII and PSI (Haldrup *et al.*, 2001; Allen, 2003). Although the precise operation of a state transition remains not fully understood, it is known that this energy rebalancing is achieved by biochemical adjustments which, according to the classical view, involves a fraction of potentially mobile LHCII which can associate with either PSII or PSI (Canaani and Malkin, 1984; Allen, 1992). Two states – state 1 and state 2 – reference these two putative docking positions in what is a bistable mechanism. A simplified representation of the classical state transition model is shown in Fig. 3. The association of this LHCII fraction with either photosystem is important since it physically alters the photosystem with which it associates, producing an increased light absorbing area and corresponding increase to light absorption by that photosystem. The impetus for this rearrangement is photosystem excitation imbalance, with the redox state of the PQ pool thought to play an important sensory and regulatory role in this regard. In state 1, mobile LHCII associates with PSII following dark-adaptation or when PSI is overexcited and PSII is rate limiting to electron transport. Reversal of this process towards state 2, such that mobile LHCII associates with PSI, occurs when PSII is overexcited and PSI is rate limiting to electron transport. Therefore, the docking location of the LHCII fraction is reciprocal to the rate limiting photosystem, increasing or decreasing photosystem absorption in a 'seesaw' manner in relation to one another. Mobility of the mobile LHCII fraction is granted by phosphorylation or dephosphorylation of mobile LHCII depending on whether state 1 or state 2 is induced. State 2 is induced by a reduced PQ pool which triggers the phosphorylation of Lhcb1 and Lhcb2 (two of the three LHCII apoproteins) and depends on

the STN7 kinase in plants and stt7 kinase in algae. The dephosphorylation process and return to state 1 in response to an oxidised PQ pool is less clear but believed to involve the phosphatases TAP38 and PPH1 (Pribil *et al.*, 2010; Shapiguzov *et al.*, 2010).
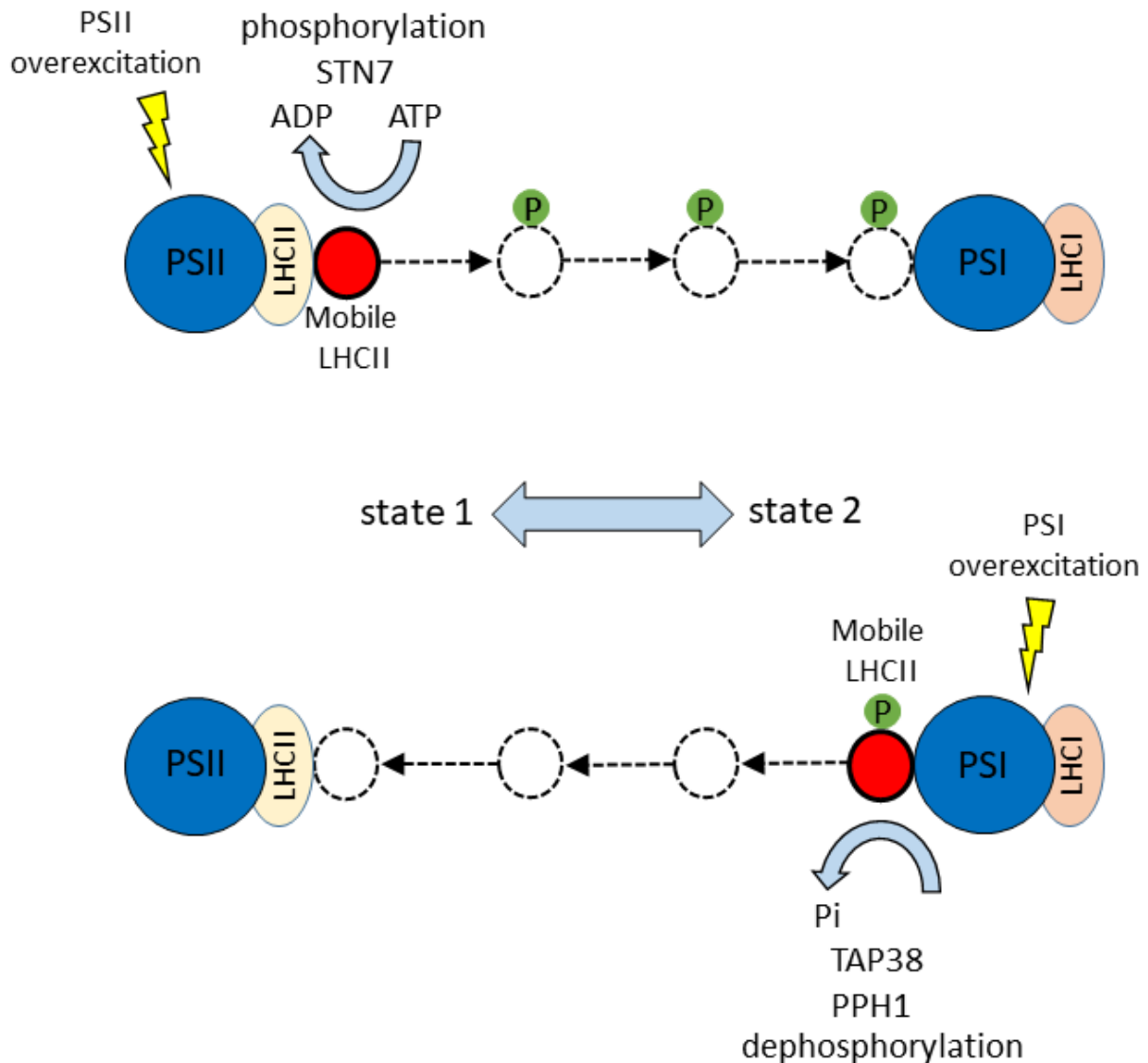

Figure 3: Simplified illustration of the classical state transition model. In state 1 a potentially mobile pool of LHCII is associated with PSII. Over-excitation of PSII creates a reduced PQ pool which triggers phosphorylation by the STN7 kinase (in plants) which grants mobility to the potentially mobile LHCII pool. This LHC pool associates with PSI, completing a transition to state 2. A return to state 1 can occur when an oxidised PQ pool caused by PSI over-excitation triggers the dephosphorylation of the potentially mobile pool involving phosphatases TAP38 and PPH1.

While the docking location of mobile LHCII in state 1 is generally accepted to be consistent with the classical model, the precise attachment point of mobile LHCII in state 2 is yet to be met with consensus. Some work has suggested that negligible or no mobile LHCII associates

with PSI in state 2 (Haworth and Melis, 1983; Ünlü *et al.*, 2014). Other findings have suggested that mobile LHCII is a part of PSI and migrates to PSII in state 1 (Galka *et al.*, 2012). What is known is that state transitions are accompanied by changes at the molecular level and these are routinely observable using chlorophyll fluorescence methods. For example, the transition from state 1 to state 2 is characterised by an initially high chlorophyll fluorescence yield which gradually quenches as the state transition proceeds (Allen, 1992). The transition to state 1 is marked by a gradual increase in fluorescence yield to a new steady level upon completion of the state transition.

Given the link between photosystem balance and Φ_{CO2} (Chow *et al.*, 1990), it was expected that if state transitions would correct imbalances between the photosystems then they should also increase Φ_{CO2} in leaves (Andrews *et al.*, 1993). However, those authors found that no increase in assimilation rate accompanied a state transition in leaves of various C3 species despite them showing the fluorescence hallmarks of this molecular reorganisation. Yet, in *Chlorella pyrenoidosa*, the green alga in which state transitions were discovered, state transitions were accompanied by an increase in oxygen evolution with similar kinetics to fluorescence yields (Bonaventura and Myers, 1969). While this finding is consistent with predictions of a higher Φ_{CO2} arising from improved photosystem balance, it does not resolve the apparent disconnect between changes at the thylakoid level and assimilation in higher plants. Despite this, the benefits of state transitions to plant fitness have been demonstrated in experiments where arabidopsis STN7 mutants (which cannot perform state transitions) were grown in alternating PSI and PSII light regimes (PSI light and PSII light referring to light which preferentially excites PSI and PSII, respectively). In these experiments the mutant accumulated less biomass (Bellafiore *et. al*, 2005) or produced half as much seed (Wagner *et al.*, 2008) as the wild type. In the same mutant grown in field conditions seed production was 19% less than in the wild type (Frenkel *et al.*, 2007) revealing a benefit of state transitions in the natural environment.

In the longer term, leaves tune their photosynthetic apparatus to their growth spectrum (Walters, 2005). This has been demonstrated by growing plants in different spectra and comparing photosystem stoichiometry (Chow *et al.*, 1990; Walters and Horton, 1994). In those studies, leaves grown in PSII light had a lower PSII:PSI ratio than leaves grown in PSI light. This involves the *de novo* synthesis of new proteins or the degradation of others to

compensate, at a molecular level, for an irradiance which would otherwise result in imbalanced excitation and reduced Φ_{CO2} (Chow *et al.*, 1990; Kim *et al.*, 1993).

1.6. The Emerson Enhancement effect

The Emerson enhancement effect (commonly referred to simply as enhancement) describes a phenomenon in which the photosynthetic rate of a leaf exposed to two (or more) irradiances together is greater than the sum of the rates for each of the irradiances when applied separately (Emerson, 1957). Instead of rates the same analysis can be made with reference to the quantum efficiencies of photosynthesis. The incidental discovery of this phenomenon by Emerson was initially made with 680 nm and 700 nm narrowband irradiances and was correctly interpreted to mean that another yet to be identified photosystem – PSI – operates in series with the then known PSII. In that instance, the 680 nm irradiance over-excited PSII whereas the 700 nm irradiance over-excited PSI. The combination of the two excited both photosystems more equally and thus led to a greater rate of oxygen evolution than expected based on the addition of the rates of oxygen evolution obtained when the 700 nm and 680 nm irradiances were applied on their own; this also results in an increased photosynthetic efficiency. Enhancement highlights the cooperative action of the series-configured photosystems and the importance of maintaining photosystem balance and hence efficient linear electron transport. On the other hand, enhancement also highlights the potential for losses in photosynthetic efficiency if this is not achieved.

While enhancement has been demonstrated using narrowband mixtures in algae (Govindjee and Rabinowitch, 1960; Myers and Graham, 1963; Senger and Bishop, 1969) and intact leaves (Canaani *et al.*, 1982), conflicting evidence exists for whether enhancement occurs in white light. Φ_{CO2} in four types of 'white' light was found to be approximately the same as predictions which assumed that each of the wavelengths was additive and independent i.e. no enhancement was found (McCree, 1972b). In cucumber, however, a 12% enhancement occurred in cucumber leaves in a simulated daylight spectrum (Hogewoning *et al.*, 2012) compared to the sum of a range of narrowband irradiances. An 18% enhancement was found in two species of green algae, *Ulva lactuca* and *Codium fragile*, subjected to irradiance from quartz iodine lamps (Dring and Lüning, 1985). Other broadband irradiances in that study yielded much smaller or negligible enhancement, suggesting that the spectral nature of broadband irradiance is significant in determining whether or not enhancement occurs with

broadband irradiance. On the other hand, it is difficult to reconcile this with the negligible enhancement found in the study by McCree (1972b) considering that a quartz iodine lamp was also one of the light sources used by McCree to test for enhancement.

1.7. Maximum quantum yield of Φ_{CO2} fixation

Given the focus of this work on spectral impacts on Φ_{CO2}, maximum Φ_{CO2} is a useful point of reference with which to quantify losses in light-use efficiency relate these to underlying biochemistry. The maximum quantum yield of photosynthesis has, however, been the subject of historical controversy (Hill and Govindjee, 2014) and a precise upper limit remains inconclusive. Whereas Emerson and Lewis (1941) reported a maximum quantum yield of oxygen evolution in *Chlorella pyrenoidosa* of about 0.10 (i.e. a minimum requirement 10 photons per O_2 molecule evolved), Warburg never deviated much from a value of 0.25 (i.e. a minimum requirement of 4 photons) (Hill and Govindjee, 2014). Theoretical calculations of maximum quantum yield based on an accounting of ATP and NADP assuming NAPDH supply is limiting and ATP demand can be met by the activity of linear electron transport alone suggests that this maximum lies around 0.125 (Singsaas *et al.*, 2001). It is important to note that this putative value applies only to low $[O_2]$ conditions in which photorespiration, which substantially reduces Φ_{CO2}, is practically eliminated. In reality Φ_{CO2} is routinely found to be less than 0.125 because meeting the demand for ATP requires the use of cyclic electron transport which competes with linear electron transport, or a reduction of NADPH supply to carbon dioxide fixation to drive non Calvin cycle sinks which 'parasitize' reducing power but then also make available more ATP for carbon dioxide fixation. These sinks include nitrite reduction, the export of reductant from the chloroplast via the Malate shuttle, and the Mehler reaction. It should also be noted that the quantum yield of O_2 evolution is slightly greater than CO_2 fixation as O_2 is evolved earlier in the photosynthetic process and subject to fewer of these non-assimilatory processes.

In practise, measured Φ_{CO2} values in C3 plants on an absorbed light basis are less than, but close to, 0.1, and therefore support the findings of Emerson and co-workers. In a survey of quantum yield in a wide variety of C3 plants, Long *et al.*, (1993) reported a maximum of value of 0.093. The same value was obtained in more recent work by Hogewoning *et al.* (2012) for cucumber leaves and a practically identical value (0.092) was reported for pea (Evans, 1987). There, nonetheless, remains variability in the measured quantum yield of C3 plants; in an

extensive meta-analysis Singsaas *et al.* (2001) attributed this to measurement error and concluded that maximum quantum yield varies little amongst diverse taxonomic groups. The similar values obtained amongst these studies is however somewhat problematic given the considerably different actinic spectra used amongst those studies. Whereas Hogewoning *et al.* (2012) found maximum Φ_{CO2} to occur under narrowband 640 nm irradiance, Long *et al.* (1993) and Evans (1987) both used broadband irradiance from quartz iodine lamps. While maximum Φ_{CO2} is well known to occur in the red region, the comparable values obtained in the broadband irradiance rich in less efficient wavelengths such as green and far-red (when used alone) is difficult to reconcile. One likely explanation is that potentially considerable enhancement occurred in work by Long *et al.* (1993) and Evans (1987). It is noteworthy that, as described earlier, significant enhancement also occurred in algae subjected to irradiance from quartz iodine lamps (Dring and Lüning, 1985).

1.8. Photomorphogenetic effects of growth irradiance

Though the focus thus far has been on spectral impacts on photosynthesis at the leaf-level, another conspicuous impact of spectrum involves a variety of potential morphological changes at the leaf and whole-plant levels. These so-called photomorphogenetic responses are mediated by different photoreceptors which sense light spectrum and intensity and translate these to physiological changes of adaptive and developmental significance (Smith, 1982, 1986). Light is therefore as much an information source about the ambient environment as it is a primary energy source for photosynthesis (Smith, 1986). A wide variety of leaf properties have been shown to be impacted by the spectrum of growth irradiance. These properties include leaf area (e.g. Wang *et al.*, 2016; Johkan *et al.*, 2012), leaf mass area (LMA; Wang *et al.*, 2021), and stomatal properties such as dimensions and density (Dai *et al.*, 1995; Savvides *et al.*, 2012; Wang *et al.*, 2016). At the whole-plant level internode spacing is often affected by spectrum leading to more or less elongation. For example, the predominantly red and far-red-absorbing phytochrome and blue-light-absorbing cryptochrome photoreceptors are known to affect plant compactness by promoting or inhibiting etiolation (Ahmad *et al.*, 2002; Nagashima and Hioksaka, 2011).

These morphological changes are important because they affect light penetration through the crop by changing the position and anatomical properties of photosynthetic surfaces. It is foreseeable that, for instance, a more compact plant morphology may create more self-

shading than a more open architecture. It cannot be assumed that an LED lighting spectrum which maximises photosynthesis at the leaf-level would lead to an optimal morphology for whole-plant light interception or whole-plant photosynthesis. Therefore, in understanding the impact of LED lighting on plant growth and development it is essential to examine not only the intrinsic photosynthetic effects of LED lighting but also the photomorphogenetic impacts which alter light distribution and absorption by the plant.

1.9. Temperature response of photosynthesis

The importance of light spectrum on light-limited photosynthesis has been the main focus of this introduction. However, as noted earlier, there are several environmental factors which impact this parameter of which temperature is one. A major impact of temperature on photosynthesis in C3 plants in air is photorespiration. Photorespiration is the fixation of O_2 in place of CO_2, leading to a decrease in Φ_{CO2} of about 30%, depending on leaf temperate and the concentrations of CO_2 and O_2 at the site of carboxylation (Björkman, 1966). As temperature increases, the specificity of Rubisco for CO_2 decreases, as does the solubility of CO_2 relative to that of O_2, leading to an increase in photorespiration with temperature (Ku and Edwards, 1978).

The majority of temperature work has focused on saturating, or non-light limiting, light intensities which has been given some justification by the frequent co-occurrence of high light and temperature in the natural environment (Sharkey and Zhang, 2009). Indeed, thin leaves exposed to direct sunlight heat up rapidly because of their low heat capacity and routinely exceed air temperature (Sharkey, 2005; Miller *et al.*, 2021). In contrast, the temperature of shaded leaves closely matches that of air temperature (Miller *et al.*, 2021). Comparatively little work has examined temperature responses of Φ_{CO2} at light-limiting intensities (e.g. Ehleringer and Björkman, 1977; Ku and Edwards, 1978; Yin *et al.*, 2014) and a comprehensive examination of the combined temperature sensitivies of light-limited Φ_{CO2}, Φ_{PSII} and Φ_{PSI} under these conditions is absent in literature. Given that most leaves are shaded and generally light-limited within the canopy, the general lack of temperature-related work on light-limited Φ_{CO2} presents a gap in our understanding of temperature effects on photosynthesis which could impact models of photosynthesis at the crop level. In greenhouses where a transition from HPS lighting to LED lighting occurs, an understanding of the temperature dependency of Φ_{CO2} is especially relevant given the reduced heat load

imposed by LEDs. For instance, knowing how much of the reduced heat load to compensate for with greenhouse heating is highly relevant to overall greenhouse energy efficiency and could significantly impact crop productivity.

1.10. Key questions of this study

A wide and ever-increasing variety of high-intensity broadband and narrowband LEDs are now available. This has spawned a LED horticultural lighting industry and the grower is afforded more lighting flexibility and control than ever before. For instance, LEDs can be used to produce spectra which are utilised efficiently for photosynthesis and photoreceptors can be targeted to produce desirable plant morphology (Zhen *et al.*, 2022) or to regulate flowering (e.g. Meng and Runkle, 2017). However, although LED lighting presents many opportunities, it is met with many accompanying unknowns. For example, while the wavelength dependence of photosynthesis has been intensively studied (Hogewoning *et al.*, 2012; Hoover, 1937; Inada, 1976; McCree, 1972a) it is not known how this dependence may change when narrowband irradiance is combined with daylight. Understanding spectral responses of Φ_{CO2} under these conditions is an important step towards the efficient use of LED lighting which itself uses valuable electrical energy and requires significant initial outlay.

The myriad of plant responses to even subtle spectral signals makes it difficult to disentangle and interpret fundamental spectral responses (Smith, 1986). This is especially relevant in the supplementary-LED-lit greenhouse in which a seemingly incalculable number of spectral compositions can occur. Nonetheless, there are some avenues to explore which can contribute to some general principles within the context of LED supplementary lighting:

(a) The conflicting findings for enhancement in broadband light reveals the need to rigorously explore broadband impacts on Φ_{CO2}, especially within the context of supplementary LED lighting, and to determine whether useful enhancement does occur under such spectral conditions. In this respect, comparatively few broadband spectra have been used to explore maximum Φ_{CO2} which is at odds with the significance of spectrum to this value.

(b) State transitions are expected to be an important acclimation mechanism in supplementary-lit greenhouses given the potential for short term spectral variability in these environments. An important focus of this thesis is to examine whether a relationship between state transitions and Φ_{CO2} does occur and, if so, to what extent.

(c) Since plant morphology is also known to be influenced by spectrum and itself affects light interception and absorbance at the whole-plant level, some attention is given in this work to the combined photomorphogenetic and photosynthetic impacts of supplementary lighting.

(d) The importance of temperature to Φ_{CO2} is explored given that it has a significant bearing on this parameter. Understanding this temperature response may assist with the calibration of spectral models which predict Φ_{CO2} at leaf and crop levels.

Several key questions emerge from the above and provide the stimulus for the present study. These are:

1.) What is the wavelength dependence of Φ_{CO2} with simulated natural spectra (sunlight or shade light) as background irradiance and how does this compare to that of narrowband irradiance alone?

2.) Does enhancement occur in the spectral combinations in (1) and how might the composition of broadband white light influence enhancement?

3.) What is the upper limit for quantum yield in practice and how does this compare with reported maxima?

4.) Is there a relationship between state transitions and Φ_{CO2}?

5.) What are the photomorphogenetic and photosynthetic impacts of blue light doses in a simulated daylight spectrum?

6.) What is the impact of temperature on underlying PSII and PSI photochemistry and how does this relate to Φ_{CO2}?

1.10. Approach of this study

The questions of this study, as outlined above, are approached as follows:

Chapter 2 addresses questions (1-3) by examining maximum Φ_{CO2} and underlying PSII and PSI photochemistry of leaves (produced in either an artificial daylight spectrum or an artificial shade light spectrum) in a total of 36 unique spectra comprising narrowband, broadband (artificial daylight or shade light), or combinations of narrowband and broadband irradiance. The occurrence of enhancement is tested for each spectrum by comparing predicted Φ_{CO2}

with measured Φ_{CO2}. The highest quantum yield obtained in this exhaustive spectral study is compared with that of other reports.

Chapter 3 addresses question (4) by probing for a relationship between state transitions and Φ_{CO2} in leaves produced under an artificial daylight and artificial shade spectrum. The use of two particularly extreme PSII and PSI spectra are used to induce state transitions while fluorescence yield and assimilation rate are measured simultaneously. The link between Φ_{CO2} and underlying photochemistry is discussed. An understanding of this short-term photosynthetic plasticity is relevant in instances where potentially sudden spectral changes can occur in greenhouses with supplementary LED lighting, but also in ecophysiological contexts.

Chapter 4 addresses question (5) by adopting a holistic approach which explores the combined photosynthetic and photomorphogenetic responses to blue light doses applied with an artificial daylight background. Quantum yields of CO_2 fixation, PSI, and PSII are examined together with A_{max}. Plant morphology is characterised and whole-plant light absorption is quantified using a ray tracing model. The impacts at leaf and whole-plant levels are discussed in relation to biomass accumulation.

Chapter 5 addresses question (6) by examining the temperature response of Φ_{CO2} and, spectroscopically, the yields of PSI and PSII. The impacts of measurement procedure on the perceived temperature response are highlighted.

Chapter 6 collates and summarises the key findings of experimental work. Suggestions are made on how intelligent lighting solutions could be implemented with efficient light use in mind and the findings are discussed in an ecophysiological context.

CHAPTER 2

Greater than the sum of the parts: Revisiting the Enhancement Effect in Photosynthesis using simulated sun- and shade-light

Abstract

The Enhancement Effect describes the phenomenon in which two irradiances, when applied to a leaf simultaneously, result in a greater rate of CO_2 fixation than the sum of rates obtained using each irradiance separately. While enhancement has been routinely demonstrated to occur in narrowband mixtures, limited and conflicting evidence exists for enhancement in leaves exposed to artificial broadband light. Additionally, the use of more natural spectra is lacking in enhancement studies and limits the understanding of the ecophysiological significance of the enhancement phenomenon. We grew tomato leaves under simulated sunlight ('SUN') or shade-light ('SHADE') and measured action spectra using 17 narrowband wavelengths with or without SUN or SHADE irradiance as background irradiance. Φ_{CO2} was measured for each of the 53 unique spectra and enhancement quantified for the broadband spectra. The light use efficiencies for PSII and PSI electron transport and the regulation of PSII were also measured to account for changes in the yield of CO_2 fixation at the level of electron transport. While no enhancement was observed in SUN-grown leaves under SUN, a 23% enhancement occurred in SHADE-grown leaves under SHADE. In SHADE-grown leaves enrichment of SHADE irradiance with wavelengths <700 nm resulted in enhancements of between 17 and 27%, and an enhancement of 76% at 720 nm. In SUN-grown leaves, enrichment of SUN irradiance with wavelengths <680 nm resulted in little to no enhancement although enhancement of 4.7, 7.6 and 46% occurred at 680, 700 and 720 nm, respectively. The participation of far-red light in broadband enhancement may be of ecophysiological significance given that the majority of leaves are shaded by other leaves and thus photosynthesize in a far-red enriched irradiance.

Taylor, C.R., van Ieperen, W. and Harbinson, J. To be submitted.

Introduction

The photosynthetically active wavelengths used by plants are commonly defined to extend over a narrow wavelength region (400 to 700 nm) of the total shortwave solar radiation that reaches the Earth's surface, which itself is generally defined as ranging from 280 to 3000 nm. This definition of 'photosynthetically active' is a practical definition rather than one based on the biophysical limits of photosynthesis. Extensive study of the spectral dependence of photosynthesis in leaves on an absorbed light basis has shown red light drives photosynthesis most efficiently followed by short-wave blue light (400 - 420 nm), and that there is a minimum in the long-wave blue region at around 480 - 500 nm (Hogewoning *et al*. 2012; Inada, 1976; McCree, 1972a). Invariably, photosynthetic efficiency falls sharply above ~680 nm and rapidly diminishes to zero as wavelength increases in a phenomenon first identified in *Chlorella* and termed the 'red drop' (Emerson and Lewis, 1943).

Losses in photosynthetic efficiency relative to the highest efficiencies encountered in the red spectral region reveal underlying limitations to efficient light utilization. Some of these losses are accounted for by the spectral absorption profiles of pigments which either do not participate in photosynthesis (e.g. non-photosynthetic pigments such as anthocyanins or flavonoids) or which transfer absorbed light energy with reduced efficiency to chlorophyll molecules (such as carotenoids) (Croce *et al.*, 2001). It is especially significant that photosystems I and II (PSI and PSII) differ in their pigment composition and thus have different spectral absorbances. The predominant form of electron transport in C3 plants is linear electron transport (LET) and depends on the cooperative action of photosystems I and II working in series. Since the two photosystems have different light-absorption spectra, spectral composition of irradiance can result in the over-excitation of one photosystem or the other. Furthermore, maximum light-use efficiencies for electron transport differ between PSI and PSII and this must be taken into account when considering the balance between the photosystems: whereas PSI operates with an efficiency of ~0.99, PSII is less efficient with a maximal operating efficiency of about ~0.9 (Pfündel, 1998). Optimal operation of LET requires that potential electron transport rate through each photosystem is the same; if the potential electron transport rate through one photosystem is greater than that through the other, the system with excess capacity will be limited by the other and lose efficiency until the capacities are in balance. The operation of cyclic electron transport (CET) around PSI could also result in

limitation to PSII. Under light-limiting conditions the limitation of one or the other photosystem by the other can result in the loss of overall photosynthetic light-use efficiency at the level of leaf assimilation (Hogewoning *et al.*, 2012). Clearly, balanced photosystem turnover and balanced activity of CET and LET is the product of numerous factors which cannot be viewed in isolation.

Whereas sunlight over-excites PSII more strongly than PSI, far-red-enriched light (a feature of light in the shade since leaves absorb far-red light very weakly) excites PSI considerably more strongly than PSII. The spectral qualities of light which preferentially excite PSI or PSII have become termed simply as PSI or PSII light (Chow, 1990). In situ, many factors can affect the spectrum of light a leaf receives. A large percentage of foliage photosynthesizes for a large part of its lifespan below other leaves in almost permanent foliar shade. Short-term spectral variations may also occur e.g. due to cloud cover and within foliage due to sun-flecks or more gradually due to changes in solar angle over the course of a day (Holmes and Smith, 1977). These changes in spectrum can result in changes in the balance of excitation of PSI and PSII.

The importance of LET and high photosynthetic efficiency is evidenced by the ability of leaves to acclimate to the spectrum in which they were produced in a quest to maintain LET. For example, leaves produced under PSI light have a greater PSII:PSI ratio than leaves produced under PSII light whereas this ratio is lower in leaves produced in PSII light (Chow *et al.*, 1990; Walters and Horton, 1994; Hogewoning *et al.*, 2012). The result of this acclimation is that leaves grown in PSI light have a higher quantum yield of CO_2 fixation than PSII-grown leaves subjected to PSI light, and the opposite is true (Chow *et al.*, 1990). Even after full leaf expansion has been achieved, the plasticity of the photosynthetic apparatus arising from acclimatory mechanisms further highlights the importance to the plant of maintaining a high photosynthetic efficiency. These acclimatory mechanisms have been divided into short-term and long-term mechanisms based on the duration which they require to take effect. The short-term state transitions occur within minutes in response to over-excitation of one of the photosystems and involve the relocation of a mobile fraction of LHCII from PSII to PSI, or vice versa, to increase cross-section and absorption of the rate limiting photosystem. State transitions have recently been shown to have a direct beneficial effect on photosynthetic efficiency through this structural reorganisation which at least partially mitigates excitation imbalance (Taylor *et al.*, 2019). A longer term acclimation mechanism occurring in the order

of days is the adjustment to the stoichiometry of PSI and PSII, alluded to earlier, which involves the synthesis and degradation of various PSII and PSI proteins (Kim *et al.*, 1993).

Since it is known that balanced potential electron transport through PSII and PSI is a prerequisite for high photosynthetic efficiency, it follows that spectral manipulations which better balance the photosystems will result in improved photosynthetic efficiency. This effect, eponymously termed the Emerson enhancement effect (Emerson, 1957; Emerson, 1958; hereafter referred to as 'enhancement') was discovered by presenting cells of *Chlorella pyrenoidosa* with PSI (700 nm) and PSII light (680 nm), applied separately and simultaneously; cells subjected to PSI and PSII light simultaneously showed a greater rate of CO_2 fixation than predicted from the sum of the rates for each of the constituent irradiances i.e. the rate of CO_2 fixation was greater than the sum of the parts. The majority of subsequent early work on enhancement also used narrowband irradiances to explore and characterise enhancement further in algal cells (e.g. (Govindjee and Rabinowitch, 1960; Myers and Graham, 1963; Senger and Bishop, 1969), isolated chloroplasts (Govindjee *et al.*, 1964) or intact leaves (Canaani *et al.*, 1982). Though the use of narrowband irradiances simplified the characterization of enhancement in these early studies, comparatively little attention was given to enhancement in white light. In spinach chloroplasts the addition of a range of narrowband red and far-red wavelengths (678 nm – 740 nm) to background white light revealed significant enhancement in terms of NADP reduction in the far-red region, increasing up to the longest narrowband wavelength used (Govindjee *et al.*, 1964). The significant 'enhancement' observed by those authors when using supplementary wavelengths as long as 740 nm indicates the importance of far-red light well outside the PAR region for which Φ_{CO2} is zero (or nearly so) when those wavelengths are used alone (e.g. in cucumber leaves measured at 736nm; Hogewoning *et al.*, 2012). Far-red light (loosely defined as wavelengths >690nm) is an important spectral region as it overexcites PSI considerably more than all shorter PAR wavelengths and is bound by two biophysical constraints relevant to photosystem balance and enhancement: sharply increasing absorption of PSII relative to PSI at shorter wavelengths and sharply diminishing absorption at longer far-red wavelengths (Laisk *et al.*, 2014). Given these biophysical properties of far-red light it is reasonable to expect that by stimulating PSI photochemistry far-red could be a common feature of not only 'narrowband' enhancement but also of 'white light enhancement'.

An investigation using leaves of selected crop species and four types of 'white' light, including a spectrum rich in far-red light from a quartz-iodine lamp, concluded that enhancement could be ignored in white light (McCree, 1972b). However, enhancement in white light has recently been revisited with emphasis on the role of far-red light in this phenomenon (Zhen and van Iersel, 2017; Zhen and Bugbee, 2020). In lettuce leaves subjected to 400 μmol m^{-2} s^{-1} cool white LED light, the addition of 60 μmol m^{-2} s^{-1} far-red light (with peak wavelength of 735 nm) resulted in comparable photosynthetic rates to when 60 μmol m^{-2} s^{-1} of the same white light was added (total PAR of 460 μmol m^{-2} s^{-1}), despite the far-red light leading to lower total absorption by the leaf (Zhen and Bugbee, 2020). This led those authors to conclude that the added far-red photons were utilized with greater efficiency than the added white light on an absorbed light basis, indicating that significant enhancement had occurred. The quantitative assessment of the role of far-red light (or any other spectral region) in enhancement is easier when using strictly light limiting intensities on an absorbed light basis. Such an approach avoids spectral additions in non-linear portions of the light response curve as well as differences in absorption between added light and background light which together create difficulties in quantifying potential enhancement. Also of importance is the spectral composition of the white light spectrum used. Notably absent in enhancement literature is the use of more natural sun- and shade-like white spectra. This limits the understanding of the potential significance of enhancement in natural ecophysiological contexts, as well as in high-tech greenhouses with supplementary LED lighting. To gain insight in this regard, we test for enhancement in simulated sun- and shade-light using leaves produced under these same spectra to create more natural, yet contrasting, spectral acclimation histories. Furthermore, unlike previous enhancement studies where action spectra have been produced using a far-red background (Govindjee and Rabinowitch, 1960; Myers and Graham, 1963), we produce an action spectrum using 17 narrowband wavelengths with a sun- or shade-like spectrum as background irradiance. This spectral diversity allows for rigorous testing for enhancement in broadband irradiance and provides clues as to which spectral region(s) may be influential in enhancement for these more natural spectra.

Materials and Methods

Apart from actinic light and measurement procedure the methods used in this study are described in detail in Taylor *et al.* (2019). Here we provide a comparatively brief description.

Plant material, growth light and climate conditions

Tomato seeds (cv. Moneymaker) were sown in rockwool blocks (Grodan, Roermond, The Netherlands) and grown in tents (80 cm × 80 cm × 50 cm) made of opaque plastic sheet in a climate-controlled room (16-h photoperiod, 20 °C air temperature, 70% relative humidity). The rockwool blocks were flooded with Hoagland solution for 15 minutes daily. Two growth spectra, described in Hogewoning *et al.* (2012), were used to produce leaves that were acclimated to a sun- or shade-like light spectrum: a sulfur plasma lamp (Plasma International, Muhlheim am Main, Germany) provided the sun-like spectrum whereas quartz-halogen lamps filtered with a plastic-film filter (Full C.T. blue, Lee Filters, Hampshire, U.K.) provided the shade-like spectrum. The sun-like spectrum comprises more short PAR wavelengths than the shade-like spectrum which is rich in far-red. Growth PAR was maintained at 100 µmol m^{-2} s^{-1} at the apical bud until the third leaf began to develop at which point the third leaf became the reference point for all subsequent light intensity measurements. Leaf temperature was controlled at 22.5 °C by adjusting the flow rate of ambient air into the tents and monitoring leaf temperature by means of a thermocouple appressed to a leaf. Fully expanded leaves were used for measurements at 30-35 days after sowing.

Light during photosynthesis measurements

Actinic light during all photosynthesis measurements comprised 17 narrowband spectra and simulated sun- and shade-light (Fig. 1), including combinations of each narrowband spectrum with each of the broadband spectra in a 1:1 ratio on an absorbed light basis. The 17 narrowband spectra (Fig. 1A) had nominal peak wavelengths of 406 nm, 427 nm, 445 nm, and from 460 to 720 nm in 20 nm increments. These were produced using a lab-built light source comprising fixed and interchangeable LEDs on an optical bench. Light from a high power white LED was filtered using bandpass filters to produce the following narrowband spectra: 460 nm with 10 nm full width at half maximum (FWHM; Thorlabs, Newton, NJ, USA) and 500 to 680 nm with 10 nm FWHM (Thorlabs with the exception of 500 and 520 nm where Edmund filters were used; Edmund, USA). In addition to the bandpass filters used in combination with the white LED, a Calflex filter and one of four dichroic filters (DT blue, DT green, DT Yellow or DT Red as appropriate, Balzers, Liechtenstein) were used for thermal management. The remaining narrowband spectra were produced using single-colour LEDs in combination with bandpass filters: UV LEDs for 406 nm with 15 nm FWHM (Semrock, Rochester, NY, USA),

420 nm LEDs (SemiLed, Taiwan, ROC) for 427 nm with 15 nm FWHM (Semrock), 440 nm LEDs for 445 nm with 15 nm FWHM (Semrock), 480 nm LEDs (Luxeon Rebel) for 480 nm with 10 nm FWHM, 700 nm LEDs (Roithner Lasertechnik, Vienna, Austria) for 700 nm with 10 nm FWHM (Thorlabs) and 720 nm LEDs (Roithner) for 720 nm with 10 nm FWHM (Thorlabs). No CO_2 fixation was detected when using 736 nm light and therefore longer wavelengths were not used. A xenon lamp (Newport Instruments, USA) was used to simulate a sunlight spectrum modelled on a standard ASTM spectrum (Fig. 1B; G173, ASTM, 2003). The xenon lamp was also used to simulate a shade spectrum (Fig. 1C) by combining it with sheet filters ('Yellow' and 'Cold Blue'; Lee Filters, Hampshire, UK). Although the simulated sun- and shade-light spectra were matched as closely as was possible to their respective natural reference spectra, they are deficient in the shorter wavelengths of the blue region and were cut off above about 740 nm. In the case of the shade spectrum a further difference is a left-shifted far-red peak. For these reasons neither spectrum can be strictly defined as either sunlight or shade light. However, the spectra are distinctly sun-like or shade-like and for the purposes of this work these spectra are referred to as 'SUN' and 'SHADE'.

Gas exchange

A custom two-part chamber was used for gas exchange measurements. The gas mix comprised 400 µmol mol^{-1} CO_2, 210 mmol mol^{-1} O_2 and 18.8 mmol H_2O with the remaining fraction being N_2. The gas stream was split into reference and sample streams and a LI-7000 CO_2/H_2O analyser (LI-7000, Li-Cor, Nebraska, USA) analysed each stream. Sample and reference streams were routinely cross-checked before measurement using nitrogen (i.e. 0 µmol mol^{-1} CO_2) and a reference gas comprising 391 µmol mol^{-1} CO_2. Analyzers were further cross checked against another calibrated gas analyser (Li-6400, Li-Cor, Nebraska, USA) by placing each stream in series with the analysers in the Li-6400 head. CO_2 readings agreed amongst the analysers to within 0.1% across a range of CO_2 concentrations. Flow rate was maintained at 250 cm^3 min^{-1} using a precision flow controller, and another flow meter, which was found to measure to within 0.2% of the flow controller controlling flow to the chamber, was used to test for leaks by monitoring the exhaust flow. Leaks were reliably eliminated by using a quick-set non-toxic silicone rubber (Body Double, Smooth-on, Macungie, USA) between the abaxial leaf surface and the lower chamber seal. Temperature was maintained at 22.5 °C and monitored using a calibrated non-contact temperature sensor (Micro Irt/c,

Exergen, Watertown, USA) mounted directly below the leaf on a PCB. Leaf temperature was controlled by circulating water from a temperature-controlled water bath through an internal channel in the upper and lower leaf-chamber halves.

Actinic light measurement

Actinic light was delivered to the chamber by a split optical fibre with an output diameter of 25mm (Schoelly, Denzlingen, Germany). A 15 cm long transparent acrylic rod on the output of the fibre homogenized the light sources. A 3 mm acrylic rod coupled a sample of light within the chamber to a photodiode (OSD15-5T, Centronic, Croydon, U.K.) connected to a transimpedance amplifier from which a voltmeter was used to measure intensity. For calibration of the chamber irradiance sensor, a custom lab-built irradiance sensor was made. This comprised 13 evenly and concentrically spaced photodiodes (TEFD4300, Vishay, Coatesville, PA, U.S.A.), housed within a nylon body with a nylon optical window for diffusion, connected to a transimpedance amplifier and, in turn, a voltmeter. This sensor has two main advantages over conventional irradiance sensors by sensing light over the entire chamber area and having a flat, basic spectral response over the range of wavelengths used. Once calibrated using a calibrated CL500a illuminance spectrophotometer (Konica Minolta, Japan) as calibration reference and 22 narrowband irradiances between 380 and 740 nm, the voltage output of the irradiance sensor was consistently found to translate to an intensity within 3.5% (typically <2%) of the output of the spectrophotometer for all the spectra used in this study. The higher reflection caused by the white optical window on the lab-built irradiance sensor (which would reflect more light than a leaf onto reflective chamber walls and back onto the sensor) had the potential to underestimate irradiance intensity measurements within the chamber. A correction factor was determined for each spectrum by comparing the difference in irradiance intensity collected by a glass fibre (connected to a USB2000 spectrophotometer; Ocean Optics, Duiven, The Netherlands) inserted through a nylon window and, separately, a tomato leaf.
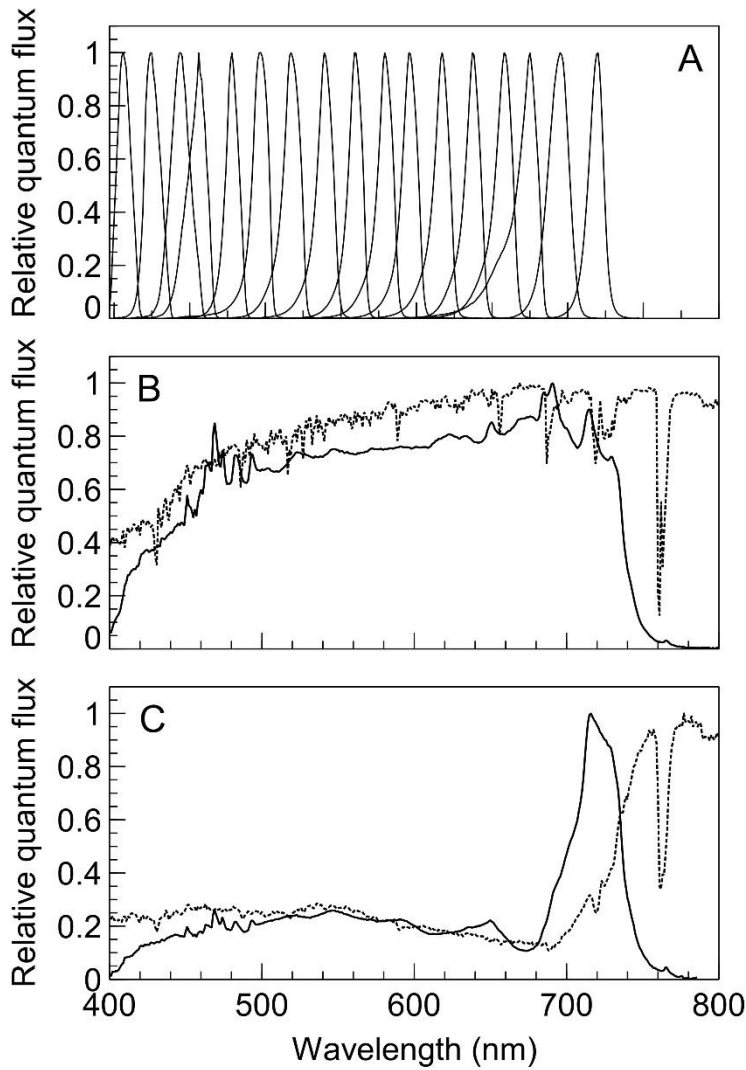
Figure 1: Relative quantum fluxes of the narrowband spectra (A), simulated sun spectrum (B, solid line), and simulated shade spectrum (C, solid line) used as actinic light for photosynthesis measurements. Actinic spectra also included the combination of each narrowband spectrum with either the simulated sun or shade spectrum in a 1:1 ratio on an absorbed light basis. Dotted lines in (B) and (C) represent, respectively, a standard solar spectrum (G173, ASTM, 2003) and a shade spectrum measured beneath a deciduous canopy during summer in the Netherlands.

Chlorophyll fluorescence

Chlorophyll fluorescence was determined using a modulated system by measuring the fluorescence produced by a red measuring beam modulated at approximately 1 kHz (the frequency was adjusted to minimise noise) with an intensity of 0.5 µmol m^{-2} s^{-1} (or 1 µmol m^{-2} s^{-1} for improved signal to noise ratio when 720 nm or SHADE was used). The output of the optical fibre which delivered the measuring beam to the chamber was filtered with a

hot mirror to prevent near-infrared fluorescence produced by the glass-fibre from entering the leaf chamber. A saturating light pulse (12000 µmol m^{-2} s^{-1}) was generated using three high power red 'Phlatlite' LEDs (Luminus Devices, Sunnyvale, USA) connected to a timer which pulsed the LEDs for 1 second. Three photodiodes (G1736, Hamamatsu, Hamamatsu city, Japan), each filtered with an RG-9 filter (Schott, Mainz, Germany) and spaced evenly on a PCB of the sensor cluster below the leaf were used to detect fluorescence. A lab-built phase-sensitive detector and amplifier amplified fluorescence signals and these signals were recorded using a data logger (National Instruments) with a 10 Hz low-pass filter on its input to limit bandwidth. All fluorescence parameters were determined and calculated according to Maxwell and Johnson (2000).

Φ_{PSI} estimation from 820 nm absorbance changes

Φ_{PSI} was estimated following the calculation of Baker *et al.* (2007) using changes in 820 nm absorption (Δ820 nm). An LED (ELJ-810-228B, Roithner Lasertechnik, Vienna, Austria) whose output was filtered was used to produce the 820 nm signal. This signal was modulated at 455 KHz and coupled to the chamber by means of a glass fibre. Three silicon photodiodes (BPW 34 FA, Osram, Regensburg, Germany) connected to a selective amplifier containing a 455 kHz ceramic filter (Murata, Kyoto, Japan) were used to recover signal which was recorded by a data recorder. Each Δ820 nm measurement, taken at each light step, involved first determining the 820 nm signal in the light and then in darkness. Obtaining darkness involved interruption of the xenon lamp and/or switching off of the LED(s) simultaneously to accommodate instances where both light sources were in use. This was achieved using a mechanical shutter affixed to the output of the xenon lamp which also switched off the LEDs electronically upon closure. Upon reaching steady state signal in darkness a far-red pulse of ca. 10 s in duration was applied to oxidise P700 centres during which a 5 ms pulse of saturating irradiance was also applied to oxidise any remaining unoxidised PSI centres (Kingston-Smith *et al.*, 1999).

Chlorophyll a/b ratio

Chlorophyll a/b ratio was determined using the method of Croce *et al.* (2002). Briefly, an extract was prepared for SUN- and SHADE-grown leaves using buffered 80% acetone. The

absorption spectrum of the extract was fitted with that of known absorption spectra for individual pigments to determine chlorophyll a/b ratio.

Measurement procedure

Actinic light treatments during photosynthesis measurements

In total 70 combinations of actinic light spectra × growth light spectra can be distinguished: SUN-grown leaves subjected to (1) 17 different narrowband spectra, (2) 17 mixtures of each of the 17 narrowband spectra in a 1:1 ratio with 'background' SUN-light on an absorbed PAR basis, and (3) to 'background' SUN-light only. Identical actinic light treatments were used for SHADE-grown leaves except with SHADE-light in place of SUN-light.

For each of the 70 actinic light × growth-light acclimated leaf combination measurements, five light-limiting irradiances ranging from about 10 to 50 µmol m^{-2} s^{-1} (on an absorbed light basis) were used to construct light-limited slopes. This approach is different to the approach often used in enhancement studies where single-point assimilation rates are measured. However, the approach used here gives a more reliable determination of Φ_{CO2}, which is of interest in this work, as it better accounts for respiration in the light and dark which can be difficult to estimate accurately. Light intensities were selected to avoid non-linearity at either low light intensities (Kok, 1948) or at higher light intensities. Leaves were dark-adapted for 20 minutes to determine dark-adapted Fv/Fm and the rate of dark respiration, estimated from CO_2 efflux. Light intensity was subsequently increased incrementally, allowing photosynthesis to reach steady state at each intensity (during ca. 8 minutes) at which point CO_2 and H_2O fluxes were logged over 30 s at a sample rate of 1Hz. The mean of these records at each light intensity was used to calculate the rate of photosynthesis according to Farquhar *et al*. (1980). Chlorophyll fluorescence and Δ820 nm were measured at each light step immediately after the CO_2 measurement had been taken. At the end of each light response curve, dark respiration in the light was again estimated after 6 minutes of darkness had elapsed.

The experiment commenced by first completing all narrowband measurements on SUN-grown leaves followed by all narrowband measurements with SUN as background irradiance (also using SUN-grown leaves). Lastly, measurements on SHADE-grown leaves were taken in the same order as for SUN-grown leaves. Narrowband spectra were applied in random order including when a background irradiance was used. Mindful of the potential for acclimation of

leaves over the two days it took for a complete set of measurements, each day commenced with measurement of Φ_{CO2} using SUN or SHADE to test for drift of biological (or non-biological) origin. As differences were negligible Φ_{CO2} for SUN and SHADE was taken as the mean of the two measurements. In an attempt to help prevent acclimation, 50 µmol m^{-2} s^{-1} of SUN or SHADE on an absorbed light basis (corresponding with growth spectrum) was also applied between different measurement spectra until gas exchange had stabilized.

Data analysis and statistics

Measurements were repeated three times using plants from a staggered sowing schedule and the data from each repetition were treated as independent. Φ_{CO2} was determined from the slope of a linear regression of the response of CO_2 fixation to light intensity. The method of (McCree, 1972b) was used to test for enhancement. This involved the linear interpolation between the 17 Φ_{CO2} values obtained for the narrowband irradiances so that each wavelength (in nm increments) had an associated Φ_{CO2} value. These values were weighted according to the relative spectral intensity of the spectrum of interest by multiplication, the product of which was summed to predict Φ_{CO2} in the absence of enhancement. An Enhancement factor (E) was calculated as the ratio of measured:predicted Φ_{CO2}; a value ≤1 indicates either no enhancement or negative interference occurred, whereas a value >1 implies enhancement did occur. T-tests were used to compare predicted and measured Φ_{CO2}. A two-way ANOVA was used to test for interaction between leaf type and enhancement. All analysis was performed in Microsoft Excel 2013.

Results

The two growth spectra (SUN and SHADE) were chosen to produce leaves with different acclimation histories. The SHADE growth spectrum produced two of the classical features associated with growth in the shade: plants were significantly more etiolated than SUN-grown plants and the chlorophyll a/b ratio in leaves of SHADE-grown plants was 2.89 compared with that of 3.08 in SUN-grown plants. Leaf absorptance tended to be slightly lower in SHADE-grown leaves than in SUN-grown-leaves, and was zero in both leaf types at about 728 nm (Fig. 2).

The response of CO_2 fixation to light was highly linear between 10 and 50 µmol m^{-2} s^{-1} in the PAR spectral region ($R^2 > 0.99$). Only at 720 nm was the linearity of the light response less

strong ($R^2 \leq 0.98$) due to lower rates of assimilation and hence a lower signal to noise ratio of the measurements of assimilation. Quantum yields for CO_2 fixation (Φ_{CO2}) on an absorbed light basis for SUN-grown and SHADE-grown leaves subjected to narrowband light alone were greatest in the red region with a shoulder at 406 nm to 440 nm and a trough at 500 nm (Fig. 3). A sharp drop in Φ_{CO2} occurred above 680 nm. Although Φ_{CO2} was generally comparable for SUN- and SHADE-grown leaves in the blue and blue-green region (i.e. ≤520 nm), the effect of growth spectrum on wavelength dependence of Φ_{CO2} was marked at wavelengths of 540 nm and greater. In this respect, Φ_{CO2} of SHADE-grown leaves was lower than that of SUN-grown leaves between 540 nm and 680 nm whereas at wavelengths >700 nm Φ_{CO2} was greater in SHADE-grown leaves. Maximum Φ_{CO2} (absorbed light basis) in SUN-grown leaves was 0.090, occurring at 680 nm, while that of SHADE-grown leaves was 0.085, occurring at 640 nm, though the difference between Φ_{CO2} at 680 and 640 nm was small for both leaf types. The minimum Φ_{CO2} within the PAR region was 0.064 in SUN-grown leaves and 0.063 in SHADE-grown leaves, occurring at 500 nm.
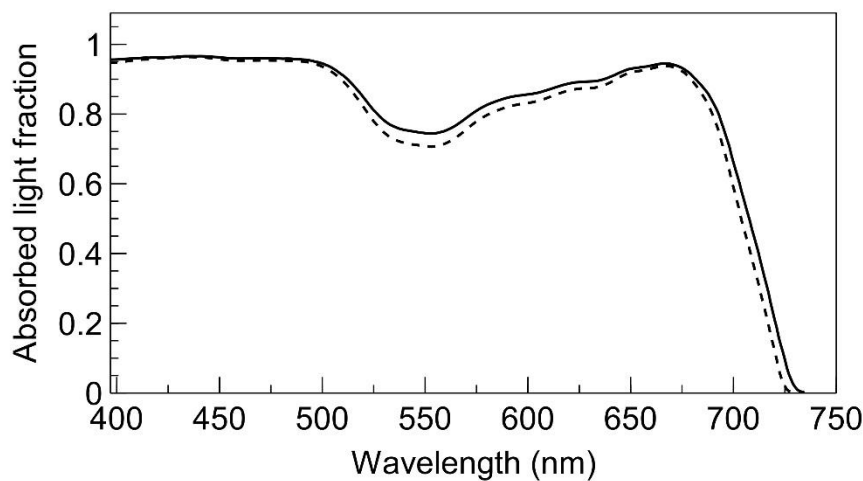

Figure 2: Leaf absorptance of SUN-grown leaves (dashed line) and SHADE-grown leaves (solid line). (*n*=3).

Φ_{CO2} for SUN-grown leaves subjected to SUN, and SHADE-grown leaves subjected to SHADE, are shown in Fig. 4 together with their predicted Φ_{CO2}. In SUN-grown leaves measured Φ_{CO2} was 0.069 and predicted Φ_{CO2} was 0.073 (with a corresponding E value of 0.94), although this difference was not significant (*p*=0.13). However, the difference between measured Φ_{CO2} in

SHADE-grown leaves (0.075) and the predicted Φ_{CO2} (0.061) was significant ($p<0.001$) and yielded an E value of 1.23. A two-way ANOVA showed significant interaction ($p<0.001$) i.e. leaf type (SUN or SHADE) was a significant factor in determining enhancement.
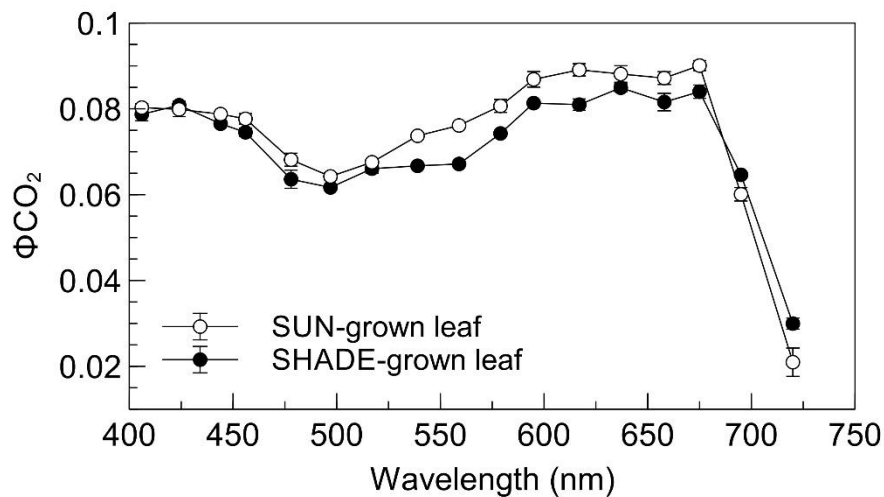

Figure 3: Wavelength dependence of Φ_{CO2} on an absorbed light basis for SUN-grown (open circles) and SHADE-grown (closed circles) tomato leaves using 17 narrowband irradiances. Error bars are ±SE of the mean and are shown where the bars are larger than the data points (n=3).
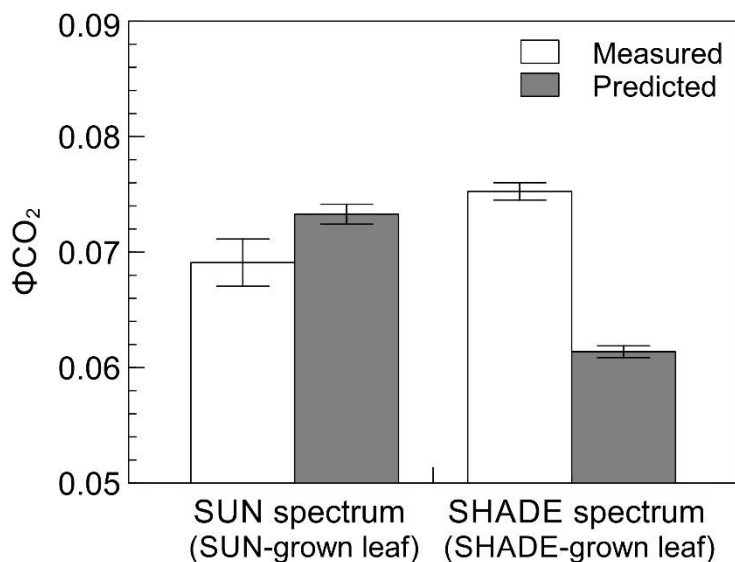
Figure 4: Measured (open bars) and predicted Φ_{CO2} (without enhancement; shaded bars) for SUN- and SHADE-grown leaves in SUN and SHADE light. Error bars are ±SE of the mean (n=3).

In general, the trends in wavelength dependency of Φ_{CO2} were preserved when a background of SUN or SHADE was used (Fig 5, row A). For example, the trough at 500nm and the peak in the red region were still evident in both leaf types. However, as expected, Φ_{CO2} traces were

considerably flattened as a result of the moderating effect of the broadband component. The maximum Φ_{CO2} with background SUN or SHADE occurred when 680 nm irradiance was used irrespective of whether leaves were SUN- or SHADE-grown; in SUN-grown leaves this value was 0.083 with SUN as background and in SHADE-grown leaves this value was 0.089 with SHADE as background. The corresponding minima Φ_{CO2} for SUN- and SHADE-grown leaves was 0.068 and 0.074, respectively, when a foreground irradiance of 500 nm was used, coinciding with the minima observed at 500 nm amongst the narrowband spectra. SHADE was used more efficiently by SHADE-grown leaves than SUN by SUN-grown leaves (0.075 compared with 0.069). Predicted Φ_{CO2} (assuming no enhancement) is shown in Fig. 5B with measured Φ_{CO2} from Fig. 3 shown again for reference. From these results the three greatest E values in SUN-grown leaves with the SUN background were (in sequence from 680 nm to 720 nm foreground irradiance): 1.047, 1.076, and 1.456 (i.e. enhancement of 4.7%, 7.5% and 46%). Mean E for the same leaves presented with SUN background and foreground irradiances of <680 nm was 1.011 (SE=0.011) indicating that enhancement was negligible at foreground wavelengths <680 nm. In SHADE-grown leaves with the SHADE background E values were substantially greater than in SUN-grown leaves across the range of foreground irradiances used. As with SUN-grown leaves the greatest E value in SHADE-grown leaves occurred with 720 nm foreground irradiance although this value was far greater (1.76), indicating a considerable enhancement of 76%. E values in SHADE-grown leaves at all other supplementary wavelengths were between 1.17 and 1.27.
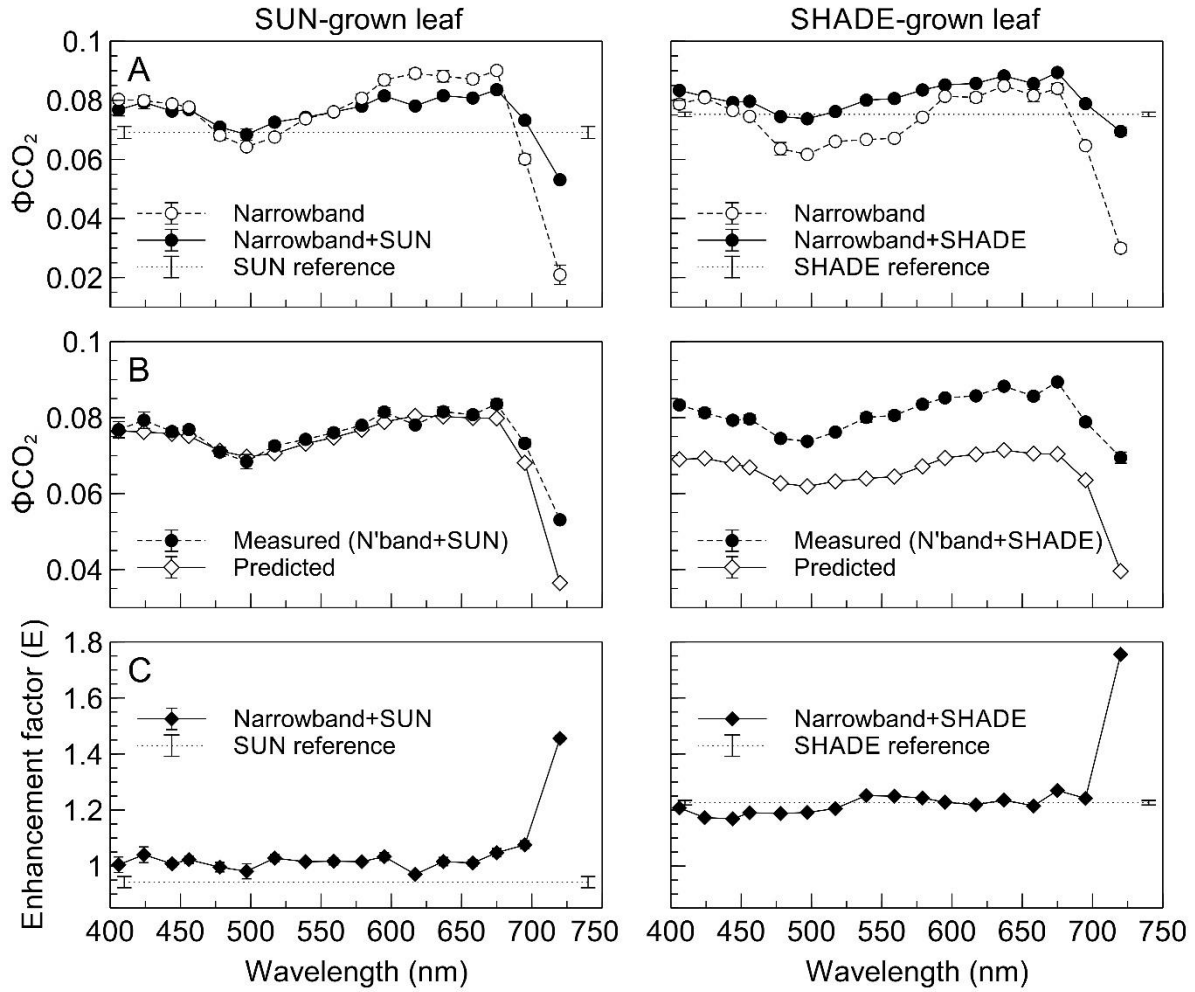
Figure 5: (Row A) Φ_{CO2} obtained when narrowband irradiances were applied with SUN (left panes) or SHADE (right panes) as background irradiance in a 1:1 ratio on an absorbed light basis (closed circles). Wavelength dependence data from Fig. 3 are shown for comparison (open circles, dashed lines). Dotted lines represent mean Φ_{CO2} when the background irradiance (SUN or SHADE) was applied alone. Row B: Predicted Φ_{CO2} for each narrowband irradiance with SUN or SHADE as background irradiance, assuming no enhancement (open circles). Estimations were made according to the method of McCree (1972b) by summing the product of interpolated narrowband Φ_{CO2} data and the relative spectral distribution of each spectrum. Measured values from Row A are shown again for comparison (closed circles, dashed lines). Row C: Enhancement factor (E) calculated as the ratio of measured:predicted Φ_{CO2} using data shown in Row B. Error bars are ±SE of the mean and are shown where the bars are larger than the data points (n=3).

The results of selected PSII parameters, Φ_{PSI}, and photosystem balance ($\Phi_{PSII}/(\Phi_{PSI}+\Phi_{PSII})$) are presented in Fig. 6. We deal first with leaves subjected to narrowband irradiance alone. Minima in Φ_{PSII} occurred at 480nm, 560nm, and 660nm in both leaf types (Fig. 6 A). Outside of these troughs, PSII in SUN-grown leaves was high (ca. 0.75-0.8) but greatest at 720 nm (>0.8). Though the trend of PSII in SHADE-grown leaves was similar to that of SUN-grown leaves, differences were amplified such that maxima were greater than, and the minima less

than, in SUN leaves. For example, the Φ_{PSII} minima in SUN leaves (corresponding values for SHADE-grown leaves in brackets) at 480, 560 and 660nm were, respectively, 0.69 (0.64), 0.74 (0.69) and 0.72 (0.70) whereas the maximum at 720nm was 0.81 (0.83). The sharp peak in PSII in SHADE-grown leaves at 520 nm is especially notable compared with the shoulder in this region in SUN-grown leaves. It is notable that Φ_{PSI} closely mirrored the response of Φ_{PSII} in both leaf types; when PSII was high, PSI was low and vice versa. For example, PSI maxima coincided with PSII minima at 480, 560 and 660nm whereas PSI minima coincided with the PSII maximum at 720 nm and also locally at 400, 520, and 700 nm, when PSII was high. The wavelength dependence of photosystem balance, taken as the ratio of Φ_{PSII} to the sum of Φ_{PSII} and Φ_{PSI} (Fig. 6C), generally ranged between ca. 0.4-0.45 in both leaf types and tended to follow the Φ_{PSII} trend (since for most wavelengths changes in Φ_{PSII} were comparatively greater than that of Φ_{PSI}). However at >700 nm the marked loss of Φ_{PSI} had a dramatic impact on the relative efficiencies of the photosystems, with $\Phi_{PSII}/(\Phi_{PSI}+\Phi_{PSII}$ ratios of 0.87 and 0.84 in SUN- and SHADE-grown leaves, respectively, at 720 nm. The qP parameter (Fig. 6D) quantifies the effect of closure of PSII reaction centres via Q_A reduction on Φ_{PSII} (Baker et al 2007) and is qualitatively correlated with Q_A reduction. The variation of qP showed striking similarity to that of Φ_{PSII} in both leaf types, with loss of qP coinciding with, and contributing to, Φ_{PSII} minima where PSII overexcitation occurred. Φ_{PSII} is the product of qP and Fv'/Fm', where Fv'/Fm' is the maximum efficiency of PSII in the light. Fv'/Fm' showed little response to wavelength, apart from increases at 700-720 nm, although values in SUN-grown leaves tended to be slightly less than 0.8 whereas in SHADE-grown leaves values were slightly greater than this, supporting the conclusion that changes in Φ_{PSII} are strongly dependent on qP.

Broadband spectra have a considerable moderating effect on Φ_{PSII}, qP, and the photosystem excitation balance (Fig. 6A-C). Φ_{PSII} varied within a tight range between 0.77 and 0.81 in SUN-grown leaves and 0.76 and 0.79 in SHADE-grown leaves and excitation balance was about 0.45 in both leaf types apart from at 720 nm. Troughs in these parameters observed for narrowband irradiance alone at 480 nm and 680 nm were however preserved but only to a reduced extent. Unlike Φ_{PSII} and qP, the response of Φ_{PSI} to a combination of narrowband and broadband (SUN and SHADE) irradiances was little different to that obtained under narrow band irradiances alone (Fig. 6) apart from 720nm. The main difference between the leaf types was in the response of Fv'/Fm'. Whereas this parameter was largely uniformly higher by about

0.03 at most wavelengths in SUN-grown leaves in the presence of the SUN background (the exceptions being at 550 nm and over 700 nm where this increase did not occur) SHADE-grown leaves with the SHADE background showed no difference apart from at 700 and 720 nm. Since Φ_{PSII} is the product of the proportion of open reaction centres (qP) and maximum efficiency of Φ_{PSII} in the light (Fv'/Fm'; see above), the values of these underpin the spectral response of Φ_{PSII}. Of qP and Fv'/Fm' it is variation in qP that most greatly effects Φ_{PSII}; the relationships between qP and Φ_{PSII} (Fig. 7) are nearly linear. Fig. 7 also shows that, in both leaf types, greater variation in qP occurred when only narrowband irradiances were used, and comparatively more variation was observed in SHADE-grown leaves than in SUN-grown leaves. Only in SUN-grown leaves does the small step-increase in Fv'/Fm' described earlier lead to the separation of two discernible relationships depending on whether narrowband irradiance was used alone (open points) or in combination with the SUN spectrum (closed points).

State transitions were monitored using the ratio of light-adapted maximum fluorescence (Fm') to dark-adapted maximum fluorescence (Fm) (Fig. 8). In SUN-grown leaves the spectral response of Fm'/Fm to narrowband irradiance alone was similar to that of Φ_{PSII} and qP. For example, the trough in Φ_{PSII} at 480 – 500 nm and local maxima occurring at 520-540 nm, 640 nm and 700-720 nm are reflected in the response of Fm'/Fm. In response to the overexcitation of PSII at 480-500 nm state 2 was induced as shown by the lower Fm'/Fm ratio of 0.9. At 520 nm and 640 nm, when PSII excitation pressure was comparatively low, Fm'/Fm was ≈1 indicating state 1. Unexpectedly, Fm'/Fm was greater than 1 at 700 and 720 nm. Also, in SUN-grown leaves the combination of the SUN spectrum with the narrowband irradiances tended to moderate Fm'/Fm values around 1 (with the exception of 700 and 720 nm), indicating the predominance of state 1 (i.e. no migration of LHCII to PSI). On the other hand, SHADE-grown leaves subjected to either the narrowband irradiance alone or in combination with the SHADE spectrum tended to have Fm'/Fm values of less than 1, indicating the predominance of state 2 irrespective of spectrum. An exception to the latter occurred when using 720 nm narrowband irradiance alone where Fm'/Fm was greater than 1.
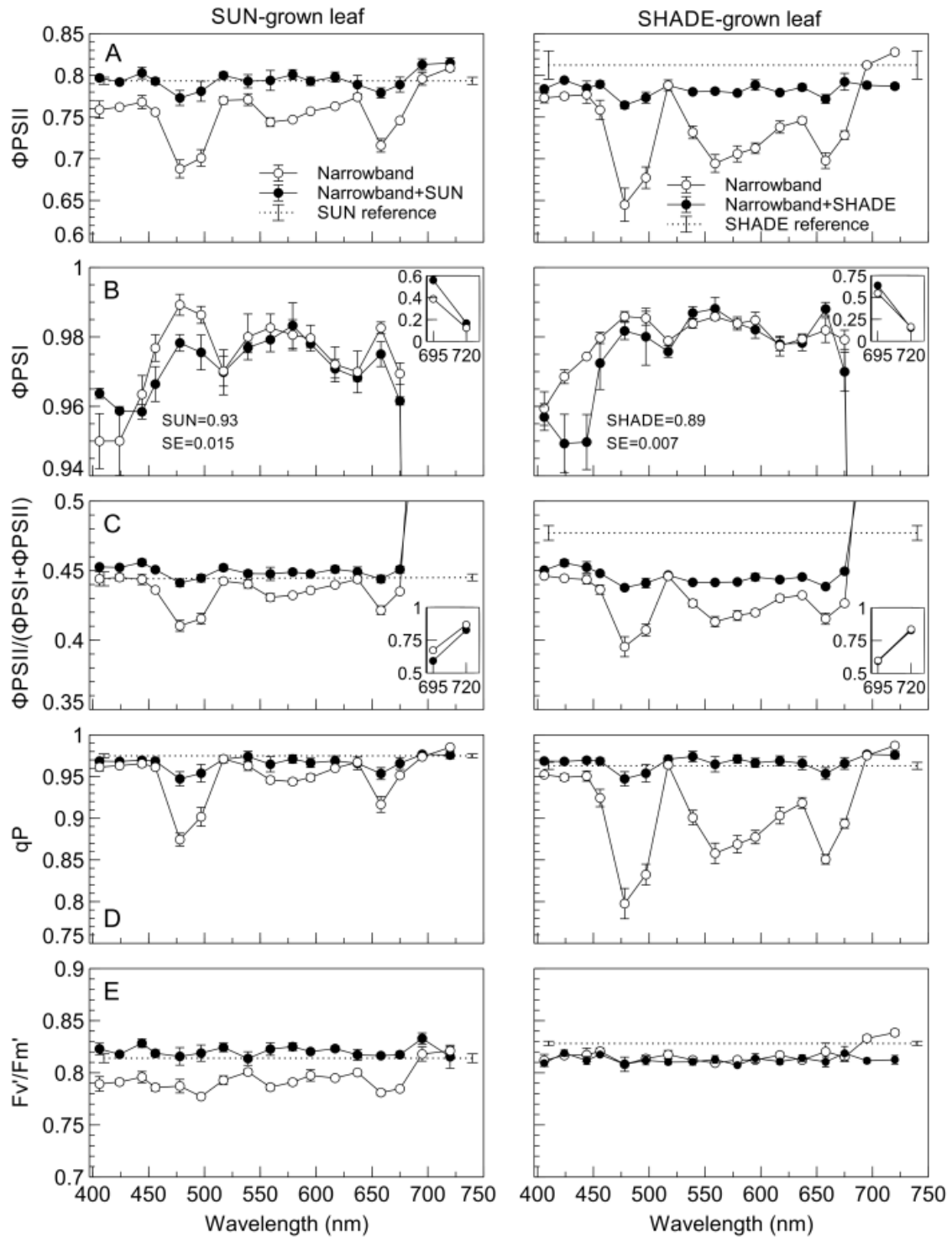
Figure 6: (A) PSII efficiency (Φ_{PSII}), (B) PSI efficiency (Φ_{PSI}), (C) photosystem balance taken as the ratio of $\Phi_{PSII}/(\Phi_{PSI}+\Phi_{PSII})$, (D) the proportion of open reaction centres (qP), and (E) maximum PSII efficiency in the light (Fv'/Fm'), measured at the highest absorbed light intensity of ca. 50 μmol m^{-2} s^{-1} for SUN- (left panes) and SHADE-grown (right panes) leaves. Measurements were taken using narrowband irradiances only (open circles) or with SUN or SHADE background irradiance in a 1:1 ratio on an absorbed PAR basis. Dotted lines represent values for the corresponding SUN or SHADE spectra. Error bars are ±SE of the mean and are shown where the bars are larger than the data points (*n*=3).
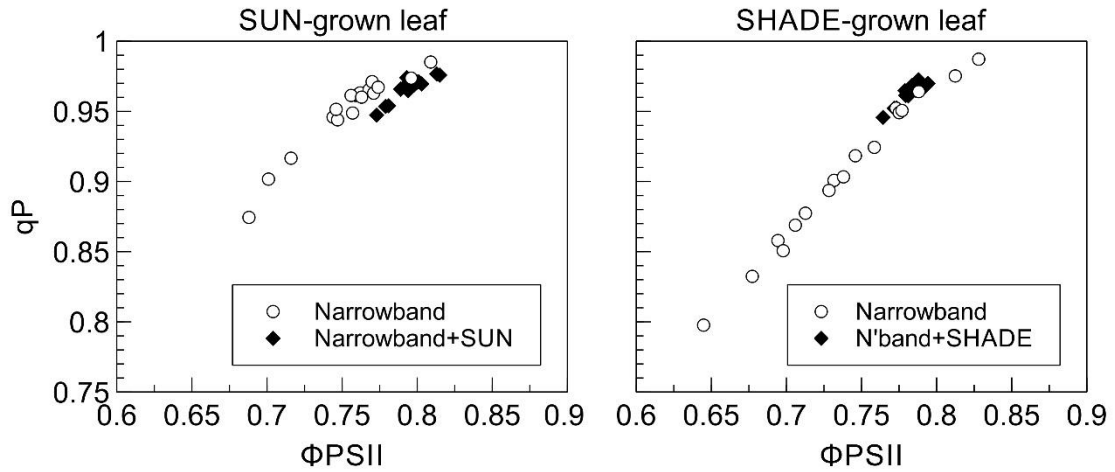
Figure 7: Relationship between qP and PSII for SUN- (left pane) and SHADE-grown (right pane) leaves. Measurements were taken using narrowband irradiances only (open circles) or with SUN or SHADE background irradiance in a 1:1 ratio on an absorbed PAR basis.

Since changes in Fm'/Fm are proportional to changes in cross-sectional area of PSII which can impact the excitation pressure on PSII, the relationship between qP and Fm'/Fm was explored (Fig. 9). For SUN- and SHADE-grown leaves subjected to narrowband irradiance alone, the general trend was an increase in qP as Fm'/Fm increased. When Fm'/Fm was high (>1) qP was also high (0.95-1), occurring at PSI irradiances when a transition to state 1 increased the cross-sectional area of PSII. The lowest Fm'/Fm values were about 0.9 in SUN-grown leaves and 0.85 in SHADE-grown leaves (state 2). At around these Fm'/Fm values qP decreased sharply to a minimum of about 0.87 in SUN-grown leaves and 0.8 in SHADE-grown leaves. In SUN- and SHADE-grown leaves subjected to narrowband plus their corresponding broadband spectra the data points were tightly clustered although in SHADE-grown leaves slight decreases in qP were observed when Fm'/Fm was at its lowest.
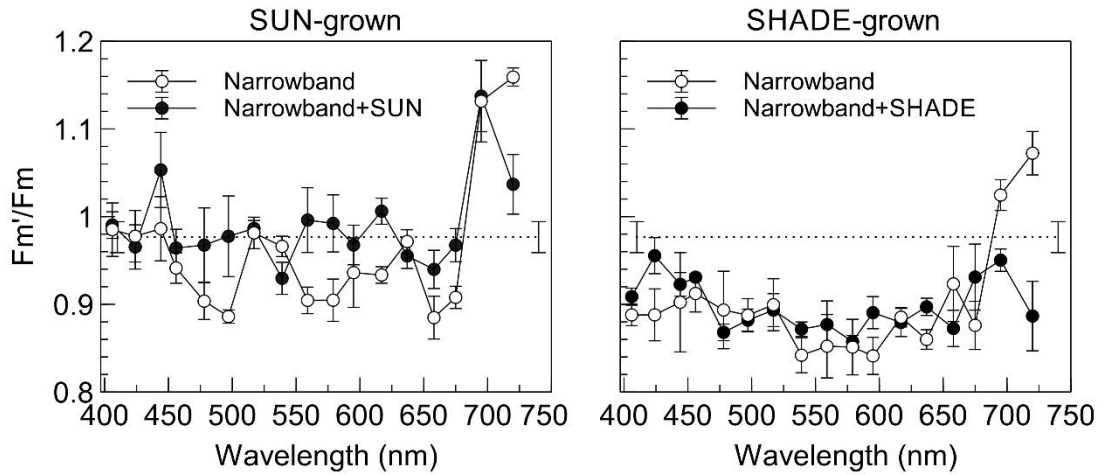
Figure 8: Fm'/Fm for SUN- and SHADE-grown leaves. Measurements were taken using narrowband irradiances only (open circles) or with SUN or SHADE background irradiance in a 1:1 ratio on an absorbed PAR basis. Dotted lines represent values for the corresponding SUN or SHADE spectra. Error bars are ±SE of the mean and are shown where the bars are larger than the data points (n=3).
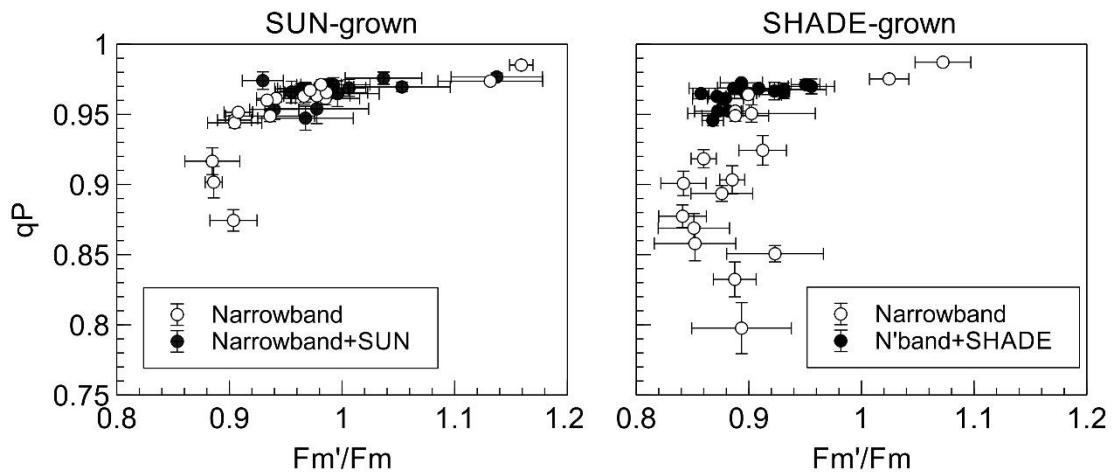

Figure 9: Relationship between Fm'/Fm and qP for SUN- and SHADE-grown leaves. Measurements were taken using narrowband irradiances only (open circles) or with SUN or SHADE background irradiance in a 1:1 ratio on an absorbed PAR basis. Error bars are ±SE of the mean and are shown where the bars are larger than the data points (n=3).

Discussion

This study demonstrates that enhancement of photosynthetic efficiency in leaves operating in permanent foliar shade can be significant. While no enhancement was observed in SUN-grown leaves illuminated with the SUN irradiance, an enhancement of 23% occurred in

SHADE-grown leaves presented with the SHADE irradiance. This figure is considerably greater than a maximum of 7% for four different types of white light (McCree, 1972b).

Since there was no enhancement found in SUN-grown leaves in SUN-light (Fig. 4) but enhancement was found in SHADE-grown leaves in SHADE-light, the question arises as to which spectral region (or regions) of the SHADE spectrum may have contributed to the observed enhancement. Analysis of Φ_{CO2} for the SUN and SHADE spectra, each enriched separately with the 17 narrowband spectra, provides clues in this regard. Enhancement of between 17 to 27% occurred in SHADE leaves with the SHADE background for all narrowband irradiances apart from 720 nm where enhancement was even greater, and substantially so, at 76%. Despite no evidence for enhancement in the SUN spectrum itself, enrichment of the SUN spectrum with 680 nm caused enhancement of 4.7%, increasing to 7.6% at 700nm and 46% at 720 nm. When the results for SUN and SHADE-grown leaves are taken together it can be deduced that the far-red tail outside the PAR spectrum plays a more significant role in Φ_{CO2} than may be expected based on its ability to drive photosynthesis only very weakly when applied alone and, by definition, its exclusion from the PAR region. In this regard the considerably greater far-red component of the SHADE spectrum (about 28% of total photon flux at wavelengths beyond 700 nm in the band 700 – 728 nm compared with a corresponding figure of 10% for the SUN spectrum) is further supportive of the participation of far-red in the enhancement. Apparent Φ_{CO2} increased by up to 41% in lettuce when far-red light (700-770nm) was added to either a red/blue mixture or warm white LED light, suggesting significant enhancement (Zhen and van Iersel, 2017). In selected species of green algae, Dring and Lüning (1985) observed enhancement of 18% when using an irradiance rich in far-red from a quartz-iodine lamp. It is notable that those authors did not observe comparable enhancement, if it was present, using four other light sources comprising little or no far-red light. Using an artificial shade spectrum similar to that of the present study i.e. also rich in far-red, a 21% enhancement was observed in leaves of cucumber (Hogewoning *et al.*, 2012). The numerous reports implicating far-red directly or indirectly in broadband enhancement lends unequivocal support for the role of far-red in this phenomenon and the similarity of reported enhancement values with our own of 23% in SHADE is noteworthy.

An unexpected result was the strong enhancement observed when the SHADE spectrum was combined with the 720 nm irradiance. The 720 nm irradiance strongly overexcites PSI

whereas the SHADE spectrum is rich in far-red irradiance itself. How might two irradiances rich in PSI-overexciting far-red irradiance combine to produce significant enhancement? The answer appears to lie in the presence of shorter wavelengths in the SHADE spectrum which drive PSII photochemistry more strongly than the 720 nm irradiance which itself drives PSII only very weakly; the complementary action of the shorter 'PSII' wavelengths with the 720 nm 'PSI' irradiance increases photosynthetic efficiency hence the observed enhancement. It is this complementary action which underpins enhancement and therefore it is not one irradiance which enhances another so much as either irradiance enhancing the other. These findings also demonstrate that, while the use of PSI and PSII narrowband irradiances simplifies an understanding of the enhancement phenomenon, predicting whether enhancement may occur in broadband spectrum demands a holistic view of the component spectra within the broadband spectrum, itself often being a mixture of PSI and PSII irradiances in various proportions.

The greatest Φ_{CO2} obtained using broadband irradiance in the present study was 0.089, obtained using SHADE-grown leaves presented with SHADE enriched with 680nm irradiance. This value compares favourably with 0.092 for pea leaves (Evans, 1987) and a mean of 0.093 for a variety of 11 C3 species (Long *et al.*, 1993). In both those studies a quartz-iodine lamp (which has a spectrum close to that of a 3200 K black-body emitter) was used for actinic light. The output from such a lamp comprises a significant fraction of red but also less efficiently used far-red wavelengths, so in some ways is similar to the SHADE spectrum enriched with 680nm irradiance. It is likely that significant enhancement also occurred in those studies given that those Φ_{CO2} values are comparable with the maximum Φ_{CO2} of 0.093 obtained by Hogewoning *et al.* (2012) on cucumber leaves as well as the Φ_{CO2} of 0.09 obtained here in SUN-grown leaves when highly efficient wavelengths for photosynthesis of 618 and 680 nm, respectively, were used. Singsaas *et al.* (2001) concluded that the maximum quantum yield deviates little across diverse taxa from the mean maximum value reported by Long (1993) of 0.093 and that variation in this value is likely due to measurement error. The use of 53 unique spectra allowed the present study to rigorously test the effect of actinic spectrum on this putative maximum value. The maximum Φ_{CO2} value obtained from our extensive analysis provides support for the conclusion of Singsaas *et al.* (2001) and also suggests that this

supposed upper limit is not exceeded even in instances where significant enhancement occurs.

In determining the underlying factors which contributed to the observed enhancement, the efficiencies of PSII and PSI are obvious candidates. Strictly these are relative efficiencies because the fluorescence-derived estimate of PSII efficiency (our Φ_{PSII}) takes no account of PSI fluorescence (Pfündel, 1998), and the redox-state based estimate of Φ_{PSI} takes no account of the actual efficiency of PSI with unoxidized P700). The differences between SUN and SHADE-grown leaves in terms of acclimation and, consequently spectral dependence of Φ_{CO2}, is further reflected in Φ_{PSII} and qP values. Whereas Φ_{PSII} and qP of SHADE-grown leaves were very slightly higher than that of SUN-grown leaves at 700 and 720 nm, these parameters were lower than SUN-grown leaves for most other wavelengths apart from a spike at 520 nm and in the blue region, where Φ_{CO2} was also similar. Changes in Φ_{PSII} in response to narrowband irradiance alone were largely due to changes in qP, one of the two components of Φ_{PSII}, the other being Fv'/Fm'. It is however interesting that in the case of SUN-grown leaves exposed to narrowband irradiances alone there were some weak decreases in Fv'/Fm' at those wavelengths where qP was low. This could possibly be due to state transitions.

We were able to detect state transitions by monitoring Fm'/Fm (Bellafiore *et al.*, 2005). It has recently been shown that state transitions positively influence Φ_{CO2} (Taylor *et al.*, 2019). When Fm'/Fm is <1 then the photosynthetic apparatus is configured in state 2 (i.e. some LHCII has become phosphorylated and migrated from PSII to PSI) whereas if Fm'/Fm approximates 1 then the photosynthetic apparatus is configured in state 1 (LHCII is not phosphorylated and has not migrated to PSI). In SUN-grown leaves exposed only to narrowband irradiances Fm'/Fm was closely related to that of Φ_{PSII} (and thus qP) and inversely related to Φ_{PSI} i.e. Fm'/Fm was high when Φ_{PSII} was low or when Φ_{PSI} was high. For example, the troughs in Φ_{PSII} at 480 and 660 nm as well as the depression in the 580 nm to 620 nm region were reflected by drops in Fm'/Fm to 0.9. In the case of SUN-grown leaves exposed to narrowband irradiances plus SUN Fm'/Fm was close to 1, consistent with a qP of 0.95 – 1 and a Φ_{PSII} of about 0.8. In SHADE-grown leaves exposed to either only narrowband irradiances or narrowband irradiances plus SHADE Fm/Fm' was consistently <1 (about 0.9) for all wavelengths apart from 700 nm and 720 nm, indicating that these leaves were in state 2 for all but the PSI irradiances. The difference in the spectral response of Fm'/Fm between the

SUN and SHADE-grown leaves once again indicates the different acclimation of the two leaf types; SHADE-grown leaves were more susceptible to entering state 2 than SUN-grown leaves as evidenced by the comparatively left-shifted spread of Fm'/Fm points in Fig. 9. The SHADE-grown leaves, likely having more PSII LHCs to compensate for the PSI-overexciting growth light, were predisposed to photosystem imbalance in most of the narrowband irradiances given that PAR wavelengths generally over-excite PSII hence the bias towards state 2 in these leaves. It is apparent that state transitions in both leaf types were not sufficient to compensate for strong imbalances as demonstrated by the troughs in PSII/(PSII+PSI) at strong PSII irradiances such as 480 and 660 nm. Furthermore, in response to strong PSII-overexcitation, qP fell sharply once Fm'/Fm showed no further decreases, revealing the limited scope of state transitions to arrest sharp decreases in qP beyond, in this instance, a transition to state 2. These findings are consistent with the findings of Taylor *et al.* (2019) who observed that state transitions mitigate, but do not eliminate, Φ_{CO2} losses caused by strong photosystem imbalances. Nonetheless the influence of state transitions on Φ_{CO2} is of significance to this study as state transitions would have served to ameliorate the response of Φ_{CO2} to irradiances which induced photosystem imbalance. The weak tendency for Fv'/Fm' to decrease in SUN-grown leaves exposed to narrowband irradiance alone could be due to only these leaves showing a marked wavelength specific variation in Fm/Fm'. If LHCII attaches to PSI it would result in an increase in PSI fluorescence which would result in a lowering of Fv'/Fm'. Significantly, in the SUN-grown leaves in both narrowband irradiances and narrowband irradiances plus SUN, and SHADE-grown leaves in only narrowband irradiance, Φ_{PSII} and qP were high at 700nm and 720 nm. In these treatments Fm'/Fm was also conspicuously high, and Fv'/Fm' was relatively high, consistent with the idea that LHCII migration can produce small changes in Fv'/Fm' as was also shown in Taylor *et al.* (2019)

It can be concluded that enhancement was significant under many of the spectral combinations presented here. A commonality amongst instances where enhancement was found to occur is a spectrum rich in far-red light, such as the SHADE spectrum or when supplementary 720 nm irradiance was combined with the SUN or SHADE spectra. Though unremarkable at the level of leaf assimilation when applied alone, far-red light has impacts on underlying photochemistry which make it an especially relevant spectral region for photosynthesis. Although we did not measure enhancement at narrowband wavelengths

greater than 720 nm, it is plausible that still greater enhancement could have been achieved at longer wavelengths as observed in spinach chloroplasts presented with 730nm irradiance with a narrowband background (Govindjee *et al.*, 1964). Because those authors did not test beyond 730 nm where enhancement was found to be greatest, the far-red wavelengths around which enhancement ceases remains to be known. On the other hand, in a lettuce canopy, enhancement in a white light background was shown to decline as supplementary far-red wavelength increased from 711 to 723 and 746 nm (Zhen and Bugbee, 2020). There could be several explanations for these apparent differences, including the absorption in the far-red region and the spectrum of background light. With respect to the latter, the extent of enhancement observed in the present study may differ from that in actual sunlight or shade. Nonetheless, the results presented here are supportive of a role for far-red light in 'white light enhancement' and consistent with a growing body of evidence on the subject (Zhen and van Iersel, 2017; Zhen and Bugbee, 2020). From a practical perspective, while the PAR definition may suffice for the majority of photosynthesis studies, care should be taken as it can lead to substantial error which is of significance in instances where absolute values are important, such as in modelling work or quantum yield studies. From an ecophysiological perspective the enhancement in the SHADE spectrum may be significant because the majority of leaves are exposed to shade beneath the canopy; these leaves may be surprisingly efficient in spectra which are classically regarded as poor for efficient photosynthesis.

Acknowledgements

CHAPTER 3

Demonstration of a relationship between state transitions and photosynthetic efficiency in a higher plant

Abstract

A consequence of the series configuration of PSI and PSII is that imbalanced excitation of the photosystems leads to a reduction in linear electron transport and a drop in photosynthetic efficiency. Achieving balanced excitation is complicated by the distinct nature of the photosystems, which differ in composition, absorption spectra, and intrinsic efficiency, and by a spectrally variable natural environment. The existence of long- and short-term mechanisms which tune the photosynthetic apparatus and redistribute excitation energy between the photosystems highlights the importance of maintaining balanced excitation. In the short term, state transitions help restore balance through adjustments which, though not fully characterised, are observable using fluorescence techniques. Upon initiation of a state transition in algae and cyanobacteria, increases in photosynthetic efficiency are observable. However, while higher plants show fluorescence signatures associated with state transitions, no correlation between a state transition and photosynthetic efficiency has been demonstrated. In the present study, state 1 and state 2 were alternately induced in tomato leaves by illuminating leaves produced under artificial sun and shade spectra with a sequence of irradiances extreme in terms of PSI or PSII overexcitation. Light-use efficiency increased in both leaf types during transition from one state to the other with remarkably similar kinetics to that of F_m'/F_m, F_o'/F_o, and, during the PSII-overexciting irradiance, Φ_{PSII} and q_P. We have provided compelling evidence for the first time of a correlation between photosynthetic efficiency and state transitions in a higher plant. The importance of this relationship in natural ecophysiological contexts remains to be elucidated.

Introduction

The optimal light-use efficiency of photosynthesis depends on the optimal excitation of photosystems I and II. This arises from the need to balance linear (through PSII and PSI) and cyclic (around PSI) electron transport fluxes (yielding reduced ferredoxin and then NADPH) and their associated proton transport fluxes (yielding ATP synthesis) with the demands of metabolism and the activity of the Mehler reaction. In the case of C3 plants linear electron transport predominates under most circumstances. The stoichiometry of proton release into the thylakoid lumen that occurs together with linear electron transport, together with the 14/3 proton:ATP ratio expected for the chloroplast ATPase, results in an ATP/NADPH ratio of ~1.28. This is close to the ATP/NADPH demand of 1.5 for carbon dioxide fixation alone, and the demand of 1.75 for photorespiration alone (Foyer *et al.*, 2012). The shortfall in ATP is made up by alternative electron transport activity (cyclic electron transport and the Mehler reaction) and the low ATP/Fd demand of other reductive metabolic activities such as nitrite reduction, sulfate reduction, fatty acid biosynthesis, and the export of reducing power from the chloroplast. Maximally efficient linear electron transport depends on the balanced electron transport through the two photosystems; this will require, however, overexcitation of PSII relative to PSI as the quantum yield for electron transport by PSI is higher (c. 0.99) than PSII (c. 0.88; based on fluorescence data and accounting for the PSI fluorescence error in the determination of Fo and Fm (Pfündel, 1998)). In the event that some of the ATP shortfall were to be made up from cyclic electron transport rather than pseudocyclic electron transport or the extra ATP arising from the activity of photosynthetic reduction processes (like nitrate reduction) with a low ATP/Fd demand, then overall excitation of PSI would need to be increased relative to that of PSII.

A further problem affecting optimal operation of photosynthesis is that the two photosystems do not have an identical light absorption spectrum and spectral light-use efficiency (Laisk *et al.*, 2014). These differences arise from differences in the pigments and the binding of pigments in the two photosystems to which should be added the lower energy transfer to chlorophyll of carotenoids compared to that of chlorophyll to chlorophyll (Croce *et al.*, 2001). Overall, it seems that at most photosynthetically active wavelengths there is an over-excitation of PSII relative to PSI. The spectrum of light incident on a leaf is not constant but highly variable due to, amongst other things, sun angle, weather, and intermittent shading by

other leaves (Holmes and Smith, 1977). It follows, therefore, that spectrum and changes in spectrum has great potential to disrupt the balanced activities of PSI and PSII required for optimal linear electron transport.

Optimum light-use efficiency - the optimal excitation of the two photosystems - is critical in any situation where light is limiting, such as low irradiances. Maintaining this optimal excitation is, however, difficult because of the changing metabolic demands changing the need for cyclic electron transport, and changing spectrum of the irradiance combined with the absorption and photophysical properties of the two photosystems. Plants possess mechanisms to balance, at least to some extent, photosystem excitation. These range from longer-term adjustments of photosystem ratio and composition to short term adjustments in pigment-binding protein associations between the two photosystems. In the order of days, leaves acclimate to growth spectrum by tuning the relative amounts of the photosystems and associated light harvesting complexes (Chow *et al*., 1990; Hogewoning *et al*., 2012). The long-term nature of this kind of adjustment is demonstrated by the 'memory' of leaves produced under a spectrum that preferentially excites PSI or PSII: leaves show a comparatively higher photosynthetic efficiency when exposed to an irradiance which, in terms of spectral composition and absorption by the photosystems, more closely matches that of the growth spectrum (Chow *et al*., 1990).

State transitions represent a considerably faster excitation-balancing mechanism, operating over minutes in response to imbalances in electron transport through PSI and PSII. This reversible process is defined by two states - 'state 1' and 'state 2' - which reference one of two putative docking positions of a potentially mobile LHCII pool (Myers, 1971). The classical view of state transitions is that, in state 1, mobile LHCII becomes associated with PSII during periods of PSI overexcitation whereas in state 2 LHCII becomes associated with PSI during periods of PSII overexcitation with the redox state of the PQ pool being pivotal in the regulation of the state transition process (Allen *et al*., 1981). In accordance with this model a state transition regulates the cross-sectional area of PSI and PSII in a reciprocal manner and helps restore balance by enhancing light capture by the rate limiting photosystem whilst limiting light capture by the overexcited photosystem. Of the three LHCII apoproteins (*viz.* Lhcb1, Lhcb2, and Lhcb3), Lhcb1 and Lhcb2 can be phosphorylated in a process which requires the STN7 kinase in plants, and the Stt7 kinase in algae, which itself is believed to be activated

by a reduced PQ pool (Bellafiore *et al*., 2005). It is this phosphorylation of LHCII that induces mobility of a proportion of LHCII and results in state 2. A return to state 1 occurs when an oxidised PQ pool triggers dephosphorylation of Lhcb1 and Lhcb2 in a process which is less well understood, although the phosphatases TAP38 and PPH1 have been shown to play a role in this regard (Pribil *et al.*, 2010; Shapiguzov *et al*., 2010). A potential overcapacity of electron transport through PSII will result in the reduction of Q_A, which will result in an increasing reduction of the PQ pool, potentially until the quantum yield of PSII decreases to bring actual electron transport activity into balance with that of PSI. A potential overcapacity of electron transport through PSI will result in oxidation of the intersystem electron transport chain, including the PQ pool, until the oxidation of P700 increases to the point where quantum yield of PSI falls to match the flux of electrons from PSII and cyclic electron transport.

The biochemical re-organisation which occurs during a state transition is readily detectable in algae, cyanobacteria and higher plants using spectroscopic (Bonaventura and Myers, 1969; Murata, 1969; Andrews *et al*., 1993), photoacoustic (e.g. Canaani and Malkin, 1984; Canaani, 1986; Veeranjaneyulu and Leblanc, 1994; Delosme *et al*., 1996) and proteomic methods (Allen *et al*., 1981). Chlorophyll fluorescence, for example, reveals distinct kinetics upon transition from state to the other (Allen, 1992). When state 1 leaves (i.e. fully adjusted to an overexcitation of PSI) are presented with so-called PSII light (light which over-excites PSII and induces a transition to state 2) fluorescence yield increases sharply and is gradually quenched until a new equilibrium in state 2 is achieved. Subsequently presenting state 2 acclimated leaves with PSI light (light which over-excites PSI) is met with a sharp decrease in fluorescence yield followed by a gradual increase in fluorescence yield to a new steady-state as a return to state 1 occurs. The changes in PSII antennae size during state transitions can be estimated by changes in Fm and Fo between the two states (Allen, 1992). In the algae *Chlorella pyrenoidosa*, light absorption by PSII is reduced by an estimated 10% when in state 2 compared to state 1 (Bonaventura and Myers, 1969) and a similar reduction of 10-15% has been reported in the cyanobacteria *Nostoc muscorum* which was accompanied by an equivalent increase in PSI antennae size (Canaani, 1986). Following a transition to state 2 in higher plants, decreases in PSII antennae size of 11% (Kim *et al.*, 2015) and 20% (Forti and Fusi, 1990) have been reported and an increase in PSI antennae size of 12% has been determined by 820 nm absorbance changes (Telfer *et al.*, 1986).

The precise location of LHCII and its three trimers in state 1 and state 2 is, however, the subject of contrasting findings that do not match with the classical model. In isolated spinach chloroplasts, for example, mobile LHCII was attached to PSII in state 1 but was not associated with PSI in state 2 (Haworth and Melis, 1983). Picosecond-fluorescence spectroscopy of the algae *Chlamydomonas reinhardtii* showed that only a negligible amount of mobile LHCII docks with PSI (Ünlü *et al.*, 2014). It has recently become possible to better purify PSI-LHCII complexes and, using this approach, mobile LHCII has been shown to be an intimate part of PSI rather than that of PSII as widely believed (Galka *et al.*, 2012). Moreover, those authors showed that mobile LHCII is a very effective antenna for PSI in state 2. An alternative finding is that mobile LHCII serves as an antenna of both photosystems and this allows for acclimation to different growth light intensities simply by regulating the amount of LHCII (Wientjes *et al.*, 2013).

Whatever the precise points of attachment are for mobile LHCII in either of the states, the perceived role of state transitions as an acclimatory mechanism whose purpose is to alleviate, or at least partially alleviate, photosystem excitation imbalance has gained widespread acceptance based on current evidence (Allen *et al.*, 1981). It is reasonable to predict that as state transitions act to optimize the balance of excitation of PSII and PSI, they ought also to positively influence the rate CO_2 assimilation and hence photosynthetic efficiency. In seminal work describing the phenomenon of a state transition, Bonaventura and Myers (1969) observed a relationship between state transitions and oxygen evolution in *Chlorella pyrenoidosa*. Those authors observed an accompanying increase in oxygen evolution with similar kinetics to that of fluorescence yield which reveals a clear functional role for state transitions that is congruent with its effects at the level of electron transport. Arabidopsis lacking the STN7 kinase and consequently unable to perform state transitions showed decreased biomass under changeable light conditions, demonstrating the significance of state transitions at the whole-plant level (Bellafiore *et al.*, 2005). In another alternating PSI/PSII light regime the stn7 mutant produced half as much seed as the wild type, further indicating a benefit to plant fitness (Wagner *et al.*, 2008). The same mutants produced 19% less seed than their wild type counterpart in field conditions, showing the significance of state transitions under natural conditions (Frenkel *et al.*, 2007). However, a study of the responses of assimilation to irradiance expected to induce changes between states 1 and 2 showed no

alterations in assimilation of the kind expected to accompany a state transition, despite bearing the same fluorescence signatures associated with state transitions in algae (Andrews *et al.*, 1993). It has therefore been suggested that the apparent beneficial effects of state transitions at the whole-plant level cannot be quantified using gas exchange measurements (Dietzel *et al.*, 2008). The apparent disconnection between responses at the thylakoid level and those of assimilation in relation to state transitions has posed problems for understanding the significance and impact of state-transitions. We re-examine the possible relationship between state transitions and photosynthetic efficiency by inducing an extreme photosystem excitation imbalance. We show that, under these extremes, changes at the molecular level which occur during a state transition are correlated with changes in the rate of CO_2 fixation and quantum yield. This not only partly resolves the puzzle of the lack of an effect of state transitions at the level of assimilation but also offers a new, relatively straightforward way of monitoring state transitions in terms of extent and kinetics.

Materials and Methods

Plant material and growth environment

Tomato seeds (*cv.* Moneymaker) were sown in rockwool blocks (Grodan, Roermond, The Netherlands) and divided equally into two light-tight plastic-lined fabric enclosures (80 cm x 80 cm x150 cm) in a climate-controlled room (16 hour photoperiod, 20 °C air temperature, 70% relative humidity). Rockwool blocks were irrigated from below with Hoagland solution via pumps which operated for 15 minutes once per day. Each enclosure was illuminated with a different light source to provide spectrally distinct growth environments. The light sources used were a plasma lamp (Plasma International, Muhlheim am Main, Germany) and a quartz-halogen lamp assembly comprising four floodlight housings, each fitted with 500W lamps (Osram, Munich, Germany). The plasma lamp provided a daylight-like spectrum (hereafter referred to as 'SUN') whereas light from the quartz-halogen lamps was diffused with a ground glass diffuser and filtered with a plastic-film filter (type 'cold blue', Lee Filters, Andover, UK) to provide a shade-like spectrum (hereafter referred to as 'SHADE', see (Hogewoning *et al.*, 2012)). Fig. 1 shows the relative quantum flux and spectral distribution of each of these light sources together with that of the two narrowband actinic irradiances used for gas exchange measurement (see 'Actinic light' section below). The lighting environments were selected based on their expected influence on photosystem excitation balance; the SUN spectrum

over-excites PSII whereas the SHADE spectrum over-excites PSI. The enclosures were impervious to light to ensure no spectral contamination from adjacent enclosures. The intensity of light incident on the apical buds of the seedlings, and subsequently the third leaf once it began to develop, was controlled at 100 µmol m^{-2} s^{-1} ±5% by measuring the irradiance using a Licor quantum sensor (Li-190, LICOR, Nebraska, USA) and adjusting plant height. It was observed that leaves tended to droop and no longer be normal to the direction of the incident irradiance. To ensure that the third leaf received the desired irradiance it was supported normal to the light using wooden stakes from below. Poor germination rates were observed in the shadelight treatment. To remedy this, seeds destined for the shadelight treatment were allowed to germinate in the daylight treatment and transferred to the shadelight treatment once the cotyledons had fully expanded. Fans within the enclosures provided air circulation around the plants and fans mounted in the walls of growth enclosures ventilated the enclosures. The high heat output from the quartz-halogen lamp compared with the plasma lamp had the potential to create large differences in leaf temperature between the treatments. The amount of ventilation for each enclosure was adjusted to ensure that leaf temperature was 22.5 °C ± 1 °C in the growth enclosures.
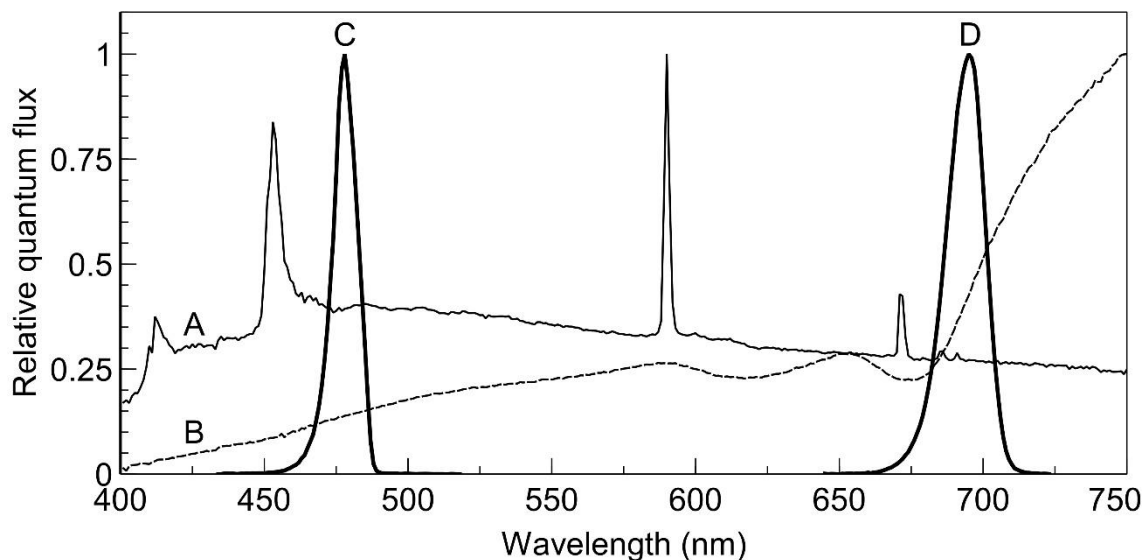

Fig. 1: Relative quantum flux and spectral distribution of (A; thin solid line) artificial daylight spectrum, (B; dotted line) artificial shade spectrum, (C; left thick line) filtered 480 nm (nominal) irradiance (peak wavelength 478 nm, 10 nm FWHP), and (D; right thick line) 700nm (nominal) irradiance (peak wavelength 695 nm, 10 nm FWHM). The broadband spectra were used as growth irradiance treatments and the narrowband spectra were applied separately as actinic irradiance during gas exchange measurements.

Gas exchange

A custom two-part gas exchange chamber, similar to that described in (Hogewoning *et al.*, 2010b), was used for gas exchange measurements. The main difference compared to the previous design is a slightly reduced chamber area (3.80 cm^2). The gas mix used for measurement comprised 400 µmol mol^{-1} CO_2, 20 mmol mol^{-1} O_2 (i.e. 2% O_2), and 18.8 mmol H_2O with the remainder being N_2. The gas stream was split into reference and sample streams with the sample stream being sent to the leaf chamber and then to the gas analysis system. The reference stream was analysed by a Li-7000 CO_2/H_2O analyser (LICOR, Nebraska, USA) operating in absolute mode while the difference between the mole fractions of the absolute and relative gas streams was measured by a Li-7000 CO_2/$H2O$ analyser operating in differential mode. The differential accuracy of the Li-7000 analysers was compared against a Li-6400 (LICOR, Nebraska, USA) by flowing the incoming and exhaust gas over the analysers in the Li-6400 head. The test showed that the differential reading for both analysers and Li-6400 was in agreement to <0.1%. A flow rate of 250 ml min^{-1} was used for all measurements and was sufficient for CO_2 depletion rates to remain within about 10 µmol mol^{-1}. The accuracy of the flow was verified by cross-checking it with a newly calibrated flow meter (Bronkhorst, Ruurlo, The Netherlands). Flow rates were within 0.2% for the two flow meters used. The same flow meter used for cross checking the chamber flow was then placed in series with the exhaust gas to test for the presence of leaks with and without a leaf in the chamber. Tests showed that gas leaks originated from the lower seal due to imperfect seals around leaf veins. A liquid, two part, non-toxic, skin-safe, quick-setting (approx. 5 minutes working time) moulding silicone rubber applied between the lower foam rubber chamber seal and the lower leaf surface (Body Double Fast Set, Allentown, PA, USA) immediately before closing the chamber eliminated all detectable leaks. Each day, before commencing measurements, standard gases comprising 491 ppm CO_2 (±2 ppm) and N_2 or pure N_2 were flowed separately through the analysers to test for calibration drift. Oxygen concentration was then verified using an oxygen analyser (type 570A, Servomex, Crowborough, UK). Leaf temperature was monitored using a non-contact temperature sensor (Micro IRt/c, Exergen, Watertown, MA, USA) directly below the leaf. In a separate test, the accuracy of the temperature sensor was verified using a type K thermocouple appressed to the abaxial surface of the leaf. This type K thermocouple had been shown to measure within 0.1 °C of an Omega high accuracy thermistor probe (Omega, Norwalk, Connecticut, USA). Leaf temperature was maintained at

22.5 °C by circulating water from a temperature-controlled water bath through an internal channel in the upper and lower chamber halves.

Actinic light

Actinic light was chosen to induce state 1 (PSI light, LHCII (largely) connected to PSII) or state 2 (PSII light, some LHCII potentially connected to PSI). Irradiance with a nominal peak wavelength of 480 nm or 700 nm (Fig. 1) was used as PSII and PSI light, respectively. These irradiances were chosen based on prior measurements which showed that, of 15 narrowband wavelengths spread across the PAR spectrum, 480 nm irradiance most strongly excites PSII whereas 700 nm irradiance most strongly excites PSI (while driving photosynthesis sufficiently strongly to avoid the problem of a low signal to noise ratio from the gas analysers). PSII light was produced using an array of 470 nm LEDs (LXZ1-PB01, Lumileds, San Jose, CA, USA) on a metal cored PCB in combination with a 480 nm interference filter (10 nm FWHM, Thorlabs, Newton, NJ, USA) and PSI light was produced using a 700 nm LED (LED700-66-60, Roithner Lasertechnik, Vienna, Austria) in combination with a 700 nm interference filter (10 nm FWHM, Thorlabs, Newton, NJ, USA). Each LED was mounted on a heatsink with forced air cooling to avoid the intensity shifts associated with increases in LED junction temperature upon switching. LED-heatsink assemblies and filters were secured on a laboratory-built optical bench which comprised a blower to force air across the filters to minimise increases in filter temperature upon switching and maintain stability of their optical characteristics. The two actinic light LEDs were coupled to the chamber using a branched fibre-optic bundle with an output diameter of 25mm. A 15 cm long transparent acrylic 25 mm diameter rod was placed at the output of the fibre to ensure that light distribution at leaf level was homogenous.

Two irradiance sensors were built and used to measure irradiance in the leaf chamber; one was used for routine measurement of irradiance incident on the leaf (sensor 1) and the other (sensor 2) was used for calibration purposes. Sensor 1 was made from a light guide with a diameter of 3 mm, which extended into the leaf chamber above the leaf and into the path of actinic light. This light guide was coupled to an external photodiode (OSD15-5T, Centronic, Croydon, UK) whose photocurrent was translated to a voltage by a transimpedance amplifier. Sensor 1 was calibrated *in situ* using sensor 2, a laboratory-built sensor comprising 13 three mm diameter photodiodes (TEFD4300, Vishay, Coatesville, PA, USA) embedded concentrically and evenly across a sensing area identical to that of the cross-sectional measurement area of

the chamber. This lab-made sensor was calibrated against a calibrated CL500a illuminance spectrophotometer (Konica Minolta, Tokyo, Japan) and a Li-Cor quantum sensor (Li-188, Nebraska, USA). The calibration wavelengths used consisted of a 'white' broadband spectrum and 22 narrowband wavelengths in the range 380-740nm which included the two narrowband spectra (480 and 700 nm) used in this study. The calibration procedure was repeated twice to test for consistency; the readings of sensor 2 for each calibration run were found to be identical. The readings of the Licor quantum sensor were on average 3% higher than those of the spectrophotometer for the narrowband spectral distributions lying within the sensitivity region of the quantum sensor (i.e. PAR region) with an 11% overestimation at 422 nm and a 6% underestimation at 519 nm. The CL500a was used as the calibration reference for the lab-made sensor 2 since it is known that the Li-Cor quantum sensor does not have a flat sensitivity across the PAR spectrum and because the CL500a is spectrally resolved and designed to measure accurately for narrow bands across its range of sensitivity. The CL500a also allowed for calibration of sensor 2 outside of the PAR region which is of importance to this study.

Since the polyacrylamide plastic body of sensor 2 had a significantly higher reflectance than the tomato leaves to be measured, it caused more light to be reflected onto chamber walls and back onto itself; the sensor and the upper part of the leaf chamber formed a cavity resulting in overestimation of irradiance relative to the same system with a leaf in place of the white diffuser of the sensor. This was corrected for each irradiance by comparing the irradiance intensity transmitted by glass fibre surrounded by a punched leaf with that obtained using a polyacrylamide disk in place of the leaf. The 4mm diameter window of the glass fibre was positioned in the centre of the chamber (at leaf level) and transmitted light to a USB2000 spectrophotometer (Ocean Optics, Duiven, The Netherlands). The percentage differences in irradiance intensity using either the leaf or polyacrylamide disk did not exceed 4% for any of the irradiances and sensor 2 was corrected accordingly for the wavelength dependent reflection component associated with these irradiance intensity measurements. Sensor 1 was, in turn, calibrated against the corrected sensor 2 and used for routine measurements of irradiance with a leaf *in situ*. Another optical difference between the leaf and sensor 2 was that some light could transmit through the leaf to the lower chamber and, by reflection onto the abaxial side and re-transmission through the leaf, could interact with

sensor 1. However, these second-order reflections from the lower chamber were negligible and ignored.

Chlorophyll fluorescence

Chlorophyll fluorescence was determined using a laboratory-built modulated system. Fluorescence was excited by the application of a red measuring beam with an intensity of 0.25 μmol m^{-2} s^{-1}, produced using a red LED (660 nm peak emission) which was filtered (660 nm) and modulated at approximately 1 kHz (the exact frequency was adjusted to minimize interference from background electrical noise). The excitation beam was coupled to the leaf chamber using a fibre-optic light-guide and a hot mirror was attached to the leaf-chamber end of the fibres to remove fibre fluorescence which otherwise results in a slightly lowered dark adapted Fv/Fm. When required, a saturating light pulse with an intensity of approximately 12 000 μmol m^{-2} s^{-1} was generated using three high power red LEDs (Phlatlite, Sunnnyvale, California, USA) controlled by a laboratory-built timer based on a PIC microcontroller (Microchip Technology, Chandler, AZ, USA). Three fibre-optic light guides, one per LED, delivered the saturating light pulse through three side ports of the leaf chamber. Chlorophyll fluorescence was detected by three GaAsP photodiodes (G1736, Hamamatsu, Hamamatsu City, Japan) spaced evenly below the leaf. Each photodiode was filtered with an RG-9 filter (3mm, Schott, Mainz, Germany) to screen them from filtered excitation light and other short-wavelength irradiances. The photocurrent from these fluorescence sensing photodiodes was pre-amplified using transimpedance amplifiers based on OPA627 operational amplifiers (Texas Instruments, Dallas, Texas, USA). Laboratory-built phase-sensitive detectors further amplified and recovered the fluorescence signals, which were then recorded using a data logger (National Instruments, Austin, Texas, USA) with a 10 Hz low-pass filter on its inputs to further smooth the signals. The maximum quantum efficiency of PSII (Fv/Fm) was determined at the start and end of measurements. Minimum fluorescence (Fo) (i.e. that measured in the dark-adapted state) was determined after the leaf had been subjected to at least 20 minutes of darkness in the leaf chamber and immediately before the measurement of Fm. Light-adapted minimum fluorescence (F'o) was determined by interrupting actinic light and providing a 1 s far-red pulse to oxidise all Q_A and so get an accurate Fo'. Calculations of Φ_{PSII}, Fv'/Fm', and NPQ were made according to (Maxwell and Johnson, 2000).

Measurement procedure

Measurements were taken on third, fully expanded leaves, at about 30 – 35 days after sowing. Leaves were placed in the leaf chamber and allowed to dark-adapt for 20 minutes to determine the rate of dark respiration and Fv/Fm. All leaves used for measurement were healthy with a Fv/Fm >0.8. Actinic light was then applied, commencing with PSII light, and then alternating with PSI light at 65 minute intervals. Light intensities were carefully chosen to meet three criteria:

1. to be sufficiently high to avoid any non-linearity occurring at very low intensities (Kok, 1948),

2. to be well within the strictly light limiting region, and

3. to ensure that CO_2 assimilation rates were comparable for PSI and PSII light to avoid any confusion of state transitions (or other changes) with any intensity-dependent effects (such as photosynthetic induction) upon changing from one light source to the other.

To be sure that the PSI and PSII irradiances produced similar assimilation rates, tests were performed on SUN and SHADE leaves in which PSI light was adjusted so that the steady state assimilation rate matched that developed under a reference absorbed PSII light intensity of 40 μmol m^{-2} s^{-1}. The required PSI-light intensities were 55.6 μmol m^{-2} s^{-1} for SUN leaves and 53.9 μmol m^{-2} s^{-1} for SHADE leaves. The measurements were divided into two sets. In one set of measurements, the rate of CO_2 depletion for 3 replicate leaves was determined with fluorescence measuring beams switched on but actinic light was not interrupted at any point throughout the measurement and saturating pulses were not applied. This had the obvious drawback that only Fs could be determined but ensured that CO_2 depletion traces were smooth and unaffected by disruptions to stable measurement conditions. A second set of measurements included simultaneous measurements of all basic chlorophyll fluorescence parameters at 0.5, 3, 6, 9, 12, 15, 20, 25, 30, 40, 50, and 60 minutes after switching from one light to the other, except for the PSII light application following dark adaptation where fluorescence measurements were taken at 50 and 60 minutes. In this latter group of measurements the responses of the assimilation to PSI or PSII light is less clear because of the superimposed saturating irradiances and interruptions in irradiance.

Leaf light absorption

Leaf light absorption for each leaf was taken as the average absorption of three disks which were punched from the area of the leaf that had been in the gas exchange chamber. The leaf absorption apparatus comprised two integrating spheres (50 mm diameter reflectance and transmittance spheres; Avantes, Appeldoorn, The Netherlands), one used for measurement of leaf light transmission and the other for leaf light reflection. These spheres were used in a light-tight enclosure. The leaf disks were clamped into an aluminum holder that fitted securely to each integrating sphere, positioning the disks above the measurement ports. Leaf transmittance and reflectance were measured using a broadband light source comprising two LED sources; one a warm white LED and the other a blue light source consisting of four LEDs that generated peak wavelengths of 380 nm, 400 nm, 420 nm, and 440 nm (Mightex Systems, Toronto, Canada) to provide improved signal to noise ratio in the blue region. These light sources were coupled to a branched glass fibre which was connected to the measuring light inlet port (angled at 8° to the vertical) of the reflectance sphere, or held at 8° to the vertical and the light focused and directed to the middle of the measurement port of the transmittance sphere. Transmission and reflectance measurements, including the transfer of each disk and light source from one sphere to the other, usually took no longer than 2 minutes. In such a short time period, any chloroplast movement induced by the high intensity broadband measurement light does not interfere to any significant extent on transmission and reflectance measurements. Two spectrometers (USB-4000, Ocean Optics, Dunedin, FL, USA), one per sphere, analysed the transmitted and reflected light with a spectral resolution of 0.2 nm. Leaf absorption was obtained by subtracting transmittance and reflectance values from 1.0. This provided a static, post-measurement leaf light absorption value. To determine how leaf absorption might have changed during gas exchange measurement, SUN and SHADE leaves were placed over the port of an integrating sphere (LiCor 1800-12, LiCor, Lincoln, Nebraska, USA) and subjected to the same irradiance regime that was used for gas exchange. Transmission measurements were taken separately and logged at each of the time intervals used for gas exchange, using the same configuration described for post-measurement absorption measurement. Reflectance was estimated using the relationship between transmission and reflectance data from the post-measurement leaf light absorption measurements.

Results

Basic characterisation of SUN-grown and SHADE-grown plants

SHADE-grown plants were considerably more etiolated than SUN-grown plants (Supplementary Fig. 1, appendix). The chlorophyll a/b ratio, determined by fitting an 80% acetone extract absorption spectrum to that of known absorption spectra for individual pigments (Croce *et al.*, 2002), was higher in SUN plants (3.08) than in SHADE plants (2.89) (Supplementary Fig. 2, appendix).

Gas exchange

Rates of assimilation for SUN and SHADE leaves are shown in Fig. 2. When leaves were exposed to PSII light following dark adaptation, assimilation increased until a steady state was reached. Upon switching from PSII light to PSI light, a sharp drop in gas exchange occurred, reaching a local minimum at about three minutes after the change. Assimilation rate then recovered, increasing over about 50 minutes to a steady state similar to that achieved under PSII light. After switching from PSI to PSII light, the assimilation rate once again decreased and subsequently recovered. However, the drop following a change from PSI light to PSII light is considerably deeper than occurs during the PSII light to PSI light alternations and, furthermore, the recovery is faster with steady state being reached after about 30 minutes. The spikes in assimilation which occurred upon switching from PSII to PSI light are conspicuous; more detailed analysis of these spikes (Fig. 3) reveals a bimodal response of assimilation when switching from PSII light to PSI light; the falling edge of the initial spike is met with a more rounded peak which is generally of lesser magnitude than the spike preceding it. These kinetics occurred within about 1 min after switching and assimilation subsequently dropped to a local minimum (about 2-3 minutes after switching) prior to commencement of recovery in assimilation rate. No such kinetics were observed when switching from PSI to PSII light; assimilation dropped sharply to a local minimum within 1 min.
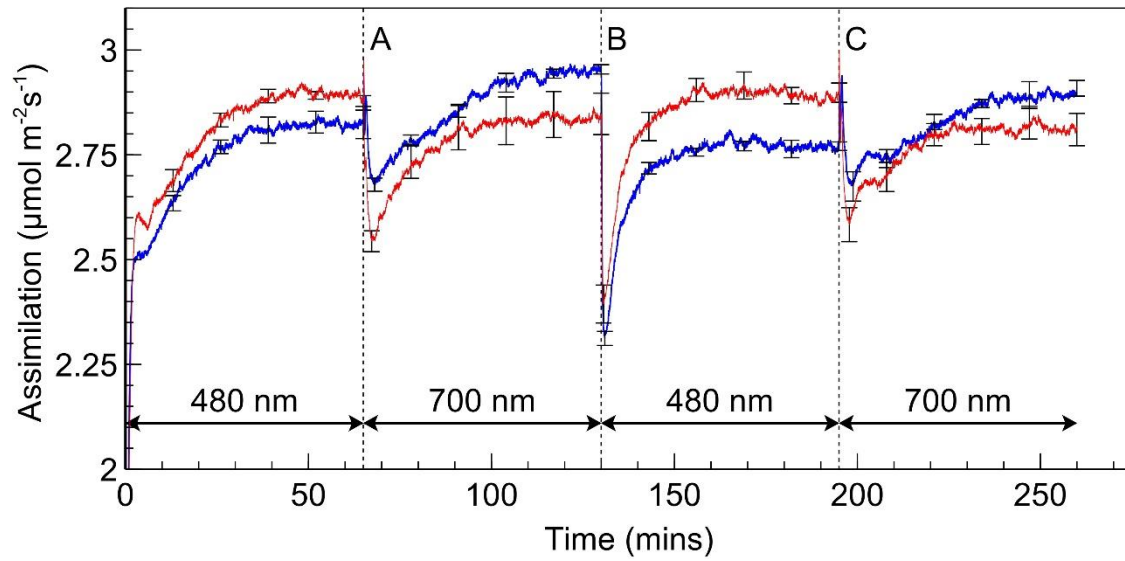
Fig. 2: Rates of assimilation for SUN (red) and SHADE (blue) leaves during a PSII/PSI light regime. Absorbed irradiance was 40 μmol m^{-2} s^{-1} for each irradiance type. Letters 'A', 'B', and 'C' are references for figure 3. Error bars shown represent the SEM (n=3).
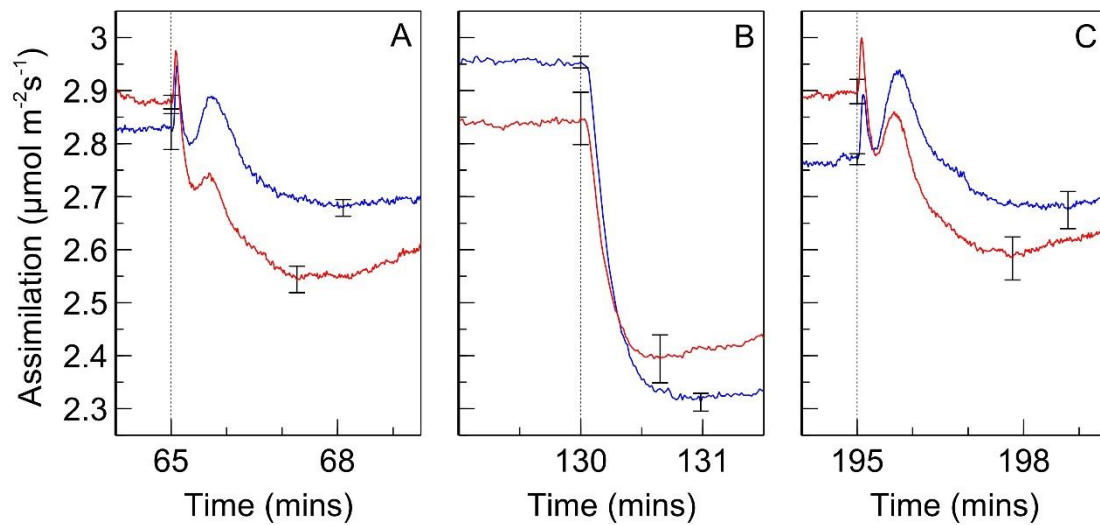

Fig. 3 (A-C): Detailed view of assimilation rate in SUN (red) and SHADE (blue) leaves during (A) switching from PSII to PSI light, (B) switching from PSI to PSII light, and (C) second switching from PSII to PSI light. Letters correspond with data segments by 'A' and 'B' in figure 2. Error bars shown represent the SEM (n=3). The set of error bars to the right of the dotted line correspond with local minima after switching.

We chose irradiances for PSI and PSII light that resulted in nearly identical steady state assimilation rates in order to minimise photosynthetic induction as a potential contributing factor to the observed recoveries in assimilation after switching of irradiance. Nonetheless, a

switch from PSII light to PSI (or back) could potentially produce local photosynthetic induction kinetics because of the different absorption profiles of the two irradiances within the leaf. When alternating to PSI light from PSII light, for example, the PSI light, which is more weakly absorbed by the leaf, more strongly illuminates deeper cell layers. The latter could produce a photosynthetic induction response in those cells, creating a slow increase in the rate of assimilation that is not associated with a state transition. On the other hand, the alternation from PSI light to PSII light, which is more strongly absorbed by the leaf, would result in upper cell layers absorbing considerably more quanta which could also induce a photosynthetic induction.

To more fully exclude photosynthetic induction as a contributing factor to the observed increases in assimilation after a wavelength change, a leaf was exposed to a sequence of PSII and PSI light at half the intensity, followed by the same intensity, used to obtain the results in Fig. 2 (Fig. 4). The same characteristic induction in assimilation was observed when the leaf was first exposed to PSII or PSI light but upon doubling the irradiance intensity the rate of assimilation increases to a new, stable, rate without any of the kinetics observed following a change in wavelength. The short-lived spikes in assimilation upon the doubling of irradiance intensity were further investigated by examining light intensity upon switching but were found to be physiological in nature and not due to an overshoot in irradiance.
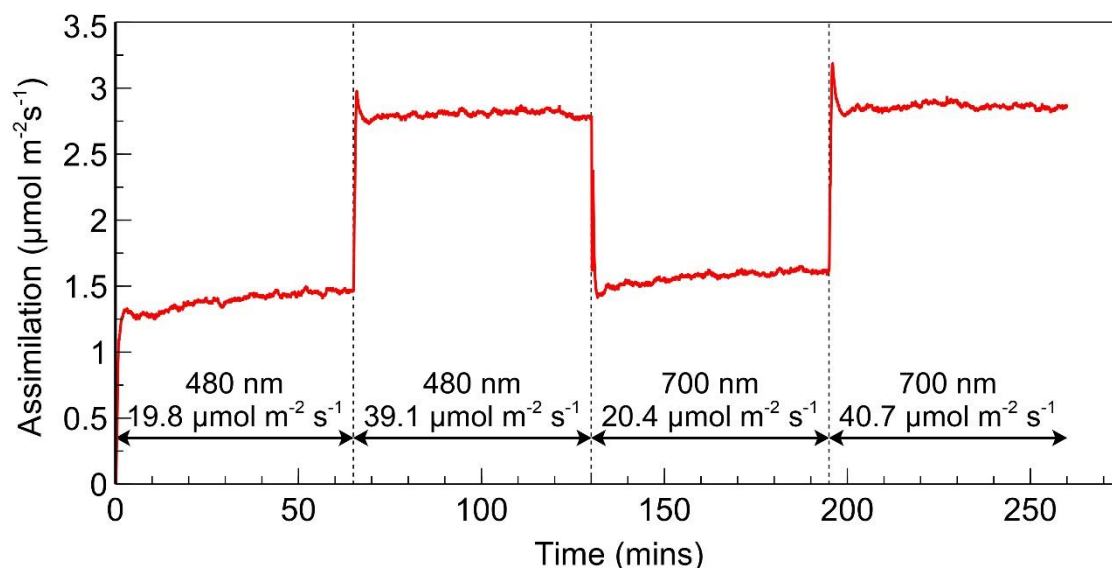

Fig. 4: Rate of assimilation for a SUN leaf initially exposed to PSII light at an absorbed irradiance of about 20 μmol m^{-2} s^{-1} followed by the subsequent doubling of intensity. PSII light was followed in the same manner by PSI light.

Although irradiance intensities were intentionally low and consequently thought unlikely to induce chloroplast movement and associated changes to leaf light absorption, it was nonetheless important to exclude this as a contributing factor to the observed recovery in assimilation after a change in the illumination spectrum. Results for light transmission, reflectance, and absorbance obtained *in situ* (i.e. when in the leaf chamber) from intact leaves subjected to PSII, and subsequently PSI, light are shown in Fig. 5. Transmission and reflectance in dark-adapted SUN and SHADE leaves increased when exposed to PSII light and subsequently decreased when exposed to PSI light. Calculated leaf light absorption for SUN leaves decreased by 2.2% during exposure to PSII light and increased by 2.1% during subsequent exposure to PSI light. The corresponding changes in leaf light absorption for SHADE leaves were 3.8% and 3.1%. In the absence of any other changes it is expected that the effect of these changes in leaf absorption would be to decrease assimilation during PSII
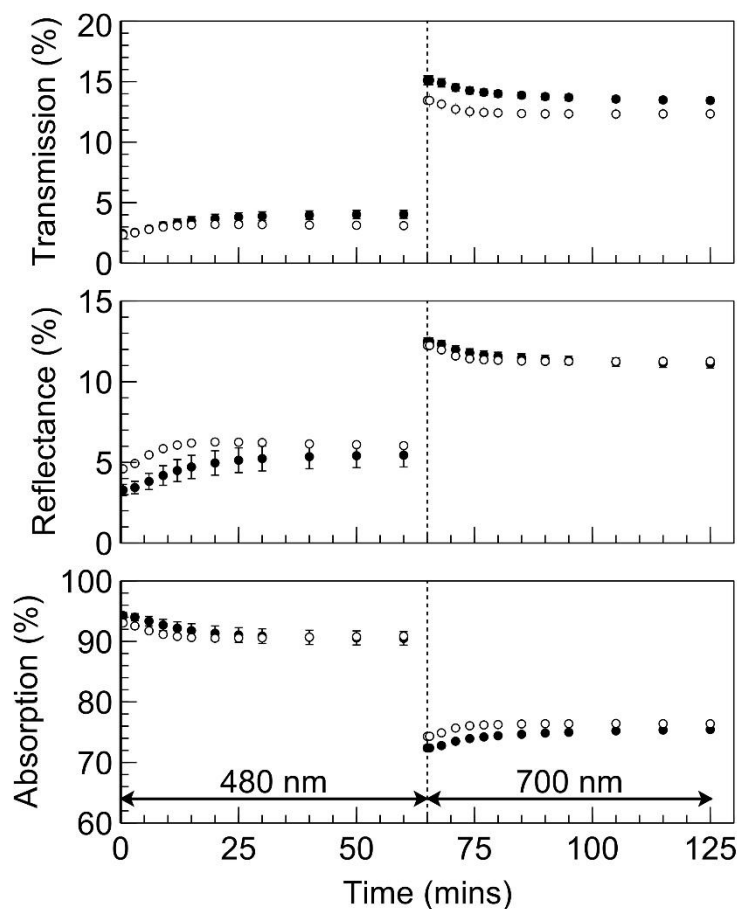

Fig. 5: Leaf light transmission determined *in situ* on intact SUN (open circles) and SHADE (closed circles) leaves together with estimated reflection (based on transmission) and calculated absorption values. Error bars shown represent the SEM (*n*=3).

light exposure as well as to increase assimilation during subsequent exposure to PSI. Φ_{CO2} is a measure of the integrated light-use efficiency of photosynthesis. Fig. 6 shows Φ_{CO2} using either (A) a single light (broadband 'white' light) absorption of leaf discs measured immediately after the gas exchange measurement i.e. a 'static' absorption value or (B) the light absorption of the leaves calculated throughout the measurement of assimilation based on actual leaf light transmission changes i.e. 'dynamic' absorption values. After correcting Φ_{CO2} for the changes in leaf-light absorption there remains a recovery in Φ_{CO2} after exposure of PSII light or PSI light. Owing to the difference in leaf absorption values obtained using either the static or dynamic approaches the quantitative effect of the correction differs between these treatments, but not the existence of the recovery of Φ_{CO2} itself.
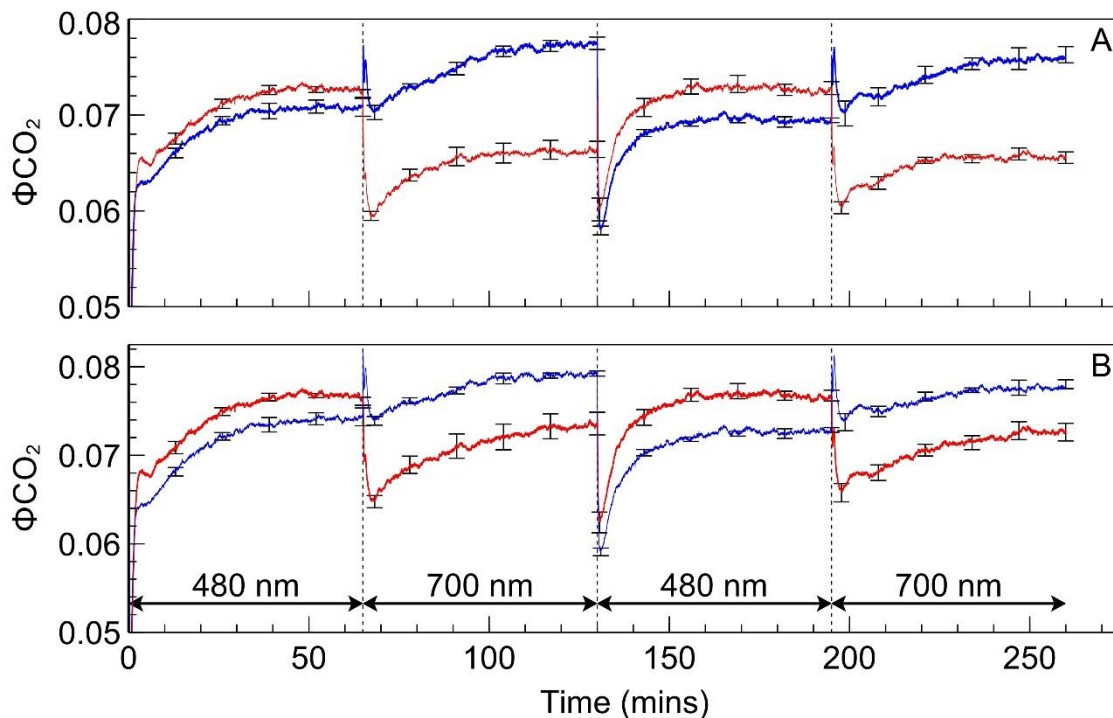

Fig. 6: Φ_{CO2} calculated for SUN (red) and SHADE (blue) leaves using (A) leaf absorption determined from leaf discs directly after gas exchange measurements or (B) calculated leaf absorption determined *in situ* on intact leaves during gas exchange measurements. Error bars shown represent the SEM (*n*=3).

Fluorescence measurements

The fluorescence yield when leaves were transferred from one irradiance to the other (Fig. 7) showed distinct kinetics associated with state transitions (Allen, 1992, Bonaventura and Myers, 1969). The application of PSII light following PSI light exposure, when leaves are in

state 1, creates a surge in fluorescence yield which is gradually quenched as transition occurs to state 2. When switching from PSII light to PSI light, in contrast, fluorescence yield falls abruptly and subsequently increases during transition to state 1. The responses of derived PSII parameters to PSII and PSI light are shown in figures 8 (SUN leaves) and 9 (SHADE leaves), along with the response of Φ_{CO2} for the corresponding leaf type. Values for each fluorescence parameter (closed circles) are scaled and superimposed on the Φ_{CO2} traces to reveal the strong correlations between these data during exposure to either PSII or PSI light.

Switching from PSII light to PSI light produced a prompt increase in Φ_{PSII} in SUN and SHADE leaves to just under 0.8; this increase was greater for the SHADE than for the SUN leaves due to the lower Φ_{PSII} in SHADE grown leaves under PSII light. Following the prompt change of Φ_{PSII} upon switching from PSII to PSI light there was only a slight subsequent slower increase in Φ_{PSII}. The changes in Φ_{PSII} produced upon changing from PSII to PSI light did not parallel the changes in Φ_{CO2}. The switch from PSI light to PSII light was accompanied by a prompt decrease in Φ_{PSII} to a global minimum in SUN (0.47) and SHADE (0.42) leaves followed by a slower increase to a stable value. The kinetics of the prompt decrease and subsequent slower recovery of Φ_{PSII} paralleled closely the changes in Φ_{CO2} produced by the irradiance changes, implying a close coupling between Φ_{CO2} and Φ_{PSII}. The extent of the prompt decrease in Φ_{PSII} was greater for the SHADE grown leaves (46% compared with 38% for SUN leaves) and the subsequent stable value of Φ_{PSII} reached after the slow increase was greater for the SUN grown leaves (ca. 0.65 compared with ca. 0.6 for SHADE leaves).

Φ_{PSII} is the product of Fv'/Fm', the quantum efficiency for electron transport by PSII when all reaction centres are open (strictly it is a relative quantum efficiency), and the photochemical efficiency factor, qP (Genty *et al.*, 1989), which is the factor by which PSII efficiency is decreased as a result of some Q_A being reduced and therefore traps being closed. Trap closure increases the trapping time and so increases the probability that the migrating excited state of chlorophyll a will be dissipated via a non-photochemical route, such as fluorescence or a non-photochemical quenching mechanism (Hendrickson *et al.*, 2004). The changes of qP and Fv'/Fm' after switching from PSII light to PSI light and back again are therefore relevant to understanding the changes in Φ_{PSII}. Qualitatively, the changes in qP are similar to the changes
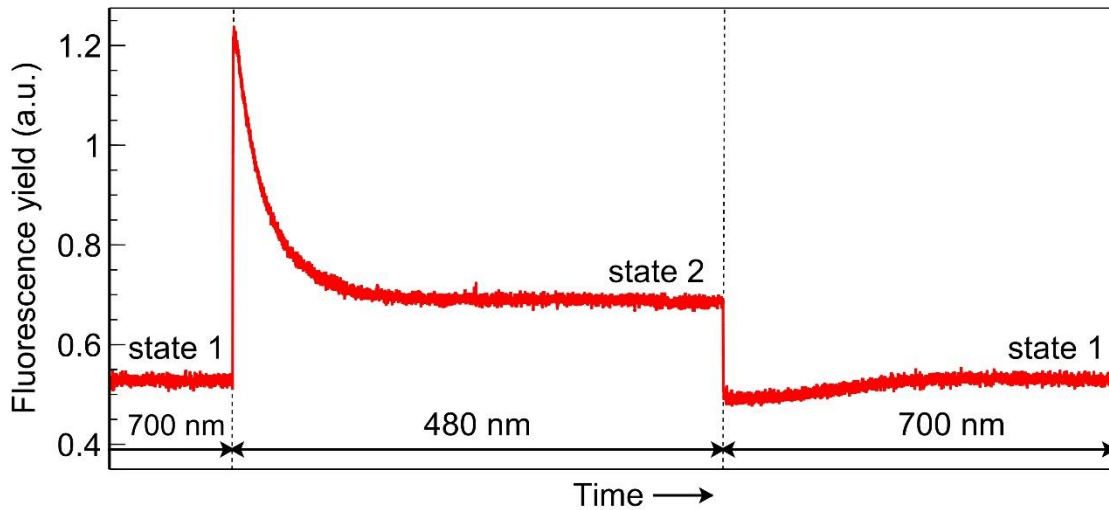
Fig. 7: Segment of fluorescence yield trace obtained with a SUN leaf and bearing classical hallmarks of a state transition. Fluorescence yield changes abruptly upon light switching and subsequent increases or decreases to a new steady state as a state transition proceeds.

in Φ_{PSII}; following a change from PSII light to PSI light qP rises to a value close to one in both SUN and SHADE grown leaves and thereafter remains stable and does not track the changes in Φ_{CO2}, while after the change from PSI light to PSII light qP decreases promptly and then increases slowly in parallel with Φ_{CO2}. Fv'/Fm' in SUN and SHADE grown leaves increases slightly (by c. 0.02) upon changing from PSII light to PSI light, and decreases slightly (by c. 0.02) upon transferring from PSI light to PSII light. In both SUN and SHADE grown leaves after a PSII light to PSI light change the increase of Fv'/Fm' tracks the increase in Φ_{CO2}. Upon switching from PSI light to PSII light Fv'/Fm' decreases while Φ_{CO2} increases; in SUN grown leaves these corresponding changes are weakly correlated whereas in SHADE grown leaves no correlation exists. The ratio of light adapted maximum fluorescence to dark adapted maximum fluorescence (Fm'/Fm) increases after a PSII light to PSI light transition by 16% in SUN leaves and 15% in SHADE leaves, indicating corresponding increases in PSII antennae size, and these increases track the increase in Φ_{CO2}. Corresponding increases in the minimum fluorescence equivalent (Fo'/Fo) were 13% in SUN leaves and 10% in SHADE leaves. Fm'/Fm and Fo'/Fo decrease after a PSI to PSII light transition and are negatively correlated with the subsequent increase in Φ_{CO2}. These decreases in Fm'/Fm were 16% for SUN leaves and 14% for SHADE leaves while corresponding decreases in Fo'/Fo were 7% for SUN and SHADE leaves. NPQ

(Fm/Fm' – 1) increases after a PSI to PSII light transition, tracking the increase in Φ_{CO2}, and is negatively correlated with increases in Φ_{CO2} following a PSII light to PSI light transition.

The relationship between fluorescence parameters and Φ_{CO2} were examined in further detail by plotting each fluorescence-derived parameter against Φ_{CO2} (Fig. 10). In SUN and SHADE leaves subjected to PSI light, the increase in Φ_{CO2} as the transition from state 1 to state 2 proceeded was not accompanied by changes in Φ_{PSII} or qP. When these leaf types were exposed to PSII light, however, increases in Φ_{CO2} were accompanied by corresponding increases in Φ_{PSII} and qP. In SHADE leaves the PSI-light data points are right-shifted and the PSII-light data points are left-shifted compared to SUN leaves. No significant changes in Fv'/Fm' occurred during either a state 1 to state 2 transition or a state 2 to state 1 transition. Parameters Fo'/Fo and Fm'/Fm were positively related to Φ_{CO2} under PSII light but negatively related to Φ_{CO2} under PSI light, implying an effect of PSII cross sectional area on Φ_{CO2}.

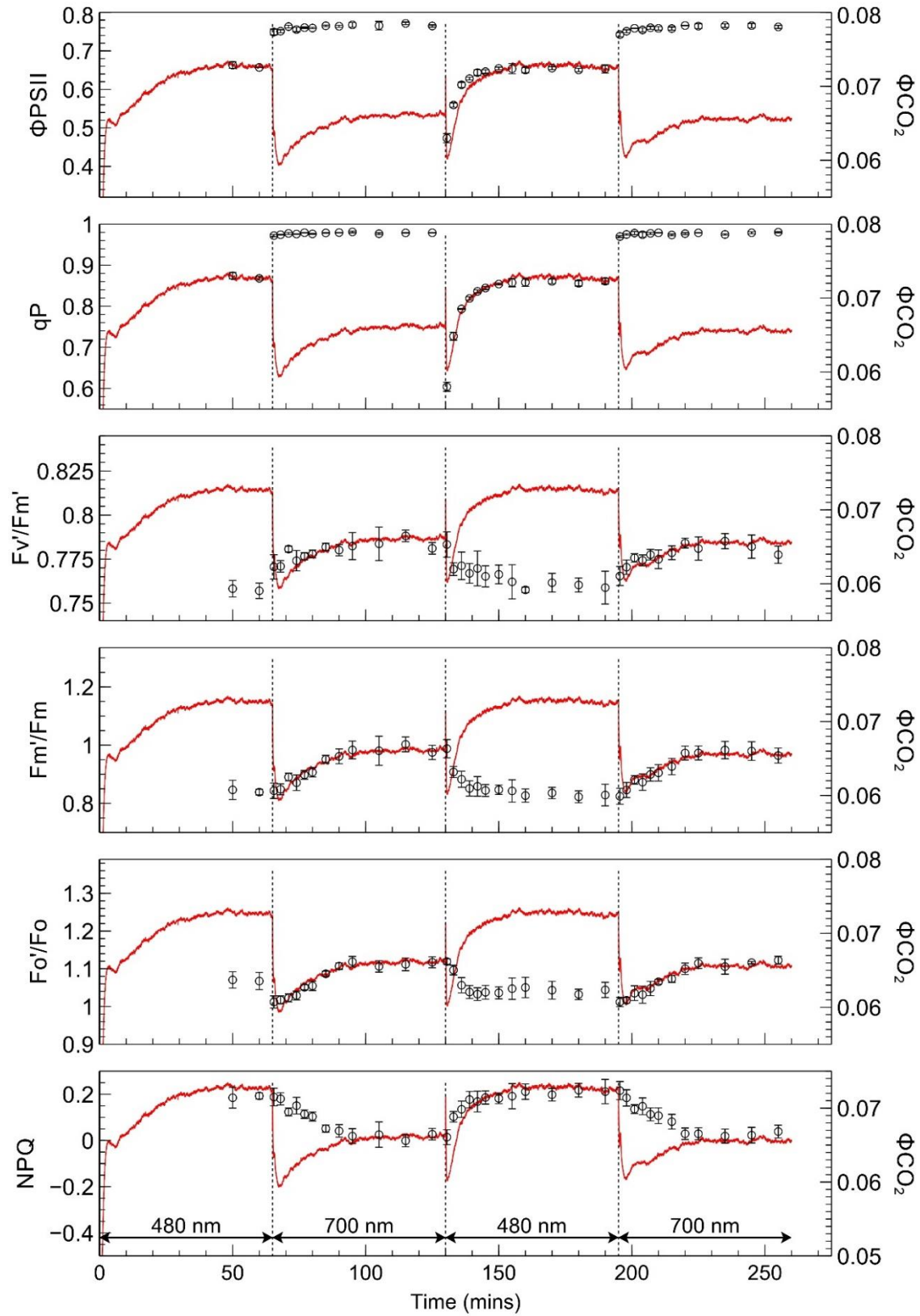Fig. 8: Measurements of Φ_{PSII}, qP, Fm'/Fm, Fo'/Fo, Fv'/Fm' and NPQ (open circles) for SUN leaves, superimposed on light-limited Φ_{CO2} traces for SUN leaves. Error bars shown represent the SEM (n=3).
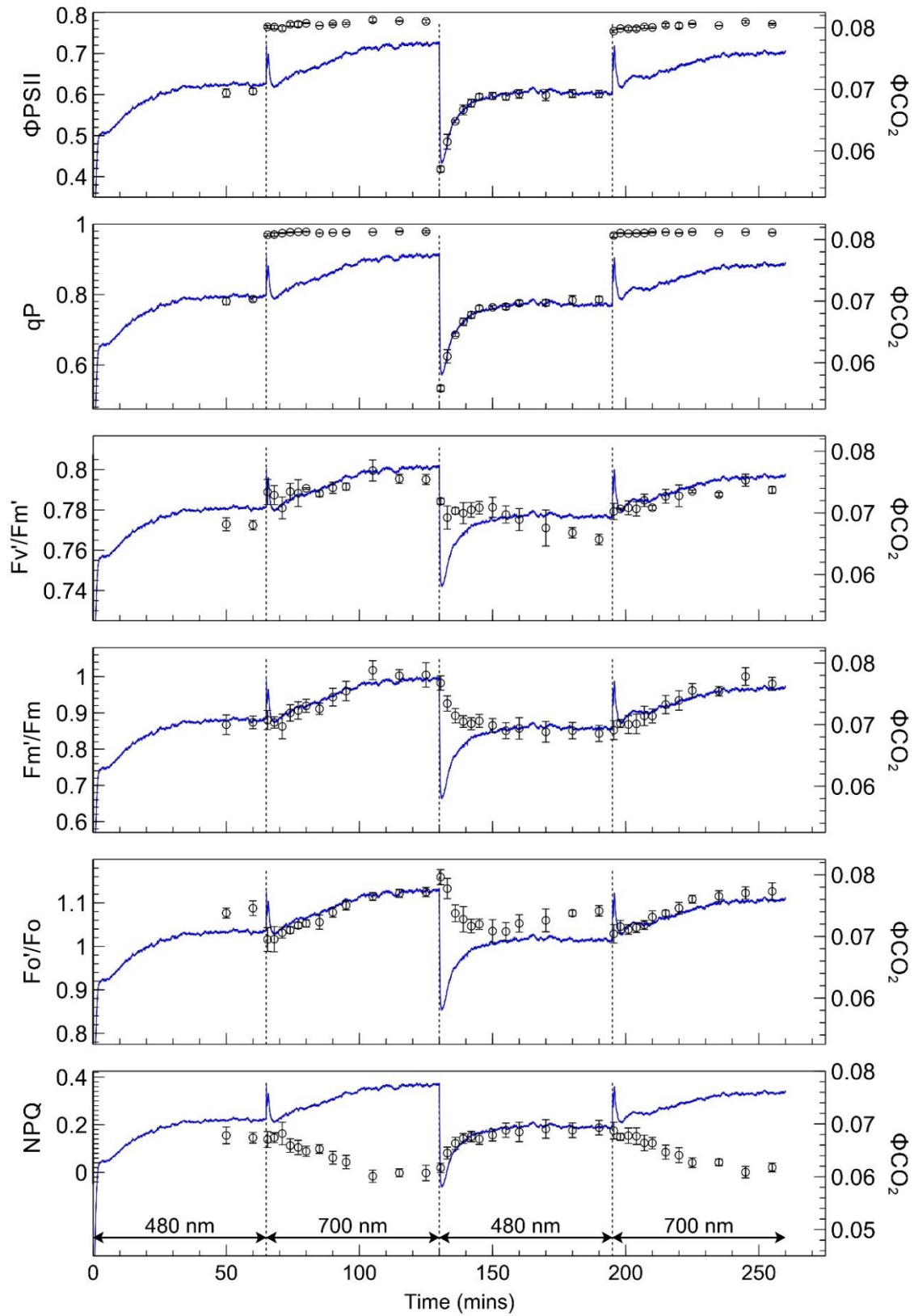
Fig. 9: Measurements of Φ_{PSII}, qP, Fm'/Fm, Fo'/Fo, Fv'/Fm' and NPQ (open circles) for SHADE leaves, superimposed on light-limited Φ_{CO2} traces for SUN leaves. Error bars shown represent the SEM (n=3).
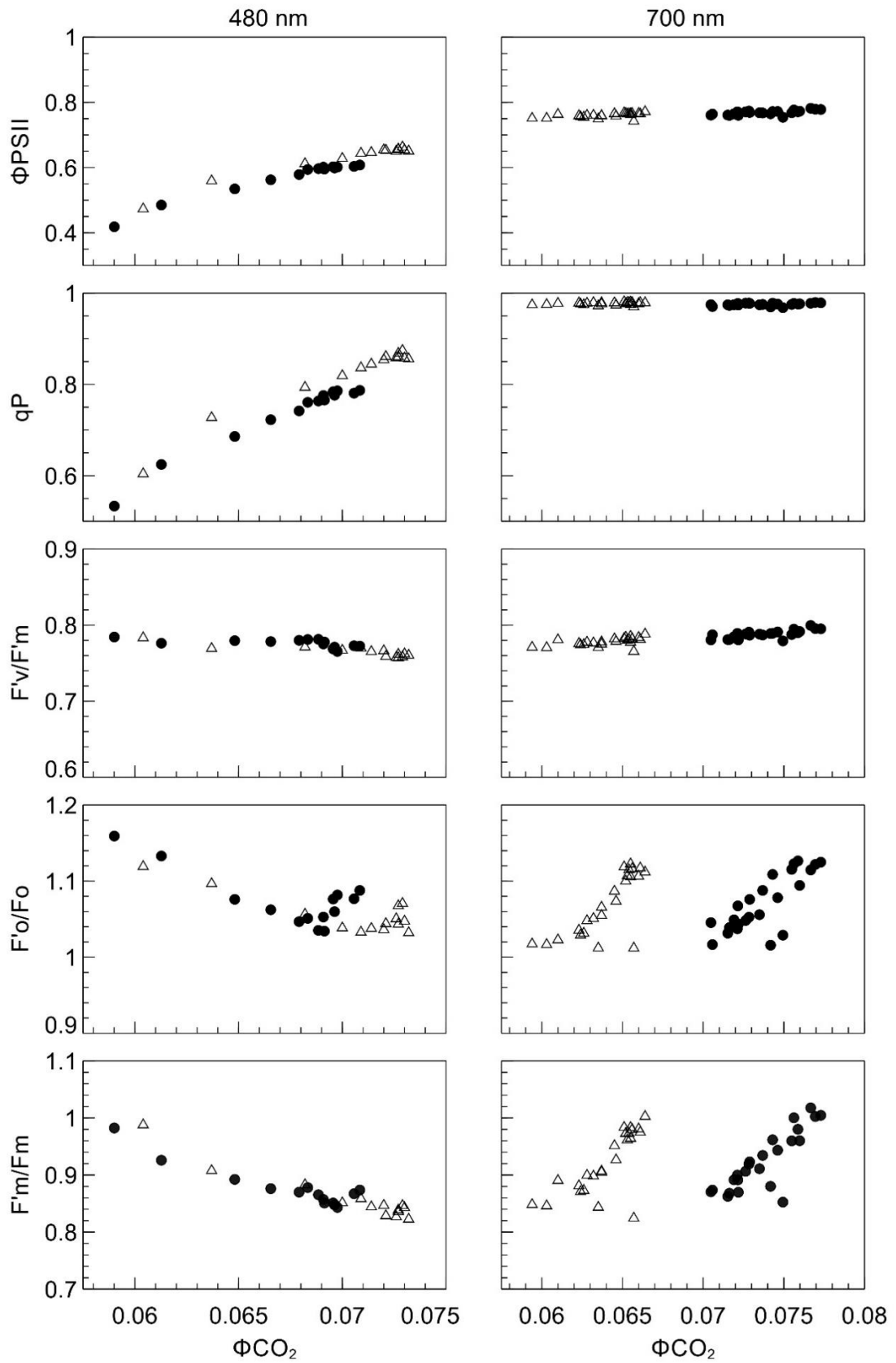
Fig. 10: Relationship between Φ_{CO_2} and Φ_{PSII}, qP, Fv'/Fm, and Fo'/Fo, Fm'/Fm for SUN (open triangles) and SHADE leaves (closed circles) presented with 480 nm and 700 nm irradiance (n=3).

Discussion

We present compelling evidence for the first time of a relationship between state transitions and photosynthetic efficiency in a higher plant. State transitions are known to occur in algae, cynaobacteria and higher plants but until now an accompanying increase in photosynthetic efficiency during a state transition had been observed only in algae and cyanobacteria (Bonaventura and Myers, 1969; Murata, 1969; Canaani, 1986; Andrews *et al.*, 1993). A relationship between state transitions and photosynthetic efficiency is predicted if the widely held view of state transitions as a short-term energy redistribution mechanism is to be accepted. The absence of such a relationship in higher plants has created difficulty in understanding the functional significance of state transitions in leaves. In the present study, SUN and SHADE leaves were subjected to a sequence of PSI and PSII light known to result in closely matched rates of assimilation at steady state. Switching between each light type was followed by a drop in assimilation rate and a subsequent increase to a steady state occurring over about 30 minutes.

Changes in Fm'/Fm and Fo'/Fo, which correspond to changes in PSII antennae size expected to occur during a state transition, closely tracked changes in Φ_{CO2} in SUN and SHADE leaves; Φ_{CO2} is a measure of the integrated light-use efficiency of photosynthesis, including PSII and PSI. If Fm'/Fm is considered as directly proportional to PSII cross-sectional area (Allen, 1992) then the latter decreased by 16% in SUN leaves and 14% in SHADE leaves during transition from state 1 to state 2 under PSII light. These figures lie between a reported 11% decrease in PSII antennae size for Arabidopsis (Kim *et al.,* 2015) and a c. 20% decrease in spinach (Forti and Fusi, 1990), and the mobile LHC pool size determined in the present study is thus also less than a figure of 20% reported for maize (Bassi *et al*., 1988). These decreases in PSII antennae size which we observed (and subsequent increases) represent fully reversible binary states, consistent with the reversible nature of state transitions. Since Φ_{CO2} increases after a switch to PSII light while PSII antennae size decreases, this raises the question about the docking location of mobile LHCII which detaches from PSII. While this study has not directly resolved this question, it has established that the reorganization at the molecular level following a switch from PSI to PSII light (state 1 to state 2) partially alleviates a limitation which affects Φ_{CO2} and thus produces an increase in photosynthetic light-use efficiency. Andrews *et al.* (1993) observed small increases in Φ_{PSI} following a switch from PSII to PSI light, implying that

the rate of electron turnover through PSI is the limitation. The findings by those authors fits well with the view that PSI is the docking location of mobile LHCII in state 2 (Galka *et al.*, 2012; Ünlü *et al.*, 2014) but conflicting findings exist in literature (e.g. Haworth and Melis, 1983). In the present study the increase in Φ_{CO2} with a decrease in PSII antenna size (e.g. a decrease in Fm'/Fm) would be consistent with detachment of LHCII from PSII and its attachment to PSI, resulting in an increase in the combined light-use efficiency for linear electron transport.

State transitions were accompanied by small changes in Fv'/Fm' which indicate that changes in the efficiency with which an electron was transferred to PSII occurred during state transitions. Fv'/Fm' increased upon exposure to PSI light when a state 2 to state 1 transition occurred and it decreased (abruptly) under PSII light when a state 1 to state 2 transition occurred. The same pattern was observed in wheat leaves exposed to a similar PSI/PSII light regime (Andrews *et al.*, 1993). Those authors suggested that changes in non-photochemical quenching, possibly through modification of PSII antennae, as a possible cause for the observed changes in Fv'/Fm'. Indeed, in the present study, steady state NPQ decreased from ca. 0.2 in leaves exposed to PSII light to zero in leaves exposed to PSI light, but such a change would be expected as the result of a decrease in the PSII antenna size occurring as a result of LHCII movement. A possible explanation for the decrease in Fv'/Fm' following exposure to PSII light is that any attachment of LHCII to PSI would increase the amount of PSI fluorescence. PSI fluorescence contributes to both the Fo or Fo' (e.g. 2) and the Fm or Fm' fluorescence yields, but the relative contribution to the Fo and Fo' signals is greater (e.g. 38) so any increase in PSI fluorescence would be expected to decrease Fv'/Fm' so this change is consistent with a state transition detaching LHCII from PSII followed by its attachment to PSI.

Following exposure to PSII light Φ_{CO2} increases in parallel with Φ_{PSII} and these changes in Φ_{PSII} are largely due to qP as the changes in Fv'/Fm' were small. The changes in qP are due to the decrease in PSII antenna size (Fm'/Fm decreases) and probably the increase in PSI antenna size. Correlation of the flux of electrons through PSII with that of the demand of reductant for carbon dioxide fixation can often be done with reference to Φ_{PSII} alone (e.g. Genty *et al.*, 1989; Genty and Harbinson, 1996). In this case, however, the changing antenna size of PSII during exposure to PSII light means that PSII electron transport is not governed by changes only in Φ_{PSII} as this measure includes no direct involvement of antenna size.

We used SUN and SHADE leaves to explore the potential impact of considerably different growth spectra on state transitions. Whereas the SUN leaves were produced under a spectrum which preferentially excites PSII (PSII light), SHADE leaves were produced under a spectrum which preferentially excites PSI (PSI light). The different leaf types displayed the 'memory' of growth spectra with respect to growth irradiance; SHADE leaves utilized the PSI light more efficiently (c. 16%) than SUN leaves whereas SUN leaves utilized PSII light only slightly more efficiently (c. 3%) than SHADE leaves. The higher chlorophyll a/b ratio of SUN leaves compared with that of SHADE leaves is indicative of a higher PSI/PSII ratio in SUN leaves (and lower PSI/PSII ratio in SHADE leaves) (7, 40) which is consistent with the differences in light use efficiency with respect to light type observed in the present study. The difference between leaf types in terms of the efficiency of PSI and PSII light utilization is further illustrated by plotting Φ_{CO2} (x-axis) against Φ_{PSII} (y-axis); data points for SUN leaves corresponding with PSII light are right-shifted compared with that for SHADE leaves and the opposite is true for the PSI light points. The same 'memory' of growth spectrum has been found to occur in leaves as a result of long term acclimatory processes which tune photosystem stoichiometry to growth spectrum (Chow *et al.*, 1990; Hogewoning *et al.*, 2012). Clearly state transitions are capable of mitigating, but not eliminating, losses in Φ_{CO2} arising from imbalanced photosystem excitation; as in cucumber leaves produced under the same artificial sun and shade growth spectra the PSII acceptor side remains strongly reduced in state 2 (Hogewoning *et al.*, 2012). This is consistent with the view of state transitions as a 'fine-tuning' energy redistribution mechanism (Anderson *et al.*, 1995). In terms of the extent of state transition and $\Delta\Phi_{CO2}$ in the two leaf types, $\Delta\Phi_{CO2}$ during transition from state 2 to state 1 was c. 10% and c. 13% during a transition from state 1 to state 2 in both leaf types. The similar changes in $\Delta\Phi_{CO2}$ are proportional to corresponding changes in antennae size of PSII and suggest that growth history does not affect the size of the mobile LHCII pool or its effect on $\Delta\Phi_{CO2}$.

The reasons why we observed a recovery in overall photosynthetic light-use efficiency (i.e. Φ_{CO2}) upon light switching while Andrews *et al.* (1993) did not cannot be resolved in the present study. However, our fluorescence results bear striking resemblance to those presented in their study in terms of characteristics and extent upon light switching. On the other hand, our results are in agreement with Bonaventura and Myers (1969) who observed

a recovery in the rate of oxygen evolution which they note had similar kinetics to that of fluorescence yield. In *Chlamydomonas* a greater proportion of LHCII is mobile than in higher plants, possibly as a result of the lower amount of thylakoid stacking in *Chlamydomonas* compared with higher plants which makes LHCII more accessible for phosphorylation kinases (Dekker and Boekema, 2005). At least in tomato we show that changes in assimilation track changes in the fluorescence-derived parameters characteristic of state-transitions, which implies that assimilation measurements could be used to measure state-transitions in leaves.

Detailed analysis of the spikes in assimilation which occurred upon switching from PSII to PSI light revealed more intricate bimodal assimilation kinetics. To exclude a spike in actinic light intensity or any other spurious in light intensity upon light switching as the cause of these kinetics, a high-speed photodiode light monitoring circuit connected to an oscilloscope was used to probe light intensity upon light switching. It was found that light intensity ramped up (and down) to the desired intensity for PSI and PSII light within a matter of microseconds and no overshoot occurred. The observed kinetics in assimilation are therefore physiological in nature. When switching from PSII light to PSI light the PQ pool is rapidly oxidised and during this very brief period a greater flux of electrons flows through PSI. This creates a temporarily better balanced flux of electrons through the photosystems which results in a brief spike in assimilation rate. The principle of this mechanism is therefore related to the Emerson enhancement effect (Emerson, 1957, 1958). The 'residual enhancement effect' which we observed in the present study shows that, under unique conditions, enhancement can be a brief artefact of previous irradiance conditions due to the capacitive nature of the PQH_2 pool.

The ability to observe state transitions by relatively straightforward gas exchange and fluorescence methods creates a new avenue to explore the link between photosystem organisation and CO_2 assimilation. Whether this relationship is preserved in a natural, ecophysiological context, remains to be elucidated.
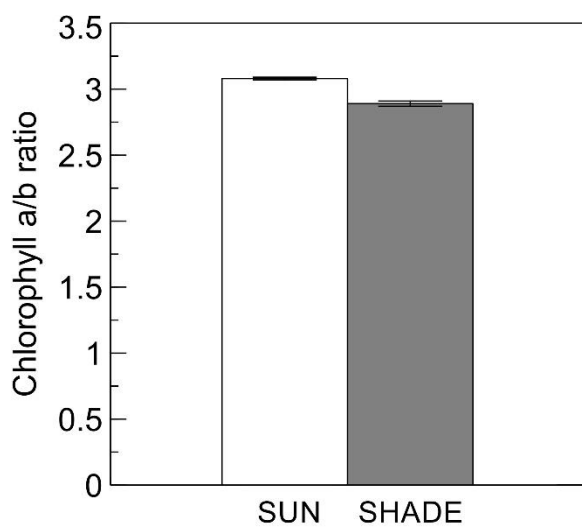
Acknowledgements

Appendix

Supplementary Fig. 1: SUN grown plant (left) and SHADE grown plant (right) at about 20 days after sowing, showing the difference in etiolation caused by the light treatments.

Supplementary Fig. 2: Chlorophyll a/b ratios for SUN and SHADE leaves. Error bars shown represent the SEM (n=3).

CHAPTER 4

Unraveling the effects of blue light in an artificial solar background light on the growth of tomato plants

Abstract

While the use of narrowband irradiance regimes containing different blue light fractions has proven useful to unravel blue light effects on plants at a fundamental level, it does not quantify the responses to blue light under natural daylight conditions. The objective of this study is to understand the blue light growth responses by combining photosynthetic measurements with measurements of whole-plant light absorption in a simulated daylight spectrum enriched with different levels of blue light. To achieve this, tomato plants were grown under six different combinations of artificial solar light and blue LED light. Light treatments were defined by the blue light (400–500 nm) fraction of total photosynthetic photon flux density (400–700 nm) and included 27% (no additional blue LED), 28%, 31%, 38%, 43% and 61% blue light with a total photosynthetic photon flux density of 100 µmol m^{-2} s^{-1} in all treatments. Whole-plant light absorption was estimated by using ray tracing simulation combined with measured 3-dimensional structure of the plant and optical properties of the leaves. The total dry weight of the plants decreased linearly with the increase of blue light fraction; the dry weight of the plants grown under 27% blue being 1.6 times greater than that of the plants grown under 61% blue. This large difference was related to lower light absorption by the plants when fraction blue light increased, due to more compact morphology, i.e. lower leaf area, leaf length/width ratio and shorter stem. Light-limited quantum yield and maximum photosynthetic capacity were not affected by blue light fraction. In the case of the latter, which in other studies has often been found to be positively related to blue light fraction, it may be that the blue light fraction already present in the daylight source had saturated this response. Overall, increasing the blue light fraction in a solar light background decreases growth mainly through its effect on plant morphology and light interception. It remains to be elucidated whether the responses observed using the low growth light intensity in the present study are maintained in high light growth environments more characteristic for tomato growth and production.

Introduction

Light is not only the source of energy for photosynthesis but also a source of information about the plant's environment. Since leaves absorb red and blue light strongly but far-red light only weakly, plants themselves greatly modify the natural light environment through the canopy in a wavelength dependant manner by acting as selective optical filters. For example, the particularly weak absorption of far-red light relative to shorter wavelengths means that transmitted light is relatively enriched with far-red light. In contrast, leaves in the upper canopy, which are exposed to direct sunlight, are exposed to a comparatively red and blue-enriched spectrum. These spectral signatures associated with either shade or direct sunlight are translated by various photoreceptors into physiological changes of adaptive benefit. For example, the red:far- red ratio – high in direct sunlight but low in shade – is sensed by phytochrome which triggers etiolation when this ratio is low. The obvious adaptive benefit of this 'shade avoidance syndrome' (SAS) (Smith, 1982) is the potential for improved light capture by at least maintaining a similar height to neighbouring plants (Nagashima and Hikosaka, 2011). Although less well characterised than the impact of the red:far-red ratio on SAS, blue light depletion also provides similar information about shading and has been associated with the SAS phenotype (Keller *et al.*, 2011; Keuskamp *et al.*, 2012, 2011). For example, Arabidopsis grown using a spectrum containing reduced blue light resulted in comparatively more hypocotyl elongation (Pierik *et al.*, 2009) whereas increasing the fraction of blue light in tomato using a white light or red light mixture had the opposite effect by decreasing plant height (Snowden *et al.*, 2016). Snowden *et al.* (2016) also observed that petiole length and leaf area index (LAI) decreased under higher blue light fractions. Similarly, several other authors have confirmed the occurrence of reduced stem elongation and increased tomato plant compactness when the fraction of blue light increased, either in narrowband blue:red combinations or under broadband light (Glowacka, 2004; Hernández *et al.*, 2016; Kaiser *et al.*, 2019; Nanya *et al.*, 2012). These photomorphogenic responses to blue light are known to be regulated by cryptochrome (Ahmad *et al.*, 2002).

At the leaf level, chloroplast movement from the anticlinal position to the periclinal position is mediated by phototropin (Suetsugu and Wada, 2013). Stomatal opening, though not exclusively an effect of blue light, is also mediated by phototropin in the guard cells. An action spectrum for stomatal opening in *Xanthium strumarium* showed that blue light exerted a considerably stronger effect on stomatal opening than red light (Sharkey and Raschke, 1981). Those authors reported that the peak efficacy in the blue region was about 10 times greater than the peak in the red region. At the thylakoid level, blue light has been shown to create 'sun type' chloroplasts compared with red

light alone; these are chloroplasts which bear the architectural features of chloroplasts produced under high light i.e. smaller grana stacks and less lamellae (Lichtenthaler *et al.*, 1980). These changes at the thylakoid level are consistent with a higher maximum photosynthetic capacity (A_{max}). In a blue light dose-response study, A_{max} in cucumber increased as the blue light fraction increased from 0% to 50% in a red light background (Hogewoning *et al.*, 2010a). In similar studies A_{max} in spinach increased when the fraction of blue light was increased up to 33%, and compared to rice grown under red light adding 25% blue light increased photosynthetic capacity by 88% (Matsuda *et al.*, 2004, 2007).

Under low light conditions, however, light-use efficiency of photosynthesis (and overall light capture), rather than A_{max}, is relevant to growth. In the short-term, blue light is known to drive photosynthesis under light-limited conditions less efficiently than red (Hogewoning *et al.*, 2012; Hoover, 1937; Inada, 1976; McCree, 1972a). This is due, at least in part, to the absorption by carotenoids which transfer energy to chlorophyll molecules with less efficiency (ca. 70%) than chlorophyll to chlorophyll energy transfer (Croce *et al.*, 2001). In the longer term, however, red irradiance alone results in abnormal PSII functioning as evidenced by suppressed Φ_{PSII} which manifests as reduced Φ_{CO2} and dysfunctional stomata compared with blue-red light mixtures (Hogewoning *et al.*, 2012). When red light was supplemented with 25% blue light the rate of light-limited photosynthesis in rice increased by 53% (Matsuda *et al.*, 2004).

The wide variety of blue light responses across different scales makes blue light a potentially useful spectral tool with which to explore relationships between photosynthetic and photomorphogenic effects at the whole-plant level. While the use of narrowband irradiance regimes containing different blue light fractions has proven useful in unravelling blue light effects at a fundamental level, these studies do not quantify the responses to blue light under natural daylight conditions. Since natural daylight already contains approximately 27% blue light (Hogewoning *et al.*, 2012), it is not known whether the addition of more blue light would enhance the potentially already saturated blue light responses even at low daylight levels. This study adopts a holistic approach to understanding blue light responses at the whole-plant level by combining photosynthetic measurements at leaf-level with estimations of whole-plant light absorption in a simulated daylight spectrum with, and without, different doses of blue light supplementation. This approach quantitatively relates photomorphogenic responses to whole-plant absorption and allows for the disentanglement of the contribution of photosynthetic and photomorphogenic changes to whole-plant biomass.

Materials and methods

Plant material and growing conditions

Tomato seeds (*Solanum lycopersicum* cv. Moneymaker) were sown in rockwool blocks (7 cm · 7 cm · 7 cm) (Grodan, Roermond, The Netherlands) and covered with a layer of vermiculite. Sown blocks were placed in a climate chamber under fluorescent tubes (TLD 36 W/840 HF, Philips, The Netherlands). The photosynthetic photon flux density (PPFD) at the rockwool level was 100 μmol m^{-2} s^{-1} and the photoperiod was 16 h. The air temperature and relative humidity in the climate chamber were set to 20 °C, and 70%. The atmospheric CO_2 concentration was ambient. A week later, when seedlings had emerged, a group of the most homogeneous seedlings were transferred to a different climate chamber and placed in groups of five inside plant growth tents (160 cm · 80 cm · 80 cm). The seedlings remained in the growth tents for 30–32 days after sowing, having developed at least seven leaves longer than 1 cm. The measured average air temperature in the growth tents was 23.5 °C and the average relative humidity 66.5%. CO_2 concentration was ambient. Plants were irrigated daily at 8:00 AM for 10 min by ebb and flood technique, using a Hoagland solution (EC 1.2, pH 5.9). Inside each tent, a transparent, spectrum-neutral (400–800 nm) heat screen above the plants separated the climates of the plant compartment (bottom) from the light source compartment (top), blocking part of the radiative heat transfer to the plants (Sonneveld *et al.*, 2006). In both compartments, two 80 mm fans were used to exchange air between the tent and the growth chamber. Additionally, the bottom compartment was equipped with four extra fans (80 mm, 12 V) to ensure a homogenous distribution of air temperature.

Light treatments

Each growth tent was equipped with a plasma lamp (AS1300, Plasma International GmbH, Offenbach am Main, Germany), suspended 153 cm above the rockwool blocks, providing an artificial solar (AS) broadband spectrum (Fig. 1). Furthermore, there was an array of blue (B) LEDs (a prototype design, Philips, Eindhoven, The Netherlands), suspended 93 cm above the rockwool blocks, providing blue light with a peak wavelength at 450 nm. The output of both light sources was controlled by digital controllers. A spectrum-neutral diffusing screen made from disposable non-woven fabric material was placed 5 cm under the LED array. The screen was used to improve uniformity of both intensity and light spectrum in the tent. All light treatments had equal PPFD and photoperiod (100 μmol m^2 s^{-1} for 16-hs). The spectrum of each treatment was adjusted by replacing part of the broadband plasma lamp light with blue LED light. Therefore, the treatments were defined

based on the fraction blue (400–500 nm) they contained in their recorded total PPFD (400–700 nm): 27% (no blue LED), 28%, 31%, 38%, 43% and 61%. The light spectrum was measured in every tent at plant apex height, using a spectroradiometer (USB2000 spectrometer, Ocean Optics, Duiven, The Netherlands) (Fig. 1). Two groups of plants were used for measurements: those for photosynthesis measurements and those for morphology measurements. For plants designated for morphology measurements, PPFD was measured at five locations at plant apex height using a quantum sensor (LI-190, Li-Cor, NE, USA). To maintain constant PPFD and blue light fraction at the apex of every growing experimental plant, both plasma and blue LED outputs were manually adjusted every two days. Additionally, plants were rotated every two days to minimize the effect of spatial variation in the environment within the tent. Plant positioning in the tents was done in such a way that mutual shading and touching were prevented. The phytochrome photostationary state (P_{fr}/P_{total}) of all light treatments was calculated according to Sager *et al.* (1988) (0.71, 0.72, 0.72, 0.70, 0.70 and 0.68 for the treatments with 27%, 28%, 31%, 38%, 43% and 61% blue light, respectively). In plants designated for photosynthesis measurements the aim was to maintain a light intensity of 100 µmol m^{-2} s^{-1} at the apex until the third leaf developed, at which point the third leaf became the reference point for light intensity adjustments. Where necessary, the third leaf was gently supported with a wooden dowel to ensure that it was positioned normal to the irradiance.
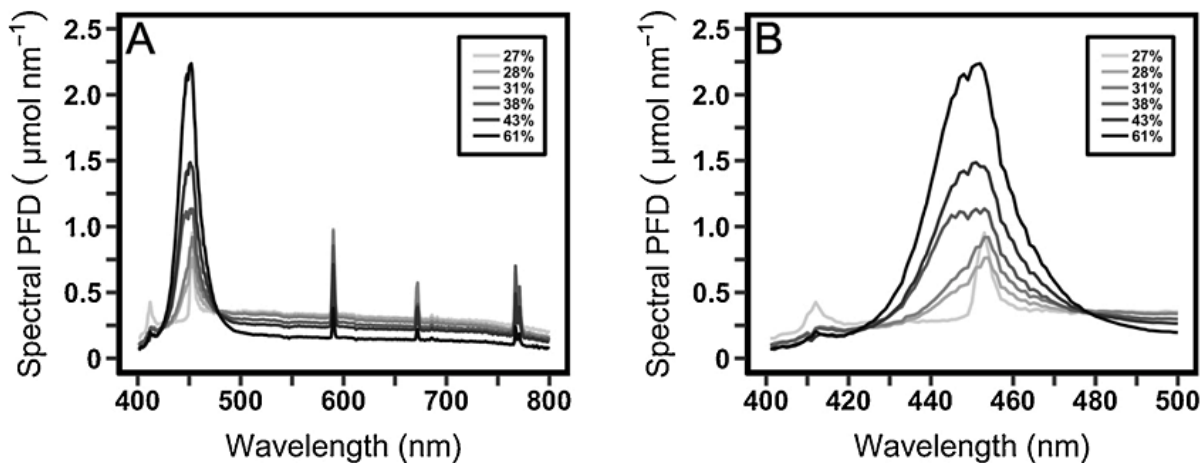

Fig. 1: Spectral light distribution (A: 400 – 800 nm, B: 400 – 500 nm) of plasma lamp without blue light supplementation (containing 27% blue light) and with blue light supplementation resulting in 28%, 31%, 38%, 43% and 61% blue light fraction.

Measurements

Thirty days after sowing, plant internode length, petiole length (distance from stem to first leaflet), leaf length (distance from first leaflet to the tip of the last leaflet) and leaf width were measured. The third leaf (counting from the bottom) was selected as representative for analysis since the first and second leaves of tomato plants have distinct and irregular shapes compared to the rest. The internode, hypocotyl and leaf dry weights were measured after oven-drying for 16 h at 70 °C initially, followed by 22 h at 105 °C. The area of every leaf was measured using an area meter (Li-3100, Li-Cor, NE, USA). The specific leaf area (SLA) of every leaf was calculated by dividing its measured area by its measured dry weight (including petiole). For the determination of the leaf number per plant, only leaves with a length of >1 cm were used. On the same day, leaf optical properties were measured on other plants. Leaves 1–3 (counting from the bottom) were taken from the plant, immediately placed inside plastic bags and stored for two hours in cold storage room (5 °C). Directly before the measurement, two leaf discs (1 cm diameter; leaf margins and veins were avoided) were taken from the fourth leaflet (counted acropetally) of each stored leaf. Optical properties were measured on both sides of the leaf disc with a custom-built integrating sphere leaf-light absorption system (Taylor *et al.*, 2019). In the range of 400–800 nm the device measured transmittance and reflectance with two integrating spheres, using a light source at a fixed angle and a non-cooled spectrophotometer (USB-4000, Ocean Optics, Dunedin, FL, USA) (Hogewoning *et al.*, 2010a). The acquired data were used to calculate the leaf light absorptance for the light of each treatment. After the measurements, the leaf material was dried like the other plant parts. An estimation of whole plant light absorption was made based on measurements of plant 3D structure and leaf optical properties, in combination with a ray tracing software mimicking the light environments. A day before the destructive measurements, plant 3D structure was measured. The plants that would be later used for biomass and destructive morphology measurements were first transferred to a 20 m^2 room and subjected to 3D laser scanning. Terrestrial laser scanning (TLS) is an active remote sensing technique that measures the distance to an object by measuring the time-of-flight of a laser pulse to and from the object (Calders *et al.*, 2015). A RIEGL VZ-400 3D terrestrial scanner (RIEGL Laser Measurement Systems GmbH, Horn, Austria) was used. This time-of-flight scanner has a range up to 350 m, the beam divergence is nominally 0.35 mrad, and the scanner operates in the near infrared (wavelength 1550 nm). This instrument records multiple-returns from each laser pulse to improve the scab resolution (up to four returns per emitted pulse) (Calders *et al.*, 2014). Each plant was

scanned from four equidistant locations (minimum separation 1.5 m, 90 degrees azimuth spacing). The TLS data from the individual locations were registered in the RiSCAN PRO software (provided by RIEGL) and points with a deviation of more than 20 were removed to increase the signal-to-noise ratio (Calders *et al.*, 2017) before exporting the final point cloud model for each plant. The plant surface was reconstructed in each point-cloud with MeshLab software (Meshlab, 2014), using the Ball Pivoting Algorithm (Bernardini *et al.*, 1999) (Supplementary Fig. 1). Laplacian smoothing was applied on each reconstructed mesh: for each vertex, the average position with the nearest vertex was calculated in three sequential smoothing steps. Finally, the smoothen meshes were exported as Alias Wavefront Object (*.obj) and Collada File Format (*. dae) file types. The. dae files were imported to SketchUp Make software where the upper angles between petiole and stem were measured. Light absorption of each plant was computed using a 3D model built in GroIMP modelling platform (Kniemeyer, 2008). This platform allows the use of a multispectral inversed ray tracer, which for this study was set to 20 million rays and a recursion depth (maximum number of light bounces) of 10. The constructed 3D scene mimicked each light treatment, including light intensity and spectrum. Spotlights facing downwards represented the plasma and LED lamps and were situated above the plant according to their positions in the growth tents. The emitted light passed through a transparent cover at ca. 30 cm above the plant model. This model was the smoothed mesh of the 3D scan of each of the treated plants (*.obj file) and was imported in the 3D scene as a wireframe object, with its surface consisting of multiple vertices. For each vertex (or polygon) the measured absorption and reflection were imported as optical parameters. Each 3D model plant was situated inside a box of 1 m · 1 m · 1 m, enclosed by vertical white walls that fully reflected light; black ground floor and ceiling fully absorbed the light. In this approach, all the given light could be traced back in the scene: the light was either absorbed by the plant, reflected to the ceiling or transmitted to the floor (and consequently absorbed by the ceiling and the floor).

Gas exchange

Gas exchange was measured by custom-made equipment with a leaf chamber similar to that described in Taylor *et al.* (2019). Actinic light comprised two light sources; artificial daylight was produced by a plasma lamp identical to the one used for growth, and blue light was produced by LEDs with a practically identical emission spectrum to those used for growth light. The blue LEDs were arranged in an array on a metal-cored printed circuit board. All light sources were coupled to the chamber with glass fibres. Light intensity from the plasma lamp was controlled with built-in electronic control but, since the lamp cannot sustain an arc below a minimum current it was used

in combination with a neutral density filter comprised one or more layers of fine wire gauze on an adjustable rotatable disk between the lamp and the optical fibre. Measurements were taken on third, fully expanded leaves, usually at about 30–32 days after seeds were sown. Two sets of gas exchange measurements were taken on each leaf. The first set of measurements was taken at low O_2 mole fraction (20 mmol mol^{-1}) to inhibit photorespiration while the subsequent second set of measurements on the same leaf were taken at ambient O_2 (210 mmol mol^{-1}). In both cases, the concentration of CO_2 was 400 μmol mol^{-1}, and the concentration of H_2O was set to 18 mmol mol^{-1} (70% RH) by adjusting the proportion of the incoming airstream which was passed through a bubbler with temperature-controlled water. The remaining gas fraction consisted of N_2. A Li-7000 infrared CO_2/H_2O analyzer (Li-Cor, Lincoln, Nebraska, USA), set in differential mode, analyzed incoming and outgoing gas streams. Leaf temperature was monitored using a calibrated infrared (non-contact) thermocouple (Micro IRt/c, Exergen, Watertown, MA, USA) and maintained at 23 °C by circulating water of the appropriate temperature through cavities in the upper and lower chamber halves. Assimilation was measured at five light-limiting irradiances (10, 25, 50, 75 and 100 μmol m^{-2} s^{-1}) at a low O_2 mole fraction. To ensure that these irradiances were light-limiting, light response curves were examined for inflection points at which the response became curvilinear. It was found that these intensities were indeed light-limiting as evidenced by the strong linearity of the assimilation response up to, and including, 100 μmol m^{-2} s^{-1}. The lowest light intensity of 10 μmol m^{-2} s^{-1} was chosen to avoid potential non-linearity associated with the Kok effect at very low light intensities (Kok, 1948). Measurements at ambient O_2 mole fraction were taken using the same light-limiting irradiances but also included higher irradiances of 200, 400, 800, 1200, 1600, and 1800 μmol m^{-2} s^{-1}. Leaves were subjected to each light intensity step for as long as necessary for the rate of gas exchange to reach a steady state. Assimilation (A) and stomatal conductance (gs) were calculated according to the model of Farquhar *et al.* (1980). The purpose of low [O_2] measurements was to remove the effect of potential differences in photorespiration amongst treatments arising from potential blue-light mediated changes in mesophyll and stomatal conductances. Maximum quantum yield of CO_2 fixation at low and ambient CO_2 (Φ_{CO2}) was taken as the slope of a linear regression of the gas exchange- irradiance response curve for the first five light-limiting irradiances (10-100 μmol m^{-2} s^{-1}). Maximum photosynthetic capacity (A_{max}) for the full light response curves at ambient CO_2 was determined using the non-linear hyperbolic function of Thornley (1976).

Chlorophyll fluorescence

Chlorophyll fluorescence parameters were measured using a lab-built system comprising a modulated measuring beam and lock-in amplifier. Upon commencement of gas exchange measurement, Fv/Fm was measured in dark-adapted leaves. Fm was determined using a saturating flash of 12 000 µmol m^{-2} s^{-1} for 1 s generated by three high-power red LEDs (623 nm, Phlatlight PT120, Luminus Devices, CA, USA) coupled to the chamber by three glass fibres. The intensity of the measuring beam, produced by a red LED (660 nm), was approximately 0.5 µmol m^{-2} s^{-1}. Three GaAsP photodiodes (G1736, Hamamatsu, Hamamatsu City, Japan) with their optical windows covered with RG-9 filters (Schott, Mainz, Germany) were used to detect fluorescence signal. $\Phi_{PSII(LL)}$ was determined at each light step up to and including the highest light-limiting intensity used of 100 µmol m^{-2} s^{-1}.

Measurement of 820 nm absorption changes and $\Phi_{PSI(LL)}$ estimation

The modulated measuring beam for Δ820 nm was produced using a LED (ELJ-810-228B, Roithner Lasertechnik, Vienna, Austria) modulated at 455 kHz coupled to the chamber by a glass fibre and the signal was detected below the leaf by three silicon photodiodes (BPW 34 FA, Osram, Regensburg, Germany) connected to a selective amplifier containing a 455 kHz ceramic filter (Murata, Kyoto, Japan). Three steady state signal levels were used to estimate $\Phi_{PSI(LL)}$: 1.) The 820 nm signal in the light, 2.) the subsequent and rapid change in 820 nm signal (ΔA820) when actinic light was turned off (i.e. in darkness), and 3.) the signal obtained when a ca. 10 s far-red pulse was applied during darkness to fully oxidise P700. The use of a saturating pulse (5 ms duration using the same saturating pulse as for the chlorophyll fluorescence) was used to oxidise any P700 which may have not been oxidized during the application of far-red light (Kingston-Smith *et al.*, 1999). These absorbance changes were used to estimate $\Phi_{PSI(LL)}$ according to the calculation of Baker *et al.* (2007).

Experimental design and statistical analysis

There were six light treatments each with three replicate plots (*n*=3), with two replicate plants per plot for measurement of growth, biomass and 3D structure, two for photosynthesis and one for optical properties measurements. Hence, there were in total always six or nine replicate plants per treatment. The plots were distributed over four tents in five separate time periods. Linear regression was applied to the response of plant morphological parameters (plant height, total leaf area, etc.) to the fraction of blue light (*p*=0.05). Additionally, linear regression was applied to test the correlation between total plant light absorption and plant morphological parameters (plant height

and total leaf area, and leaf length, width, length/width and angle) and photosynthesis (p=0.05). For every measured response, the normality of the data was confirmed with Shapiro-Wilk normality test. All analyses were conducted in R (R Development Core Team, 2010). All figures were also created in R using the ggplot2 data visualization package (Wickham, 2016).

Results

Plant growth, morphology and development

Plant height decreased linearly with the increase of fraction blue light (p<0.001) (Figs. 2A, 3). The plant height decreased by 55% and the hypocotyl length by 35% at the highest (61%) compared to lowest (27%) fraction blue treatment. Length, width, and length/width ratio of the third leaf decreased linearly with the increase of fraction blue (p<0.05) (Fig. 2C-E), but petiole length was not affected (p=0.053). The total plant leaf area also decreased linearly (p<0.05), being 30% lower in plants growing under 61% compared to plants growing at 27% fraction blue treatment (Fig. 2F). The dry weight of plants decreased linearly with the increase of fraction blue light (p<0.05) (Fig. 2B). Plant dry weight decreased by 37% under the highest compared to lowest fraction blue treatment. Leaf number, specific leaf area and angle of the third leaf (upper angle between petiole and stem) were not affected by the increase of fraction blue (p>0.05) (Table 1). The fraction of dry weight partitioned to the leaves increased linearly with the increase of fraction blue (p<0.001), at the expense of stem (Table 2).

Leaf light absorptance

The light absorptance per unit leaf area of both the adaxial and abaxial sides of the third leaf increased linearly with the increase of fraction blue light (p<0.05), but relative effects were rather small (Fig. 4). Plants grown under 61% blue light fraction had a light absorptance which was 2.5% (adaxial) and 2% (abaxial) higher than when grown under 27% blue light fraction. The spectral distribution of the absorptance did not vary among treatments, hence optical properties of the leaves were not affected by the treatments (data not shown).
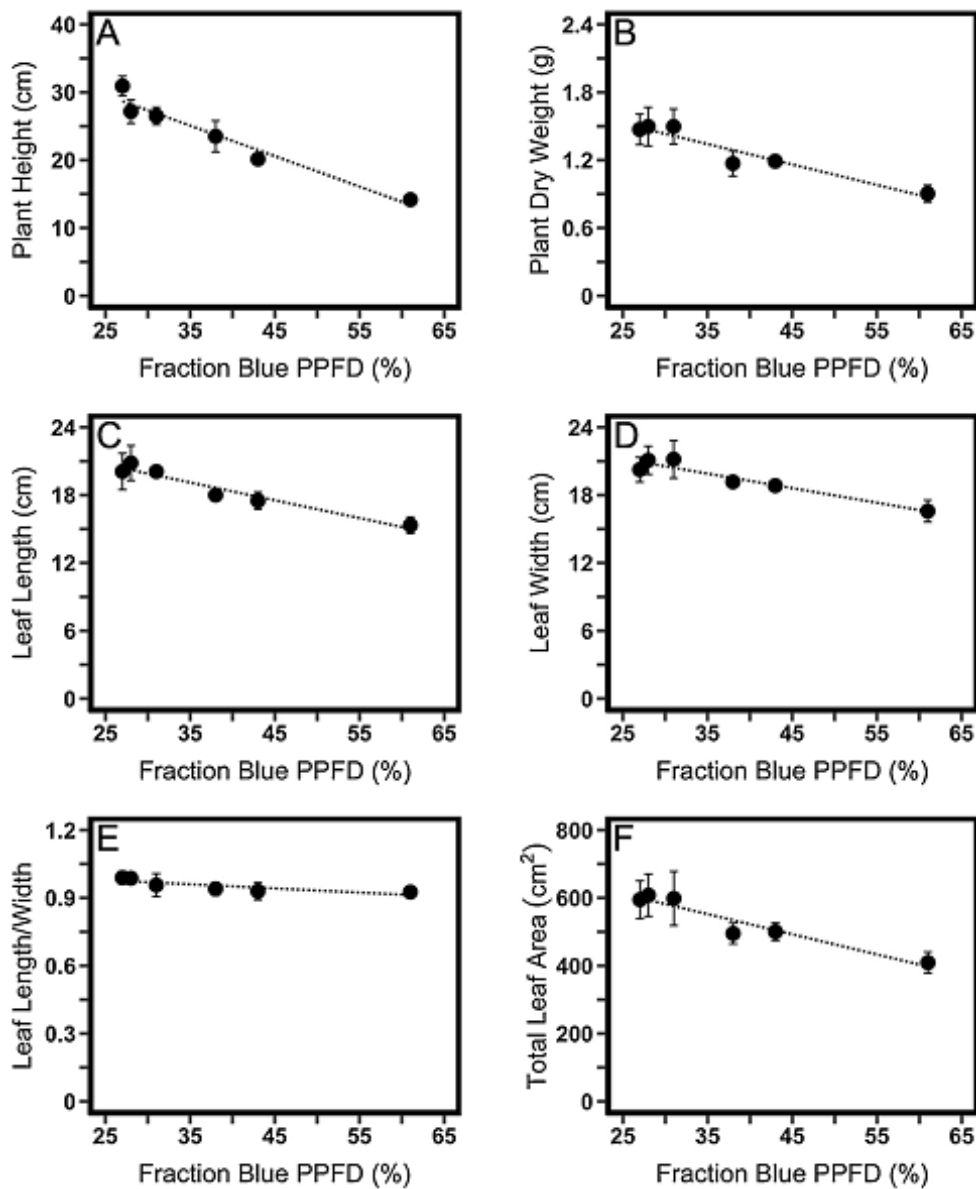
Fig. 2: Effects of fraction blue light on (A) height, (B) dry weight, (C) length of the third leaf counting from the bottom, (D) width of the third leaf counting from the bottom, (E) length to width ratio of the third leaf counting from the bottom and, (F) total leaf area of tomato plants grown for 23 days under a total of 100 μmol m^{-2} s^{-1} blue +artificial solar PPFD. Error bars indicate means ±SEM from three plots (*n*=3) with two replicate plants per plot. The lines represent significant linear regression (P <0.05).
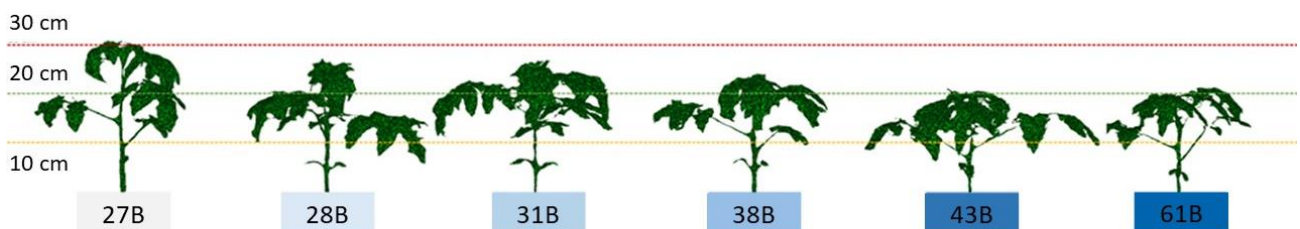

Fig. 3: Effects of fraction blue light on the architecture of tomato plants grown for 23 days under a total of 100 μmol m^{-2} s^{-1} blue +artificial solar PPFD. Images are 3D scans acquired with a terrestrial laser scanner (TLS). The colour of the block under each plant resembles the fraction blue. All 3D scans are presented in Supplementary Fig. 2.

Table 1: Effects of blue light fraction on the leaf number of plants, specific leaf area (SLA) and upper angle between petiole and stem of leaf number 3. The tomato plants were grown for 23 days under a total of 100 μmol m^{-2} s^{-1} blue +artificial solar PPFD. Data are means ±SEM from three plots (n=3) with two replicate plants per plot. P-value indicates the significance of the F-ratio of the linear regression.

	27%	28%	31%	38%	43%	61%	P
Leaf number	6.33±0.17	6.50±0.29	6.50±0.50	6.00±0.00	6.17±0.17	6.00±0.00	0.113
SLA (cm^2 g^{-1})	574±4.4	562±26.3	544±21.1	564±18.7	551±27.3	551±27.3	0.576
Leaf angle (°)	67.6±7.6	71.7±4.4	53.4±1.0	62.3±5.6	58.3±5.3	58.3±5.3	0.273

Table 2: Effects of blue light fraction on dry weight partitioning (%) to leaves and stems of tomato plants grown for 23 days under a total of 100 μmol m^{-2} s^{-1} B+AS PPFD. Data are means ±SEM from three plots (n=3) with two replicate plants per plot. P-value indicates the significance of the F-ratio of the linear regression.

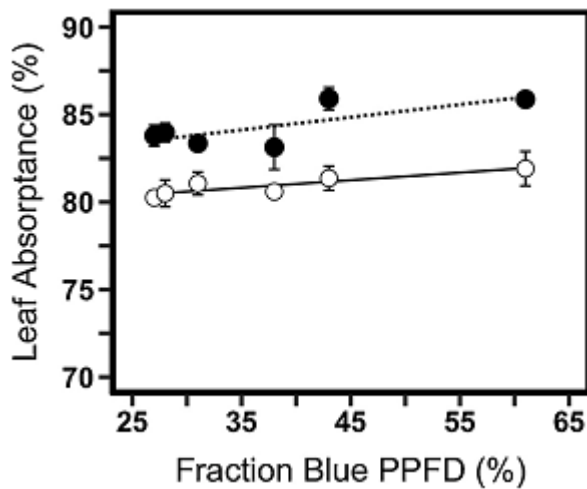|	27%	28%	31%	38%	43%	61%	P
Leaves (%)	71.1±1.01	73.4±0.40	74.3±1.86	75.9±1.24	76.0±1.24	83.1±0.33	<0.001
Stem (%)	28.9±0.69	26.6±0.56	25.7±1.23	24.1±0.83	24.0±1.03	16.9±0.74	<0.001

Fig. 4: Effects of fraction blue light on the integrated light absorptance (400 – 700 nm) of the third appeared leaf of tomato plants grown for 23 days under a total of 100 μmol m^{-2} s^{-1} blue +artificial solar PPFD (adaxial side: ●; abaxial side: ○). Error bars indicate means ±SEM from three plots (n=3) with two replicate plants per plot. The lines (adaxial side: dotted; abaxial side: solid) represent significant linear regression (p<0.05).

Photosynthesis

Mean Fv/Fm amongst all treatments was 0.78 (SE=0.004). The response of assimilation to light intensity between 10–100 μmol m^{-2} s^{-1} was highly linear with a mean R^2 of 0.997 (SE=0.0008), indicating that photosynthesis was light-limited within this range. The light-limited quantum yield of CO$_2$ fixation ($\Phi_{CO2(LL)}$; μmol m^{-2} s^{-1} CO$_2$.μmol photons^{-1}) was substantially higher at 2% O$_2$ than at

88

21% due to the suppression of photorespiration at the lower O_2 concentration (Fig. 5A). The response of $\Phi_{CO2(LL)}$ at the higher O_2 concentration generally mirrored the response at low $[O_2]$. $\Phi_{CO2(LL)}$ amongst treatments ranged from 0.064 to 0.069 at 2% O_2 and 0.046 to 0.050 at 21% O_2. However, the treatment effects on $\Phi_{CO2(LL)}$ were small and not significant. Likewise, $\Phi_{PSII(LL)}$ was similar amongst treatments, ranging from 0.75 – 0.76 at the highest light-limiting intensity used of 100 µmol m^{-2} s^{-1} (Fig. 5B). $\Phi_{PSI(LL)}$, on the other hand, was comparatively more affected by blue light fraction at the same light intensity (Fig. 5C). $\Phi_{PSI(LL)}$ ranged from 0.81 to 0.9 at 2% O_2 and from 0.82 to 0.88 at 21% O_2 with the lowest efficiency at 31% and greatest at 61% blue. $\Phi_{PSI(LL)}$ and $\Phi_{PSII(LL)}$ generally showed opposite trends i.e. when ΦPSII was greatest at 31% blue, $\Phi_{PSI(LL)}$ was lowest. The excitation balance of PSII and PSI (Fig. 5D), calculated as the yield of PSII divided by the sum of the yield of PSI and PSII, also showed a peak at 31%. Stomatal conductance (gs) was highest at 31% blue (Fig. 5E) while no effect of the fraction blue light in the growth irradiance was observed for the maximum photosynthetic capacity (A$_{max}$) (Fig. 5F).

Plant light absorption

The total plant light absorption decreased linearly ($p<0.01$) with the increase of fraction blue light (Fig. 6A). At 61% blue fraction treatment plants had total light absorption which was 22% lower than that of plants at 27% blue fraction. Plant dry weight correlated linearly with plant light absorption ($p<0.01$) (Fig. 6B), which correlated linearly with leaf area ($p<0.01$) (Fig. 6C). Additionally, the total plant light absorption decreased linearly with a decrease of plant height ($p<0.001$) and length, width ($p<0.01$) and length/width ratio of the third leaf ($p<0.05$) (Supplementary Fig. 3). Total plant light absorption did not correlate with leaf angle or petiole length ($p>0.05$). Lastly, plant dry weight correlated linearly with $\Phi_{PSI(LL)}$ (negatively) and photosystem excitation balance ($p<0.05$), but not with $\Phi_{PSII(LL)}$, Φ_{CO2} ($p>0.05$) (Supplementary Fig. 4).
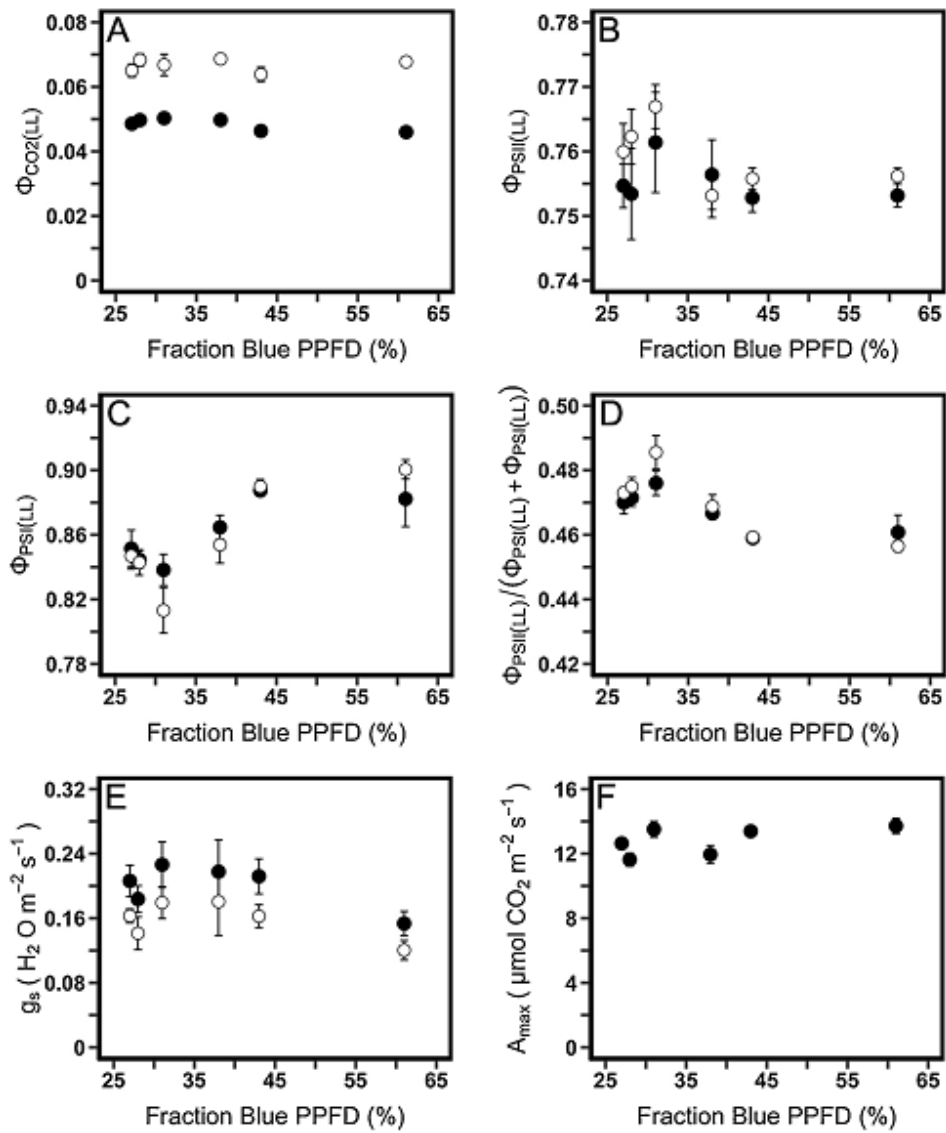
Fig. 5: Effects of different fractions of blue light in actinic irradiance on (A) $\Phi_{CO2(LL)}$; µmol m^{-2} s^{-1} CO_2.µmol photons^{-1}, (B) $\Phi_{PSI(LL)}$, (C) $\Phi_{PSII(LL)}$, (D) photosystem excitation balance calculated as the fraction of $\Phi_{PSII(LL)}$ relative to the sum of $\Phi_{PSI(LL)}$ and $\Phi_{PSII(LL)}$, (E) stomatal conductance and (F) maximum photosynthetic capacity as determined on tomato leaves grown under the same growth irradiance and spectrum of 100 µmol m^{-2} s^{-1} blue+artificial solar PPFD. Different symbols indicate measurements under 2% (○) and 21% (●) oxygen levels. Error bars indicate means ±SEM (n=3).
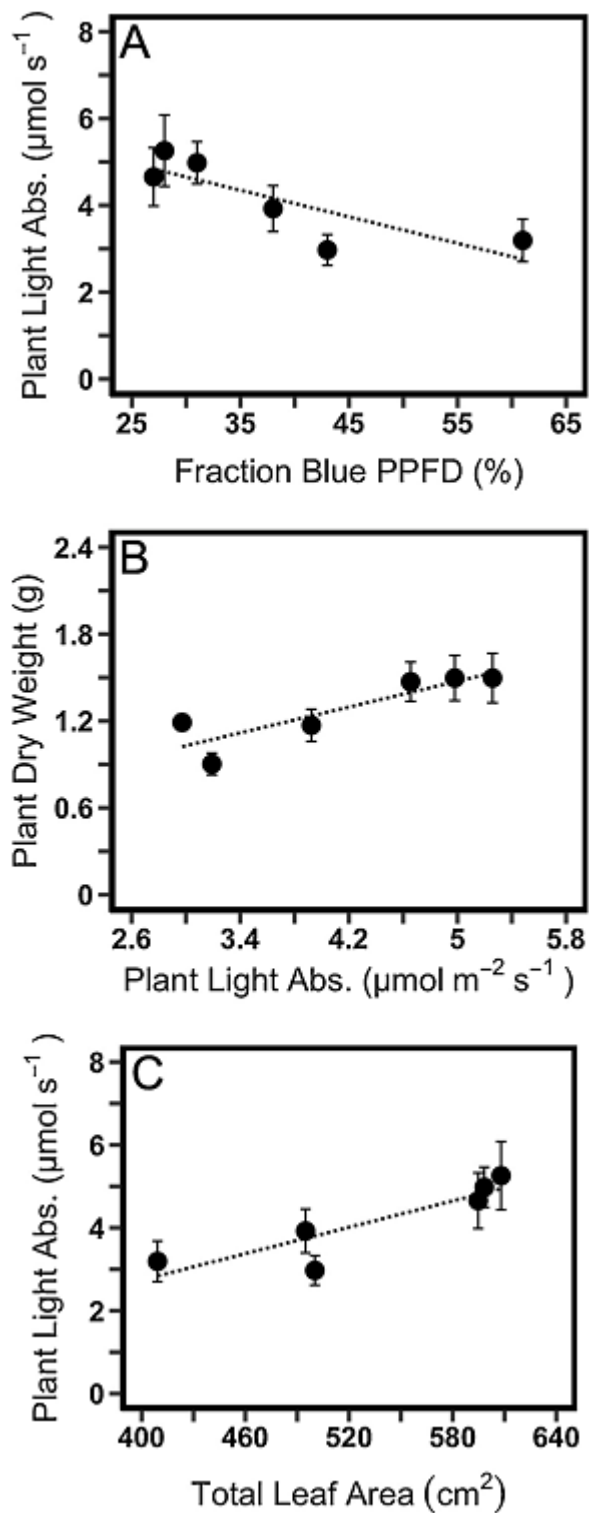
Fig. 6: (A) Effects of fraction blue light on the estimated plant light absorption, (B) effects of the estimated plant light absorption on the plant dry weight and, (C) effects of plant leaf area on the estimated plant light absorption of tomato plants at day 23, when grown under a total of 100 µmol m^{-2} s^{-1} blue +artificial solar PPFD. Error bars indicate means ±SEM from three plots (n=3) with two replicate plants per plot. The dotted lines represent significant linear regression (p<0.05).

Discussion

Plant morphology and photosynthesis

Total plant light absorption decreased linearly with the increase of the blue light fraction (Fig. 6A), in agreement with the findings of Snowden *et al.* (2016). Specifically, total plant light absorption decreased linearly with the decrease of plant leaf area (Fig. 6C), height, third leaf length and width, and length/with ratio ($p<0.05$). The results are in accordance with the findings of Sarlikioti *et al.* (2011) who showed through simulations performed with an FSPM, that increased internode length and leaf length:width ratio increased total light absorption in tomatoes, due to the reduction in leaf mutual shading. In our study, it is safe to conclude that increased blue light fraction induced a set of phenotypic traits that decreased the total light absorption mainly due to decreased leaf area. Although the leaf area decreased linearly with the increase of fraction blue light (Fig. 2F), the percentage of assimilates partitioned to the leaves increased (Table 2). These two responses combined resulted in a decreased SLA (although not significant) as blue light fraction increased (Table 1). Similar responses to increasing fraction blue light under low irradiance (100 µmol m^{-2} s^{-1}) have often been associated with leaf responses to high irradiances (Hogewoning *et al.*, 2010a; Poorter *et al.*, 2009). Moreover, the decrease of leaf area and SLA (or 1/LMA) with the increase of fraction blue light has often been reported (Hernández *et al.*, 2016; Hernández and Kubota, 2016; Hogewoning *et al.*, 2010a).

Despite the greatly differing spectra used for growth and measurement, the fraction of blue light used for growth and measurement had a negligible effect on $\Phi_{CO2(LL)}$ (Fig. 5A). In cucumber grown under different blue light doses in a red background, $\Phi_{CO2(LL)}$ remained within a narrow range between 0.045 and 0.053, with the lowest values at 0% and 100% blue (Hogewoning *et al.*, 2010a). The similar $\Phi_{CO2(LL)}$ values obtained in the present study are not surprising given that, individually, the blue light and simulated daylight spectra used drive photosynthesis with similar efficiencies; in the present study Φ_{CO2} in simulated daylight of 0.065 (2% O$_2$) is comparable to that of 0.058 – 0.063 obtained by Hogewoning *et al.* (2012) when cucumber leaves produced under diverse growth spectra were presented with narrowband blue irradiance with a peak wavelength of 444 nm. There are however two different reasons for the relative inefficiency of daylight and blue light compared with, for example, red light: in the case of blue light energy transfer from carotenoids to chlorophyll is less efficient than chlorophyll-chlorophyll energy transfer (Croce *et al.*, 2001) whereas, apart from blue light, daylight contains other less efficient wavelengths such as green and far-red which, on their own, are used less efficiently for photosynthesis. The relatively small difference in $\Phi_{CO2(LL)}$

between treatments may also be partly due to acclimatory mechanisms which act to improve photosynthetic light-use efficiency and so maximise $\Phi_{CO2(LL)}$ and partly mitigate losses in $\Phi_{CO2(LL)}$. For example, leaves can adjust the relative amounts of PSI and PSII to maintain a high light-use for electron transport and thus a high $\Phi_{CO2(LL)}$ (Chow et $al.$, 1990). The same adjustments could have reduced any potential differences in $\Phi_{CO2(LL)}$ arising from the amount of blue light in the growth spectrum, causing leaves to converge upon similar $\Phi_{CO2(LL)}$ values. A_{max}, on the other hand, has been shown to be a plastic trait which responds strongly to blue light fraction. In the same study by Hogewoning et $al.$ (2010a), A_{max} was shown to increase up to the 50% blue light dose treatment and in a similar study A_{max} in spinach leaves was shown to increase up to 33% blue light in a red light background (Matsuda et $al.$, 2007). However, a key difference between our study and that of others where narrowband red-blue mixtures were used is that the background artificial daylight spectrum we used comprised 27% blue light (i.e. the irradiance between 400 and 500 nm). This is only slightly less than the blue light fraction which resulted in saturation of A_{max} in the study by Matsuda et $al.$ (2007). It is possible, therefore, that the blue content of our 'white light' background had saturated the blue light mechanisms which contribute to higher A_{max}. This explanation may also account for the lack of effect of blue light on stomatal conductance, which is otherwise known to be stimulated by blue light (Sharkey and Raschke, 1981). While $\Phi_{PSII(LL)}$ was remarkably similar across the spectra used, $\Phi_{PSI(LL)}$ showed a more varied response (Fig. 5C). The latter can be accounted for by the far-red fraction (700–720 nm) of the white light used which was 5.7% of irradiance in the spectral range 400–720 nm. Compared to other wavelengths (including blue light) far-red light is known to over-excite PSI compared to PSII (Hogewoning et $al.$, 2012; Laisk et $al.$, 2014). In cucumber leaves, Φ_{PSI} at 720 nm (ca. 0.1 – 0.15) was considerably less than for most wavelengths in the PAR region including 450 nm where Φ_{PSI} was high (>0.9) (Hogewoning et $al.$, 2012). Laisk et $al.$ (2014) calculated PSI absorption to be approximately 0.8 and greater at wavelengths <700 nm whereas at 450 nm this figure was ca. 0.3. Therefore, as blue light fraction increased from 27% to 61%, far-red irradiance between 700 and 720 nm decreased from 5.7% to 2.7% so decreasing the relative over-excitation of PSI and resulting in an increase in $\Phi_{PSI(LL)}$. This highlights the need to consider not only direct blue light impacts but also indirect effects which inevitably occur in spectral dose response studies in which one irradiance flux is partially replaced by another. The opposite trends in Φ_{PSI} and Φ_{PSII} further serves to highlight the differences between the photosystems in terms of composition and absorption. At the higher blue fractions, it is likely that cyclic electron flow was enhanced to account for the relatively increased excitation of PSII compared with PSI which may account for the slight corresponding reduction in Φ_{CO2}.

Plant growth

Since $\Phi_{CO2(LL)}$ was unaffected and integrated leaf light absorptance increased slightly with blue light fraction (Figs. 4, 5A), a likely contributor to the reduction of plant dry weight is the decrease in total plant light absorption (Fig. 6B). Similar results were reported by Hernández and Kubota (2014) for cucumber plants grown under equal light intensities with different fractions blue light. Although no differences were found in net leaf photosynthesis, biomass accumulation decreased significantly with the increase of fraction blue light due to the decrease of total plant leaf area. The linear correlation between total plant light absorption and plant dry mass production confirms the findings of Snowden *et al.* (2016) i.e. the effect of blue light on tomato dry mass is primarily determined by total plant light absorption rather than by direct effects on photosynthesis. Lastly, the 'sun-type' plant leaf morphology and overall phenotype resulting from high fractions of blue in some studies (e.g. Hogewoning *et al.*, 2012) may not be advantageous for growth acclimation when plants are growing under low light intensities characteristic of the present study.

Plant development

Blue light fraction did not affect the leaf initiation rate as indicated by the unaltered leaf number (Table 1). Increasing the blue light fraction did not increase the phototropic response (and therefore the angle) of the third leaf as expected (Table 1) (Huché-Thélier *et al.*, 2016). However, when multiple regression (ANCOVA) was used to assess the angle response of the most developed leaves (1–3 counting from the bottom), the effect of blue light fraction upon them was significant ($p<0.05$).

Signalling

The linear reduction in plant height (Figs. 2A, 3) due to increased blue light fraction is possibly cryptochrome-regulated (Fraser *et al.*, 2016). This response is consistent with previous studies on tomato (Glowacka, 2004; Hernández *et al.*, 2016; Nanya *et al.*, 2012; Snowden *et al.*, 2016; Wollaeger and Runkle, 2014). The response cannot be related to phytochrome-regulated shade avoidance, since P_{fr}/P_{total} decreased by only 0.03 in the highest blue fraction treatment. Moreover, it is known that cryptochromes are the main photoreceptors inhibiting hypocotyl and epicotyl elongation, when absorbing light in the range of 390–480 nm (Ahmad and Cashmore, 1996; Ahmad *et al.*, 2002; Hartmann, 1967). In the present study, the peak wavelength of the blue LED used was 450 nm.

Conclusions

The present study revealed strong photomorphogenic responses to blue light doses whereas leaf level photosynthetic responses were negligible or absent. This proved a potentially useful tool which allowed for the significance of whole-plant light absorption to plant biomass to be gauged. Total dry weight of tomato plants grown under different combinations of artificial solar light enriched with blue light, while keeping photosynthetic photon flux density constant, decreased linearly as blue light fraction increased. This decrease is most likely a consequence of reduced whole-plant light absorption. The fraction of blue light contained in the artificial solar light appeared to saturate all previously reported positive effects of blue light on maximum photosynthetic capacity and had no significant impact on Φ_{CO2}. When plants are grown under constant light intensities increasing the blue light fraction in a solar light background decreases growth. This reduction in performance is primarily a consequence of the effect of blue light on plant morphology and light interception. This highlights the significance of whole-plant light absorption as a major determinant of whole-plant biomass but also indicates that leaf-level photosynthetic effects may not reliably be extrapolated to whole-plant performance in the absence of an understanding of specific effects on plant morphology and whole-plant light absorption. Clearly, neither of these two factors can be viewed in isolation in relation to whole-plant biomass especially since spectra which are used efficiently at the leaf-level may not result in a morphology which is efficient for light capture.

Supplementary data

Supplementary material accompanying this chapter can be found in the online version of the published article at doi:https://doi.org/10.1016/j.envexpbot.2021.104377.

CHAPTER 5

Temperature dependence of quantum yield of CO_2 fixation in tomato

Abstract

Temperature is an important abiotic variable which influences the rate of photosynthesis in C3 species considerably. However, despite the impact of temperature on photosynthesis, our understanding of the effects of temperature on photosynthesis is, in some places, weak. The majority of work on the subject has used high or light-saturating light intensities to determine temperature dependence of photosynthesis, and the effects of light-stress at extreme temperatures is also well studied. The potential contribution of light stress in conjunction with temperature extremes, makes it difficult to relate these results to lower light intensities. This is of ecophysiological relevance given that most leaves photosynthesize within the canopy where light availability limits the rate of photosynthesis. The quantum yield (Φ_{CO2}) of photosynthesis under these conditions is a useful and sensitive metric to probe temperature related impacts on photosynthetic operation. We tested the temperature dependence of Φ_{CO2} in tomato at 7 temperatures ranging from 15 - 35 °C in ambient (21%) or low (2%) oxygen. Corresponding changes in Φ_{PSII}, Φ_{PSI} and ECS_{520} were examined. Φ_{CO2} showed an optimum at 18 °C in 2% and 21% O_2. Φ_{CO2} was 29% lower in 2% O_2 at 35 °C than at the temperature optimum, revealing a fairly marked temperature response despite practically no photorespiration. Φ_{PSII} and qP showed little temperature dependence at 2% O_2 but, unexpectedly, these parameters were lower in 21% O_2 across all temperatures with a distinct parabolic trend and a temperature optimum at 25 °C. A possible explanation for these observed differences is more cyclic electron transport at 21% O_2. A more rapid measurement procedure to test for potential artefacts of comparatively long exposure time (ca. 1 h) to each of the different temperatures revealed quite different results especially in terms of Φ_{CO2} and Fv/Fm, suggesting that exposure time may have a bearing on results even within a temperature range considered to be typically moderate. The latter has practical implications when interpreting temperature responses within more dynamic, ecophysiological, contexts.

Introduction

Photosynthesis and its many interrelated and coordinated biochemical processes is affected by the leaf temperature at which these operate. A major short-term impact of temperature on photosynthesis in C3 species is through photorespiration, a product of the catalytic activity of RuBisCo for both the carboxylation and the oxygenation of ribulose-1,5-bisphosphate. In practice the relative rates of each of these reactions is readily manipulated by increasing or decreasing the ambient concentration of one or both of the substrates i.e. CO_2 and O_2. For example, increasing the mole fraction of CO_2 or decreasing the mole fraction of O_2 will increase the rate of the carboxylation reaction and decrease the rate of the oxygenation reaction. Each oxygenation reaction results in the formation of one phosphoglycerate and one phosphoglycolate (PGO) molecule, and in the subsequent metabolism of PGO one CO_2 is released for every two PGO. This formation of CO_2 antagonises the CO_2 fixation process and further decreases the light-use efficiency of assimilation. The oxygenation reaction is favoured as temperature increases because the solubility of CO_2 decreases relatively more than that of O_2 as temperature increases (Ku and Edwards, 1978). A typical C3 leaf photosynthesising in air will experience a 30% loss of light-use efficiency as a result of the combined effects of oxygenation of RuBP and the subsequent release of CO_2 by photorespiration (Björkman, 1966), although this figure depends greatly on temperature. Strictly speaking photorespiration refers to the release of CO_2 during the metabolism of PGO but it is common to use photorespiration to include the oxygenation of RuBP as it is the starting point of the photorespiratory pathway.

Other short-term temperature impacts are on conductance to CO_2, including impacts on stomatal (Urban *et al.* (2017) or mesophyll conductance (Bernacchi *et al.*, 2002). At constant vapour pressure deficit, stomatal conductance was shown to increase by about 40% in Poplar and Pine when temperature was increased from 30 °C to 40 °C (Urban *et al.*, 2017). In a survey of 9 species, mesophyll conductance generally increased with temperature (von Caemmerer and Evans, 2015). At the thylakoid level, temperatures above 20 °C were shown in spinach thylakoids to induce a state transition to state 2 in which the antenna size of PSI is increased whereas that of PSII is decreased (Weis, 1985). This was explained as being needed to increase cyclic electron transport around PSI in order to meet the increased demand for ATP relative

to NADPH arising from the increase in the rate of oxygenation of RuBP relative to its carboxylation that occur with increasing temperature (Weis, 1985).

Work on the temperature effects on photosynthesis has included extensive analysis of temperature responses of the light-use efficiency for electron transport by PSII and PSI, and the rate of CO_2 fixation. These responses are however difficult to interpret in a simple, consistent way. For example, at an irradiance of 300 µmol m^{-2} s^{-1}, Φ_{PSII} of leaves of *F. pringlei* was independent of temperature between 15 °C and 35 °C whereas at a higher irradiance of 1100 µmol m^{-2} s^{-1} Φ_{PSII} increased from about 0.3 to 0.55 (Oberhuber and Edwards, 1993). In barley, and at even higher irradiance (1600 µmol m^{-2} s^{-1}), the temperature response of Φ_{PSII} was dependent on O_2 concentration (Clarke and Johnson, 2001); Φ_{PSII} (shown in brackets) was greatest at 25 °C (0.13) and 30 °C (0.21) at 2% and 21% O_2, respectively, and Φ_{PSII} at 21% O_2 was greater than at 2% O_2 for all temperatures apart from the lowest temperature of 10 °C where Φ_{PSII} was the same. This contrasts with the findings of Oberhuber and Edwards (1993) where no difference in Φ_{PSII} was observed between 2% and 21% O_2. In leaves of *Glycine max* measured at an irradiance of 1200 µmol m^{-2} s^{-1}, Φ_{PSII} followed a similar parabolic function to that obtained by Clarke and Johnson (2001) but with maximum Φ_{PSII} (ca. 0.56) occurring at a higher temperature of about 35°C (June *et al.*, 2004). The latter authors reported that the temperature dependence of Φ_{PSII} was dependent on growth temperature. In isolated spinach thylakoid membranes electron transport through PSII was maximal at 35°C (Yamori *et al.*, 2008). Clarke and Johnson (2001) observed a parabolic response of Φ_{PSI} with a peak at 25 °C whereas in potato decreases in ΦPSI were observed only at higher temperatures (ca. >40°C) (Havaux, 1996). Yamori *et al.* (2008) observed increasing electron transport though PSI throughout a temperature range of 10-40°C.

It is possible that the varied and somewhat inconsistent results on the temperature dependence of Φ_{PSII}, Φ_{PSI} and rate of CO_2 fixation and are due not only to different growth acclimations but also different measurement conditions, especially irradiance. In this regard, most work on temperature dependence has focused on high, or saturating, irradiances (Baker *et al.*, 1988). Although these two factors (i.e. high irradiance and temperature) are often expected to accompany one another under natural conditions (Zhang and Sharkey, 2009), such as in leaves exposed to direct sunlight, the combination of two stresses – high light and temperature extremes – make it difficult to disentangle the impact of temperature or

temperature stress alone. In a variety of C3 and C4 species the application of light following chilling stress was found to aggravate reductions in photosynthetic rate in an intensity-dependent manner (Taylor and Rowley, 1971). Furthermore, limitations to photosynthesis in high light are different to those under light limited conditions (Baker *et al.*, 1988). Limitations at high irradiance could include limitation of RuBP regeneration due to reaching the maximum electron transport rate or limitations in the regeneration phase of the Bassham-Benson-Calvin cycle, limitation due to Rubisco and end-product limitation, or to supply-side limitation due to leaf CO_2 conductance. Limitations of this kind are not relevant at low, light-limiting irradiances.

In this study we examine Φ_{CO2} at low, strictly light-limiting intensities and moderate temperatures (15 °C - 35 °C) which shaded leaves may routinely encounter in the natural environment. The responses of the thylakoid-level processes, including Φ_{PSII}, Φ_{PSI} and the electrochromic shift, are also investigated. Light-limitation provides some standardisation to such measurements and is physiologically more simple to define in terms of which processes are relevant to understanding any phenomena we observe. Since most leaves photosynthesize within the canopy where light availability limits the rate of photosynthesis (Long and Drake, 1991; Long *et al.*, 1996), the temperature response of Φ_{CO2} could be useful for modelling photosynthesis at crop level.

Materials and methods

Growth environment

Seeds of tomato were sown in vermiculite in a central depression of rockwool blocks (Grodan, Roermond, The Netherlands) and placed in plastic lined fabric tents in a climate-controlled room. The top of each rockwool block was covered with black plastic sheet, cut to allow light to reach only the vermiculite, which greatly reduced algal growth on the rockwool. Rockwool blocks were irrigated once daily by flooding with Hoagland solution for 15 minutes. Seedlings were thinned to the most vigorous seedling per block a few days after germination. Leaf temperature of the third leaf was maintained at 23 °C ±1 °C. This was achieved by controlling the temperature of air which ventilated each tent. Leaf temperature was verified using a thermocouple appressed to the abaxial side of the leaf. Light was provided by plasma lamps (Plasma International, Muhlheim am Main, Germany), one per tent, and light intensity was

routinely measured with a PAR sensor (Li-190R, Li-Cor, Lincoln, Nebraska, USA) and adjusted to an intensity of 100 µmol m^{-2} s^{-1} at the apical tip or the third leaf, once it began to develop.

Gas exchange

The gas exchange system used was as described in Taylor *et al.* (2019). Gas exchange was monitored using two Li-7000 infra-red gas analysers (Li-Cor, Lincoln, Nebraska, USA) with one set to absolute mode for reference stream analysis and the other set to differential mode for sample stream analysis. Both analysers were checked daily (before measurements commenced) with a 391 ppm CO_2 reference gas and nitrogen gas (i.e. 0 ppm CO_2). No drift was found from the original calibration throughout the experiment. Since condensation was initially found to occur within gas tubing when the leaf was subjected to the higher temperatures it was necessary to heat the tubes using heating cable (10W/m). To ensure no condensation occurred within the gas analyzer cells, cell temperature was increased to approximately 35 °C by partly insulating the analysers with bubble wrap without impeding airflow from the cooling fans of each unit. Actinic irradiance was provided by nine red LEDs (peak wavelength of 660 nm) arranged in a matrix on a metal core board attached to a metal cylinder for cooling which slotted snugly above the window of the upper chamber half. A Li-cor quantum sensor (Li-190R, with the optical window visible through a punched hole in a sample tomato leaf, was used to calibrate a chamber photodiode which received light from a light guide in the light path above the leaf. Average light intensity in the chamber was determined using the method of Hogewoning *et al.* (2010b) to correct for error in light intensity determination arising from the point source measurement. The gas mix used comprised 400 µmol CO_2, 20 or 210 µmol O_2 (low and high $[O_2]$, respectively). The amount of H_2O in the gas mix was adjusted for each temperature to maintain a relative humidity of 70% and controlled by bubbling gas through a temperature-controlled water bath. N_2 comprised the remaining gas fraction.

Determination of leaf temperature

Leaf temperature was determined using a non-contact temperature sensor (Micro IRt/c, Exergen, Watertown, Massachusetts, USA) facing the abaxial side of the leaf i.e. positioned in the lower chamber half, the mV signal of which was amplified and read using a data recorder. The non-contact thermocouple was calibrated as follows: an aluminium block served as a

reference temperature source by clamping it in the gas exchange chamber in place of a leaf and the heating or cooling the block to a series of known temperatures determined with a PT100 resistance temperature detector (RTD) temperature probe (Omega Engineering, Connecticut, USA) which tightly friction-fitted into the block. A type k thermocouple was also used for more precise point measurements and appressed to the lower side of the block. Heating and cooling of the block was achieved using a hotplate or ice prior to placing it in the chamber. The block temperature homogenised evenly as evidenced by comparable readings of the temperature probe and thermocouple. As the temperature of the block slowly increased or decreased (depending on whether it has been heated or cooled) the temperature of the block and the corresponding voltage reading from the non-contact sensor were recorded at 1 °C increments (within a range of 0 °C to 40 °C) to produce a calibration curve. This procedure was repeated twice after several leaf temperature measurements, and the results of the initial calibration were faithfully reproduced. Leaf temperature was controlled by manipulating the temperature of the chamber by circulating water from a temperature-controlled bath through an internal loop in the chamber block. This in turn controlled the temperature of the gas stream which entered the leaf chamber through small channels.

Spectroscopic measurements

Chlorophyll fluorescence and Φ_{PSI}

Chlorophyll fluorescence was determined using a modulated red measuring beam produced by a 660 nm LED (LED engine) and filtered with a 660 nm filter. Modulation frequency and intensity were set to approximately 1kHz and 0.25 µmol m^{-2} s^{-1}, respectively. The measuring beam was coupled to the chamber by glass fibre with a hot mirror at the chamber end to eliminate fluorescence arising from the fibre itself. Three photodiodes capped by RG-9 filters (Schott, Mainz, Germany) were used to detect fluorescence, the signal of which was amplified by a phase-sensitive detector. Maximum fluorescence (Fm) was determined using a saturating flash of ca. 12000 µmol m^{-2} s^{-1} for a duration of 1 s. This flash was produced by three high-power red LEDs (Phlatlite, Luminus Devices, Sunnyvale, CA, USA) coupled to the chamber with glass fibre. Minimum fluorescence in the light Fo' was determined in darkness with the application of a far-red pulse (ca. 12 µmol m^{-2} s^{-1} for 1 s) to ensure complete oxidation of PSII reaction centres.

102

Φ_{PSI} was determined from the absorbance change at 820 nm using the calculation of Baker *et al.* (2007). The 820 nm beam was produced by an LED (ELJ-810-228B, Roithner Lasertechnik, Vienna, Austria) modulated at 455 kHz, filtered, and delivered to the chamber via a glass fibre. Three photodiodes below the leaf (BPW 34 FA, Osram, Regensburg, Germany) were used to detect the signal which was amplified using a lab-built lock in amplifier and recorded by a high-speed recorder. The PSI oxidation state at steady state was recorded at each light step before actinic light was interrupted, followed by the application of a far-red light for approx. 10 s. While the far-red light was on a saturating pulse of 1 ms duration was used to fully oxidise PSI centres.

Electrochromic shift

The electrochromic shift at 520 nm (ECS_{520}) was determined using a modulated 520 nm measuring beam coupled to the chamber by a glass fibre. The measuring beam was produced by a modulated green LED with a 520 nm filter (Thorlabs, Newton, NJ, USA) using the same modulation and demodulation system described for the Φ_{PSI} measurements. 520 nm absorbance changes were determined at the highest light intensity for each light-limited slope by switching the actinic light on for 1 s and then off for 20 s. Δ520 was taken as the mean amplitude of 8 consecutive on-off cycles.

Measurement procedure

Third, fully expanded leaves were used for all measurements. For each replicate leaf a complete set of measurements comprised measurements at low (2%) and high (21%) O_2. All 2% O_2 measurements were taken first before proceeding to 21% O_2 measurements. Leaves were clamped into the gas exchange chamber with a quick setting non-toxic moulding silicone (Body Double, Smooth-on, Macungie, USA) on the lower seal which was found to eliminate gas leaks. The efflux of CO_2 following a period of dark adaptation for 30 minutes was used to estimate dark respiration (Rd) and, subsequently, Fv/Fm was determined by applying a saturating pulse. Actinic light intensities were chosen to result in absorbed light-limiting intensities of ca. 30, 45, 60, and 75 µmol m^{-2} s^{-1}. After corrections for a slightly heterogeneous chamber light distribution (ca. 5% lower intensity at chamber edges compared to the chamber centre; Hogewoning *et al.*, 2010b), average incident chamber light intensities used were ca. 33, 49, 65, and 81 µmol m^{-2} s^{-1}. These irradiances were applied in sequence allowing ample

time for gas exchange to stabilize (ca. 13 min). Previous tests had shown that the highest light intensity was light-limiting (i.e. within the linear region of the light response curve before the response became curvilinear at higher light intensities) and the lowest intensity was more than sufficient to avoid possible non-linearity associated with the Kok effect (Kok, 1948; Sharp, 1984). Φ_{CO2} was taken as the slope of the linear regression of CO_2 assimilation rate and light intensity. Light-limited slopes were taken at each of 7 temperatures with a complete slope being completed at a given temperature before changing temperature. The temperatures used were 15, 18, 22, 25, 28, 32 and 35 °C and were applied in no particular order with the exception of the highest and lowest temperatures which were reserved for last. The complete set of measurements comprised measurements on 5 replicate leaves.

Results

Linearly interpolated rates of CO_2 fixation under light-limitation at 2% O_2 and 21% O_2 are shown in figures 1A and B, respectively. Calculated R^2 for the slopes were high at all temperatures, with mean values of 0.999 for 2% O_2 and 0.994 for 21% O_2. Quantum yields for each of the temperatures, taken as the slopes of linear regressions, are shown in figure 2. As expected, the response of Φ_{CO2} was higher and was less affected by temperature in 2% O_2 compared with 21% O_2. Φ_{CO2} was greatest at 18 °C in both low and high [O_2], with values of 0.085 and 0.060, respectively. This represents a 29% lower quantum yield at 21% O_2 due to photorespiration. Φ_{CO2} was slightly reduced at the lowest temperature (15 °C) but decreases above 18 °C were more marked, and especially so, in 21% O_2. The lowest Φ_{CO2} were 0.069 and 0.022 at the highest temperature we used (35 °C) for high and low [O_2], respectively, representing a 69% reduction in Φ_{CO2} in 21% O_2. To show how the temperature response of Φ_{CO2} may differ from that of A_{max}, three replicate leaves grown under identical conditions were measured at a saturating irradiance of 1400 µmol m^{-2} s^{-1} and 21% O_2 between 15-30 °C in 5 °C increments (Fig. 3). Unlike Φ_{CO2}, A_{max} showed no drop-off at the higher temperatures, showing that temperature influences each of these parameters through different limitations.
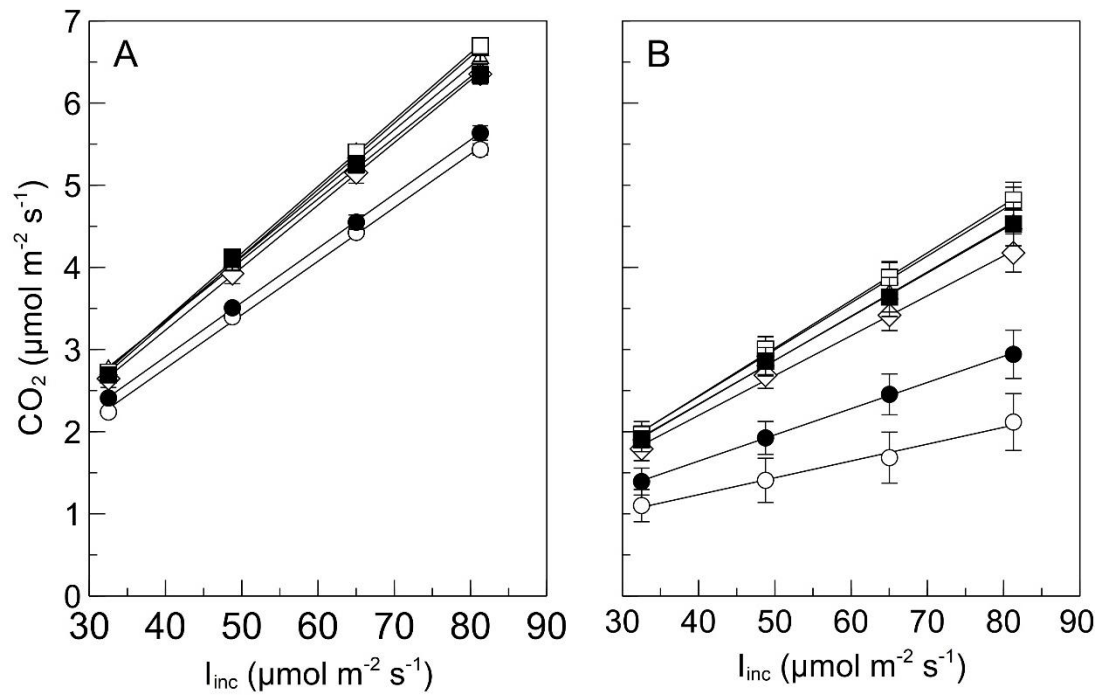
Figure 1: Light-limited rates of CO_2 fixation measured at low $[O_2]$ (2%) and leaf temperatures of 15 °C (closed squares), 18 °C (open squares), 22 °C (closed triangles), 25 °C (open triangles), 28 °C (open diamonds), 32 °C (closed circles) and 35 °C (open circles). Incident irradiances ranged from about 33 μmol m^{-2} s^{-1} to 81 μmol m^{-2} s^{-1} Lines represent linear regressions fitted to each set of data. Where shown error bars represent SEM (n=5).
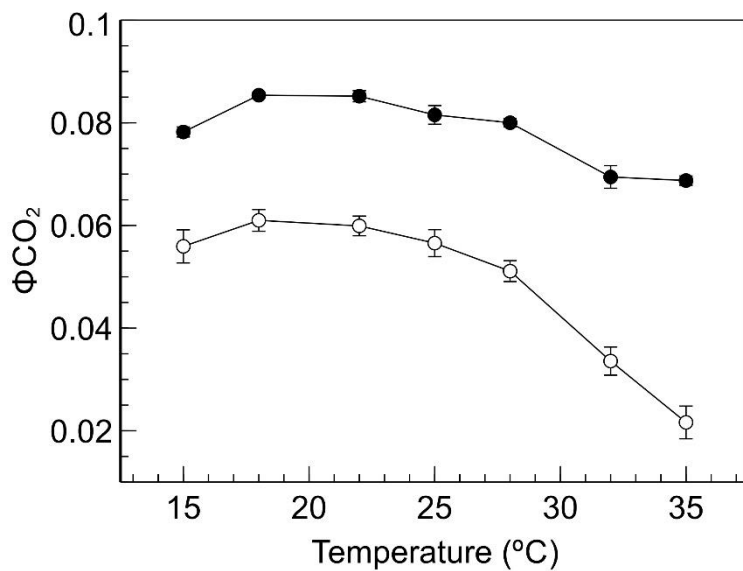

Figure 2: Temperature dependence of quantum yield of tomato leaves, measured at low $[O_2]$ (2%, closed circles) or high $[O_2]$ (21%, open circles). Where shown error bars represent SEM (n=5).
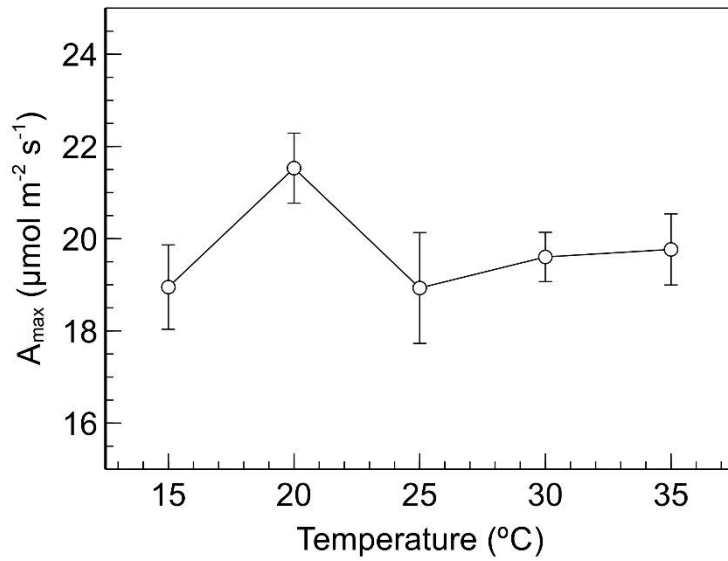
Figure 3: Temperature dependence of A_{max} of tomato leaves, measured at 21% O_2 and a saturating irradiance of 1400 µmol m^{-2} s^{-1}. Where shown error bars represent SEM (*n*=3).

The temperature dependence of selected Φ_{PSII} parameters are shown in Fig. 4. The maximum (dark adapted), chlorophyll fluorescence-derived yield of PSII electron transport (Fv/Fm) was generally about 0.8 at temperatures of ≤28°C, with decreases in this parameter above this temperature (Fig. 4A). For the highest and lowest temperatures used Fv/Fm was lower when measured at 21% O_2 than at 2% O_2. Further differences between high and low $[O_2]$ measurements reveal themselves in other PSII parameters. For example, PSII efficiency (Φ_{PSII}) was generally lower at 21% O_2 and with a trend that was convex in nature with a maximum of 0.67 at 25 °C (Fig. 4B) decreasing to 0.42 at 35 °C. At 2% O_2, however, Φ_{PSII} was considerably less affected by temperature, with less marked decreases at the lower and higher temperatures used. A similar trend in qP (Fig. 4C) was observed to that of Φ_{PSII} but the decrease in qP at 21% O_2 for the lower temperatures was more marked than the corresponding decrease in Φ_{PSII}. The efficiency of electron transport (fluorescence-derived) excitation capture by PSII reaction centres in a light adapted state (Fv'/Fm', Fig. 4D) was comparable between 2% and 21% O_2 at temperatures ≤28°C but the traces diverged at higher temperatures (32 and 35 °C) with lower Fv'/Fm' at 21% O_2 at these temperatures. Since PSII is the product of PSII and qP and Fv'/Fm', the observed differences in Φ_{PSII} between the low and high oxygen concentrations is the result of qP alone at temperatures of 28°C and below but qP and Fv'/Fm' at higher temperatures.
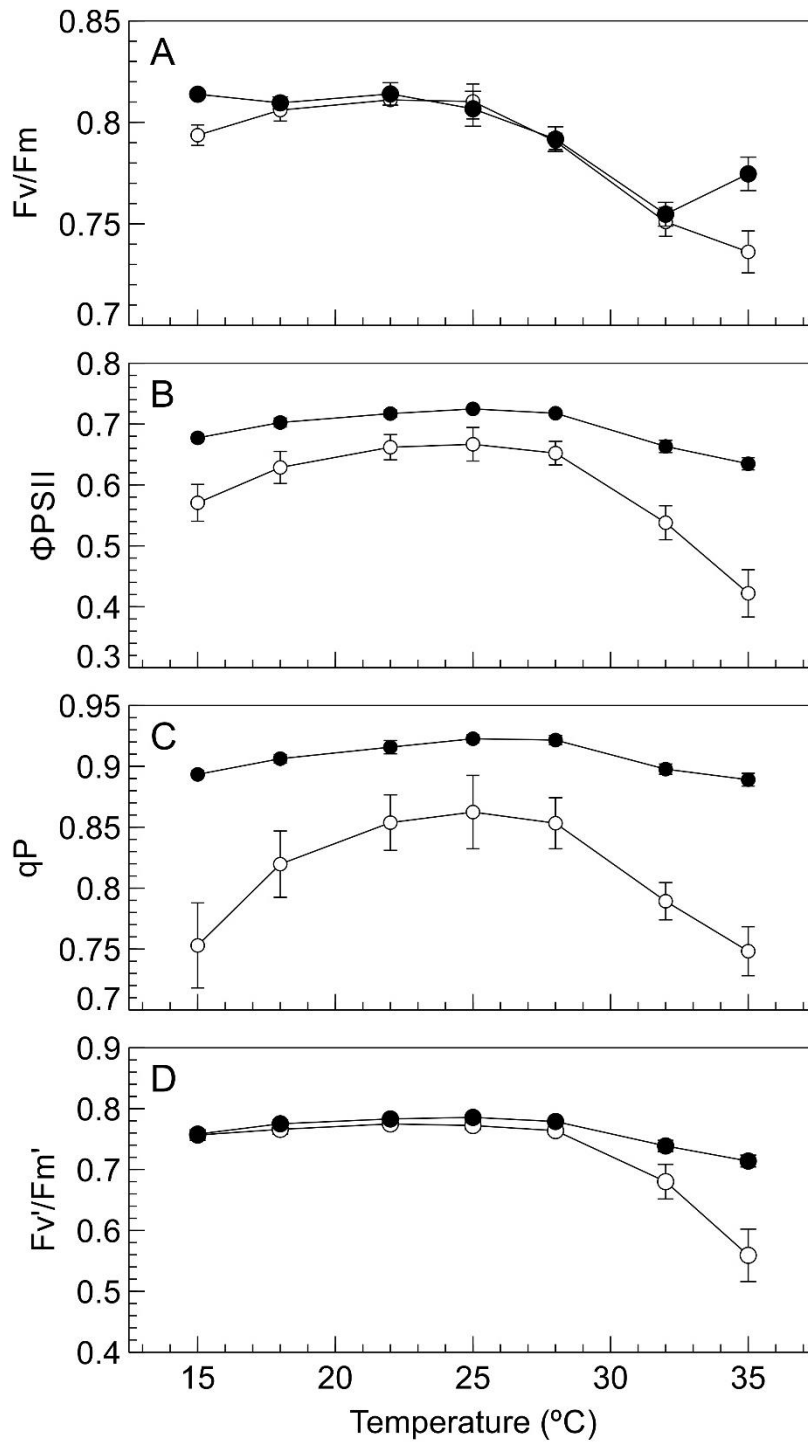
Figure 4: Temperature dependence of (A) dark adapted Fv/Fm and (B) Φ_{PSII}, (C) qP, and (D) Fv'/Fm'of tomato leaves at an absorbed irradiance of 75 μmol m^{-2} s^{-1}. Measurements were taken at low [O_2] (2%, closed circles) and high [O_2] (21%, open circles). Where shown error bars represent SEM (*n*=5).

The effect of light intensity of Φ_{PSII}, qP and Fv'/Fm' are shown in Fig. 5. In general, these parameters showed slight decreases as light intensity increased, and the decreases in Φ_{PSII} and qP were more marked at 21% O_2 than at 2% O_2.

Figure 5: Temperature dependence of selected fluorescence parameters of tomato leaves at incident irradiances ranging from about 33 µmol m^{-2} s^{-1} to 81 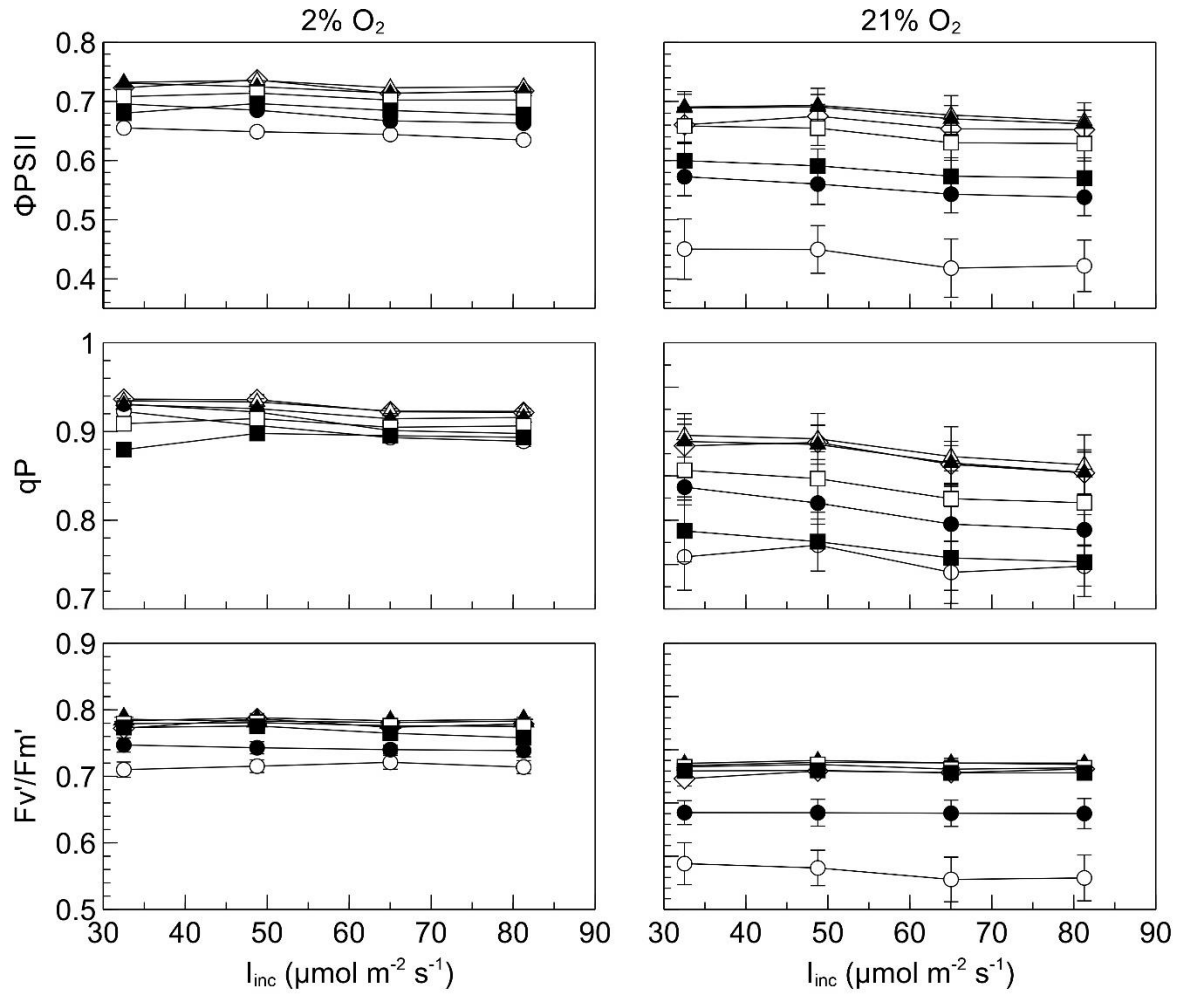µmol m^{-2} s^{-1}, measured at low [O$_2$] (2%, left panes) or high [O$_2$] (21%, right panes). Where shown error bars represent SEM (n=5).

The Fm'/Fm ratio was used to probe for state transitions. These results are presented together with Φ_{PSI} and $\Phi_{PSII}/(\Phi_{PSII}+\Phi_{PSI})$ in Fig. 6. At all temperatures Fm'/Fm values were <1 and at temperatures of ≥32 °C Fm'/Fm was especially low. The response of Φ_{PSI} at both high and low [O$_2$] was somewhat varied. At 21% O$_2$ a reduction in Φ_{PSI} was observed at 32 °C and 35 °C. On the other hand, at 2% O$_2$ Φ_{PSI} was lower and higher, respectively, at 15 °C and 35 °C than corresponding values at 21% O$_2$. Changes in this parameter were however negligible compared with equivalent responses of Φ_{PSII}, and difficult to resolve given that the actinic irradiance stimulated PSI weakly.
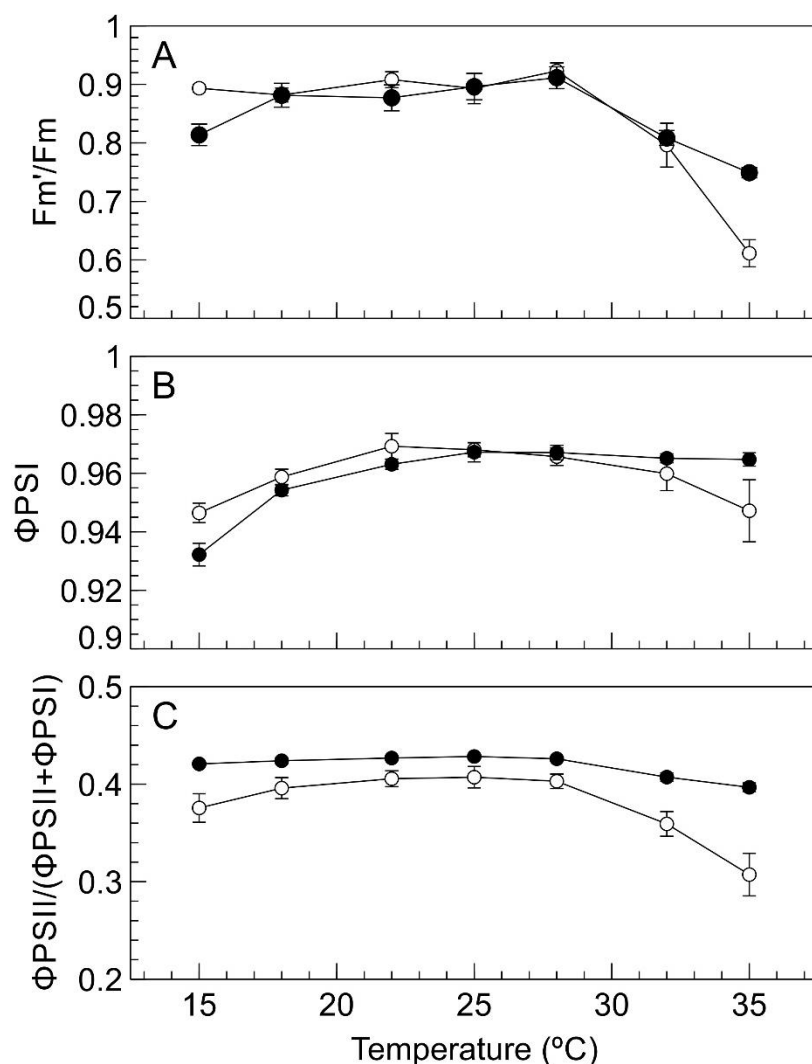
108

Figure 6: Temperature dependence of (A) Fm'/Fm, (B) Φ_{PSI}, and (C) $\Phi_{PSII}/(\Phi_{PSII}+\Phi_{PSI})$ of tomato leaves, measured at an absorbed irradiance of about 75 µmol m^{-2} s^{-1} at low [O_2] (2%, closed circles) or high [O_2] (21%, open circles). Where shown error bars represent SEM (*n*=5).

The results of NPQ at high and low [O_2] are shown in Fig. 7A. NPQ was low for all treatments (<0.25) apart from 32 °C and 35 °C where NPQ increased considerably, especially under high [O_2]. Since mechanisms involved in NPQ are known to be induced by an increase in ΔpH across the thylakoid lumen, the amplitudes of 520nm absorbance (ECS$_{520}$) were also probed (Fig. 7B). The ECS at 21% O_2 was lower than at 2% O_2 across all temperatures and whereas the amplitude changes at 2% showed a negligible response to temperature, the response at 21% O_2 was slightly greater at the temperature extremes and depressed at intermediate temperatures. The relationship between NPQ and Fv'/Fm', shown in Fig. 8, was explored and a generally linear negative relationship between these two variables was observed.
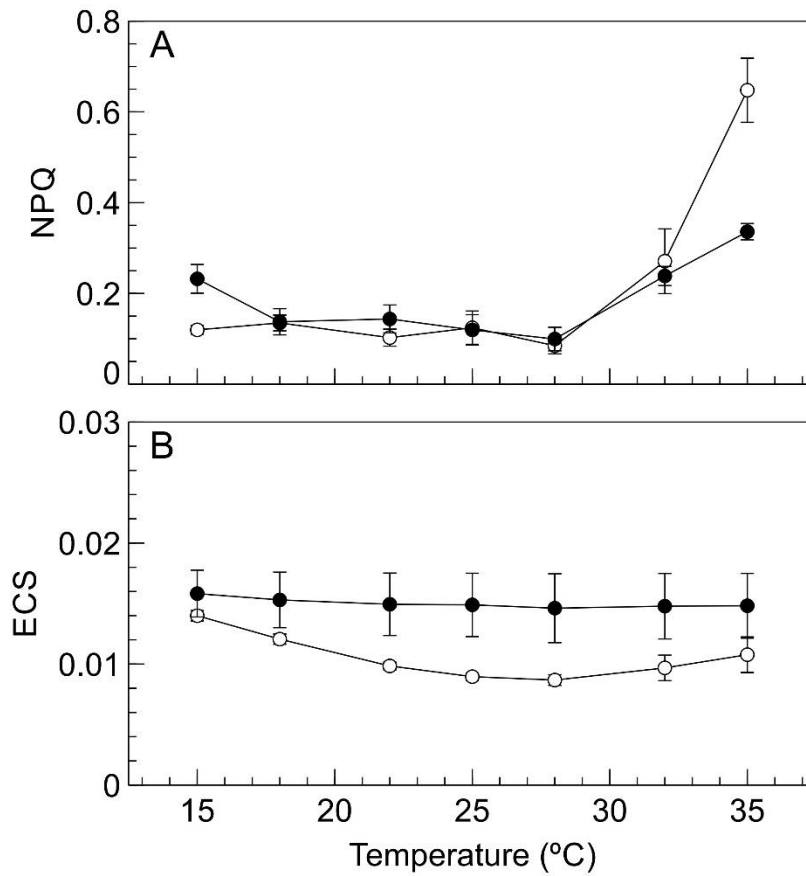
Figure 7: Temperature dependence of NPQ and ECS of tomato leaves, measured at an absorbed irradiance of about 75 μmol m^{-2} s^{-1} at low [O_2] (2%, closed circles) or high [O_2] (21%, open circles). Where shown error bars represent SEM (*n*=5).
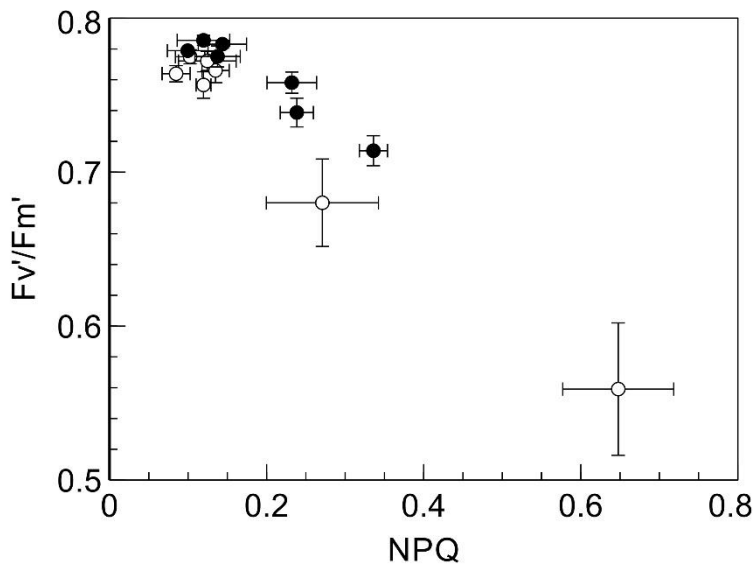
Figure 8: Relationship between NPQ and Fv'/Fm' in tomato leaves at low [O_2] (2%, closed circles) or high [O_2] (21%, open circles). All data points were taken at an absorbed irradiance of about 75 μmol m^{-2} s^{-1}. Where shown error bars represent SEM (*n*=5).

The relationship between Φ_{PSII} and Φ_{CO_2} in relation to temperature is examined in more detail in figures 9 and 10. Whereas the response of Φ_{PSII}/Φ_{CO2} was negligible at 2% O_2, this parameter displayed an exponential response in relation to temperature (Fig. 9). Hook-like relationships between Φ_{PSII} and Φ_{CO_2} were observed for both O_2 concentrations, with a tighter cluster of points for the low [O_2] treatments (Fig. 10). An Arrhenius plot (Fig. 11) of the difference in Φ_{CO2} between 2% and 21% O_2 indicates a linear portion from 15 – 25 °C with deviation from linearity at 28 °C.
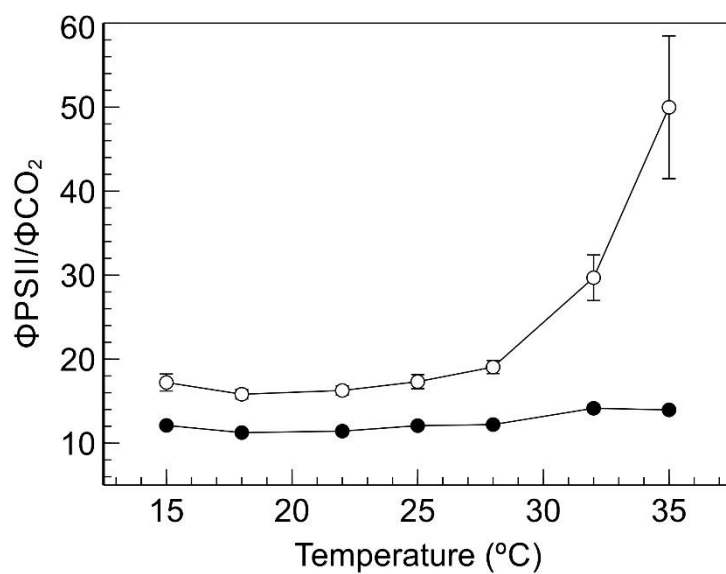
Figure 9: Temperature dependence of Φ_{PSII}/Φ_{CO2} ratio of tomato leaves, measured at an absorbed irradiance of about 75 µmol m^{-2} s^{-1} at low [O_2] (2%, closed circles) or high [O_2] (21%, open circles). Where shown error bars represent SEM (*n*=5).
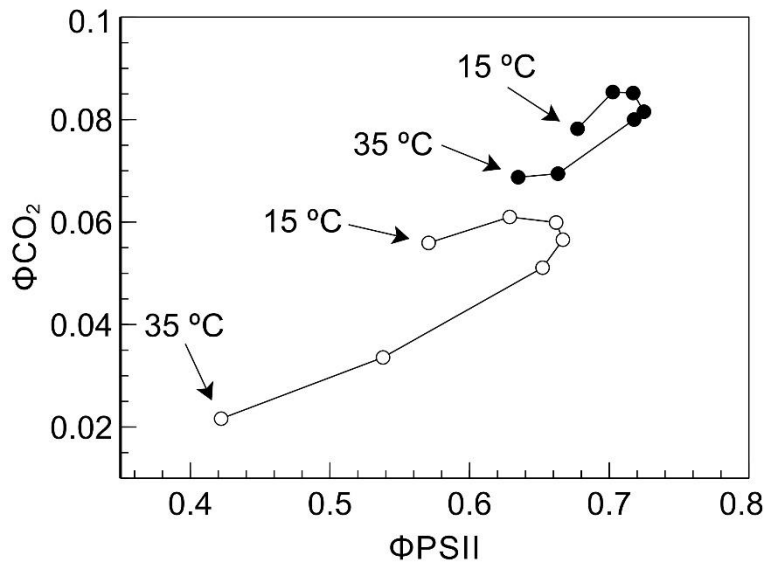
Figure 10: Relationship between Φ_{PSII} and Φ_{CO2} in tomato leaves, measured at leaf temperatures ranging from 15 – 35 °C and low [O_2] (2%, closed circles) or high [O_2] (21%, open circles). Absorbed irradiance was about 75 μmol m^{-2} s^{-1}. Where shown error bars represent SEM (*n*=5).
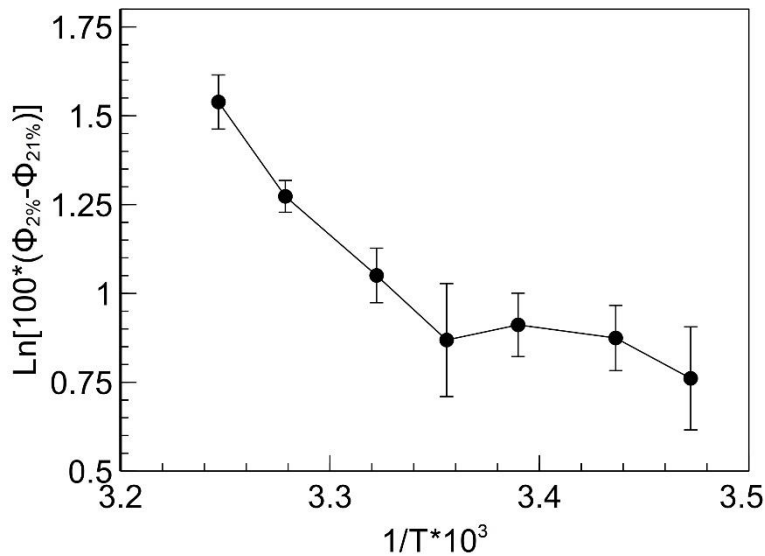
Figure 11: Arrhenius plot of $\Delta\Phi_{CO2}$ (2%-21%) of tomato leaves. Error bars represent SEM (*n*=5).

Since leaves were held at each temperature for about an hour to construct each light-limited slope before proceeding to another temperature, it was thought that this exposure time may have induced temperature related effects that depended on this longer-term exposure, especially at the lowest and highest temperatures. To test what effect a more brief exposure to each temperature may have, leaves were held at each temperature (using a constant

112

background irradiance of 100 µmol m^{-2} s^{-1}), in a sequence from 15 °C to 35 °C, until gas exchange had stabilized (about ten minutes at each temperature). Each measurement sequence was taken using 2% and 21% O_2. The results of Φ_{CO2} and Φ_{PSII} using this method are presented in figure 11.
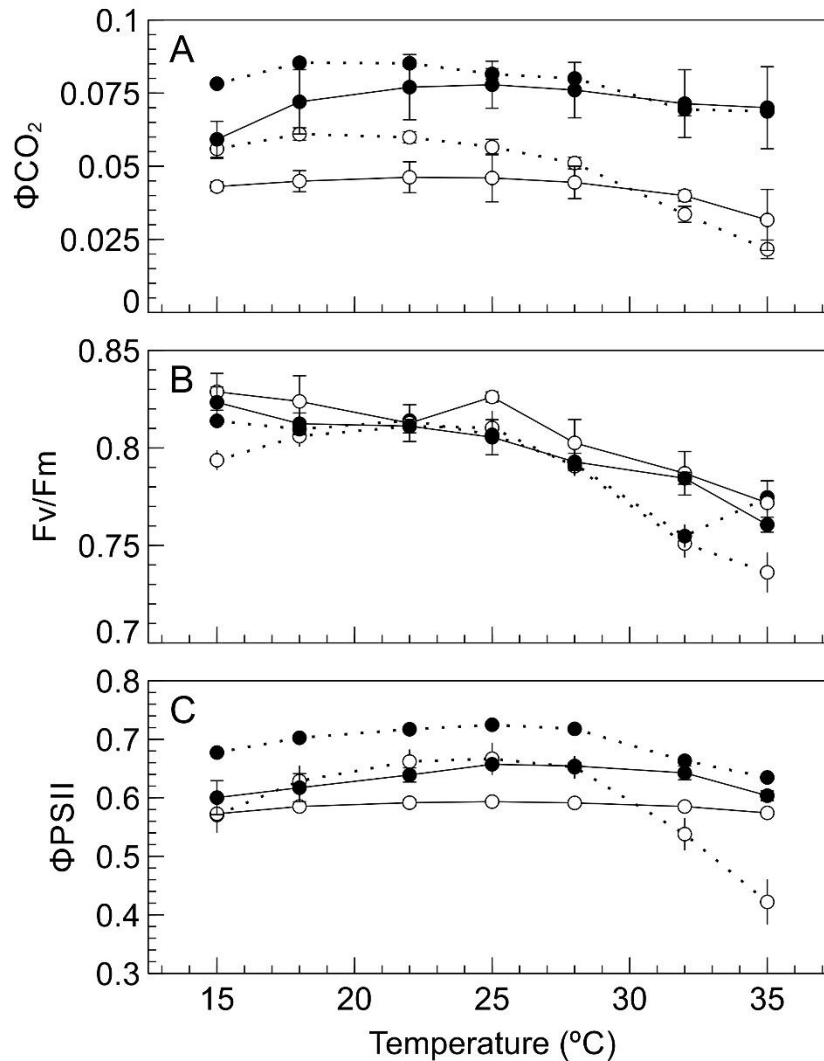
Figure 12: (A) Φ_{CO2}, (B) dark-adapted Fv/Fm, and (C) Φ_{PSII} of tomato leaves measured over a rapid sequence of temperatures from 15 – 35 °C and 2% O_2 (closed circles) or 21% O_2 (open circles). Φ_{PSII} data was taken at an absorbed light intensity of about 75 µmol m^{-2} s^{-1}. Where shown error bars represent SEM (*n*=2). Data from figures 2 and 4 are shown for reference (dashed lines).

Comparing the two methods for measuring the temperature response of assimilation we used, Φ_{PSII} is still greater at all temperatures in 2% O_2 than at 21% O_2 and the convex trend of Φ_{PSII} under 21% is maintained using the fast-response method. Furthermore, in both methods

113

and both oxygen concentrations peak Φ_{PSII} occurred at 25 °C. However, a marked difference between the two methods lies in the response of Φ_{PSII} to temperature at 2% O_2; whereas Φ_{PSII} showed little response to temperature using the longer duration exposure method, a strong convex response, much more marked in 2% O_2 than at 21% O_2, was observed. Fv/Fm was also measured using the fast-response method and, unlike the results obtained using the first method, values tended to decrease linearly as temperature increased. At 21% O_2, Φ_{CO2} also showed a linear decrease with temperature when measured using the fast-response method, although the response at 2% O_2 was convex in nature with a peak occurring at 25 °C.

Discussion

The response of Φ_{CO2} to the moderate temperatures used here indicates the sensitivity of this parameter to temperature. It is safe to consider the temperatures used as 'moderate' given that the lowest (15 °C) and highest (35 °C) temperatures are greater, or less than, those which have been shown to cause chilling or heat injury to PSII or PSI. In chilling-sensitive plants, such as tomato, chilling injury is typically considered to occur below about 10 °C (Terashima *et al.*, 1994). On the other hand, being a warm-climate species, tomato is not expected to be susceptible to heat injury at 35 °C. Accordingly, investigations into heat and chilling injury in tomato leaves have tended to use lower and higher temperatures (e.g. 4 °C and 40 °C; Zushi *et al.*, 2012).

The temperature response of Φ_{CO2} at 2% and 21% oxygen (Fig. 2) revealed a temperature optimum at 18 to 22 °C with decreases at sub-optimal and supraoptimal temperatures. This contrasts with the findings of Yin *et al.* (2014) in the same species, where Φ_{CO2} decreased linearly between 16 and 35 °C under photorespiratory conditions (i.e. the temperature optimum was ≤16 °C). Those authors also observed a flat Φ_{CO2} response at high CO_2 (760 ppm) and low [O_2] (2%). Also in tomato, but at light saturation, the temperature optimum was about 27 °C under photorespiratory conditions but increased up to the highest temperature used of about 32 °C (Sharkey and Sage, 1987). It is however important to note that the underlying limitations imposed by temperature at saturating light intensity can be expected to be quite different from the limitations under strict light limitation. In this respect, the different responses of Φ_{CO2} and A_{max} to temperature (Figs. 2 and 3) show how any given temperature response is relevant only to a specific set of measurement conditions, especially where another potential stress is involved.

Understanding the temperature response of Φ_{CO2} relies on an understanding of the underlying limitations to photosynthesis and the different limitations which may exist at different temperatures. As expected, the most significant impact of temperature on photosynthesis was through its impact on photorespiration, and photorespiration has a strong effect on Φ_{CO2} as evidenced by the considerably greater Φ_{CO2} at 2% O_2 when photorespiration is practically eliminated. At higher temperatures the difference between Φ_{CO2} at 2% and 21% O_2 was more marked, as shown by the increasing divergence with increasing temperature of the high and low [O_2] Φ_{CO2} traces (Fig. 2). The effect of photorespiration is further reflected in the temperature dependence of Φ_{PSII}/Φ_{CO2} (Fig. 9) which in high [O_2] conditions increased exponentially as temperature increased. At low [O_2], however, Φ_{PSII}/Φ_{CO2} showed little to no response to temperature as a result of the lack of photorespiration (Oberhuber and Edwards, 1993), implying that the temperature response of Φ_{CO2} at 2% O_2 can attributed to variation in Φ_{PSII}.

An Arrhenius plot of the difference between Φ_{CO2} at 2% and 21% O_2 (i.e. the relationship ln[100*(2% Φ_{CO2} - 21% Φ_{CO2}) and 1/T; Ehleringer and Bjorkman (1977)) revealed a linear region coinciding with temperatures between 25 and 35 °C but a break from linearity occurred at 28 °C (Fig. 11). The same plot by Ehleringer and Bjorkman (1977) for *E. Californica* revealed an entirely linear response which suggests that, in the present study, distinct differential rate limiting steps exist between the lower (15-25 °C) and higher (28-35 °C) temperatures. Possible candidates for this transition are problems arising from maintaining the balance of supply of ATP and NADPH, and thus possibly alternative electron pathways such as cyclic or pseudocyclic electron flows, or changes in photosynthetic metabolism that affect the balance of ATP/NADPH required by the BCC and photo-respiratory pathways.

The responses of Fm'/Fm and NPQ on the one hand, and Fv'/Fm' on the other, need to be considered as a whole. Fm'/Fm and NPQ (which is Fm/Fm' – 1) are basically different ways of expressing the same physical change, that of a reduction in Fm' relative to Fm. Fm'/Fm is useful as a measure of the effect of state transitions on PSII cross-section (e.g. Bellafiore *et al.*, 2005). NPQ is a useful parameter with which to measure the activity of any qE type non-photochemical quenching activity in PSII that occurs in competition with the decay of excited states of chlorophyll *a* via fluorescence. Unfortunately a state transition will affect NPQ, and a change in non-photochemical quenching will affect Fm'/Fm. Fv'/Fm' is affected by non-

photochemical quenching, but only very slightly by state-transitions (Harbinson, 2018, Taylor *et al.*, 2019), so by comparing changes in NPQ or Fm'/Fm and Fv'/Fm' it is possible, to some extent, to unravel changes in NPQ or Fm'/Fm into changes in qE type non-photochemical quenching or state transitions. From Fig. 8 it is evident that decreases in NPQ and Fv'/Fm' parallel each other; as NPQ increased at 32 °C and 35 °C, Fv'/Fm' decreased. NPQ has been shown to increase at higher temperatures (Georgieva and Yordanov, 1994). Nonetheless, higher temperatures have also been shown to induce state transitions (Weis, 1985). Pea which was heat-treated at 38 and 42 °C showed, respectively, 10% and 17% more LHCII in non-appressed thylakoid regions than that of the control (25 °C) indicative of increased phosphorylation and LHCII migration towards PSI (state 2) at the higher temperatures (Mohanty *et al.*, 2002). In field-grown cotton a transition to state 2 was also observed at high temperature as determined by the ratio of PSI:PSII fluorescence which was greater when field temperature was 41 °C compared to 28 °C (Schrader *et al.*, 2004). A transition to state 2 has also been reported in arabidopsis in darkness at high temperature (Nellaepalli *et al.*, 2011). We cannot say for sure if state transitions contribute to the increase in NPQ and the decrease in Fm'/Fm, but qE type quenching certainly is present. It is noteworthy that in 21% O_2 the increase in NPQ, and decrease in Fv'/Fm', is greater than for 2% O_2.

The response of Φ_{PSII} to temperature in the present study shows the same parabolic trend of modelled Φ_{PSII} in the work of Yin *et al.* (2014) in which data from tomato leaves between 16 and 35 °C in light-limited conditions was used. In potato leaves under low-light intensity (150 μmol m^{-2} s^{-1}), increases in temperature from about 3 °C to about 50 °C also showed a parabolic response (Havaux, 1996b). In that study Φ_{PSII} decreased below about 10 and above about 35 °C, respectively, leaving a broad plateau of nearly constant Φ_{PSII} between these temperatures. On the other hand, practically no change in Φ_{PSII} was observed between 15 and 35 °C in *F. pringlei* under 300 μmol m^{-2} s^{-1} (Oberhuber and Edwards, 1993). Under all measurement conditions, qP was less than 1.0 suggesting that PSII was being over-excited relative to the fraction of PSI engaged in linear electron transport and net QA reduction was occurring even though light-limiting irradiances were being used.

We observed that Φ_{PSII} was lower at all temperatures at 21% O_2 compared with 2% O_2. Only negligible differences in Φ_{PSII} were found between photorespiratory and non-photorespiratory conditions in the C3 species *F. pringlei* (Oberhuber and Edwards, 1993),

including under light-limiting conditions, or nearly so (Oberhuber *et al.*, 1993). On the other hand, oxygen dependence of Φ_{PSII} has been observed in intact leaves of Barley (Clarke and Johnson, 2001). In that study Φ_{PSII} was greater at 21% O_2 than 2% O_2 for all temperatures used – the opposite of what we observed here – although it is also important to note that those authors used a higher, non-light-limiting, irradiance intensity (1600 µmol m^{-2} s^{-1}). One explanation for our results may be increased cyclic electron transport in 21% O_2. This is supported by the negligible temperature response shown by Φ_{PSI} while Φ_{PSII} was greatly impacted by temperature at 21% O_2 but not at 2% O_2. Increased cyclic electron transport may be needed to compensate for the added ATP demand by oxygenation of Rubisco at 21% O_2. However, this explanation does not account for the difference at lower temperatures; when oxygenation of Rubisco is less, the difference in Φ_{PSII} between 2% and 21% O_2 increases rather than decreases. Therefore, a conclusive explanation for suppressed PSII activity at 21% O_2 cannot be reached in the present study.

The amplitude of the 520 nm absorbance changes (the electrochromic shift or ECS) measured following a light to dark transition, is a measure of the light dependent transthylakoid voltage and is a proxy for the transthylakoid proton motive force (Baker *et al.*, 2007). The ECS showed no response to temperature at 2% O_2 and was greater than at 21% O_2 for all temperatures. The ECS at 21% O_2 did vary with temperature, increasing with decreasing or increasing temperatures from a minimum at 28 °C. The lower ECS in 21% O_2 compared to 2% O_2 could be explained by the relatively greater demand for ATP relative to NADPH in the presence of photorespiration. This could lower the phosphorylation potential in the stroma and result in a lower driving force being required to drive ATP synthesis. Non-photochemical quenching of Fm at 2% O_2 was higher than at 21% O_2 at 35 °C, but the same at all other temperatures apart from 15 °C where NPQ was lower in the 21% O_2 treatment. This explanation, therefore, does not fully account for the perceived differences in PSII across temperatures.

Since low [O_2] measurements were always taken first for a given set of high and low [O_2] measurements, it was initially suspected that these differences may be an artefact of injury occurring from the exposure to low [O_2], though no such damage had been observed in the past to tomato in similar experiments. Fv/Fm was examined to exclude this possibility, and no differences in this parameter were found to occur apart from at 15 °C and 35 °C where Fv/Fm was slightly lower at 21% O_2. These small differences do not account for the impact of

temperature at other temperatures within the temperature extremes including moderate temperatures. It is furthermore unlikely that temperatures of 15 °C and 35 °C, and an exposure time to these temperatures of not more than 60 mins using low actinic light intensity, were damaging to PSII. Maximum Φ_{PSII} at the highest light intensity (Fv'/Fm') was lower at 32 °C and 35 °C at 21% O_2 but was comparable at all other temperatures, further supportive of there being no artefact of previous measurements on PSII operation. The more rapid measurement procedure, which switched rapidly between temperatures at each light intensity, showed slightly different results for Φ_{CO2}, Fv/Fm, and Φ_{PSII} than the more conventional method of constructing full light-limited slopes for each temperature at a time. These differences raise the question as to whether the rapid procedure was in fact measuring the response to rapidly changing temperature rather than the intended steady state temperature response. In this regard the generally weaker linearity of Φ_{CO2} using the rapid approach may have been a result of state transitions, which would also have impacted Φ_{PSII}.

The somewhat different results obtained using two methods – a slower, more conventional approach and a fast-response approach - revealed the impact of measurement procedure in temperature work. In particular it is apparent that leaves may possess 'memory' of exposure to different temperatures even from exposure to the moderate temperatures used here, which impacts the perceived temperature response. It is important to note that temperature changes in the natural environment are highly dynamic and considerably more complex than the comparative temperature stability provided in most temperature studies. For example, leaves can undergo temperature changes on a wide range of timescales such as briefly during a sunfleck, to longer term changes including diurnal variation and seasonal fluctuations. Special care should care should therefore be taken in the design of temperature response experiments and when interpreting results, especially within ecophysiological contexts.

Acknowledgements

CHAPTER 6

GENERAL DISCUSSION

This thesis was stimulated by the need to better understand the response of photosynthesis to the potentially diverse spectral possibilities associated with LED supplementary lighting in greenhouses. Since, even with supplementary lighting, the rate of photosynthesis in most leaves remains light-limited (apart from unshaded leaves in the canopy), the focus of this thesis is on spectral effects on light-limited photosynthesis (Φ_{CO2}).

Although the use of narrowband lighting has proved useful in deciphering the functioning and nature of the photosynthetic apparatus as well as spectrally sensitive sensors (e.g. the existence of the two photosystems and various photoreceptors), the natural environment presents a considerably more complex light environment. An added layer of complexity is introduced in the greenhouse when using supplementary LED lighting which produces a considerably different spectrum to that of daylight. An understanding of the impact of light spectrum on leaf photosynthesis and whole-plant morphology is necessary if LED lighting technology is to be implemented effectively.

Two principle environmental factors which impact Φ_{CO2} – light and temperature – received attention in this work. In chapter 1 a literature review explored the response of Φ_{CO2} to light spectrum as well as the underlying biophysical phenomena which underpin this response. Chapter 2 revealed that enhancement of photosynthesis does occur in certain 'white' light spectra. A relationship between state transitions and Φ_{CO2} is shown in chapter 3. Given the spectral impacts on plant morphology, chapter 4 adopted a holistic view by investigating the combined impact of blue supplementary lighting on photosynthesis and morphology, and how this impacts whole-plant performance. Chapter 5 examined the effect of temperature on Φ_{CO2} as well as Φ_{PSII} and Φ_{PSI}. In this chapter the key findings are collated and discussed in relation to the practical implications for greenhouse supplementary LED lighting with some attention given to the broader ecophysiological significance of results.

6.1. Basic spectral dependency of Φ_{CO2}

Chapter 2 examined the spectral dependency of Φ_{CO2} of leaves in 17 narrowband irradiances and the same narrowband irradiances combined with either a simulated daylight or shade-

light spectrum as background irradiance. Dealing with the results for the narrowband irradiances alone, the spectral response of Φ_{CO2} which we obtained is characterised by peak Φ_{CO2} in the red region, a trough in the longer blue wavelength region (480-500 nm) and a shoulder in the shorter blue wavelength region (400-460 nm). This is a typical response which has been observed for Φ_{CO2} in plants (McCree, 1972a; Inada, 1976; Evans, 1987; Hogewoning *et al.*, 2012) and Φ_{O2} in algae (Emerson and Lewis, 1943). However, there are some apparent differences amongst these studies and our own in terms of the precise spectral response which are noteworthy. For example, the marked trough which we observed at 480-500 nm was absent in cucumber (Hogewoning *et al.*, 2012) as was also the case in a few of the 33 species surveyed by Inada (1976) where this trough was not present or very minor. Inter-species differences in the spectral dependence of Φ_{CO2} in surveys by Inada (1976) and McCree (1972a) was small in the majority of cases but sizeable in others, and these differences ought to be further explored and understood. Growth spectrum also influences the spectral dependence of Φ_{CO2}, as evident from the different responses of Φ_{CO2} to spectrum in SUN-grown and SHADE-grown leaves (chapter 2, Fig. 3). The underlying causes of these spectral differences arising from growth spectrum are discussed below.

6.2. Impact of growth spectrum on spectral dependence of Φ_{CO2}

A longer-term acclimation mechanism, in contrast to state transitions, is the adjustment of PSI and PSII stoichiometry. For example, the PSII:PSI ratio of thylakoids from pea leaves was greater when plants were grown in PSI-overexciting irradiance (Chow *et al.*, 1990). Likewise, work by those same authors also showed a lower PSII:PSI ratio of thylakoids in leaves of plants grown in PSII-overexciting irradiance. When Arabidopsis was transferred from white light to far-red light the PSI:PSII ratio decreased to about one-third of the ratio in white light over a period of 5-8 days (Wientjes *et al.*, 2017). Therefore, leaves demonstrate a 'memory' of growth spectrum by means of long-term acclimation. The result of this acclimation is greater Φ_{CO2} when leaves have a photosystem excitation balance which closely matches that of their growth spectrum (Chow *et al.*, 1990). The effect of growth spectrum on spectral dependence of Φ_{CO2} is evident in results shown in chapters 2 and 3. In chapter 2, Fig. 5A, SHADE-grown leaves have a higher Φ_{CO2} under PSI irradiance (700 nm) than leaves produced in the SUN spectrum. On the other hand, SUN-grown leaves had a higher Φ_{CO2} than SHADE-grown leaves when subjected to the PSII irradiance (480 nm).

There are two main reasons for the lower Φ_{CO2} for most wavelengths in SHADE-grown leaves than in SUN-grown leaves. First, the majority of wavelengths in the PAR spectrum preferentially excite PSII as shown by comparatively lower PSII and qP values. The latter has also been shown in cucumber (Hogewoning *et al.*, 2012). Second, as discussed, SHADE-grown leaves have comparatively more PSII than SUN-grown leaves which is beneficial to Φ_{CO2} under their PSI-overexciting growth irradiance but detrimental under PSII irradiance which leads to a loss of qP (chapter 2, Fig. 6). In general, a commonality in instances where SHADE-grown leaves had a similar or greater Φ_{CO2} than SUN-grown leaves were wavelengths where Φ_{PSII} was similar between SUN- and SHADE-grown leaves (e.g. 400-460 nm, 520 nm and 700 – 720 nm). It is noteworthy that a marked peak in Φ_{PSII} at 520 nm was observed in SHADE-grown leaves. The cause of this peak is not known but the same phenomenon was also found in shade-grown cucumber leaves (Hogewoning *et al*., 2012). This could be due to a potentially different pigment composition of shade-grown leaves (e.g. non photosynthetic pigments or carotenoids) which would attenuate the energy of this spectral region which reaches PSII reaction centres and, in the case of carotenoids, result in less efficient energy transfer to chlorophyll (Croce *et al.*, 2001).

6.3. Spectral dependency of PSI and PSII efficiency

The biophysical nature of the photosystems, which are diverse in terms of pigment composition and hence absorption spectrum, inherently leads to certain spectra which preferentially excite PSI or PSII. Classically, wavelengths less than about 690 nm have been regarded as PSII irradiances whereas wavelengths greater than this have been regarded as PSI irradiances (e.g. Evans, 1987). Although this is true in a general sense it is an oversimplification. In chapter 2 it is evident that not all shorter wavelengths exert the same excitation pressure on PSII or PSI. For example, as shown in chapter 2, Fig. 6, while some wavelengths strongly overexcite PSII (e.g. global minimum at 480 nm and local minimum at 660 nm), other shorter wavelengths (e.g. 400-460 nm, 520-540 nm, and 640 nm) exert considerably less excitation pressure on PSII and more on PSI. In fact, at 400-460 nm, ΦPSI is relatively efficient compared to other wavelengths <700 nm. Essentially a continuum exists in terms of the excitation pressure imposed on PSII with all other shorter wavelengths falling somewhere between the extremes at 480 nm and at 660 nm in the case of the tomato leaves in this study. The transition from 'PSII irradiance' to 'PSI irradiance' occurs very sharply

between 680 and 700 nm as shown by the increase in Φ_{PSII} and sharp drop in Φ_{PSI} (chapter 2; Fig. 6). Furthermore, the see-saw nature of photosystem efficiency in relation to spectrum is illustrated by the inverted responses of Φ_{PSI} and Φ_{PSII} i.e. when Φ_{PSII} is high, Φ_{PSI} is low and *vice versa*. This difference in the spectral response of the photosystems is expected based on the different absorption spectra of PSI and PSII (Laisk *et al.*, 2014).

6.4. Relevance of enhancement to Φ_{CO2}

The enhancement model holds that two irradiances, when applied in combination, result in greater rates of photosynthesis than would be predicted based on the sum of the rates of photosynthesis measured in each of the irradiances on their own. A prerequisite for enhancement to occur is that one of the irradiances must over-excite PSII while the other must over-excite PSI, to some extent; the combination of the two irradiances better balances the excitation of the photosystems compared to when either irradiance is applied alone. It is this improved photosystem excitation balance which leads to an increase in photosynthetic efficiency and a corresponding increase in the rate of photosynthesis beyond what can be accounted for by the sum of the rates of photosynthesis for each of the irradiances. While enhancement has routinely been shown to occur in narrowband mixtures, no consensus has been reached on the involvement of this phenomenon in 'white' light (e.g. McCree, 1972b).

In chapter 2, Φ_{CO2} obtained from light-limited slopes was used to test for enhancement instead of single-point assimilation measurements often used in enhancement work. An advantage of this approach is that it is not affected by potential error in the estimation of dark respiration. Measurements of Φ_{CO2} using 17 narrowband irradiances produced 17 corresponding data points for Φ_{CO2} which were interpolated to produce a curve with an associated Φ_{CO2} per wavelength (chapter 2, Fig. 3). If the effect of each wavelength on Φ_{CO2} is assumed to be additive and independent, and the spectrum of an irradiance is known, then Φ_{CO2} can easily be predicted for the spectrum of interest by summing the product of interpolated narrowband Φ_{CO2} data and the relative spectral distribution of each spectrum (McCree, 1972b). However, by combining narrowband spectra with one of two broadband irradiances (SUN and SHADE), chapter 2 shows that this assumption is not always valid. Whereas differences between measured and predicted Φ_{CO2} were negligible in SUN-grown leaves subjected to SUN (i.e. no or little enhancement occurred for that spectrum), in SHADE-grown leaves subjected to SHADE measured Φ_{CO2} was 23% greater than predicted Φ_{CO2} using

the method described above, indicating enhancement of 23%. Clearly, the prediction of Φ_{CO2} in broadband irradiance (or a mixture of irradiances) is not a straightforward exercise since enhancement can cause significant deviation of measured Φ_{CO2} from predicted Φ_{CO2}. As noted earlier, a prerequisite for enhancement is that the applied spectrum must result in better balance of PSII and PSI photochemistry than the component spectra (or wavelengths) on their own and by so doing ameliorate or eliminate Φ_{CO2} losses otherwise caused by photosystem imbalance. Almost all narrowband wavelengths within the PAR region preferentially excite PSII and only somewhere in a very narrow band somewhere between 680 nm and 700 nm, where a sharp decrease in PSII absorbance and increase in PSI absorbance occurs, could a narrowband irradiance lead to relatively balanced excitation of the photosystems. Having observed enhancement for only the SHADE spectrum, the question arose as to which spectral region(s) underpinned the enhancement response. A key difference between the broadband spectra is that the SHADE spectrum is rich in more PSI-overexciting far-red irradiance - 28% of total photon flux between 700 and 728 nm - whereas this figure is only 10% for the SUN spectrum, which is comparatively rich in PSII irradiances. The impact of these compositional differences is evident on the photosystem excitation balance, whereas SHADE leaves subjected to SHADE had a $\Phi_{PSII}/(\Phi_{PSI}+\Phi_{PSII})$ ratio of 0.48, this ratio was 0.46 in SUN leaves subjected to SUN. Though small, this difference could be expected to be greater in SUN leaves subjected to SHADE, and SHADE leaves subjected to SUN, because of their acclimation bias towards their corresponding PSI light (shade light) or PSII light (daylight) growth spectrum. It may be useful for future work to measure sun-grown leaves in shade and shade-grown-leaves in daylight, similar in concept to the PSII light/PSI light transfer experiments by Chow *et al.* (1990), to establish the extent of photosystem imbalance and corresponding impact on Φ_{CO2} in more natural spectra.

The addition of narrowband spectra from across the PAR spectrum and including 700 and 720 nm (in a 1:1 ratio with each of the SUN and SHADE spectra on an absorbed PAR basis) revealed the participation of far-red in instances where enhancement was found to occur. In SUN leaves enhancement increased from 4.7% to 7.5% and 37% as added narrowband irradiance increased from 680 to 700 and 720 nm. In SHADE leaves enhancement was 17-27% for all added narrowband wavelengths between 400 and 700 nm but 76% for SHADE plus 720 nm. An explanation for the latter enhancement was less obvious given that SHADE irradiance and

720 nm irradiance are both 'PSI' irradiances. However, the SHADE irradiance also comprises some PSII irradiances which lead to enhancement even when PSI-overexciting narrowband irradiances were added to it. Clearly, predicting whether enhancement may occur requires a holistic view of the irradiances used and careful examination of their component spectra with respect to stimulation of PSII and PSI photochemistry.

Such was the enhancement in SHADE-grown leaves subjected to SHADE plus 680 nm that Φ_{CO2} was as high as 0.089, comparable with the highest Φ_{CO2} of 0.09 measured in this work in SUN leaves in 680 nm irradiance. This demonstrates three things: 1.) As a result of enhancement, Φ_{CO2} in broadband 'white' spectra comprising many less efficient wavelengths for photosynthesis can be comparable to Φ_{CO2} in the red spectral region where Φ_{CO2} is at a maximum, 2.) high Φ_{CO2} values reported using broadband light (e.g. 0.093 by Long *et al.* (1993) and 0.092 by Evans (1987)) must be the result of significant enhancement (as proposed by Hogewoning, 2012) if not an over-estimation of Φ_{CO2}, and 3.) SHADE-grown leaves, which generally showed lower Φ_{CO2} than SUN-grown leaves for the narrowband spectra alone, can potentially have a high Φ_{CO2} comparable to that of SUN-grown leaves. In fact, SHADE-grown leaves were compromised compared to SUN-grown leaves when using mostly PSII-overexciting narrowband irradiances since they have comparatively more PSII-LHCs which makes them better suited to their growth spectrum but not to PSII irradiances. Consequently, SHADE leaves were in state 2 for all PAR wavelengths with the exception of 700 nm as shown in chapter 2, Fig. 8. On the other hand, the greater Φ_{CO2} in SHADE-grown leaves at 700 nm and 720 nm compared to SUN-grown leaves is simply the reciprocal of the latter i.e. SUN-grown leaves have more PSI-LHCs. By eliminating the photosystem balance problem in SHADE-grown leaves it becomes apparent that these leaves can utilise broadband light with high efficiency provided the spectrum is conducive.

Since narrowband and broadband irradiances were combined in an arbitrarily-chosen 1:1 ratio, a natural question is how changes in this ratio, which will be routinely encountered in supplementary-lit greenhouses due to changeable daylight intensity (e.g. arising from cloudcover or sun angle), may impact enhancement. A corollary is whether the extent of enhancement can be predicted (or Φ_{CO2} in broadband light). Though it was beyond the scope of this work, it seems that the answer may lie in weighting irradiances according to PSII or PSI excitation of component wavelengths.

6.5. Impact of state transitions on Φ_{CO_2}

Alternations between PSII and PSI irradiances have previously been performed to induce state transitions during gas exchange measurements (Anderson *et al.*, 1993) but no relationship between state transitions and Φ_{CO_2} were observed in that study. Those authors used white light and white light supplemented with far-red light as PSII and PSI irradiances. The conspicuous nature of the 480 and 700 nm irradiances in terms of PSII and PSI over-excitation was observed in chapter 2. In this respect, the 480 nm irradiance was the most extreme PSII-extreme irradiance in our study (chapter 3, Fig. 6A) as well as that of Hogewoning *et al.* (2012) and the 700 nm irradiance was the second most strongly PSI-overexciting irradiance (chapter 3, Fig. 6B) (the 720 nm irradiance being the strongest PSI-overexciting irradiance but too weakly absorbed to resolve Φ_{CO_2} with sufficient accuracy). The question arose as to whether these extreme irradiances would reveal any relationship between state transitions and Φ_{CO_2}.

Upon switching from one irradiance to the other, Φ_{CO_2} fell sharply to a local minimum before gradually increasing to a new steady state. These increases were accompanied by closely related changes in the cross-sectional area of PSII as gauged by Fm'/Fm and Fo'/Fo. These changes in cross-sectional area serve to reduce the excitation pressure on the over-excited photosystem, while simultaneously increasing the excitation pressure on the other, less excited, photosystem. Therefore, our findings are in agreement with the generally accepted state transition model in algae and higher plants. One possible exception to the latter is the location of mobile PSII-LHC in state 2, which is not resolved in this work. The generally accepted model holds that PSI is the docking point of mobile PSII-LHC although no consensus has been reached (Haworth and Melis, 1983). It seems reasonable that, based on the findings in chapter 3, that mobile LHCII associates with PSI since photosynthetic efficiency continues to increase during a state 2 to state 1 transition while Φ_{PSII} falls.

In terms of their impact on photosystem efficiency, a state transition was able to increase Φ_{CO_2} by 10-13% in both SUN- and SHADE-grown leaves compared to the local minimum observed immediately about light switching. Our results show, however, that state transitions mitigate, but do not eliminate, losses arising from such extreme imbalance. This is evident from the low values of Φ_{PSII} or Φ_{PSI} even after completion of a state transition. Longer term acclimatory differences between the leaf types (discussed in section 6.2.) are also not compensated for by state transitions as shown by the lower photosynthetic efficiency in

SHADE-grown leaves than in SUN-grown leaves under the PSII irradiance (or the lower photosynthetic efficiency in SUN-grown leaves than shade-grown leaves under PSI irradiance). Our results are therefore consistent with the view of state transitions as a 'fine-tuning' mechanism (Andrews, 1995).

Another notable aspect is the duration over which a state transition occurred. It took about 30 minutes for cessation of a state transition in either direction. Though this is rapid when one considers the extent of LHCII redistribution (and considerably more rapid than longer-term acclimation), it remains slow compared to rapidly induced photosystem excitation imbalances such as those caused by a sun-fleck which can occur in the order of seconds or less. The results obtained here can only mean that state transitions are ineffective against such rapid changes and their utility may instead lie in the acclimation to more gradual changes, such as when changing sun angle illuminates previously shaded leaves or changes the angle of illumination of leaves (e.g. He *et al.*, 1996). Changes in solar spectrum with sun angle including the increase in far-red at twilight (Hughes *et al.*, 1984) could also be a target for state transitions. Alternations between PSI and PSII growth irradiances have been performed hourly (Bellafiore *et al.*, 2005) or as little as every 20 minutes (Wagner *et al.*, 2008). Even more rapid PSI/PSII growth irradiance alternations could better reveal the limitations of state transitions in changeable spectra. Where does mobile LHCII come to rest when spectral changes favouring PSI or PSII alternate more rapidly than the kinetics of state transitions? Another pertinent question is whether the relationship between state transitions and Φ_{CO2} in the present work is preserved in more natural spectra, given that the spectra used in the present work are very different to what occurs in natural conditions. Alternations between simulated sun and shade spectra – such as the ones used in the present work will likely provide some clarification in this regard. Andrews *et al.* (1993) used white light from a quartz halogen lamp as PSII light and the same white light together with far-red light as PSI light to probe for a relationship between state transitions and Φ_{CO2}. These spectra are however also very different from what could be encountered by a leaf in the natural environment, being especially deficient in blue light and rich in red and far-red. Addressing these questions will contribute significantly to understanding the relevance of state transitions in an ecophysiological context.

6.6. Maximum Φ_{CO2} of leaves

Apart from its ecophysiological significance, maximum Φ_{CO2} is an important figure within the context of maximising the efficiency with which supplementary LED lighting is used. It seems more useful in practice to gauge the efficiency with which light is used relative to a known intrinsic maximum Φ_{CO2} rather than by comparison with Φ_{CO2} values for other light spectra. In this way lighting strategies or algorithms can target a known maximum. Maximum Φ_{CO2} has a history of controversy (Govindjee, 1999) and remains somewhat inconclusive. In a meta-analysis, Singsaas et al. (2001) concluded that maximum Φ_{CO2} deviates little across diverse taxa from the mean maximum value reported by Long (1993) of 0.093 and that variation in this value is likely due to measurement error. Apart from the testing for enhancement in chapter 3, the use of 53 unique spectra, including 17 narrowband irradiances and two natural broadband spectra (simulated sunlight and shade-light), provided an extensive spectral survey with which to test maximum Φ_{CO2}. Furthermore, since the simulated sunlight and shade-light were also used as growth spectra, two diverse growth acclimations could be tested. The greatest maximum Φ_{CO2} out of all spectra and growth spectra combinations was 0.09 μmol CO_2 μmol photons^{-1}, occurring in SUN leaves subjected to 680 nm irradiance. This value compares favourably with other reported maximum Φ_{CO2} values, such as a mean of 0.093 in a survey of 11 C3 species of diverse taxa (Long et al., 1993) and the same value in cucumber (Hogewoning et al., 2012). Evans (1987) observed a maximum Φ_{CO2} of 0.092 in pea. It would seem unlikely, given the tight clustering of our values and the other values reported here, that maximum Φ_{CO2} should be materially different from, if not very close to, 0.09.

One factor, amongst several, that could be expected to change the value of Φ_{CO2} is leaf nitrate assimilation of which at least the nitrite reduction step depends on light-generated chloroplast reducing power. Viewed simply, less nitrate reduction taking place in the leaves could be expected to increase Φ_{CO2} as result of diminished competition between chloroplast CO_2 fixation and nitrite reduction (and including even nitrate reduction with nitrate assimilation taking place in the roots or with no nitrate reduction at all in the case of ammonia assimilators, our measurements were made under conditions where we exercised no control over the extent nitrate reduction occurring in the leaves or roots.

Can the maximum Φ_{CO2} in the present work be explained? The maximum theoretical quantum efficiency of assimilation on an absorbed light-basis is often given in textbooks as 0.125. This

value is based on a very idealised model of 2 NADPH required per CO_2 fixed, so 4 e-, which requires 8 photons, 4 by PSII and 4 by PSI, and with both photosystems operating with a quantum efficiency of 1. However, in this reckoning, no account is taken of the supply of ATP. Returning to a NADPH-centred calculation there are some obvious shortcomings. The maximum efficiency of PSII for electron transport is only ~ 0.9, and maximum efficiency of PSI for electron transport is usually reported as being near 1. Assuming balanced excitation of the two photosystems (i.e. neither photosystem limits the other) and only linear electron transport takes place, the decreased efficiency of PSII results in a loss of maximum efficiency from 0.125 to 0.119 (a factor of 0.95). The maximum efficiencies of about 0.093 reported here and elsewhere under non-photorespiratory conditions are, however, considerably less than 0.119. The value of 0.119, like that of 0.125, is however based on the assumption that Φ_{CO2} is limited by NADPH formation. Assuming NADPH limitation means no account is taken of the shortfall in ATP formation compared to NADPH formation by LET compared to the demands Calvin-Bassham-Benson cycle (CBB). The CBB running without any oxygenation of RuBP has an ATP/NADPH ratio of 1.5 while linear electron transport has an ATP/NADPH of 1.28. This assumes 3 H^+ are deposited in the thylakoid lumen per unit linear electron transport and 4.67 H^+ are required per ATP. This shows that linear electron transport acting alone to drive the CBB alone is ATP limited. Extra ATP must be provided from some source to allow the CBB to operate and the fact that CO_2 fixation does occur implies that this shortfall of ATP is made up for, and this is likely to occur by the action of an alternative electron transport route that makes an excess of ATP compared to the formation of reducing power. These alternative electron transport pathways could include, for example, linear electron transport leading to nitrite reduction in the chloroplast, the export of reductant from the chloroplast via the Malate valve, or the reduction of O_2 in the chloroplast via the pseudocyclic path (which depends on the Mehler reaction); or cyclic electron transport around PSI.

It is not yet possible account for the contribution made by different alternative electron transport pathways to the total ATP/NADPH budget of the CBB (or the CBB plus photorespiration under natural O_2 partial pressures. The activity, however, of these alternative electron transport pathways needed to make this ATP will result in a loss of the light-use efficiency for assimilation. This can be illustrated using a scenario in which a leaf is photosynthesising in a 2% O_2 atmosphere with 400 ppm CO_2 (so no photorespiration) and in

which pseudocyclic electron transport provides the extra ATP for the CBB. As noted earlier for these conditions the ATP/NADPH demand for the CBB is 1.5 but the ATP/NADPH production ratio of the LET is only 1.28, resulting in a shortfall of 0.22 ATP per 2 electrons moving through the LET chain, or 0.11 ATP per single electron. To meet the demands of the CBB we would need the NADPH produced by 4 LET and the ATP produced by 4.68 LET, so 0.68 LET would need to operate pseudocyclic electron transport and produce only ATP. Combining this scenario with a maximum average photochemical efficiency of 0.95 would result in a maximum quantum yield for assimilation of 0.102. Using purely cyclic electron flow to produce the extra ATP would result in a higher yield. This scenario illustrates the need to consider the energetic realities of running the CBB or CBB+PCO when estimating maximum light-use efficiencies and the 0.125 yield so widely encountered in textbooks and lectures is in practice not realistic. Fully accounting for the observed quantum efficiencies of light-limited assimilation remains, however, 'work in progress'.

6.7. Practical challenges and considerations when determining Φ_{CO2}

It should be noted that Φ_{CO2} is difficult to measure accurately and multiple sources of potential error exist, as alluded to by Singsaas *et al.* (2001). This arises because of the many individual measurements which are involved in the calibration of measurement apparatus especially that of light intensity which is often not measured properly (Hogewoning *et al.*, 2010b). Errors in individual calibration measurements can easily compound to create erroneously low or high determinations of Φ_{CO2}. Furthermore, errors at low CO_2 flux, such as under light-limiting conditions, can have a much greater impact than at higher CO_2 fluxes (Long and Bernacchi, 2003). The present work went to great lengths in an effort to obtain absolute Φ_{CO2} values which involved careful and exhaustive analysis of all aspects relating to Φ_{CO2} measurement. For light calibration, a 13-photodiode cosine corrected light sensor with an optical window identical to the chamber area was designed to provide an average chamber light intensity. This eliminated errors associated with point source light measurement since chamber light intensity is known to be heterogeneous to some extent (Hogewoning *et al.*, 2010b). The lab-made sensor was repeatedly tested using diverse spectra and its performance was found to compare very favourably with a calibrated spectrophotometer. The lab-made sensor was also found to have a more flat spectral response than a commercial PAR sensor (Li-190, LICOR, Nebraska, USA). The latter sensor was found to have a maximum error of

6.43% for 14 narrowband spectra with peak wavelengths between 431 and 676 nm (average error=4.11%). Though this may be inconsequential for most light intensity measurements, it is significant in this kind of work especially when considering error arising from point source measurement if no suitable correction for heterogenous chamber light intensity is made. The lab-made sensor, on the other hand, was found to have a maximum error of 2.99% (average error=1.18%) for the same range of wavelengths. For matters related to gas exchange, several types of chamber material were tested before a neoprene seal was found to be superior. A quick-set non-toxic moulding silicone was used to eliminate the presence of any leaks which originated from the abaxial side of the leaf, undoubtedly as a result of the slightly imperfect contouring of the neoprene around larger leaf veins. Infrared gas analysers were cross-checked with other calibrated infrared gas analyzers at high (21%) and low oxygen (2%) concentrations. Gas flow path length was minimised and different gas tubing materials were tested for permeability to CO_2 or H_2O. Despite these comprehensive tests it was only after many design iterations and adjustments that ostensibly low and erroneous Φ_{CO2} values were eliminated.

6.8. Effect of spectrum at leaf-level vs whole-plant level

Chapter 2 examined only the short-term impact of spectrum at the leaf-level in plants grown in artificial daylight and shade light spectra. However, since spectrum is known to affect not only leaf-level photosynthesis but also plant morphology, the examination of leaf-level spectral effects alone may lead to incorrect assumptions about what an optimal spectrum may be at the whole-plant level. For example, a spectrum which leads to efficient photosynthesis at leaf-level may result in a sub-optimal plant morphology with corresponding decreases to light penetration through the canopy and hence lower whole-plant photosynthesis. Blue light is conspicuous by its involvement in the development of leaves with sun-type characteristics (such as high photosynthetic capacity) and also for its role in the inhibition of etiolation. The combination of leaf-level and whole-plant effects of blue light made it an interesting candidate to explore these relationships, further stimulated by the absence of study of blue light doses in a more natural daylight background.

Chapter 4 shows that higher blue-light doses (and consequently higher blue fraction) exerted several morphological effects at leaf and whole-plant levels, including decreases in leaf length, leaf width, leaf area and plant height. Snowden *et al*. (2016) reported decreasing leaf

area index and plant height in tomato in response to increasing blue light fraction of growth irradiance. Blue light is known to regulate etiolation via the cryptochrome photoreceptor (Ahmad *et al.*, 2002) and this impact of blue light is evidently preserved in a daylight background. Plant dry biomass was found to be generally negatively related to blue light fraction (chapter 4, Fig. 2B). Does leaf-level photosynthesis or whole-plant light interception (or both) account for the observed impact of blue light fraction on plant biomass? Plant dry biomass was generally positively related to whole-plant light absorption (6A) which, at the highest blue light fraction (61%; defined as fraction between 400-500 nm), was 22% less than in simulated daylight alone (comprising 27% blue light). At the leaf-level, however, the response of Φ_{CO2} to blue light fraction was negligible as was the response of A_{max}. Therefore, the impacts of blue light fraction on plant biomass appear to be predominantly the result of whole-plant light interception rather than leaf-level photosynthesis. Cucumber plants grown under HPS lamps, fluorescent tubes (FT), and an artificial solar (AS) spectrum developed markedly different plant morphologies with HPS and FT-grown plants being considerably more compact than AS-grown plants (Hogewoning *et al.*, 2010c). In that same study, whole-plant dry biomass in the AS spectrum was greater than that of HPS and FT grown plants by a factor of 1.6 and 2.3, respectively. This was despite a slightly lower rate of net photosynthesis in the AS-grown plants at 100 μmol m^{-2} s^{-1}. Though the latter may have been a product of the red and blue actinic light spectrum used for gas exchange measurements, the results of those authors suggest how plant morphology and radiation capture are import factors in the determination of whole-plant biomass.

The reason for the negligible response of Φ_{CO2} is likely due to the similar Φ_{CO2} for the daylight and blue spectrum. In chapter 2, Φ_{CO2} for blue narrowband irradiance with a similar peak wavelength to this study (456 nm) was 0.078 whereas this figure was 0.067 for the daylight spectrum used in chapter 4. Differences between these values for the component blue and daylight spectra are evidently small and, since enhancement was not found for a combination of SUN plus 456 nm blue light in chapter 2 (Fig. 5), it can be expected that different blue doses would have a negligible effect on Φ_{CO2} notwithstanding potential differences in pigmentation arising from the different growth spectra. Perhaps more difficult to explain is the negligible response in A_{max}. This parameter has been shown to respond positively and strongly to blue light in red and blue mixtures (Hogewoning *et al.*, 2010a). It may be that the response of A_{max}

observed by those authors was saturated at daylight levels, which in the case of the artificial daylight spectra used was 27% without blue light supplementation. Indeed, those authors also observed saturation of the A_{max} response, although the highest A_{max} occurred at 50% blue which is considerably greater than the 27% blue fraction in the daylight spectrum.

Taken together, the results of chapter 4 highlight the need for a holistic approach in spectral work especially if the goal is to maximise yield. Maximum Φ_{CO2} at leaf level but poor morphology (in terms of whole-plant absorption) is unlikely to be desirable and so too is poor Φ_{CO2} at leaf level and good morphology (unless one compensates for the other). If the unremarkable impacts of blue light fraction on Φ_{CO2} or A_{max} in the present study were the only factors to be considered in the choice of supplementary light spectrum this could easily lead to erroneous assumptions about plant productivity. In practice it is likely that some compromise needs to be made between leaf level and whole-plant effects. In other words, the optimal lighting strategy may result in maximum whole-plant CO_2 fixation yet neither maximum Φ_{CO2} at the leaf level nor optimal morphology. Light recipes must therefore balance the imperatives of high photosynthetic efficiency at leaf level and desirable morphology to maximise yield.

6.9. Response of Φ_{CO2} to temperature

The results obtained in chapter 5 on the response of Φ_{CO2} to temperature, including Φ_{PSII} and qP, were unexpected in several ways. Firstly, with photorespiration abolished in 2% O_2, Φ_{CO2} showed a marked temperature response. In terms of the extent of this response, Φ_{CO2} was 29% lower at 35 °C than at the temperature optimum of 18 °C. In general, the response of Φ_{CO2} to temperature under non-photorespiratory conditions is remarkably flat, resembling that of C4 species in which photorespiration is inhibited by the carbon concentrating mechanism (Ku and Edwards, 1978). Yin *et al.* (2014) observed that Φ_{CO2} in tomato was practically independent of temperature between 16 and 35 °C at 2% O_2 and 760 ppm CO_2 Φ_{CO2}. The loss of photosynthetic efficiency at the lowest and higher temperatures is unlikely to be a result of injury since neither the lowest and highest temperatures used are typically associated with chilling or heat injury (Weis and Berry, 1988). Certainly, injury at 32 °C, where Fv/Fm and PSII were already significantly lower than at their temperature optima, is highly unlikely to have occurred. If damage did occur then this was fully and rapidly reversible since

Fv/Fm of leaves returned to the temperature optimum was the same as prior to higher or lower temperature exposure.

Surprisingly little work has been reported on the temperature dependence of light-limited Φ_{CO2} since the work of Ehleringer and Björkman (1977) which limits meaningful comparisons with similar work. It is shown in chapter 5 (Fig. 3) that the temperature response of A_{max} is quite different to that of Φ_{CO2}. The limitations to photosynthesis in high light are expected to be different to those at low light (Baker *et al.*, 1988). Therefore, the abundance of work which has examined the temperature dependence of the rate of CO_2 assimilation in high, or nearly saturating light (e.g. Yamasaki *et al.*, 2002; Nagai and Makino, 2009; Lin *et al.*, 2012), is of limited practical value in the interpretation of our results.

Also unexpected was the marked temperature response of Φ_{PSII} at 21% O_2 whereas at 2% O_2 Φ_{PSII} was mostly independent of temperature (chapter 5, Fig.4). Furthermore, Φ_{PSII} at 21% O_2 was lower than that at 2% O_2 at all temperatures. In *F. pringlei*, O_2 concentration had no impact on Φ_{PSII} across different temperatures (Oberhuber and Edwards, 1993). In only one account, in Barley, were differences in Φ_{PSII} observed in relation to O_2 concentration (Clarke and Johnson, 2000). In that instance Φ_{PSII} was generally higher at 21% O_2 than at 2% O_2 across temperatures whereas we observed the opposite. The irradiance intensity in that work (1600 μmol m^{-2} s^{-1}) was far higher than the highest irradiance intensity of 80 μmol m^{-2} s^{-1} in the present work, making comparisons difficult. In terms of the general parabolic response of Φ_{PSII}, this was also observed in tomato (Yin *et al.*, 2014). The temperature optimum of the Φ_{PSII} response was 25 °C, which differs from the temperature optimum for Φ_{CO2} of 18 °C. It is interesting, therefore, that Φ_{CO2} increased from 25 °C to 18 C despite this drop in Φ_{PSII}.

Given the relationship between state transitions and Φ_{CO2} shown in chapter 3, the potential occurrence of state transitions was of interest. State transitions are known to occur even in response to moderate temperatures; Weis (1985) observed a tendency towards state 2 in spinach leaves starting at temperatures as low as 20 °C. The Fm'/Fm ratio, which is commonly used to probe state transitions (e.g. Bellafiore *et al.*, 2005; chapter 3), suggested that a transition to state 2 occurred at temperatures of 32 and 35 °C. However, this was likely the result of NPQ, which also increased at these higher temperatures and would have impacted

Fm'. Although a transition to state 2 cannot be ruled out, it is difficult to disentangle from other temperature impacts.

The slightly different results obtained using the rapid method points to the importance of measurement procedure in the determination of temperature responses. Overall, the temperature dependence of Φ_{CO2} is less well understood than may be assumed for such an important parameter.

6.10. Practical significance of current work for greenhouse lighting

6.10.1. Challenges associated with LED supplementary lighting

Although daylight spectrum can itself change dramatically within seconds due to, for instance, a passing cloud, or more gradually during the course of a day as sun angle changes, the use of LED lighting adds another layer of spectral complexity. For example, at twilight daylight intensity wanes and the spectral environment becomes gradually more skewed towards the supplementary light spectrum. Therefore, within a single day a leaf can routinely encounter either full sunlight alone (when sunlight intensities are high and supplementary irradiance is not needed), sunlight and supplementary irradiance, or supplementary irradiance alone. For irradiance to be used efficiently leaves must be acclimated to a similar spectrum in terms of PSII or PSI excitation. Yet, because almost all PAR irradiances (including red and blue light which are commonly used in supplementary lighting) appear to over-excite PSII more than the simulated sunlight spectrum (chapter 2, Fig. 6), the challenge facing leaves is which spectrum to acclimate to amongst diverse spectral possibilities. These dramatic spectral shifts may be well beyond the scope of photosynthetic acclimatory mechanisms to effectively counteract, and within such a short period of time. Though state transitions are regarded as a fine-tuning mechanism, they produce a remarkably large increase in Φ_{CO2} when the rapidity of their operation is taken into consideration (10-13%, chapter 3, Fig. 6). Even so, state transitions do not fully mitigate losses in Φ_{CO2} as a result of dramatic spectral shifts disrupting photosystem balance.

While longer term adjustments are capable of providing greater adjustment such mechanisms are far slower than a state transition, operating over days (Kim *et al.*, 1993). Thus, while longer term mechanisms may be capable of acclimating to spectral shifts their kinetics of operation are too slow to be effective under the changeable spectral conditions which can be

encountered by leaves in supplementary-lit greenhouses. This is problematic insofar as maximising Φ_{CO2} because state transitions and longer term acclimatory mechanisms are reciprocal to each other in terms of scale and rapidity of operation. While state transitions are rapid, they lack the capacity of larger adjustments to the PSI:PSII ratio which are necessary for some larger spectral shifts. The longer-term adjustments, on the other hand, are too slow to be effective under such conditions. A potential solution to this problem is discussed below.

6.10.2. Candidate spectra for LED lighting

Apart from morphological consequences, it seems that one reasonable approach is to employ a supplementary irradiance which matches sunlight as closely as possible in terms of photosystem excitation balance. Such an approach has two main advantages. First, it means that changes in the ratio of sunlight:supplementary irradiance, such as at dusk, will not have a significant impact on photosystem balance despite the potentially dramatic spectral shift. Second, by maintaining as constant a photosystem balance as possible, acclimatory mechanisms which rebalance photosystem excitation do not need to be invoked, or not to a significant extent. These mechanisms take time to complete and in the case of state transitions about 30 minutes was required for completion as shown in chapter 3. During this time Φ_{CO2} is suppressed and the integral of these losses over a day could be significant.

There are several candidate narrowband spectra which achieved a similar excitation balance to the simulated sunlight spectrum used in chapter 2, these being the shorter blue wavelengths (400-460 nm), 520 nm, 640 nm and a wavelength somewhere between 680 nm and 700 nm. Of these spectra, blue light and 520 nm are not good options because neither results in a high Φ_{CO2} and both are more expensive to produce electrically than the red spectral options (Kusuma *et al.*, 2020). Blue light especially is also absorbed by carotenoids which decrease Φ_{CO2} because of inefficient energy transfer by carotenoids to chlorophyll molecules (Croce *et al.*, 2001). Additionally, chapter 4 showed that plant biomass decreased in response to supplementary blue light in a simulated daylight background. For these reasons blue light ought to be used as sparingly as needed. A narrowband irradiance somewhere between 680 and 700 nm, which results in a photosystem balance which matches that of the simulated sunlight spectrum, is a particularly interesting candidate. From the results of chapter 2 it appears that such an irradiance has a peak wavelength at or around 685 nm. It is noteworthy that the highest Φ_{CO2} in sun-grown leaves for all narrowband wavelengths

occurred in this region (680 nm). The width of the spectral peak, which can be quite large in LEDs, could be a significant factor in choosing an appropriate irradiance in such a sensitive spectral region. On the other hand, significant enhancement was observed when longer far-red wavelengths were used (chapter 2, Fig. 3), increasing up to 37% at 720 nm (by comparison, enhancement in sunlight plus 680 nm was 4.7% and 7.5% at 700 nm). The greater enhancement at longer far-red wavelengths and greater penetration into the canopy to PSI light-acclimated leaves (which use this irradiance quite efficiently) may make 700 nm another attractive option. However, in the absence of sunlight (and hence enhancement) this irradiance is not used as efficiently as slightly shorter wavelengths and so the suggestion of about 685 nm appears to be the best compromise.

It is important to note that different leaf types exist within a single plant. Leaves in the canopy are acclimated to a more PSII-rich spectrum whereas shaded leaves within the canopy are acclimated to a more PSI-rich spectrum. From the results in chapter 2, where enhancement of 17-27% occurred in shade-grown leaves illuminated with shade-light plus narrowband wavelengths of 680 nm and below, it seems that these leaves may benefit from stimulation of PSII photochemistry by interlighting using PSII light. However, one caveat regarding the latter approach is that extreme leaf curling has been observed in cucumber when using red and blue intra-canopy lighting which reduced whole-plant light interception (Trouwborst *et al.*, 2010).

6.10.3. Importance of far-red light

Increasing attention is being given to the impact of additional far-red light on photosynthesis, with emphasis on enhancement (Zhen and van Iersel, 2017; Zhen and Bugbee, 2020). Those studies used red and blue or white LED light combined with far-red light as actinic irradiance. Chapter 2 showed for the first time that enhancement can occur in more natural spectra, either by the composition of the broadband spectrum itself or by the addition of far-red. These more natural spectra were an artificial shade-light spectrum and an artificial sun-spectrum. The sun spectrum was very closely matched to a solar reference spectrum whereas the shade-spectrum was matched as closely as possible to a reference shade spectrum measured within a deciduous canopy in the Netherlands during summer. One particular shortcoming of the shade-spectrum was a disproportionate amount of spectral energy between 690 – 720 nm compared to the shade reference spectrum. Nonetheless these more

natural spectra provide some insight into the extent of enhancement in more natural contexts, and in leaves at different levels (e.g. canopy and understory leaves).

Enhancement of Φ_{CO2} was 76% was observed in shade-grown leaves were subjected to the artificial shade spectrum supplemented with 720 nm and 43% enhancement was observed in sun-grown leaves subjected to the artificial sun spectrum supplemented with 720 nm. This means that Φ_{CO2} was 76% and 43% greater, respectively, when compared to the sum of Φ_{CO2} for the 720 nm spectrum and artificial shade-light or artificial sun spectrum. These are significant enhancements which draw attention to the potential usefulness of far-red as a component of LED lighting in horticulture. Furthermore, these findings further highlight the need to improve the current PAR definition to include wavelengths beyond 700 nm which has been suggested by Zhen *et al.* (2021). While the PAR definition may suffice in studies using narrowband irradiance, potential for serious underestimation of useable light intensity by photosynthesis exists in natural spectra which contain a large fraction of far-red light; this is especially relevant in shade-light which contains a much higher far-red fraction than daylight because of poor absorption by leaves of far-red light.

The impact of far-red attention on plant productivity in greenhouses has also been gaining attention (Kalaitzoglou *et al.*, 2019; Zhang *et al.*, 2019). Greenhouse-grown tomato plants with red and blue intra-canopy lighting and far-red overhead lighting had greater total dry biomass and increased fruit yield than when the far-red was absent (Zhang *et al.*, 2019). Also in greenhouse-grown tomato, the same benefits were reported by Kalaitzoglou *et al.* (2019) when far-red was included with red and blue overhead lighting. Furthermore, increased whole-plant light interception when far-red was added was noted by Kalaitzoglou *et al.* (2019). Another potential benefit of far-red addition is that its poor absorption by leaves means that it penetrates deeper into the canopy; the poor Φ_{CO2} associated with 720 nm irradiance alone may be (partly) compensated by this greater penetration to deeper leaf layers.

6.10.4. Temperature setpoint in greenhouses

A transition to LEDs from, for example, HPS lamps means that increased greenhouse heating is required to compensate for the lower heat production of LEDs (Katzin *et al.*, 2021). Choosing the amount of heating to compensate for depends on, amongst other things,

compromises between energy cost and price and quantity of yield at any point in time (Jones *et al.*, 1990). At least at the leaf-level, higher temperatures will increase photorespiration, especially in ventilated greenhouses where CO_2 is lower than in closed greenhouses. Selecting greenhouse temperature setpoints based on the temperature optimum for Φ_{CO2} is a potentially useful step towards increasing productivity. This is not a straightforward exercise, however, as there can be many other impacts of temperature at the whole-plant level. Furthermore, temperature responses may differ depending on the spectrum of supplementary lighting, specifically in terms of Φ_{PSII} or Φ_{PSI} over-excitation, as temperature can impact efficiencies of the photosystems quite differently (e.g. Havaux, 1996a).

6.10.5. Breeding for plants with greater adaptability to changing light conditions

Adaptability of leaves to changeable spectra is a desirable trait which allows photosynthesis to operate as efficiently as possible under the given spectrum. During acclimation Φ_{CO2} increases gradually as an acclimatory mechanism proceeds. The acclimation capacity afforded by an acclimation mechanism is significant. State transitions are useful for mitigating short term impacts of spectrum on Φ_{CO2}. However, in higher plants only a relatively small fraction of PSII (10-13% in our work) becomes mobile during a state transition. In *Chlamydomonas* this figure is substantially greater at about 80% (Delosme *et al.*, 1996). This raises two questions: which genes control the size of the potentially mobile PSII pool and does natural variation exist for the size of this pool? Genetic variation for phosphorylation of LHCII has already been observed in Arabidopsis, which may play a role in mobile LHCII pool size (Flood *et al.*, 2014). Exploring for natural variation in this trait could be performed using high-throughput phenotyping systems (e.g. Flood *et al.*, 2016) using Fm'/Fm as a simple and reliable indicator of LHCII size. It may then be possible to select for individuals with greater mobile PSII and possibly greater adaptability to short term spectral changes. Might there also be natural variation in the time taken for a state transition to complete? These questions reveal the infancy of the characterisation of state transitions despite the phenomenon being known for about half a century. Large acclimatory adjustments to photosynthetic apparatus, performed rapidly, would be highly desirable in horticulture in general.

6.11. Concluding remarks

The complexity of plant-light interactions cannot be understated. It is against this backdrop that decisions must nonetheless be made regarding the choice of spectrum for LED supplementary lighting using available data. By focusing mainly on the short-term spectral impacts on light-limited photosynthesis, this work has made a small contribution towards the foundational knowledge required to inform such decisions. A next step could be to see whether, for example, the apparent benefits of enhancement and a better understanding of short-term acclimation to spectrum in particular will translate to increased productivity in a greenhouse environment. The conditions in a greenhouse are far more variable than the highly controlled environments used in this work and long-term acclimation could lead to unexpected results. Nonetheless, it has been necessary in this work to use such highly controlled environments as a first step to uncover principal responses.

It is apparent that far less is known about some of the responses of Φ_{CO2} to ambient conditions – in this case spectrum and temperature – than might be supposed for such an important parameter. Three key findings have been made in this regard: Firstly, significant enhancement of photosynthesis can occur in spectra rich-in far-red, such as shade light, or by the addition of far-red to an artificial daylight spectrum. Secondly, the previously unknown relationship between state transitions on Φ_{CO2} in a higher plant reveals the limits of photosynthetic acclimation in the short-term and caution against the use of irradiances which upset the photosystem excitation balance. In future intelligent lighting applications it may be possible to determine photosystem balance spectroscopically, with real-time adjustments made to light spectrum to create as stable a photosystem excitation balance as possible. Thirdly, atypical responses of Φ_{CO2} and Φ_{PSII} to temperature were observed, the cause of this is not known and requires further investigation, especially given the paucity of light-limited temperature-response data to compare with. The work on enhancement and state transitions reveals the potential value in revisiting classical work.

Optimising spectrum for optimal leaf photosynthesis and optimal morphology for light interception remains an especially challenging duality. The often dramatic physiological responses to subtle spectral cues makes spectral work particularly difficult, especially when considering the vast number of potential spectral combinations which can be encountered in controlled or natural environments. Improved knowledge of physiological responses to

spectrum will aid in the development of advanced LED lighting control algorithms. Machine-learning may soon also play a role in solving this complex problem.

REFERENCES

Ahmad, M. and Cashmore, A.R. (1996). Seeing blue: the discovery of cryptochrome. *Plant Molecular Biology*, 30, 851–861.

Ahmad, M., Grancher, N., Heil, M., Black, R.C., Giovani, B., Galland, P. and Lardemer, D. (2002). Action spectrum for cryptochrome-dependent hypocotyl growth inhibition in Arabidopsis. *Plant Physiology*, 129, 774–785.

Allen, J.F., Bennett, J., Steinback, K.E. and Arntzen, C.J. (1981). Chloroplast protein phosphorylation couples plastoquinone redox state to distribution of excitation energy between photosystems. *Nature*, 291, 25–29.

Allen, J.F. (1992). Protein phosphorylation in regulation of photosynthesis. *Biochimica et Biophysica Acta*, 1098, 275–335.

Allen, J.F. (2003). State transitions–a question of balance. *Science*, 299(5612), 1530–1532.

Andrews, J.R., Bredenkamp, G.J. and Baker, N.R. (1993). Evaluation of the role of State transitions in determining the efficiency of light utilisation for CO_2 assimilation in leaves. *Photosynthesis Research*, 38, 15–26.

Anderson, J., Chow, W.H. and Park, YI. (1995). The grand design of photosynthesis: Acclimation of the photosynthetic apparatus to environmental cues. *Photosynthesis Research*, 46, 129–139.

Badger, M.R., Björkman, O. and Armond, P.A. (1982). An analysis of photosynthetic response and adaptation to temperature in higher plants: temperature acclimation in the desert evergreen Nerium oleander L. *Plant, Cell and Environment*, 5(1), 85–99.

Baker, N.R., Long, S.P. and Ort, D.R. (1988). Photosynthesis and temperature, with particular reference to effects on quantum yield. *Symposia of the Society for Experimental Biology*, 42, 347–375.

Baker, N.R., Harbinson, J. and Kramer, D.M. (2007). Determining the limitations and regulation of photosynthetic energy transduction in leaves. *Plant, Cell & Environment*, 30, 1107–1125.

Bassi, R., Rigoni, F., Barbato, R. and Giacometti, G.M. (1988). Light-harvesting chlorophyll a/b proteins (LHCII) populations in phosphorylated membranes. *Biochimica et Biophysica Acta*, 936, 29–38.

Bellafiore, S., Barneche, F., Peltier, G. and Rochaix, J. (2005). State transitions and light adaptation require chloroplast thylakoid protein kinase STN7. *Nature*, 433, 892–895.

Bernacchi, C.J., Portis, A.R., Nakano, H., von Caemmerer, S. And Long, S.P. (2002). Temperature Response of Mesophyll Conductance. Implications for the Determination of Rubisco Enzyme Kinetics and for Limitations to Photosynthesis in Vivo. *Plant Physiology*, 130(4), 1992–1998.

Bernardini, F., Mittleman, J., Rushmeier, H., Silva, C. and Taubin, G. (1999). The ball-pivoting algorithm for surface reconstruction. *IEEE Transactions on Visualization and Computer Graphics*, 5, 349–359.

Bird, R. E., Hulstrom, R. L., Kliman, A. W. and Eldering, H. G. (1982) Solar spectral measurements in the terrestrial environment. *Applied Optics*, 21, 1430–1436.

Björkman, O. (1966). The effect of oxygen concentration on photosynthesis in higher plants. *Physiologia Plantarum*, 19(3), 618–633.

Björkman, O. and Demmig, B. (1987). Photon yield of O_2 evolution and chlorophyll fluorescence characteristics at 77 K among vascular plants of diverse origins. *Planta*, 170, 489–504.

Bonaventura, C. and Myers, J. (1969). Fluorescence and oxygen evolution from Chlorella pyrenoidosa. *Biochimica et Biophysica Acta*, 189, 366–383.

Calders, K., Armston, J., Newnham, G., Herold, M. and Goodwin, N. (2014). Implications of sensor configuration and topography on vertical plant profiles derived from terrestrial LiDAR. *Agricultural and Forest Meteorology*, 194, 104–117.

Calders, K., Newnham, G., Burt, A., Murphy, S., Raumonen, P., Herold, M., Culvenor, D., Avitabile, V., Disney, M., Armston, J. and Kaasalainen, M. (2015). Nondestructive estimates of above-ground biomass using terrestrial laser scanning. *Methods in Ecology and Evolution*, 6, 198–208.

Calders, K., Disney, M.I., Armston, J., Burt, A., Brede, B., Origo, N., Muir, J. and Nightingale, J., (2017). Evaluation of the range accuracy and the radiometric calibration of multiple terrestrial laser scanning instruments for data interoperability. *IEEE Transactions on Geoscience and Remote Sensing*, 55, 2716–2724.

Canaani, O., Cahen, D. and Malkin, S. (1982). Photosynthetic chromatic transitions and Emerson enhancement effects in intact leaves studied by photoacoustics. FEBS LETTERS, 50(1), 142–146.

Canaani, S. and Malkin, S. (1984). Distribution of light excitation in an intact leaf between the two photosystems of photosynthesis. Changes in absorption cross-sections following state 1-state 2 transitions. *Biochimica et Biophysica Acta*, 766, 513–524.

Canaani, O. (1986). Photoacoustic detection of oxygen evolution and State 1-State 2 transitions in cyanobacteria. *Biochimica et Biophysica Acta*, 852, 74–80.

Chow, W.S., Melis, A. and Anderson, J.M. (1990). Adjustments of photosystem stoichiometry in chloroplasts improve the quantum efficiency of photosynthesis. *Proceedings of the National Academy of Sciences of the United States of America*, 87, 7502–7506.

Clarke, J.E. and Johnson, G.N. (2001). In vivo temperature dependence of cyclic and pseudocyclic electron transport in barley. *Planta*, 212, 808-816.

Croce, R., Müller, M.G., Bassi, R., and Holzwarth, A.R. (2001). Carotenoid-to-chlorophyll energy transfer in recombinant major light-harvesting complex (LHCII) of higher plants. I. Femtosecond transient absorption measurements. *Biophysical Journal*, 80, 901–915.

Croce, R., Canino, G., Ros, F. and Bassi, R. (2002). Chromophore organization in the higher-plant photosystem II antenna protein CP26. *Biochemistry*, 41, 7334–7343.

Dai, Q., Peng, S., Chavez, A.Q. and Vergara, B.S. (1995). Effects of UVB radiation on stomatal density and opening in rice (*Oryza sativa* L.). *Annals of Botany*, 76, 65–70.

Dekker, J.P. and Boekema, E.J. (2005). Supramolecular organization of thylakoid membrane proteins in green plants. *Biochimica et Biophysica Acta*, 1706, 12–39.

Delosme, R., Olive, J. and Wollman, F. (1996). Changes in light energy distribution upon state transitions: an in vivo photoacoustic study of the wild type and photosynthesis mutants from *Chlamydomonas reinhardtii*. *Biochimica et Biophysica Acta – Bioenergetics*, 1273, 150–158.

Dietzel, L., Bräutigam, K. and Pfannschmidt, T. (2008). Photosynthetic acclimation: State transitions and adjustment of photosystem stoichiometry – functional relationships between short-term and long-term light quality acclimation in plants. *The FEBS Journal*, 275, 1080–1088.

Dring, M.J. and Lüning, K. (1985). Emerson enhancement effect and quantum yield of photosynthesis for marine macroalgae in simulated underwater light fields. Marine Biology, 87, 109–117.

Ehleringer, J. and Björkman, O. (1977). Quantum yields for CO2 uptake in C3 and C4 plants. *Plant Physiology*, 59, 86–90.

Emerson, R. and Lewis, C.M. (1941). Carbon dioxide exchange and the measurement of the quantum yield of photosynthesis. *American Journal of Botany*, 28, 789–804.

Emerson, R. and Lewis, C.M. (1943). The dependence of the quantum yield of Chlorella photosynthesis on wave length of light. American Journal of Botany, 30 (3), 165–178.

Emerson, R. (1957). Dependence of yield of photosynthesis in long wave red on wavelength and intensity of supplementary light. *Science*, 125, 746.

Emerson, R. (1958). Yield of photosynthesis from simultaneous illumination with pairs of wavelengths. *Science*, 127, 1059–1060.

Engelmann TW (1882) Über Sauerstoffausscheidung von Pflanzenzellen im Mikrospectrum. *Botanische Zeitung*, 40, 419–426.

Evans, J.R. (1987). The dependence of quantum yield on wavelength and growth irradiance. *Australian Journal of Plant Physiology*, 14, 69–79.

Farquhar, G.D., von Caemmerer, S. and Berry, J.A. (1980). A biochemical model of photosynthetic CO2 assimilation in leaves of C3 species. Planta, 149, 78–90.

Forti, G. and Fusi, P. (1990). Influence of thylakoid protein phosphorylation on Emerson enhancement and the quantum requirement of Photosystem I. *Biochimica et Biophysica Acta*, 1020, 247–252.

Foyer, C.F. and Noctor, G. (2000). Tansley Review No. 112 Oxygen processing in photosynthesis: Regulation and signalling. *New Phytologist*, 146(3), 359–388.

Foyer, C. H., Neukermans, J., Queval, G., Noctor, G., and Harbinson, J. (2012). Photosynthetic control of electron transport and the regulation of gene expression. *Journal of Experimental Botany*, 63, 1637-1661.

Flood, P.J., Yin, L., Herdean, A., Harbinson, J., Aarts, M.G.M. and Spetea, C. (2014). Natural variation in phosphorylation of photosystem II proteins in Arabidopsis thaliana: is it caused by genetic variation in the STN kinases? *Philosophical Transactions of the Royal Society*, B3692013049920130499.

Flood, P.J., Kruijer, W., Schnabel, S.K., van der Schoor, R., Jalink, H., Snel, J.F.H., Harbinson, J. and Aarts, M.G.M. (2016). Phenomics for photosynthesis, growth and reflectance in *Arabidopsis thaliana* reveals circadian and long-term fluctuations in heritability. *Plant Methods*, 12, 14.

Fraser, D.P., Hayes, S. and Franklin, K.A. (2016). Photoreceptor crosstalk in shade avoidance. *Current Opinion in Plant Biology*, 33, 1–7.

Frenkel, M., Bellafiore, S., Rochaix, J-D., and Jansson, S. (2007). Hierarchy amongst photosynthetic acclimation responses for plant fitness. *Physiologia Plantarum*, 129, 455–459.

Fujiwara, K. and Sawada, T. (2006). Design and development of an LED-artificial sunlight source system prototype capable of controlling relative spectral power distribution. *Journal of Light and Visual Environment*, 30(3), 170–176.

Galka, P., Santabarbara, S., Khuong, T.T.H., Degand, H., Morsomme, P., Jennings, R.C., Boekema, E.J. and Caffarri, S. (2012). Functional analyses of the plant photosystem I–light-harvesting complex II supercomplex reveal that light-harvesting complex II loosely bound to photosystem II is a very efficient antenna for photosystem I in State II. *Plant Cell*, 24, 2963–2978.

Gayral, B. (2017). LEDs for lighting: Basic physics and prospects for energy savings. *Comptes Rendus Physique*, 18, 453–461.

Genty, B., Briantais, J. and Baker, N. (1989). The relationship between the quantum yield of photosynthetic electron transport and quenching of chlorophyll fluorescence. *Biochimica et Biophysica Acta*, 990, 87–92.

Genty, B. and Harbinson, J. (1996). Regulation of light utilization for photosynthetic electron transport. In: Baker, N.R. (ed). Photosynthesis and the environment. Kluwer Academic Publishers, 67–99.

Georgieva, K. and Yordanov, I. (1994). Temperature dependence of photochemical and non-photochemical fluorescence quenching in intact pea leaves. *Journal of Plant Physiology*, 144, 754–759.

Glowacka, B. (2004). The effect of blue light on the height and habit of the tomato (*Lycopersicon esculentum* Mill.) transplant. *Folia Horticulturae*, 16, 3–10.

Govindjee and Rabinowitch, E. (1960). Action spectrum of the "Second Emerson Effect". Biophysical Journal 1(2), 73–89.

Govindjee, R, Govindjee, and Hoch, G. (1964). Emerson Enhancement Effect in chloroplast reactions. Plant Physiology, 39(1), 10–14.

Haitz, R. and Tsao, J.Y. (2011). Solid-state lighting: 'The case' 10 years after and future prospects. *Physica status solidi (a)*, 208(1), 17-29.

Haldrup, A., Jensen, P.E., Lunde, C. and Scheller, H.V. Balance of power: a view of the mechanism of photosynthetic state transitions. *Trends in Plant Science*, 6(7), 301–305.

Harbinson, J. (2018). Chlorophyll fluorescence as a tool for describing the operation and regulation of photosynthesis in vivo. In Croce, R, Grondelle, R.V., Amerongen, H.V. and Stokkum, I.V. (Eds.), *Light Harvesting in Photosynthesis*. CRC Press.

Hartmann, K.M. (1967). An action spectrum of photomorphogenesis under high energy conditions and its interpretation on the basis of phytochrome (hypocotyl growth inhibition in *Lactuca sativa* L). *Zeitschrift fur Naturforschung. Teil B, Chemie, Biochemie, Biophysik, Biologie und Verwandte Gebiete, 22(11), 1172-1175*, 1172–1175.

Havaux, M. (1996a). Short-term responses of photosystem I to heat stress. *Photosynthesis Research*, 47, 85–97.

Havaux, M. (1996b). Temperature-dependent adjustment of the thermal stability of photosystem II in vivo: possible involvement of xanthophyll-cycle pigments. *Planta*, 198, 324–333.

Haworth, P. and Melis, A. (1983). Phosphorylation of chloroplast thylakoid membrane proteins does not increase the absorption cross-section of photosystem 1. *FEBS Letters*, 160, 277–280.

He, J., Chee, C.W. and Goh, C.J. (1996). 'Photoinhibition' of Heliconia under natural tropical conditions: the importance of leaf orientation for light interception and leaf temperature. *Plant, Cell & Environment*, 19, 1238-1248.

Hendrickson, L., Furbank, R.T. and Chow, W.S. (2004). A simple alternative approach to assessing the fate of absorbed light energy using chlorophyll fluorescence. *Photosynthesis Research*, 82, 73–81.

Hernández, R. and Kubota, C. (2014). Growth and morphological response of cucumber seedlings to supplemental red and blue photon flux ratios under varied solar daily light integrals. *Scientia Horticulturae*, 173, 92–99.

145

Hernández, R. and Kubota, C. (2016). Physiological responses of cucumber seedlings under different blue and red photon flux ratios using LEDs. *Environmental and Experimental Botany*, 121, 66–74.

Hernández, R., Eguchi, T., Deveci, M. and Kubota, C. (2016). Tomato seedling physiological responses under different percentages of blue and red photon flux ratios using LEDs and cool white fluorescent lamps. *Scientia Horticulturae*, 213, 270–280.

Heuvelink, E., Bakker, M. J., Hogendonk, L., Janse, J., Kaarsemaker, R. and Maaswinkel, R. (2006). Horticultural lighting in the netherlands: new developments. *Acta Horticulturae*, 711, 25–34.

Hikosaka, K., Ishikawa, K., Borjigidai, A., Muller, O. and Onoda, Y. (2006). Temperature acclimation of photosynthesis: mechanisms involved in the changes in temperature dependence of photosynthetic rate. *Journal of Experimental Botany*, 57(2), 291–302.

Hill, J.F. and Govindjee. (2014). The controversy over the minimum quantum requirement for oxygen evolution. *Photosynthesis Research*, 122, 97–112.

Hogewoning, S.W., Trouwborst, G., Maljaars, H., Poorter, H., van Ieperen, W. and Harbinson, J. (2010a). Blue light dose–responses of leaf photosynthesis, morphology, and chemical composition of Cucumis sativus grown under different combinations of red and blue light. *Journal of Experimental Botany*, 61, (11), 3107–3117.

Hogewoning, S. W., Trouwborst, G., Harbinson, J., and Van Ieperen, W. (2010b). Light distribution in leaf chambers and its consequences for photosynthesis measurements. *Photosynthetica*, 48, 219–226.

Hogewoning, S.W., Douwstra, P., Trouwborst, G., van Ieperen, W. and Harbinson, J. (2010c). An artificial solar spectrum substantially alters plant development compared with usual climate room irradiance spectra. *Journal of Experimental Botany*. 61, 1267–1276.

Hogewoning, S.W., Wientjes, E., Douwstra, P., Trouwborst, G., van Ieperen, W., Croce, R. and Harbinson, J. (2012). Photosynthetic quantum yield dynamics: from photosystems to leaves. *Plant Cell*, 24, 1921–1935.

Holmes, M.G. and Smith, H. (1977). The function of phytochrome in the natural environment–I. Characterization of daylight for studies in photomorphogenesis and photoperiodism. *Photochemistry and Photobiology*, 25, 533–538.

Hoover, W.H. (1937). The dependence of carbon dioxide assimilation in a higher plant on wave length of radiation. *Smithsonian Miscellaneous Collections*, 95, 1–13.

Huché-Thélier, L., Crespel, L., Gourrierec, J.L., Morel, P., Sakr, S. and Leduc, N. (2016). Light signaling and plant responses to blue and UV radiations–perspectives for applications in horticulture. *Environmental and Experimental Botany*, 121, 22–38.

Hughes, J.E., Morgan, D., Lambton, P., Black, C. and Smith, H. (1984). Photoperiodic time signals during twilight. *Plant, Cell & Environment*, 7, 269-277.

Inada, K. (1976). Action spectra for photosynthesis in higher plants. *Plant and Cell Physiology*, 17, 355–365.

Johkan, M. Shoji, K., Goto, F., Hahida, S. and Yoshihara, T. (2012). Effect of green light wavelength and intensity on photomorphogenesis and photosynthesis in *Lactuca sativa*. *Environmental and Experimental Botany*, 75, 128–133.

Jones, P., Jones, J. W. and Hwang, Y. (1990). Simulation for determining greenhouse temperature setpoints. *Transactions of the American Society of Agricultural Engineers*, 33(5) 1722-1728.

June, T., Evans, J.R. and Farquhar, G.D. (2004). A simple new equation for the reversible temperature dependence of photosynthetic electron transport: a study on soybean leaf. Functional Plant Biology, 31(3), 275–283.

Kaiser, E., Ouzounis, T., Giday, H., Schipper, R., Heuvelink, E. and Marcelis, L.F.M. (2019). Adding blue to red supplemental light increases biomass and yield of greenhouse-grown tomatoes, but only to an optimum. *Frontiers in Plant Science*, 9, 2002.

Kalaitzoglou, P., van Ieperen, W., Harbinson, J., van der Meer, M., Martinakos, S., Weerheim, K., Nicole, C.C.S. and Marcelis, L.F.M. (2019). Effects of continuous or end-of-day far-red light on tomato plant growth, morphology, light absorption, and fruit production. *Frontiers in Plant Science*, 10, 322.

Kalaitzoglou, P., Taylor, C., Calders, K., Hogervorst, M., van Ieperen, W., Harbinson, J., de Visser, P., Nicole, C.C.S. and Marcelis, L.F.M. (2021). Unraveling the effects of blue light in an artificial solar background light on growth of tomato plants. *Environmental and Experimental Botany*, 184, 104377.

Katzin, D., van Mourik, S., Kempkes, F. and van Henten, E.J. (2020). GreenLight – An open source model for greenhouses with supplementary lighting: Evaluation of heat requirements under LED and HPS lamps. *Biosystems Engineering*, 194, 61–81.

Katzin, D., Marcelis, L.F.M. and van Mourik, S. (2021). Energy savings in greenhouses by transition from high-pressure sodium to LED lighting. *Applied Energy*, 281, 116019.

Keller, M.M., Jaillais, Y., Pedmale, U.V., Moreno, J.E., Chory, J. and Ballare, C.L. (2011). Cryptochrome 1 and phytochrome B control shade-avoidance responses in Arabidopsis via partially independent hormonal cascades. *The Plant Journal*, 67, 195–207.

Keuskamp, D.H., Sasidharan, R., Vos, I., Peeters, A.J., Voesenek, L.A. and Pierik, R. (2011). Blue-light-mediated shade avoidance requires combined auxin and brassinosteroid action in Arabidopsis seedlings. *The Plant Journal*, 67, 208–217.

Keuskamp, D.H., Keller, M.M., Ballare, C.L. and Pierik, R. (2012). Blue light regulated shade avoidance. *Plant Signaling and Behaviour,* 7, 514–517.

Kim, J.H., Glick, R.E. and Melis, A. (1993). Dynamics of photosystem stoichiometry adjustment by light quality in chloroplasts. *Plant Physiology*, 102, 181–190.

Kim, E., Ahn, T.K. and Kumazaki, S. (2015). Changes in Antenna Sizes of Photosystems during State Transitions in Granal and Stroma-Exposed Thylakoid Membrane of Intact Chloroplasts in Arabidopsis Mesophyll Protoplasts, *Plant and Cell Physiology*, 56, 759–768.

Kingston-Smith, A.H., Harbinson, J. and Foyer, C.H. (1999). Acclimation of photosynthesis, H_2O_2 content and antioxidants in maize (Zea mays) grown at sub-optimal temperatures. Plant, Cell and Environment, 22, 1071–1083.

Kniemeyer, O. (2008). Design and implementation of a graph grammar based language for functional-structural plant modelling. Doctoral dissertation. Brandenburg University of Technology, Germany.

Kolberg, D., Schubert, F., Lontke, N., Zwigart, A. and Spinner, D.M. (2011). Development of tunable close match LED solar simulator with extended spectral range to UV and IR. *Energy Procedia*, 100–105.

Kowalczyk, K., Olewnicki, D., Mirgos, M. and Gajc-Wolska, J. (2020). Comparison of selected costs in greenhouse cucumber production with LED and HPS supplementary assimilation lighting. *Agronomy*, 10, 1–14.

Ku, S.-B. and Edwards, G.E. (1978). Oxygen inhibition of photosynthesis. III. Temperature dependence of quantum yield and its relation to O_2/CO_2 solubility ratio. Planta, 140, 1–56.

Kusuma, P., Morgan Pattison, P. and Bugbee, B. (2020). From physics to fixtures to food: current and potential LED efficacy. *Horticulture Research*, 7, 1–9.

Laisk, A., Vello, O., Eichelmann, H. and Dall'Osto, L. (2014). Action spectra of photosystems II and I and quantum yield of photosynthesis in leaves in State 1. *Biochimica et Biophysica Acta*, 1837, 315–325.

Lichtenthaler, H.K., Buschmann, C. And Rahmsdorf, U. (1980). The importance of blue light for the development of sun-type chloroplasts. In: Senger, H. (ed). The blue light syndrome. Springer, 485–494.

Lichtenthaler, H.K. (1987). Chlorophylls and carotenoids: Pigments of photosynthetic biomembranes. *Methods in Enzymology*, 148, 350–382.

Lin, Y-, Medlyn, B.E. and Ellsworth, D.S. (2012). Temperature responses of leaf net photosynthesis: the role of component processes. *Tree Physiology*, 32, 219–231.

Long, S.P. and Bernacchi, C.J. (2003). Gas exchange measurements, what can they tell us about the underlying limitations to photosynthesis? Procedures and sources of error. *Journal of Experimental Botany*, 54, 2393–2401.

Long, S.P. and Drake, B.G. (1991). Effect of the long-term elevation of CO_2 concentration in the field on the quantum yield of photosynthesis of the C3 sedge, Scirpus olneyi. *Plant Physiology*, 96, 221–226.

Long, S.P., Postl, W.F. and Bolharnordenkampf, H.R. (1993). Quantum yields for uptake of carbon dioxide in C3 vascular plants of contrasting habitats and taxonomic groupings. *Planta*, 189, 226–234.

Long, S.P., Farage, P.K., and Garcia, R.L. (1996). Measurement of leaf and canopy photosynthetic CO_2 exchange in the field, *Journal of Experimental Botany*, 47(11), 1629–1642.

Matsuda, R., Ohashi-Kaneko, K., Fujiwara, K., Goto, E. and Kurata, K. (2004). Photosynthetic characteristics of rice leaves grown under red light with or without supplemental blue light. *Plant and Cell Physiology*, 45, 1870–1874.

Matsuda, R., Ohashi-Kaneko, K., Fujiwara, K. and Kurata, K. (2007). Analysis of the relationship between blue-light photon flux density and the photosynthetic properties of spinach (*Spinacia oleracea* L.) leaves with regard to the acclimation of photosynthesis to growth irradiance. *Soil Science and Plant Nutrition*, 53, 459–465.

Maxwell, K. and Johnson, G.N. (2000). Chlorophyll fluorescence – a practical guide. *Journal of Experimental Botany*, 51, 659–668.

Meng, Q. and Runkle, E.S. (2017). Moderate-intensity blue radiation can regulate flowering, but not extension growth, of several photoperiodic ornamental crops. *Environmental and Experimental Botany*, 134, 12–20.

McCree, K.J. (1972a) Action spectrum, absorptance and quantum yield of photosynthesis in crop plants. *Agricultural Meteorology*, 9, 191–216.

McCree, K.J. (1972b). Significance of enhancement for calculations based on action spectrum for photosynthesis. *Plant Physiology*, 49, 704–706.

Melis, A. and Harvey, G.W. (1981). Regulation of photosystem stoichiometry, chlorophyll a and chlorophyll b content and relation to chloroplast ultrastructure. *Biochimica et Biophysica Acta*, 637, 138 – 145.

Meshlab. (2014). Visual Computing Lab - ISTI - CNR.

Miao, Y., Chen, Q., Qu, M., Gao, L. and Hou, L. (2019). Blue light alleviates 'red light syndrome' by regulating chloroplast ultrastructure, photosynthetic traits and nutrient accumulation in cucumber plants. *Scientia Horticulturae*, 257, 108680.

Miller, B.D., Carter, K.R., Reed, S.C., Wood, T.E. and Cavaleri, M.A. (2021). Only sun-lit leaves of the uppermost canopy exceed both air temperature and photosynthetic thermal optima in a wet tropical forest, *Agricultural and Forest Meteorology*, 301–302, 108347.

Morrow, R.C. (2008). LED lighting in horticulture. *HortScience*, 43, 1947–1950.

Murata, N. (1969). Control of excitation transfer in photosynthesis. 1. Light-induced change of chlorophyll *a* fluorescence in Porphyridium cruentum. *Biochimica et Biophysica Acta*, 172, 242–251.

Myers, J. and Graham, J.R. (1963). Enhancement in Chlorella. Plant Physiology, 38(1), 105–116.

Myers, J. (1971). Enhancement studies in photosynthesis. *Annual Review of Plant Biology*, 22, 289–312.

Nagai, T. and Makino, A. (2009). Differences between rice and wheat in temperature responses of photosynthesis and plant growth. *Plant and Cell Physiology*, 50(4), 744–755.

Nagashima, H. and Hikosaka, K. (2011). Plants in a crowded stand regulate their height growth so as to maintain similar heights to neighbours even when they have potential advantages in height growth. *Annals of Botany*, 108, 207–214.

Nagy, F., Fejes, E., Wehmeyer, B., Dallman, G. and Schafer, E. (1993). The circadian oscillator is regulated by a very low fluence response of phytochrome in wheat. *Proceedings of the National Academy of Sciences of the United States of America*, 90(13), 6290–6294

Nanya, K., Ishigami, Y., Hikosaka, S. and Goto, E. (2012). Effects of blue and red light on stem elongation and flowering of tomato seedlings. *Acta Horticuluturae*, 956, 264–266.

Nellaepalli, S., Mekala, N.R., Zsiros, O., Mohanty, P. and Subramanyam, R. (2011). Moderate heat stress induces state transitions in Arabidopsis thaliana. *Biochimica et Biophysica Acta*, 1807, 1177–1184.

Nelson, J.A. and Bugbee, B. (2014). Economic analysis of greenhouse lighting: light emitting diodes vs. high intensity discharge fixtures. *PLoS ONE*, 9, e99010.

Oberhuber, W. and Edwards, G.E. (1993). Temperature dependence of the linkage of quantum yield of photosystem II to CO_2 Fixation in C4 and C3 Plants. *Plant Physiology*, 101, 507–512.

Oberhuber, W., Dai, Z. and Edwards, G.E. (1993). Light dependence of quantum yields of Photosystem II and CO_2 fixation in C3 and C4 plants. *Photosynthesis Research*, 35, 265–274.

Ouzounis, T., Giday, H., Kjaer, K.H. and Ottosen, C.-O. (2018). LED or HPS in ornamentals? A case study in roses and campanulas. *European Journal of Horticultural Science*, 83, 166–172.

Pastenes, C. and Horton, P. (1996). Effect of High Temperature on Photosynthesis in Beans. *Plant Physiology*, 112, 1245–1251.

Pfannschmidt, T. (2005). Acclimation to varying light qualities: Toward the functional relationship of state transitions and adjustment of photosystem stoichiometry. *Journal of Phycology*, 41, 723–725.

Pfündel, E. (1998). Estimating the contribution of photosystem I to total leaf chlorophyll fluorescence. *Photosynthesis Research*, 56, 185–195.

Pribil, M., Pesaresi, P., Hertle. A., Barbato, R. and Leister, D. (2010). Role of plastid phosphatase TAP38 in LHCII dephosphorylation and thylakoid electron flow. *PLOS Biology*, 8, e1000288.

Paucek, I., Appolloni, E., Pennisi, G., Quaini, S., Gianquinto, G. and Orsini, F. (2020). LED lighting systems for horticulture: Business growth and global distribution. *Sustainability*, 12(18), 7516.

Pierik, R., Djakovic-Petrovic, T., Keuskamp, D.H., de Wit, M. and Voesenek, L.A.C.J. (2009). Auxin and ethylene regulate elongation responses to neighbor proximity signals independent of gibberellin and DELLA proteins in Arabidopsis. *Plant Physiology*, 149, 1701–1712.

Pfannschmidt, T. (2005). Acclimation to varying light qualities: toward the functional relationship of state transitions and adjustment of photosystem stoichiometry. *Journal of Phycology*, 41, 723–725.

Poorter, H., Niinemets, U., Poorter, L., Wright, I.J. and Villar, R. (2009). Causes and consequences of variation in leaf mass per area (LMA): a meta-analysis. *New Phytologist*, 182, 565–588.

R Development Core Team (2010). R: a Language and Environment for Statistical Computing. R Foundation of Statistical Computing, Vienna, Austria.

Radetsky, L.C. (2018) LED and HID horticultural luminaire testing report. http://www.lrc.rpi.edu/programs/energy/pdf/HorticulturalLightingReport-Final.pdf.

Raven, J.A. and Cockell, C.S. (2006). Influence on photosynthesis of starlight, moonlight, planetlight, and light pollution (Reflections on photosynthetically active radiation in the universe). *Astrobiology*, 6(4), 668–675.

Sage, R.F. and Sharkey, T.D. (1987). The effect of temperature on the occurrence of O_2 and CO_2 insensitive photosynthesis in field grown plants. *Plant Physiology*, 84, 658–664.

Sager, J.C., Smith, W.O., Edwards, J.L. and Cyr, K.L. (1988). Photosynthetic efficiency and phytochrome photoequilibria determination using spectral data. *Transactions of the American Society of Agricultural Engineers*, 31, 1882–1889.

Sarlikioti, V., de Visser, P.H.B., Buck-Sorlin, G.H. and Marcelis, L.F.M. (2011). How plant architecture affects light absorption and photosynthesis in tomato: towards an ideotype for plant architecture using a functional-structural plant model. *Annals of Botany*, 108, 1065–1073.

Savvides, A., Fanourakis, D. and van Ieperen, W. (2012). Co-ordination of hydraulic and stomatal conductances across light qualities in cucumber leaves. *Journal of Experimental Botany*, 63, 1135–1143.

Senawiratne, J., Chatterjee, A., Detchprohm, T., Zhao, W., Li, Y., Zhu, M., Xia, Y., Li, X., Plawsky, J. and Wetzel, C. (2010). Junction temperature, spectral shift, and efficiency in GaInN-based blue and green light emitting diodes. *Thin Solid Films*, 518, 1732–1736.

Senger, H. and Bishop, N.I. (1969). Emerson Enhancement effect in synchronous Scenedesmus cultures. Nature, 221, 975.

Shapiguzov, A., Ingelsson, B., Samol, I., Andres, C., Kessler, F., Rochaix, J.-D., Vener, A.V. and Goldschmidt-Clermont, M. (2010). The PPH1 phosphatase is specifically involved in LHCII dephosphorylation and state transitions in Arabidopsis. *Proceedings of the National Academy of Sciences of the United States of America*, 107, 4782–4787.

Sharkey, T.D. and Raschke, K. (1981). Effect of light quality on stomatal opening in leaves of Xanthium strumarium L. *Plant Physiology*, 68, 1170–1174.

Sharkey, T.D. (2005). Effects of moderate heat stress on photosynthesis: importance of thylakoid reactions, rubisco deactivation, reactive oxygen species, and thermotolerance provided by isoprene. *Plant, Cell and Environment*, 28, 269–277.

Sharp, R.E., Matthews, M.A., and Boyer, J.S. (1984). Kok Effect and the quantum yield of photosynthesis: light partially inhibits dark respiration, *Plant Physiology*, 75(1), 95–101.

Singsaas, E.L., Ort, D.R. and DeLucia, E.H. (2001). Variation in measured values of photosynthetic quantum yield in ecophysiological studies. Oecologia, 128, 15–23.

Smith, H. (1982). Light quality, photoperception, and plant strategy. *Annual Review of Plant Physiology*, 33(1), 481–518.

Smith, H. (1986). The perception of light quality. In: Kendrick, R.E. and Kronenberg, G.H.M. (eds) Photomorphogenesis in plants. Springer, 187–217.

Snowden, M.C., Cope, K.R. and Bugbee, B. (2016). Sensitivity of seven diverse species to blue and green light: interactions with photon flux. PLoS ONE 11(10), e0163121.

Sonneveld, P.J., Swinkels, G.L.A.M., Kempkes, F., Campen, J.B. and Bot, G.P.A. (2006). Greenhouse with an integrated NIR filter and a solar cooling system, *Acta Horticulturae*, 719, 123–130.

Suetsugu, N. and Wada, M. (2013). Evolution of three LOV blue light receptor families in green plants and photosynthetic stramenopiles: phototropin, ZTL/FKF1/LKP2 and aureochrome. *Plant and Cell Physiology*, 54, 8–23.

Tähkämö, L., Räsänen, R.S. and Halonen, L. (2016). Life cycle cost comparison of high-pressure sodium and light-emitting diode luminaires in street lighting. *The International Journal of Life Cycle Assessment*, 21, 137–145.

Tavakoli, M., Jahantigh, F. and Zarookian, H. (2021). Adjustable high-power-LED solar simulator with extended spectrum in UV region. *Solar Energy*, 220, 1130–1136.

Taylor, A.O. and Rowley, J.A. (1971). Plants under climatic stress: I. Low temperature, high light effects on photosynthesis. *Plant Physiology*, 47(5), 713–718.

Taylor, C.R., van Ieperen, W. and Harbinson, J. (2019). Demonstration of a relationship between state transitions and photosynthetic efficiency in a higher plant. *Biochemical Journal*, 476, 3295–3312.

Telfer, A., Whitelegge, J.P., Bottin, H., and Barber, J. (1986). Changes in the efficiency of P700 photo-oxidation in response to protein phosphorylation detected by flash absorption spectroscopy. *Journal of the Chemical Society, Faraday Transactions 2*, 82, 2207–2215.

Thornley, J.H.M. (1976). *Mathematical models in plant physiology: a quantitative approach to problems in plant and crop physiology*, London, Academic Press.

Trouwborst, G., Oosterkamp, J., Hogewoning, S.W., Harbinson, J. and van Ieperen, W. (2010). The responses of light interception, photosynthesis and fruit yield of cucumber to LED-lighting within the canopy. *Physiologia Plantarum*, 138, 289–300.

Trouwborst, G., Hogewoning, S.W., van Kooten, O., Harbinson, J. and van Ieperen, W. (2016). Plasticity of photosynthesis after the 'red light syndrome' in cucumber. *Environmental and Experimental Botany*, 121, 75–82.

Ünlü, C., Drop, B., Croce, R. and van Amerongen, H. (2014). State transitions in *Chlamydomonas reinhardtii* strongly modulate the functional size of photosystem II but not of photosystem I. Proceedings of the National Academy of Sciences of the United States of America, 111, 3460–3465.

Urban, J. Ingwers, M., McGuire, M.A. and Teskey, R.O. (2017). Stomatal conductance increases with rising temperature. *Plant Signalling and Behaviour*, 12(8), e1356534.

Veeranjaneyulu, K. and Leblanc, R.M. (1994). Action spectra of photosystems I and II in state 1 and state 2 in intact sugar maple leaves. *Plant Physiology*, 104, 1209–1214.

von Caemmerer, S. and Evans, J.R. (2015). Temperature responses of mesophyll conductance differ greatly between species. *Plant, Cell and Environment*, 629–637.

Wagner, R., Dietzel, L., Bräutigam, K., Fischer, W. and Pfannschmidt, T. (2008). The long-term response to fluctuating light quality is an important and distinct light acclimation mechanism that supports survival of *Arabidopsis thaliana* under low light conditions. Planta, 228, 573–87.

Walters, R.G. and Horton, P. (1994). Acclimation of Arabidopsis thaliana to the light environment: changes in composition of the photosynthetic apparatus. *Planta*, 195, 248–256.

Walters, R.G. (2005). Towards an understanding of photosynthetic acclimation. *Journal of Experimental Botany*, 56(411), 435–447.

Wang, J., Lu, W., Tong, Y and Yang, Q. (2016). Leaf morphology, photosynthetic performance, chlorophyll fluorescence, stomatal development of lettuce (*Lactuca sativa* L.) exposed to different ratios of red light to blue light. *Frontiers in Plant Science*, 7, 250.

Wang, Q.-W., Liu, C., Robson, T.M., Hikosaka, K., and Kurokawa, H. (2021). Leaf density and chemical composition explain variation in leaf mass area with spectral composition among 11 widespread forbs in a common garden. *Physiologia Plantarum*, 173(3), 698–708.

Weis, E. (1985). Light- and temperature-induced changes in the distribution of excitation energy between Photosystem I and Photosystem II in spinach leaves. *Biochimica et Biophysica Acta*, 807, 118–126.

Weis, E. and Berry, J.A. (1988). Plants and high temperature stress. *Symposia of the Society for Experimental Biology*, 42, 329–345.

Wickham, H. (2016). ggplot2: Elegand Graphics for Data Analysis. Springer-Verlag, New York.

Wientjes, E., van Amerongen, H. and Croce, R. (2013). LHCII is an antenna of both photosystems after long-term acclimation. *Biochimica et Biophysica Acta*, 1827, 420–426.

Wientjes, E., Philippi, J., Borst, J.W. and van Amerongen, H. (2017). Imaging the Photosystem I/Photosystem II chlorophyll ratio inside the leaf. *Biochimica et Biophysica Acta*, 1858(3), 259–265.

Wollaeger, H.M. and Runkle, E.S. (2014). Growth of impatiens, Petunia, Salvia, and tomato seedlings under blue, Green, and red light-emitting diodes. *HortScience*, 49, 734–740.

Yamasaki, T., Yamakawa, T., Yamane, Y., Koike, H., Satoh, K., and Katoh, S. (2002). Temperature acclimation of photosynthesis and related changes in photosystem II electron transport in winter wheat. *Plant Physiology*, 128(3), 1087-1097.

Yamori, W., Noguchi, K., Kashino, Y. And Terashima, I. (2008). The role of electron transport in determining the temperature dependence of the photosynthetic rate in spinach leaves grown at contrasting temperatures. *Plant and Cell Physiology*, 49, 583–591.

Yamori, W., Hikosaka, K., and Way, D. (2014). Temperature response of photosynthesis in C3, C4, and CAM plants: temperature acclimation and temperature adaptation. *Photosynthesis Research*, 119, 101–117.

Yin, X., Belay, D.W., van der Putten, P.E.L. and Struik, P.C. (2014). Accounting for the decrease of photosystem photochemical efficiency with increasing irradiance to estimate quantum yield of leaf photosynthesis. *Photosynthesis Research*, 122, 323–335.

Zhang, R. and Sharkey, T.D. (2009). Photosynthetic electron transport and proton flux under moderate heat stress. *Photosynthesis Research*, 100, 29–43.

Zhang, Y.-T., Zhang, Y.-Q, Yang, Q.-C., and Li, T. (2019) Overhead supplemental far-red light stimulates tomato growth under intra-canopy lighting with LEDs. *Journal of Integrative Agriculture*, 18(1), 62–69.

Zhen, S., and Bugbee, B. (2020). Far-red photons have equivalent efficiency to traditional photosynthetic photons: Implications for redefining photosynthetically active radiation. *Plant, Cell and Environment*, 43, 1259–1272.

Zhen, S. and van Iersel, M.W. (2017). Far-red light is needed for efficient photochemistry and photosynthesis. *Journal of Plant Physiology*, 209, 115–122

Zhen, S., van Iersel, M.W, and Bugbee, B. (2021). Why far-red photons should be included in the definition of photosynthetic photons and the measurement of horticultural fixture efficacy. *Frontiers in Plant Science*, 12, 693445.

Zhen, S., Kusuma, P. and Bugbee, B. (2022). Toward an optimal spectrum for photosynthesis and plant morphology in LED-based crop cultivation. In: Kozai, T., Niu, G. and Masabni, J. (eds) Plant Factory Basics, Applications and Advances. Academic Press, 309–327.

Zushi, K., Kajiwara, S. and Matsuzoe, N. (2012). Chlorophyll a fluorescence OJIP transient as a tool to characterize and evaluate response to heat and chilling stress in tomato leaf and fruit. *Scientia Horticulturae*, 148, 39–46.

SUMMARY

The ability of plants to sense spectral attributes indicates the importance of spectrum for plant growth. Therefore, apart from being the source of energy to drive photosynthesis, light is also a carrier of data about the ambient environment which imparts valuable information such as shading by competitors or day length. Various photoreceptors play a role in the interpretation of this information which is translated into physiological changes of adaptive significance at leaf-level and whole-plant level. A low red:far-red ratio, for example, signifies shading. Phytochrome responds to a low red:far-red ratio by causing etiolation in an attempt to compete with neighbouring plants for light. On the other hand, a high blue fluence indicates the presence of high light which leads to cryptochrome-mediated inhibition of stem elongation and a range of phototropin-mediated responses including leaf-level effects (e.g. chloroplast movement and stomatal opening) and photonastic movement at the whole-plant level (i.e. phototropism).

Although LEDs represent an efficient lighting technology in horticulture and allow for a diversity of spectral possibilities which were previously not possible with traditional horticultural lighting technologies, it is not known how these spectra interact with natural daylight in terms of photosynthetic and photomorphogenetic impacts. These impacts of LED lighting in the greenhouse need to be understood with the goal of maximizing yield. To begin to do this, it is important to recognise the typically extreme difference in light spectrum produced by LEDs compared to that of daylight, as well as the spectral fluctuations which can occur as the spectrum (and intensity) of daylight can itself fluctuate unpredictably (e.g. as a result of cloudcover or other meteorological conditions) or predictably (e.g. sunset and sunrise times).

This thesis places emphasis on the photosynthetic impacts of greenhouse LED lighting with some attention given to the photomorphogenetic impacts. Given the spectral possibilities and potential for spectral variability associated with LED supplementary lighting, two aspects in particular are given special attention: the efficiency with which light is used by photosynthesis under light-limiting conditions (Φ_{CO2}) and the acclimation of leaves to short-term changes in growth spectrum and temperature. For narrowband irradiances Φ_{CO2} is well understood to be highest in the red region with a minimum in the green region and, generally, a shoulder in the

blue region. One factor which influences the wavelength dependence of Φ_{CO2} is the absorption of light by pigments other than chlorophyll such as non-photosynthetic pigments and photosynthetic pigments such as carotenoids which do not transfer energy to chlorophyll molecules as efficiently as energy transfer between chlorophyll molecules. Another significant contributor to the wavelength dependence of Φ_{CO2} has to do with the different wavelength dependences of PSII and PSI. Since the photosystems operate in series, and have intrinsically different operating efficiencies, it is possible for a given spectrum to overexcite one photosystem. This leads to less linear electron transport and a decrease in Φ_{CO2}. Leaves are known to acclimate to growth spectrum by enacting short-term or long-term acclimation mechanisms. In the short term, occurring in the order of minutes, state transitions redistribute excitation energy between the photosystems to alleviate over-excitation of the rate-limiting photosystem. This involves a potentially mobile pool of LHCII which, according to the classical model, associates with either PSI or PSII thereby increasing cross-section for light absorption. Occurring in the order of days, long term acclimation involves the production of more PSII or PSI proteins, also to address photosystem excitation imbalances. These responses are especially relevant in a greenhouse which employs LED supplementary lighting given the typically very unnatural spectra produced by this lighting.

In this work tomato is used as a model plant as it is represents a significant fraction of greenhouse production and the results are broadly applicable amongst similar high-light requiring crops. Attention is given to the impact of state transitions on Φ_{CO2} given that many of the fluctuations in the LED lit greenhouse are short-term (for example, as the proportion of LED irradiance increases at twilight or decreases at sunrise). Detailed work is undertaken on the wavelength dependence of Φ_{CO2} using simulated daylight or shadelight as background spectra. The potential for lighting which achieves better photosystem balance under those conditions, hence increasing Φ_{CO2} by enhancement, is explored. Also given attention in this work is the maximum attainable Φ_{CO2} in practice. A holistic study examines the photomorphogenetic and photosynthetic effects of blue light doses under a simulated daylight background. Lastly, the impact of temperature is examined given its impact on Φ_{CO2}.

Chapter 2: This chapter explores the wavelength dependence of photosynthesis with, and without, the presence of a broadband background spectrum. This study is stimulated by two main questions: First, does enhancement occur in broadband white light and, second, what

is the upper limit for quantum yield in practice? To answer these questions a rigorous approach was adopted using tomato leaves produced under two growth spectra: an artificial sun spectrum and an artificial shade spectrum. Light-limited slopes of CO_2 fixation were constructed using each of these spectra alone or combined with each of 17 narrowband spectra from 400 nm to 720 nm. This resulted in a total of 53 unique spectra. The conventional means to test for enhancement in broadband light is by way of weighted summation of interpolated Φ_{CO2} for narrowband spectra. The basis for this is that, if Φ_{CO2} for individual spectra are additive and independent, then the weighted summation should equal or approximate Φ_{CO2} for the spectrum of interest. On the other hand, if Φ_{CO2} calculated in this way is less than measured Φ_{CO2} for the spectrum of interest then enhancement has occurred. The extent of enhancement can be quantified by the ratio of measured Φ_{CO2}:predicted Φ_{CO2}. Enhancement was found to occur within the shade spectrum itself (23%) and for all narrowband and shade combinations, particularly when 720 nm was added (76% enhancement). In contrast, enhancement was not found to occur within the sun spectrum and did not occur for all added wavelengths apart from an increasing tail of enhancement in the deep red and far-red regions from 4.7% at 680 nm to 7.6% at 700nm and 46% at 720 nm. A commonality amongst instances where enhancement occurred is a spectrum rich in far-red, either by composition (i.e. the shade spectrum) or by addition of far-red. The unresolved question of the upper limit for quantum yield in practice is addressed by the large number of irradiances surveyed. Maximum Φ_{CO2} was measured at 0.090 in sun-grown leaves (at 680 nm) which is strikingly similar to upper limits reported elsewhere. Interestingly, Φ_{CO2} approximated this maximum in shade-grown leaves (Φ_{CO2}=0.089) when the shade spectrum was combined with 680 nm; enhancement accounts for this similarity since Φ_{CO2} of the 680 nm irradiance (Φ_{CO2}=0.084) and especially that of the shade spectrum (Φ_{CO2}= 0.076) were both less than 0.089 when these irradiances were combined. The significance of far-red to enhancement shows the shortcomings of the PAR definition in broadband white light.

Chapter 3: State transitions are known to occur in algae, cyanobacteria and higher plants as evidenced by the spectroscopic hallmarks of this phenomenon (changes in fluorescence yield as a state transition proceeds) in each of these diverse taxa. In seminal work on state transitions, an increase in O_2 evolution was shown to accompany a state transition in the green algae Chlorella pyrenoidosa. The latter fits well with the known positive impact of state

transitions on photosystem excitation imbalance, leading to more linear electron transport which should also improve photosynthetic efficiency. However, the absence of a known relationship between Φ_{CO2} and state transitions in higher plants is problematic and provided the basis for this chapter. State 1 and state 2 were induced using alternating narrowband irradiance which strongly over-excites either PSII or PSI; 480 nm was established to over-excite PSII most strongly out of 17 narrowband wavelengths ranging from 400 to 720 nm (demonstrated in chapter 2) whereas 700 nm was used to over-excite PSI. Parameters Fo'/Fo and Fm'/Fm, used routinely to monitor and track state transitions, indicated the alternation between state 1 and 2 in tandem with light switching. Each state transition took about 30 minutes to reach completion. Fo'/Fo and Fm'/Fm, together with Φ_{PSII}, qp, and Fv'/Fm' showed a striking correlation with Φ_{CO2} in both artificial sun and shade-grown leaves. The extent of the change in Φ_{CO2} upon light switching to completion of a state transition was 10-13%, representing a significant impact of state transitions on Φ_{CO2} under these conditions. While it is not possible to conclude the docking point of mobile LHCII in state 2, it is likely associated with PSI since, during a transition to state 2, Φ_{CO2} increased while Φ_{PSII} fell. As the spectra used to induce state transitions were very unnatural, it remains to be conclusively determined whether the observed relationship between state transitions and Φ_{CO2} is preserved in natural environments.

Chapter 4: The conspicuous photosynthetic and photomorphogenetic impacts of blue light provide the basis for this chapter. A common means of quantifying the effect of specific spectral regions is by observing the effect of the addition of a range of doses of the irradiance of interest. A key distinction between this dose response study and previous dose response work is the use of an artificial daylight spectrum as background irradiance – rather than less natural spectra - which aids in the understanding of blue light responses in a more natural context. This is also relevant to understanding the role of blue light in greenhouse horticulture where blue light is a typical component of supplementary light. The well-known inhibition of etiolation by blue light was preserved in the presence of the daylight background, with hypocotyl length showing a 35% decrease at the highest blue light fraction (61%) compared with daylight alone (27% blue light fraction). The corresponding decrease in whole-plant light absorption between the highest and lowest blue light fraction was 22%, due to the more compact nature of plants at the highest blue fraction creating more self-shading. In contrast

with the photomorphogenetic effects of blue light, photosynthetic effects were unremarkable. A_{max}, a property which is known to relate positively to blue light addition under narrowband red background irradiance, showed no such trend in the present study and showed little variation amongst treatments. Additionally, Φ_{CO2} showed only negligible responses amongst treatments. This is because Φ_{CO2} for each of the individual spectra (i.e. blue light and artificial daylight) were established to be similar, allowing for relatively stable Φ_{CO2} across treatments despite the large spectral shifts which occurred as blue light fraction changed. The results of chapter 2 suggest that there was likely no enhancement in the daylight and blue light combinations, further accounting for the negligible changes in Φ_{CO2}. The only photosynthetic parameters which responded to blue light fraction were Φ_{PSII} and Φ_{PSI}; these acted oppositely to one another as blue light fraction changed since the blue light overexcites PSII whereas the daylight overexcites PSI. Taken together, the marked photomorphogenetic changes and unremarkable photosynthetic results indicate that plant morphology and hence whole-plant light absorption were determinants of plant biomass, which decreased as whole-plant light absorption decreased. It is concluded that care should be taken when extrapolating leaf-level performance to whole-plant performance without an awareness and understanding of the potential spectral impacts on plant morphology and hence whole-plant light absorption.

Chapter 5: The temperature response of light-limited Φ_{CO2} is examined in this Chapter. Most temperature work has examined the temperature response of photosynthesis at high, non-light-limiting, or saturating light intensities. Some justification for the latter has been that high temperature and high light frequently accompany one another in natural environments. While this is indeed the case, the combination of high light, which is a potential stress in itself, combined with potential temperature stress limits the applicability of the results to light-limiting conditions. A temperature range of 15-35 °C was used for this work as it was the response of light-limited Φ_{CO2} to moderate temperatures which were of interest; the highest and lowest temperatures are not typically considered to be stressful for a species like tomato. At both 2% (non-photorespiratory) and 21% O_2 Φ_{CO2} showed an optimum at 18 °C. The temperature dependency at 2% O_2 was such that at 35 °C Φ_{CO2} was 29% lower than at the temperature optimum. This contrasts with other studies were Φ_{CO2} showed no temperature response at 2% O_2. A particularly unexpected result was the lower Φ_{PSII} and qP at 21% O_2 than

at 21% O_2 across the temperature range used. The cause of the latter cannot presently be resolved but is speculated to be the result of cyclic electron transport. An apparent transition to state 2 at 32 and 35 °C based on the Fm'/Fm ratio was inconclusive based on the accompanying increase in non-photochemical quenching at those temperatures. Φ_{PSI} was comparatively less impacted by temperature than Φ_{PSII}. An interesting finding was that, when using a more rapid measurement procedure designed to limit the exposure time of leaves to each temperature, results for Φ_{PSII}, Φ_{CO2}, and Fv/Fm were slightly different than when the slower, more conventional, procedure for Φ_{CO2} was used. It is possible that leaves possess 'memory' of previous temperatures, despite the moderate temperatures used in this work, which impacts the perceived temperature response and highlights potential pitfalls of single-leaf measurement in this kind of work.

Chapter 6: This final chapter deals with the physiological responses to spectrum observed in this work and relates these more broadly to plants in supplementary-lit greenhouse environments. Suggestions for the development of horticultural lighting strategies are put forward and some potentially beneficial avenues for future research are discussed.

ACKNOWLEDGEMENTS

I am truly grateful to have been given the opportunity to live and study abroad, especially in the Netherlands, a country renowned for its contribution to horticulture. I am also grateful to have attended a university as respected as Wageningen University. This was an experience of a lifetime for someone who had never travelled far beyond his own country and I look back at all the experiences abroad with a great deal of fondness and some disbelief that I have been so fortunate. I still remember the day I received a phone call from my promoter, Leo Marcelis, to say that I had been selected for this exciting project. It really was a dream come true.

Naturally, this work has been the culmination of many hours of hard work, and the setbacks and successes were not navigated alone. I am humbled as I recount those who helped me with this work and made my experience at Wageningen such a pleasant one. Firstly, I extend my gratitude to my co-supervisors, Jeremy Harbinson and Wim van Ieperen. Jeremy, it was a privilege to work in your lab. The first few years were especially difficult as I learned to understand and work with lab-made measuring equipment. I appreciate your patience in the face of my relative ignorance. Soon I was contributing to your 'lab-made' culture by building my own electronic circuitry for control and measurement. From this I emerged better at a technical level but I also learned the importance of truly knowing one's measuring equipment. I appreciate your 'open-door' approach and how willing you were to discuss results or problems. Your insight and attention to detail encouraged me to think more critically within, and beyond, plant science. Wim, your no-nonsense approach and commitment to sound, rigorous experimentation and analysis proved especially useful to this work. Leo, I appreciate how quickly you responded to my many questions and I admire your commitment and hard-work. You were instrumental in helping me bring this work to a conclusion.

Part of this work was done in close cooperation with fellow PhD candidate Pavlos Kalaitzoglou. Pavlos, I appreciated our many discussions and generation of ideas. To Sander Pot from Plant Dynamics and the team from Philips (now Signify) – Esther de Beer, Esther Hogeveen-van Echtelt, Marcel Krijn, Sjoerd Mentink, Celine Nicole, and Eugen Onac – with whom regular discussions were held, your critical input and guidance helped shape the outcomes of this project and is greatly appreciated.

Last but not least, I extend thanks to my wife, Rachnild, whom I met during my studies. I appreciate the many unreasonable sacrifices you made to allow me to spend many evenings behind a computer compiling this work.

Craig

CURRICULUM VITAE

Craig Robert Taylor was born on 30th September 1986 in Durban, South Africa. He attended Pinetown Boys' High School and subsequently University of KwaZulu-Natal, commencing with a BSc in environmental science in 2005. This was followed by a BSc(Hons) in 2008, during which time he worked in the laboratory of the late Prof. P. Berjak on recalcitrant seed storage techniques. In 2009, he began field trials towards an MSc. The field trials explored the potential of fecal sludge from pit latrines – a major and problematic waste source in the region - for plant production. It was during this work that he first became acquainted with gas exchange measurement and chlorophyll fluorescence. In 2011 he began work to a PhD. In the interim he returned to South Africa in 2016 where he managed a commercial blueberry tissue culture facility. This provided him with valuable experience in not only the commercial side of plant production but also in the management of people. Since late 2019 he has been running his own tissue culture laboratory in Franschhoek, South Africa, where he is developing protocols for a variety of economically important crop species. He is happily married to his wife Rachnild, whom he met during his study in the Netherlands, and is proud father to his daughter, Elsa.

PEER-REVIEWED PUBLICATIONS

Taylor, C.R., van Ieperen, W. and Harbinson, J. (2019). Demonstration of a relationship between state transitions and photosynthetic efficiency in a higher plant. Biochemical Journal, 476(21), 3295-3312.

Kalaitzoglou, P., Taylor, C.R., Calders, K.; Hogervorst, M.; van Ieperen, W.; Harbinson, J.; de Visser, P.; Nicole, C.C.S and Marcelis, L.F.M. (2021). Unraveling the effects of blue light in an artificial solar background light on growth of tomato plants. Environmental and Experimental Botany, 184.

PE&RC Training and Education Statement

With the training and education activities listed below the PhD candidate has complied with the requirements set by the C.T. de Wit Graduate School for Production Ecology and Resource Conservation (PE&RC), which comprises of a total of 44 ECTS exceeding the minimum total of 32 ECTS (= 22 weeks of activities).

Review of literature (4.5 ECTS)

- LED Lighting in greenhouse horticulture: photosynthesis

Writing of project proposal (4.5 ECTS)

- LED Lighting in greenhouse horticulture: photosynthesis

Post-graduate courses (4.8 ECTS)

- Photosynthesis, climate and change; PE&RC (2013)
- The art of modelling; PE&RC (2015)

Competence strengthening / skills courses (1.5 ECTS)

- Techniques for writing and presenting a scientific paper; PE&RC (2015)
- Scientific publishing; PE&RC (2016)

PE&RC Annual meetings, seminars or weekends (1.2 ECTS)

- PE&RC Weekend (2011)
- PE&RC Day (2011)

Discussion groups / local seminars or scientific meetings (4.5 ECTS)

- Frontier literature in plant physiology (2011-2014)

International symposia, workshops and conferences (7.2 ECTS)

- International workshop photosynthesis: from science to industry (2012)
- The 16th International Congress on Photosynthesis Research (2013)
- The photosynthetic phenome (2014)

Lecturing / supervision of practicals / tutorials (1.2 ECTS)

- Concepts in environmental plant physiology (2013)
- Concepts in environmental plant physiology (2014)

BSc / MSc thesis supervision (6 ECTS)

- Effect of blue light doses in an artificial solar background on photosynthesis in tomato
- Examining the temperature response of photosynthesis in tomato

169